Formulación, procesado y caracterización física de emulsiones con mezclas de disolventes verdes.

Jenifer Santos García

PhD. Thesis

Thesis supervisors

José Muñoz García (Profesor Titular de Universidad)

Nuria Calero Romero (Profesor Contratado Doctor)

Department of Chemical Engineering

Faculty of Chemistry

Sevilla, 2017

INDEX

Summary

This PhD. Thesis is a part of the research project “Caracterización Reológica y Estabilidad Física de Emulsiones Formuladas con Disolventes Verdes” (CTQ2011-27371) supported by the Spanish Ministerio de Economica y Competitividad (MINECO) and by European Commission (FEDER program). In addition, this PhD was financially supported by V Plan Propio of University of Sevilla.

Emulsions are thermodynamically unstable systems, in which a liquid in dispersed in other liquid in form of droplets. These systems are unstable due to different destabilization processes which can take place such as creaming, coalescence, flocculation and Ostwald ripening. In order to improve the emulsions stability, it is of prime importance to detect destabilization processes at an early stage. The rheology of emulsions from both a fundamental and an applied point of view is an important tool to detect some destabilization processes that can occur in emulsions. In addition, emulsions for agrochemical use should possess an adequate rheological structure to prevent destabilization processes such as creaming and coalescence during the product’s lifetime. Furthermore, they must be fluid enough to be dispersed in water before its application. On the other hand, laser diffraction is the best method to characterize droplet sizes distribution (DSD) and coalescence process. In addition, confocal laser scanning and optical microscopy can be an important tool when flocculation or coalescence take place. On the top of that, the technique of Multiple Light Scattering (MLS) is able to characterize droplet or aggregate size variation and droplet/aggregate migration as a function of aging time. This PhD Thesis wants to demonstrate that the combined use of different techniques such as rheology, laser diffraction, different microscopies and multiple light scattering provide very interesting information at an early stage about the destabilization mechanisms occurring in emulsions.

This PhD Thesis is based on two of the twelve principles of green chemistry: use eco-friendly substances and reduce the energy input in chemical processes. Green solvents have attracted a lot of attention in the recent years due to the necessity to replace the organic traditional solvents by more environmentally favourable ones. N,N-dimethyldecanamide(AMD-10) is considered a safe biosolvent, according to the Enviromental Protection Agency. This solvent is partially soluble in water, which may provokes some problems of the emulsion stability such as Ostwald ripening. A possible solution to this problem may be the addition of a second disperse phase component such as D-limonene, which is rather insoluble in the continuous phase. D-limonene, a naturally occurring hydrocarbon, is a cyclic monoterpene, which is commonly found in the rinds of citrus fruits such as grapefruit, lemon, lime, and in particular, oranges. D-limonene exhibits good biodegradability, hence it may be proposed as an interesting alternative to organic solvents. These solvents can meet the ever-increasing safety and environmental demands of the 21st Century. Polyoxyethylene glycerol esters derived from cocoa oil, which possess ecolabel, are non-ionic surfactants obtained from a

renewable source which fulfil the environmental and toxicological requirements to be used as ecofriendly foaming and/or emulsifying agents.

The main goal of this PhD Thesis was to develop new eco-friendly oil-in-water emulsions, which could be used as matrices for agrochemical use. This was carried out under the frame of sustainable chemical engineering. Hence, according to that, a specific strategy was followed considering the emulsion formulation and the reduction of energy input in order to obtain fine stable emulsions.

This PhD book is comprised in eight chapters. Firstly, main concepts of emulsions, green chemistry and emulsification methods were introduced.

Chapter two shows the influence of ratio of solvents on DSD, rheology and physical stability for 30 wt% green emulsions processed in a rotor-stator device. Submicron emulsions was achieved when AMD-10 was in the dispersed phase, regardless the ratio. Furthermore, chapter three deals with ecofriendly O/W emulsions using membrane emulsification for preparation. The influence of membrane emulsification parameters on DSD was studied. These chapters could be considered the starting point for further chapters since they show the different nature of the solvents. The ration 75 wt% AMD-10 /25 wt% D-Limonene was fixed for following chapters.

In chapter four, the influence of a key variable (surfactant concentration) was presented. This chapter shows that the increase of surfactant concentration does not improve the physical stability of these ecological-formulated emulsions.

The target of chapter five was to examine the microfluidization process. In spite of the fact Microfluidizer applies high energy input, there could be other advantages which are worth to study. Emulsions with 280 nm were obtained with this process, the lowest obtained in this PhD Thesis.

Chapter six shows the influence of homogenization rate on stability of 30 wt% and 40 wt% emulsions. While 30 wt% emulsions underwent creaming as main destabilization process, 40 wt% emulsions showed an increase of droplet size with aging time. In order to avoid coalescence, a pluronic was also used as surfactant in chapter seven.

The target of chapter seven was to compare the different coarsening processes in emulsions depending on the surfactant and, hence, the continuous phase used. In addition, it shows a rheological, MLS and droplet size analysis about the differences between coalescence and Ostwald ripening in emulsions.

Chapter eight deals with the influence of processing temperature in a rotor-stator device. This parameter makes important changes in the rheology of these emulsions.

Finally, the main conclusions of this PhD Thesis research are presented.

Chapter 1. State-of-the-art in green emulsions.

1.1. Green Chemistry

The objective of green chemistry is to achieve sustainability through science and technology (Anastas, 2000). There are 12 Principles of Green Chemistry which provide a framework for scientists and engineers to take into account when they design new materials, products, processes, and systems. A design based on the 12 principles considers not only environmental but also economic and social factors. Two of the 12 principles of Green Engineering, namely 5 and 6, are referred to the use of safer solvents and formulations and to reduce energy requirements during processing, respectively. (Anastas, 1998) In this way, the application of the 5th principle guides to replace the traditional organic solvents by more environmentally favourable ones. Alternative solvents form a significant portion of research in green chemistry. This is in part due to the hazards of many conventional solvents (e.g. toxicity and flammability) and the significant contribution that solvents make to the waste generated in many chemical processes. Solvents are important in analytical chemistry, product purification, extraction and separation technologies, and also in the modification of materials. Therefore, in order to make chemistry more sustainable in these fields, a knowledge of greener solvents has attracted recently much attention. (Kerton, 2013) Low or null toxicity and fast biodegradability are requirements that green solvents must fulfil. Furthermore, these eco-friendly solvents should be obtained from renewable resources and must play the same role as traditional organic solvents, with the same or even enhanced efficiency. (Hernaiz, 2010)

The 6th principle of Green Chemistry is related to the energy efficiency. Energy requirements of chemical processes should be recognized for their environmental and economic impacts and should be minimized. If possible, synthetic methods should be conducted at ambient temperature and pressure. The design of chemical reactions or systems that do not require intensive energy use is highly desirable. Reducing the energy barrier of a chemical reaction or choosing appropriate reactants so that the transformation may proceed at room temperature is one example of what chemists can do to reduce energetic requirements, with all the direct and indirect benefits associated with it.(Anastas, 1998) One way to reduce energy input in emulsions can be using of an optimal formulation.

1.2. Introduction to emulsions

A single emulsion is a dispersion of one phase in another with which it is immiscible. These two immiscible liquids are usually an oil phase or organic solvent and an aqueous phase (Morrison & Ross, 2002). In an emulsion, one liquid phase is dispersed in the other phase in the form of droplets. A layer of a surface-active component, the so-called emulsifiers, coats the droplets of the dispersed phase. Emulsions can be classified according to the distribution of the oil and the aqueous phases (McClements, 2004). When oil droplets are the dispersed phase and the aqueous is the continuous phase, it is called oil-in-water (O/W) emulsions (see figure 1.1). Conversely, a system that consists in water droplets dispersed in an oil continuous phase is designated as water-in-oil (W/O) emulsions. In addition of these conventional O/W and W/O emulsions, it is also possible to obtain multiple emulsions, i.e. water-in-oil-in-water (W/O/W) and oil-in-water-in-oil (O/W/O) emulsions.

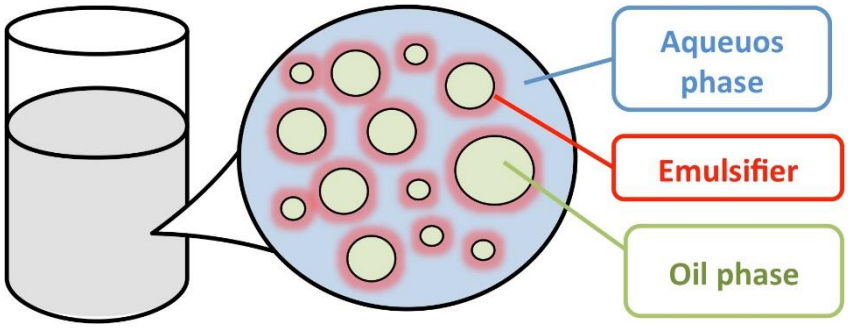

Figure 1.1. Scheme of an oil-in-water emulsion consisting of oil droplets dispersed in an aqueous medium.

Emulsion science and technology has been used for many years to create a diverse range of commercial products such as mayonnaises, salad creams, deserts, dry-cleaning formulations, pharmaceutical products as well as personal care and cosmetics, for example, hand creams, lotions, hair sprays, and sunscreens. Other field in which emulsions have a great impact is agrochemistry. In this way, it is worth to mention the self-emulsificable oils which produce emulsions on dilution with water, emulsion

concentrates (EWs), and crop oil sprays. The above importance of emulsion in industry justifies a great deal of basic research to understand the origin of instability and methods to prevent their break down.

Almost all industrially processed emulsion-based products are made up of a wide variety of constituents, including oils, emulsifiers, texture modifiers, preservatives, antimicrobial agents, antioxidants, pH adjusters, salts, and, of course, water. (Rayner, 2015)

1.3. Formulation in green emulsions for agrochemical use.

1.3.1. Eco-friendly solvents.

The nature of the oil phase has a big influence on the formation and stability of emulsions (McClements, 2005). Different molecular characteristics of the solvents lead to changes in their properties such as density, melting point, polarity, viscosity and solubility in water. Many of these properties have a great influence on the formation, stability and properties of emulsions (Piorkowski & McClements, 2014). For example, the solubility in water of the oil phase determines the physical stability of an emulsion to Ostwald ripening phenomenon due to diffusion of solvent molecules through the continuous phase. Dispersed phase viscosity influences the efficiency of droplet disruption during high energy homogenization, the closer the ratio of dispersed phase viscosity to continuous phase viscosity (η_D/η_C) is to unity, the more efficient is droplet disruption and the smaller is the particle size produced (Walstra, 1993). Oil density determines the rate of particle creaming or sedimentation within emulsions, the greater the density contrast between the droplets and surrounding fluid, the faster the rate of gravitational separation (McClements, 2005). In addition, the concentration of oil droplets in an oil-in-water emulsion influences its physical stability and rheological properties (McClements & Rao, 2011). Droplet concentration is usually characterized in terms of the dispersed phase mass fraction (Θ_m), which is the mass of the oil phase (m_{oil}) divided by the total mass of emulsion (m_E):

$$F_m(\%) = 100 \cdot \frac{m_{oil}}{m_E} \qquad \text{(EQ 1.1)}$$

A biodegradable and ecological option to substitute classical petrochemical solvents used in agrochemical formulations could be Fatty Acid Dimethylamides (FAD). FAD are solvents that fulfil the requirements to be considered green solvents and may find application in agrochemicals use due to the lack of risk to the farmer satisfying the needs of customers, which is the basic principle of the product design.(Bigorra, 2010) D-limonene, a naturally occurring hydrocarbon, is a cyclic monoterpene, which is commonly found in the rinds of citrus fruits such as grapefruit, lemon, lime, and in particular oranges. D-limonene exhibits good biodegradability, hence it may be proposed as an interesting alternative to organic solvents. (Medvedovici, 2012; Jäger, 2010). These solvents can meet the ever-increasing safety and environmental demands of the 21st century.

1.3.2. Stabilizers

Despite the fact that emulsions are thermodynamically unstable systems, it is possible to form emulsions that are kinetically stable for a long period of time by adding ingredients known as stabilizers. Stabilizers can be classified according to their mode of operation as emulsifiers or texture modifiers.

- Emulsifiers

An emulsifier is a surface-active substance that adsorbs to the surface of emulsion droplets to form a protective coating that prevents the droplets from aggregating with one another and merge, e.g., certain proteins, polysaccharides, phospholipids, surfactants and solid particles (Stauffer, 1999; Whitehurst, 2008). An emulsifier also reduces the interfacial tension and therefore facilitates the formation of emulsion droplets during homogenization (Walstra, 2002). The type of emulsifier used to stabilize an emulsion is one of the most important factors determining its overall performance and long-term stability.

The suitability of an emulsifier for a specific use is determined by a number of factors, including the optimum concentration required to stabilize an emulsion, its ability to form small droplets during homogenization, and its ability to prevent droplets from aggregating (McClements, 2005). These factors depend on the nature of the emulsifier, but they also depend on the characteristics of the emulsion in which it is present, e.g.,

pH, ionic strength, ion type, oil type, ingredient interactions, and thermo-mechanical history. For this reason, it is usually difficult to predict the behaviour of an emulsifier from knowledge of its chemical structure alone (McClements, 2005).

The main property to characterize a surfactant is its HLB number. This concept was introduced as an empirical scale that could be used to describe the balance of the size or strength of the hydrophilic and lipophilic groups on an emulsifier molecule. The HLB scale ranges from 0 to 20 for non-ionic surfactants. A low HLB (<9) is related to a lipophilic surfactant (oil soluble) and a high HLB (>11) to a hydrophilic (water soluble) surfactant. Generally, emulsifiers to form W/O emulsions exhibit HLB values in the range of 3-8 whereas emulsifiers which are adequate for O/W emulsions have HLB values of about 8-18.

Environmentally friendly surfactants have attracted significant interest recently. Polyoxyethylene glycerol esters derived from cocoa oil are non-ionic surfactants obtained from a renewable source. These fulfil the environmental and toxicological requirements to be used as ecofriendly foaming and/or emulsifying agents, hence their consideration as green surfactants (Castán and González, 2003). Their use in detergents and personal care products is disclosed in several patents (Lutz, 2006; Denolle et al., 2011).

- Modifiers

A texture modifier is a substance that either increases the viscosity of the continuous phase (thickening agent) or forms a gel network within the continuous phase (gelling agent), thereby slowing down the movement of droplets due to gravity or Brownian motion. A variety of substances have the molecular characteristics to make them suitable as thickening or gelling agents for use in emulsions. The most commonly used texture modifiers are biopolymers that are added to the aqueous phase in O/W emulsions. Thickening agents or gelling agents are usually an individual type of biopolymer or a mixture of different types of biopolymers. The most commonly used biopolymers as thickening agents are polysaccharides (carrageenans, alginates pectins, seed gums, exudates gums, xhantam gum, gellan gum, starch, cellulose…) and proteins

(gelatin, caseins…) or biopolymer blends. Mixtures of hydrocolloids may be used to impart novel and improved rheological characteristics to emulsions.

1.4. Emulsion formation.

The outcome of an emulsification process is generally a combination of two competing processes: disruption of the drop interface from dynamic destabilizing forces and thermodynamically driven coalescence.

The methods used to prepare emulsions can be divided into two categories based on the underlying principles involved in droplet formation: high and low energy methods. High-energy approaches utilize mechanical devices ("homogenizers") that generate intense disruptive forces capable of disrupting and intermingling the oil and aqueous phases, e.g., high shear mixers, high pressure valve homogenizers, microfluidizers, and sonication methods (Leong et al, 2009; Wooster et al, 2008; Gutiérrez et al, 2008). Low energy approaches rely on the spontaneous formation of tiny droplets within mixed surfactant–oil–water systems when solution or environmental conditions are altered, e.g., phase inversion and spontaneous emulsification methods (Anton et al, 2008). The droplet characteristics that can be achieved using each approach depend on equipment design, operation conditions, and system formulation. (McClements, 2012).

1.4.1. Principles of emulsion formation using high-energy methods.

The formation of an emulsion can be divided in two steps: firstly, the creation of the droplets from two separates liquids; secondly, the reduction in size of the existing droplets. They are called first and second homogenization, respectively. The formation of an emulsion may involve one or more steps depending on the nature of starting material, the application of the emulsion and the method used to create it. Usually, one type of homogenizer is used to prepare the coarse emulsion that contains large droplets (e.g. a rotor-stator device) and another device is used to reduce the size of droplets (e.g., a high-pressure homogenizer) (see figure 1.2).

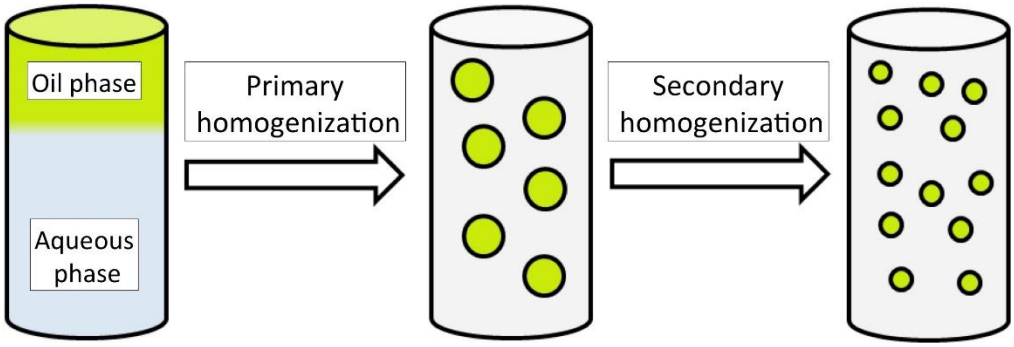

Figure 1.2. Scheme of the emulsification process divided in two steps: primary homogenization and secondary homogenization.

The physical processes that occur during homogenization can be highlighted by considering the formation of an emulsion from the four main ingredients of an emulsion: a dispersed phase (an oil in O/W emulsions), a continuous phase (water in O/W emulsions), a surfactant and energy input. The way energy can be converted from bulk mechanical stresses during emulsification to generate and stabilize the new interfacial area created is the central study of the emulsification technologies. When an oil and water are placed in a recipient they tend to adopt their thermodynamically most stable state, minimizing the contact between the two immiscible liquids. This is the reason why an emulsion droplet tends to be spherical. To create an emulsion it is necessary to supply energy in order to disrupt and mix the dispersed phase and the continuous phase. The surfactant adsorbs to the surface of the droplets during homogenization forming a protective layer that prevents the droplets merges.

1.4.2. Homogenization devices

Rotor-stator devices

Rotor–stator devices (RSDs) are probably the most widely used emulsifying system. The distinguishing feature of a rotor-stator mixer is a high-speed rotor (the driving mixing element) in close proximity to a stator (the fixed mixing element). The complexity of these components ranges from simple stirrer systems, such as propeller stirrers rotating in a vessel as a stator, to rotor–rotor systems with two rotating parts, but with no stator. One of the main benefits of RSDs is the fact that they can be run in batch, semibatch, and alternating as well as in a continuous mode, each having its respective merits. (Rayner, 2015)

The batch mode offers the advantage of realizing many process operation steps in parallel. Thus, products are mixed, pasteurized, homogenized and cooled in one vessel, which is used for mayonnaise-type products or sauces in food industry. However, it cannot be ensured that the product volume in total is processed on equal terms, which presents the main disadvantage in batch processing. Especially the broad distribution of stresses acting on emulsion droplets and residence time may result in a broad distribution of droplet sizes. Therefore, extreme process conditions as required; for example, emulsions with droplets in the submicron-size range have to be realized by continuous process.

In rotor–stator type equipment such as colloid mills and toothed-disc dispersing machines, drops are disrupted in the gap between the rotating rotor and the stationary stator. In colloid mills, drops are disrupted in the conical gap, which can be either smooth or serrated with various designs. Here, the droplet disruptive stresses are determined by the gap width (typically 100–3000 μm), rotor radius, rotational rate (typical peripheral speeds between 5 and 40 m s^{-1}), and the liquid flow rate through the gap, which can range between 4 and 20,000 l h^{-1} (Karbstein and Schubert, 1995). Colloid mills are most suitable for production of intermediate to high viscosity products and can achieve droplet diameters between 1 and 5 μm (McClements 2005). Toothed disc dispersing machines are similar to a colloid mill, except that the flow is not specifically bounded, consisting of single or several.

Ultrasonic devices

Ultrasonic homogenizers use high-intensity sound waves to generate intense shear and pressure gradients within the liquid that disrupts droplets mainly by cavitation and turbulent effects (McClements 2005). There are two methods commonly used in the industry to produce ultrasonic waves. Piezoelectric transducers are used for small batch volumes ranging from a few cubic centimeters to a few hundred cubic centimeters, and liquid jet generators are used on a larger scale where a jet coarse emulsion is pumped to impinge on a sharp-edged blade. This jet flow causes the blade to vibrate rapidly, thus generating the ultrasonic field that breaks droplets in its immediate vicinity. Ultrasonic jet-type homogenizers can produce larger volumes continuously with fluid flow rates ranging from 1 to 500,000 l h^{-1}. The factors that govern droplet disruption are intensity,

duration, and frequency of the ultrasonic waves in relationship to the volume of emulsion they are applied on (McClements 2005).

High Pressure valve Homogenizers (HPvH)

The HPH is used for size reduction or the disintegration of dispersed particles such as cells, macromolecules, or emulsion drops. The by far largest application is the size reduction of emulsion drops.

A schematic drawing of an HPH valve can be seen in Figure 1.3. Fluid enters the valve from the bottom through a feed pipe. The forcer (upper part of the figure) forces the flow radially through the narrow gap created between the forcer and the seat. Often, the seat is inclined, giving rise to a narrowing region upstream of the gap, referred to here as the inlet chamber. Downstream of the gap, the fluid exits into a larger volume, referred to as the outlet chamber. Special impact rings are sometimes mounted on the valve in order to modify the outlet chamber geometry. The gap height, h, can be varied by lowering or raising the position of the forcer. Fluid-flow frictional forces increase with decreasing gap height, and thus a higher pressure is required for a smaller gap height. In practice, the homogenizing pressure, is set by adjusting the force applied on the forcer, which, in turn, sets the gap height. Homogenization pressures are usually in the range of 5–40 MPa for food applications, such as dairy processing of milk, but can be above 100 MPa for special applications, such as cell breakage (Middelberg, 1995) or the disruption of macromolecules (Floury et al., 2002).

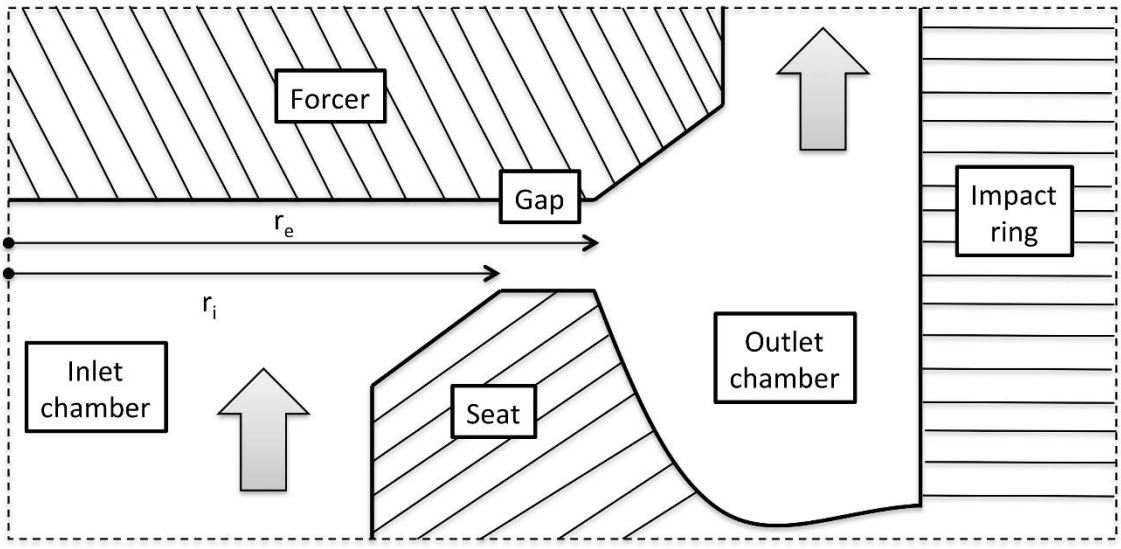

Figure 1.3. Scheme of a High Pressure valve Homogenizer.

Microfluidization.

Conventional microfluidizers can be described as two-step single-channel devices because the premixed coarse emulsions are fed into the microfluidizer from a single inlet reservoir (McClements, 2015; Galooyak and Dabir, 2015). (Figure 1.4)

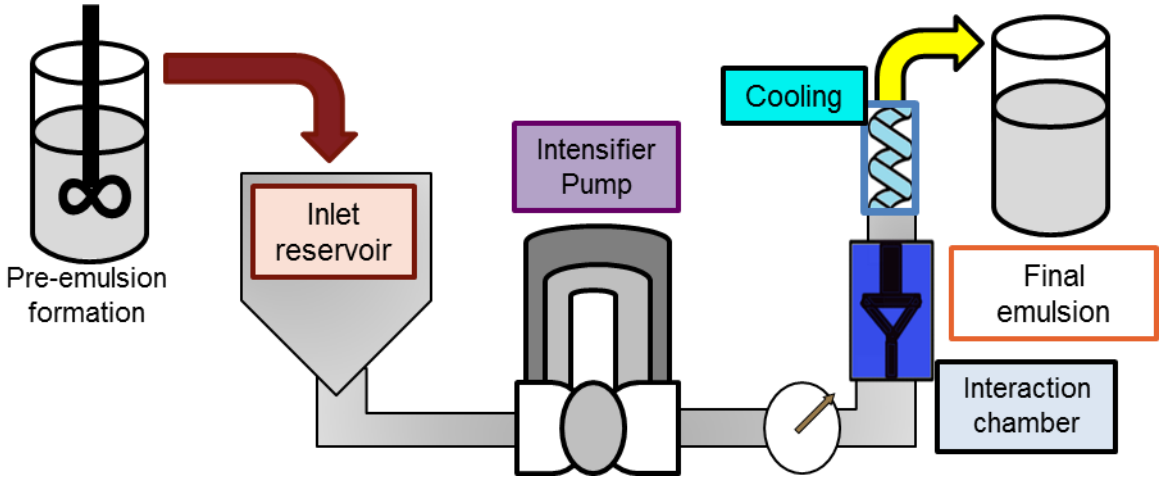

Figure 1.4. Scheme of the Microfluidizer.

Droplet breakup occurs in the Microfluidizer due to the impact of two impinging jets in the interaction chamber achieving similar pressures as those obtained in a HP_VH. In this process, high turbulence and tremendous shearing action are created. Consequently, this forces flow stream to pass though well-defined microchannels. As a result, extraordinarily fine emulsions are created. In fact, it has been observed that emulsions produced by microfluidization possess narrower DSD to those prepared using a HP_VH (Strawbridge et al, 1995; Perrier-Cornet et al, 2005). It is also shown that a continued increase in the homogenization pressure in the Microfluidizer provoked a decrease in droplet size (Qian and McClements,2011). However, this fact was not observed under all circumstances. Furthermore, microfluidization is unfavorable in some specific situations, such as higher pressures and longer emulsification times. This could lead to over-processing, namely the re-coalescence of emulsion droplets (Jafari et al, 2008).

Interactions chamber can be divided in Z-type and Y-type chambers. The latter is the most used for O/W emulsions (Figure 1.5). In this chamber, the pre-emulsion is separated in two channels and impact in the high impact zone which measures 75 µm.

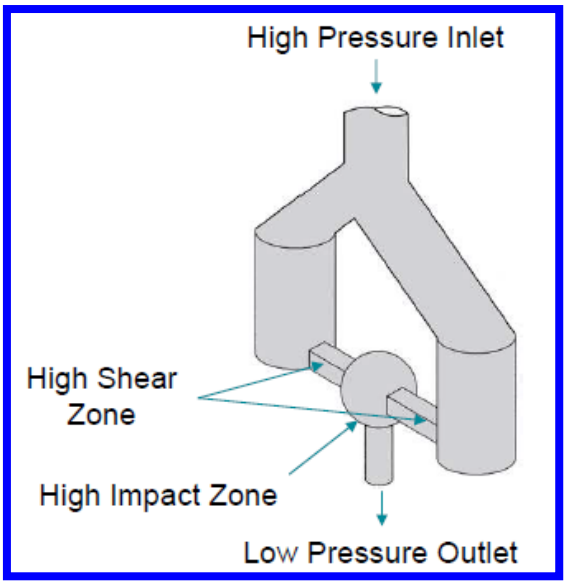

Figure 1.5. Scheme of Y-type interaction chamber.

The design of this chamber allow to make easily a change of scalability multiplying the microstructures in a larger housing. (Figure 1.6). Microchannels with characteristic dimensions enable compact operations by reducing space compared to conventional technologies. (Dietrich, 2009)

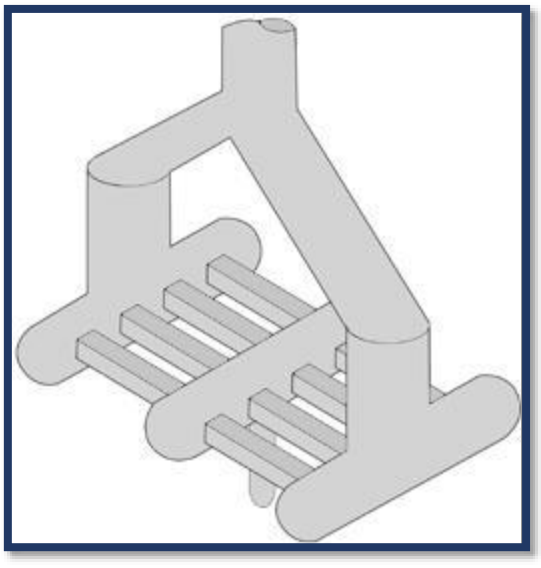

Figure 1.6. Scheme of scalability change for Y-type interaction chamber.

Membrane emulsification.

Recently, membrane emulsification (ME) has received much attention due to its ability to control the mean droplet size over a wide range together with the ability to provide

a narrow size distribution (Kosvintsev et al., 2005). The reduction in energy requirements by using ME is very significant when compared with other homogenization processes. In fact, energy densities required to achieve a mean droplet size of 1–10 μm using premix ME typically range from $10^4$to 10^6J m^{-3}, while those of rotor-stator devices and high pressure homogenizers range from 10^6 to 10^8 J m^{-3} (Karbstein and Schubert, 1995). In addition, the ability to form uniform dispersions with a technique that can be scaled from small scale to industrial production makes the process very attractive (Peng and Williams, 1998); cross flow membrane emulsification being the technique of choice for scaling-up. Two main types of ME processes have been developed: direct ME involving the permeation of pure dispersed phase through a microporous membrane into agitating or recirculating continuous phase and premix ME involving the passage of previously prepared coarse emulsion through the membrane (Charcosset et al., 2004). Premix ME provides several advantages over direct ME: (i) the dispersed phase flux is higher, so the time required for the production is very short; (ii) the mean droplet-to-pore size ratios are smaller than in direct ME. In direct ME, the mean droplet-to-pore size ratio can range between 2 and 50 (Ma, 2003; Yuan et al., 2009; Zhou et al., 2009),but it is often below 10. In premix ME, the mean droplet-to-pore size ratio is typically between 0.6 and 2 (Vladisavljevíc et al., 2006); (iii) the process parameters are easier to control than in direct ME. One of the disadvantages of premix ME is a higher emulsion polydispersity compared to direct ME.

1.5. Emulsion properties

1.5.1. Interfacial properties

Surfactants lower the interfacial tension, γ, which in turn causes a reduction in droplet size. The amount of surfactant required to produce the smallest drop size will depend on its activity a (concentration) in the bulk, which in turn determines the reduction in γ, as given by the Gibbs adsorption equation:

$$-d\gamma = RT\ \Gamma d\ ln\ a \quad \text{(EQ 1.2)}$$

where R is the gas constant, T is the absolute temperature and Γ is the surface excess (the number of moles adsorbed per unit area of the interface). Γ increases with an

increase in surfactant concentration until it eventually reaches a plateau value (saturation adsorption). The value of γ obtained depends on the nature of the oil and surfactant used. (Tadros, 2009) For instance, small molecules such as non-ionic surfactants reduce γ to a greater degree than do polymeric surfactants such as polyvinyl alcohol (PVA).

1.5.2. Droplet Size Distribution (DSD)

A polydisperse emulsion is characterized by its "droplet size distribution", which defines the concentration of droplets in different size classes (McClements, 2005). The particle concentration is usually presented as either the volume percent (Volume%) or number percent (Number%) of droplets within a particular size class. The large particles present in the emulsion cannot be seen in the DSD when the particle concentration is represented as a number percent, even though the large particles represent an appreciable amount of the overall droplets present (>25% by volume). Polydisperse emulsions may also be characterized as being "monomodal," "bimodal" or "multimodal" depending on whether there are one, two or more peaks in the droplet size distribution.

In some situations it is more convenient to represent this full droplet size distribution by a measure of the central tendency and a measure of the spread of the distribution. The mean, median or modal particle sizes are often used as measures of the central tendency, whereas the relative standard deviation is often used as a measure of the spread of the distribution (Walstra, 2002).

The three most commonly used mean particle size values are the number-weighted mean diameter (d_{10}), the surface-weighted mean diameter or so-called Sauter diameter (d_{32}) and the volume-weighted mean diameter (d_{43}).

$$d_{10} = \frac{\sum n_i d_i}{\sum n_i} \quad (EQ\ 1.3)$$

$$d_{32} = \frac{\sum n_i d_i^3}{\sum n_i d_i^2} \quad (EQ\ 1.4)$$

$$d_{43} = \frac{\sum n_i d_i^4}{\sum n_i d_i^3} \ (EQ\ 1.5)$$

Generally, the volume-weighted mean diameter is more sensitive to the presence of large droplets than the number-weighted mean diameter. Appreciable differences between the values of d_{10}, d_{32} and d_{43} generally indicate that the particle size distribution is broad or multimodal.

1.5.3. Rheology of emulsions.

Rheology is the science that studies the deformation and flow of materials. All forms of shear behaviour can be viewed as being in between two extremes: the flow of ideal viscous liquids on one hand and the deformation of ideal elastic solids on the other. Ideal liquids follow Newton law where the shear stress is proportional to the shear rate. By contrast, the solid behaviour is based on the Hooke´s law where the force (stress) is proportional to the deformation. The behaviour of all real materials is based on the combination of both the viscous and the elastic part and therefore, it is called viscoelastic. (Makosko, 1994)

The rheological properties of an emulsion are obviously among some of its more important physical attributes in either technical or aesthetic terms. As to technical matters encountered in manufacturing, such as mixing, pumping, filling or packing of emulsions, all require a good knowledge of the flow properties to assess mixing efficiency, power consumption, pump ratings etc. As to the many consumer-perceived attributes of a commercial emulsion, the visual and sensory properties are among the most important. Consumers have various expectations of emulsion: creaminess, body and consistency for instance, and these dictate their buying preference of different products. (Barnes, 1994)

The basic rheology-determining parameters of an emulsion are (i) continuous phase rheology; (ii) nature of the droplets, size distribution, deformability, internal viscosity, concentration; (iii) nature of droplet-droplet interaction.

The viscosity of a dispersed system of droplets is well described by a simplified form of the so-called Krieger-Dougherty equation:

$$\eta = \eta_c \left(\frac{\Phi}{\Phi_m}\right)^{-2} \quad (EQ\ 1.6)$$

where η is the viscosity of the emulsion (usually defined at a specific shear rate); η_c is the viscosity of the continuous phase (usually but not always constant); Φ is the phase volume of the dispersed phase and Φ_m, is the maximum phase volume when the viscosity diverges. This shows that: (i) the sensitivity of the viscosity to that of the continuous phases is multiplicative not additive, so that the effect of, for instance, temperature is, all else being equal, pro rata,(ii) the sensitivity to phase volume becomes very important for Φ greater than about 0.3, and (iii) for high phase volume the viscosity is very sensitive to the precise value of Φ, and particularly so given the nature of the exponent -2.

It has often been stated that decreasing droplet size, viscosity increase. Usually size effects are due to significant colloidal interaction between droplets, that is to say when the droplets are considerably smaller than 1 µm. However, many emulsions have sizes in excess of this, and any charge effects that might produce similar effects are negligible. Two reasons might be put forward: first that particle deformability decreases with particle size and secondly increasing the width of the distribution of droplet size, the maximum packing fraction increases, which in terms of viscosity means a decrease in viscosity.

The rheology of emulsions from an applied point of view is an important tool to detect the various destabilization processes that occur in emulsions. For instance, measurements of the viscosity at very low stresses may be quite suitable in order to predict creaming. In addition, that measurement with aging time can detect coalescence (Tadros, 2010)

1.5.4. Physical stability.

Emulsions are, by their nature, unstable. Instability is caused by different instability mechanisms, which describe the loss of the dispersed state by overcoming the threshold energies that keep the emulsions stable. Typically, we distinguish between

creaming/sedimentation, flocculation, coalescence, Ostwald ripening and phase inversion. (Figure 1.7)

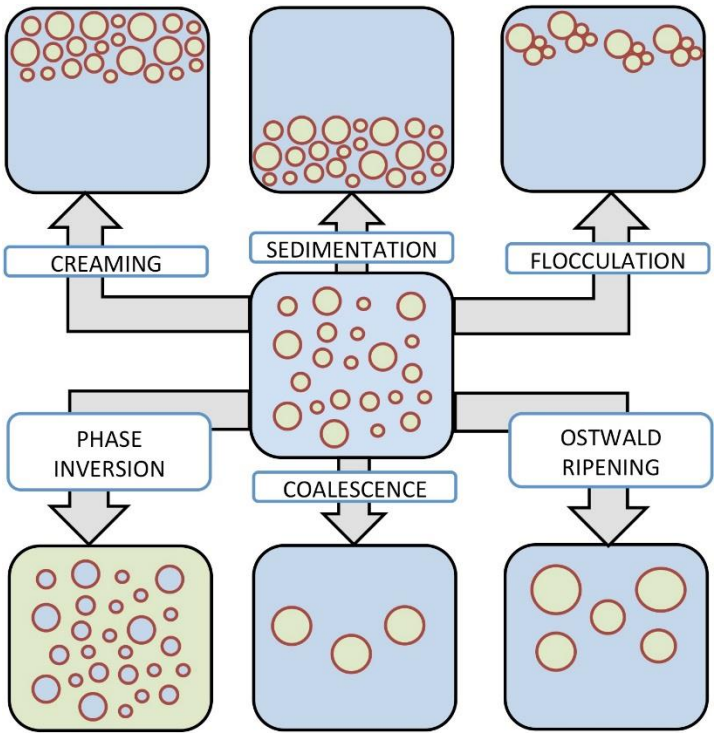

Figure 1.7. Main destabilization processes in oil-in-water emulsions

1.5.3.1. Creaming and Sedimentation

This process results from external forces, namely gravitational or centrifugal. When such forces exceed the thermal motion of the droplets (Brownain motion), a concentration gradient builds up in the system with the larger droplets moving faster to the top (if their density is lower than that of the medium) or to the bottom (if their density is larger than that of the medium) of the container. Creaming/sedimentation leads to a change in concentration in space. The change in concentration may change the rate of other destabilizing mechanisms such as flocculation or coalescence.

In principle, the long-term stability of emulsions to gravitational separation can be predicted from Stokes' Law (and its modifications) (McClements, 2005). It is necessary to have information about the densities of the dispersed and continuous phases, the droplet size, and the rheological properties of the continuous phase) to use Stokes' Law,

which predicts the rate at which gravitational separation occurs in an emulsion (Equation 1.7).

$$v_{Stokes} = -\frac{2\,g\,r^2(\delta_2-\delta_1)}{9\eta_1} \text{ (EQ 1.7)}$$

where, v_{Stokes} is the creaming velocity, r is the radius of the particle, g is the acceleration due to gravity, δ is the density, η is the shear viscosity, and the subscripts 1 and 2 refer to the continuous and dispersed phases, respectively. The sign of v_{Stokes} determines whether the particle moves upwards (+) or downwards (−), i.e., whether the particles cream or sediment, respectively. As the droplets move upwards, a droplet-depleted "serum layer" will be formed at the bottom of the container and a droplet-rich "cream layer" will be formed at the top of the container because the droplets cannot move upwards any further and so they pack closely together. The droplet concentration in the intermediate layer that separates the serum and cream layers will initially be similar to that in the original emulsion, and hence it can be referred to as the "emulsion layer". In a monodisperse emulsion, the serum layer is usually transparent because it contains no droplets that scatter light, the emulsion layer has an appearance similar to that of the original emulsion (which therefore depends on the initial droplet concentration), and the cream layer is optically opaque because the droplet concentration is high enough to cause appreciable light scattering. The extent of creaming can then be simply characterized by a creaming index (CI) (McClements, 2007):

$$CI = \frac{H_S}{H_E} \cdot 100 \; (EQ\ 1.8)$$

where, H_E is the total height of the emulsion and H_S is the height of the serum layer (Figure 1.8).

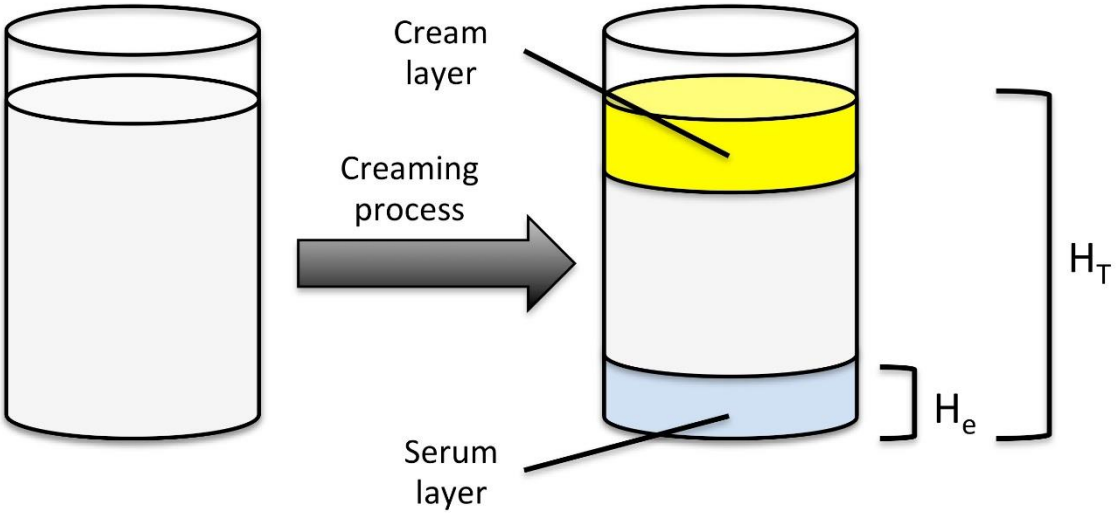

Figure 1.8. Scheme of creaming process in emulsions.

1.5.3.2. Flocculation

Flocculation is the process whereby two or more droplets associate with each other, but maintain their individual integrities. It tends to occur when the attractive interactions between droplets dominate the long-range repulsive interactions but not the short-range repulsive interactions. Hence, the droplets remain in close proximity to each other (flocculate), without coming close enough together to merge into each other (coalesce). Droplet flocculation is usually detrimental to emulsion quality, but in some cases it may be desirable. In relatively dilute emulsions (such as soft drinks, infant formula and nutritional beverages), flocculation leads to an increase in particle size that accelerates the rate of gravitational separation, which is usually undesirable because it reduces shelf-life (Chanamai et al., 2000b). Flocculation also causes a pronounced increase in emulsion viscosity ("thickening"), and may even lead to the formation of a gel in a sufficiently concentrated emulsion (Demetriades & McClements, 1999; Quemada & Berli, 2002). In some products, a controlled amount of droplet flocculation may be advantageous because it leads to the generation of desirable textural characteristics (Parker et al., 1995). The tendency for droplet flocculation to occur in an emulsion depends mainly on the balance of attractive and repulsive forces acting between the droplets: if the attractive forces dominate then the droplets will tend to aggregate, but if the repulsive forces dominate then they will be stable to aggregation. The main

attractive interactions in emulsions are van der Waals, depletion and hydrophobic forces, whereas the main repulsive interactions are electrostatic and steric forces. The rate at which droplet flocculation occurs can be characterized in terms of the droplet-droplet collision frequency and collision efficiency. The collision frequency (f_c) is the number of droplet collisions per unit volume of emulsion per unit time. It depends mainly on the dominant mechanism responsible for droplet movement in the system: Brownian motion, applied mechanical forces. The collision frequency increases with increasing droplet concentration, decreasing droplet size, and decreasing continuous phase viscosity (McClements, 2005).

1.5.3.3. Coalescence

Coalescence is defined as the process whereby two or more liquid droplets merge together to form a single larger droplet. Coalescence causes the droplets in an emulsion to cream or sediment more rapidly because of the increase in their size. In oil-in-water emulsions, coalescence eventually leads to the formation of a layer of oil on top of the material, which is referred to as oiling off. In water-in-oil emulsions, it leads to the accumulation of water at the bottom of the material.

When coalescence is the main destabilization mechanism, the time evolution of the average droplet size can follow very different behaviors: from perfectly homogeneous growth (monomodal distribution whose average size increases in time) to strongly heterogeneous growth (plurimodal distribution with the possibility of very early phase separation). Except in particular cases, the heterogeneous case is the rule (Deminiere, 1999a; Deminiere, 1999b; Schmitt, 2004). Coalescence tends to occur after the droplets have been in contact for extended periods (e.g., in a cream layer, a floc or concentrated emulsions), particularly when shear forces are applied (van Aken & van Vliet, 2002).

1.5.3.4. Ostwald ripening

Ostwald ripening (OR) is the process whereby large droplets grow at the expense of smaller ones because of mass transport of dispersed phase from one droplet to another through the intervening continuous phase (Kabalnov, 2001; Kabalnov & Weers, 1996)

Coalescence usually leads to a bimodal distribution (heterogeneous coalescence), whereas Ostwald ripening leads to a monomodal distribution with the cube of the mean

particle diameter increasing linearly with time (Kabalnov, 2001). Ostwald ripening occurs because the solubility of the material in a spherical droplet increases as the size of the droplet decreases (Kabalnov, 2001; Weers, 1998). For oil droplets dispersed in aqueous solution in absence of excess surfactant, the ripening process is generally modelled with the well-know Lifshitz-Slyozov-Wagner (LSW) theory, based on the assumption that the diffusion of oil through the water determines the overall ripening rate.(Ardell,1972; Solans, 2005). This theory predicts that, at asymptotically long times, there is a constant ripening rate ω_T that is determined by the growth in the cube of the number weighted mean droplet radius $\bar{r}$.

$$\omega_T = \frac{d\bar{r}^3}{dt} = \frac{8\gamma c_w^{eq} D_w V_m}{9kT} \quad (EQ\ 1.9)$$

Here, γ is the interfacial tension between oil and aqueous phases at the drop surface, V_m is the molecular volume of the oil, c_w^{eq} is the aqueous oil solubility , D_w is the diffusivity of the oil molecule, k is Bottzmann´s constant and T is absolute temperature. This equation based on diffusion controlled ripening has been recognized in sub-micron diluted emulsions stabilized by ionic or non-ionic surfactant. Diffusion could be accelerated due to the micellar solubilization of oil that increases the solubility of the oil in the aqueous phase. In addition, the micelles might act as a carriers that substantially increase the ripening rate (Ariyaprakai, 2010)

1.5.3.5. Phase inversion

This refers to the process whereby there will be an exchange between the disperse phase and the medium. For example, an O/W emulsion may invert to a W/O emulsion with time or change of conditions.

Earlier theories of phase inversion were based on packing parameters. When φ exceeds the maximum packing (~0.64 for random packing and~0.74 for hexagonal packing of monodisperse spheres; for polydisperse systems, the maximum packing exceeds 0.74), inversion occurs. However, these theories are not adequate, because many emulsions invert at φ values well below the maximum packing as a result of the change in surfactant characteristics with variation of conditions. Many emulsions show phase

inversion at a critical temperature (the PIT) that depends on the HLB number of the surfactant as well as the presence of electrolytes. (Tadros, 2013)

References

Anastas, P. T., & Warner, J. C. (1998). Principles of green chemistry. Green chemistry: Theory and practice, 29-56.

Anastas, P. T., Heine, L. G., & Williamson, T. C. (2000). Green chemical syntheses and processes. American Chemical Society; Distributed by Oxford University Press.

Anton, N., Benoit, J. P., & Saulnier, P. (2008). Design and production of nanoparticles formulated from nano-emulsion templates—a review. Journal of Controlled Release, 128(3), 185-199.

Ardell, A. J. (1972). The effect of volume fraction on particle coarsening: theoretical considerations. Acta metallurgica, 20(1), 61-71.

Ariyaprakai, S., & Dungan, S. R. (2010). Influence of surfactant structure on the contribution of micelles to Ostwald ripening in oil-in-water emulsions. Journal of colloid and interface science, 343(1), 102-108.

Barnes, H. A. (1994). Rheology of emulsions—a review. Colloids and Surfaces A: Physicochemical and Engineering Aspects, 91, 89-95.

Bigorra, J. (2010). Innovative solvents based on renewable raw materials. In Proceedings of 40th Annual Meeting of CED. Barcelona, Spain.

Castán P., González X. (2003) Skin properties of glycerine polyethoxylene esters. In: Proceedings of 40th Annual Meeting of CED, 325–338.

Chanamai, R., & McClements, D. J. (2000). Creaming stability of flocculated monodisperse oil-in-water emulsions. Journal of Colloid and Interface Science, 225(1), 214-218.

Charcosset, C., Limayem, I., & Fessi, H. (2004). The membrane emulsification process—a review. Journal of chemical technology and biotechnology, 79(3), 209-218.

Demetriades, K., & McClements, D. J. (1999). Ultrasonic attenuation spectroscopy study of flocculation in protein stabilized emulsions. Colloids and Surfaces A: Physicochemical and Engineering Aspects, 150(1), 45-54.

Deminiere, B., Colin, A., Leal-Calderon, F., Muzy, J. F., & Bibette, J. (1999a). Cell growth in a 3D cellular system undergoing coalescence. Physical review letters, 82(1), 229.

Deminiere, B., Stora, T., Colin, A., Leal-Calderon, F., & Bibette, J. (1999b). Surfactant phase transition inducing coalescence in dense emulsions. Langmuir, 15(7), 2246-2249.

Denolle Y, Seita V, Delaire V. European Patents and Applications. EP 2368971 A1 20110928, 2011.

Dietrich, T. (2011). Microchemical engineering in practice. John Wiley & Sons.

Floury, J., Desrumaux, A., Axelos, M. A., & Legrand, J. (2002). Degradation of methylcellulose during ultra-high pressure homogenisation. Food Hydrocolloids, 16(1), 47-53.

Galooyak, S. S., & Dabir, B. (2015). Three-factor response surface optimization of nano-emulsion formation using a microfluidizer. Journal of food science and technology, 52(5), 2558-2571.

Galooyak, S. S., & Dabir, B. (2015). Three-factor response surface optimization of nano-emulsion formation using a microfluidizer. Journal of food science and technology, 52(5), 2558-2571.

Gutiérrez, J. M., González, C., Maestro, A., Sole, I., Pey, C. M., & Nolla, J. (2008). Nano-emulsions: New applications and optimization of their preparation. Current Opinion in Colloid & Interface Science, 13(4), 245-251.

Hernaiz, M. J., Alcantara, A. R., Garcia, J. I., & Sinisterra, J. V. (2010). Applied biotransformations in green solvents. Chemistry–A European Journal,16(31), 9422-9437.

Jafari, S. M., Assadpoor, E., He, Y., & Bhandari, B. (2008). Re-coalescence of emulsion droplets during high-energy emulsification. Food hydrocolloids, 22(7), 1191-1202.

Jäger, W. (2010). Metabolism of terpenoids in animal models and humans (pp. 209-234). CRC Press: Boca Raton, FL, USA.

Kabalnov, A. (2001). Ostwald ripening and related phenomena. Journal of Dispersion Science and Technology, 22(1), 1-12.

Kabalnov, A., & Weers, J. (1996). Kinetics of mass transfer in micellar systems: surfactant adsorption, solubilization kinetics, and ripening. Langmuir, 12(14), 3442-3448.

Karbstein, H., & Schubert, H. (1995). Developments in the continuous mechanical production of oil-in-water macro-emulsions. Chemical Engineering and Processing: Process Intensification, 34(3), 205-211.

Karbstein, H., & Schubert, H. (1995). Developments in the continuous mechanical production of oil-in-water macro-emulsions. Chemical Engineering and Processing: Process Intensification, 34(3), 205-211.

Kerton, F. M., & Marriott, R. (2013). Alternative solvents for green chemistry (No. 20). Royal Society of chemistry.

Kosvintsev, S. R., Gasparini, G., Holdich, R. G., Cumming, I. W., & Stillwell, M. T. (2005). Liquid-liquid membrane dispersion in a stirred cell with and without controlled shear. Industrial & engineering chemistry research, 44(24), 9323-9330.

Leong, T. S. H., Wooster, T. J., Kentish, S. E., & Ashokkumar, M. (2009). Minimising oil droplet size using ultrasonic emulsification. Ultrasonics Sonochemistry, 16(6), 721-727.

Lutz PJ. Ca. Patents Applications.CA 2537554 A1 20060822, 2006.

Ma, G. (2003). Control of polymer particle size using porous glass membrane emulsification: a review. China Particuology, 1(3), 105-114.

Macosko, C. W., & Rheology, P. (1994). Measurements and Applications. VCH, New York.

McClements, D. J. (2004). Protein-stabilized emulsions. Current opinion in colloid & interface science, 9(5), 305-313.

McClements, D. J. (2005). Food emulsions: principles, practices, and techniques. CRC press.

McClements, D. J. (2007). Critical review of techniques and methodologies for characterization of emulsion stability. Critical Reviews in Food Science and Nutrition, 47(7), 611-649.

McClements, D. J. (2012). Advances in fabrication of emulsions with enhanced functionality using structural design principles. Current Opinion in Colloid & Interface Science, 17(5), 235-245.

McClements, D. J. (2015). Food emulsions: principles, practices, and techniques. CRC press.

McClements, D. J., & Rao, J. (2011). Food-grade nanoemulsions: formulation, fabrication, properties, performance, biological fate, and potential toxicity. Critical reviews in food science and nutrition, 51(4), 285-330.

Medvedovici, A., Udrescu, S., & David, V. (2013). Use of a green (bio) solvent–limonene–as extractant and immiscible diluent for large volume injection in the RPLC-tandem MS assay of statins and related metabolites in human plasma. Biomedical Chromatography, 27(1), 48-57.

Middelberg, A. P. (1995). Process-scale disruption of microorganisms. Biotechnology advances, 13(3), 491-551.

Morrison, I. D., & Ross, S. (2002). Colloidal dispersions: suspensions, emulsions, and foams. Wiley-Interscience.

Parker, A., Gunning, P. A., Ng, K., & Robins, M. M. (1995). How does xanthan stabilise salad dressing?. Food Hydrocolloids, 9(4), 333-342.

Peng, S. J., & Williams, R. A. (1998). Controlled production of emulsions using a crossflow membrane: Part I: Droplet formation from a single pore. Chemical Engineering Research and Design, 76(8), 894-901.

Perrier-Cornet, J. M., Marie, P., & Gervais, P. (2005). Comparison of emulsification efficiency of protein-stabilized oil-in-water emulsions using jet, high pressure and colloid mill homogenization. Journal of Food Engineering, 66(2), 211-217.

Piorkowski, D. T., & McClements, D. J. (2014). Beverage emulsions: Recent developments in formulation, production, and applications. Food Hydrocolloids, 42, 5-41.

Qian, C., & McClements, D. J. (2011). Formation of nanoemulsions stabilized by model food-grade emulsifiers using high-pressure homogenization: factors affecting particle size. Food Hydrocolloids, 25(5), 1000-1008.

Quemada, D., & Berli, C. (2002). Energy of interaction in colloids and its implications in rheological modeling. Advances in colloid and interface science, 98(1), 51-85.

Rayner, M., & Dejmek, P. (Eds.). (2015). Engineering Aspects of Food Emulsification and Homogenization. CRC Press.)

Schmitt, V., Cattelet, C., & Leal-Calderon, F. (2004). Coarsening of alkane-in-water emulsions stabilized by nonionic poly (oxyethylene) surfactants: The role of molecular permeation and coalescence. Langmuir, 20(1), 46-52.

Solans, C., Izquierdo, P., Nolla, J., Azemar, N., & Garcia-Celma, M. J. (2005). Nano-emulsions. Current opinion in colloid & interface science, 10(3), 102-110.

Stauffer, C. E.(1999). Emulsifiers.

Strawbridge, K. B., Ray, E., Hallett, F. R., Tosh, S. M., & Dalgleish, D. G. (1995). Measurement of particle size distributions in milk homogenized by a microfluidizer:

estimation of populations of particles with radii less than 100 nm. Journal of Colloid and Interface Science, 171(2), 392-398.

Tadros, T. F. (2009). Emulsion science and technology: a general introduction. Emulsion science and technology, 1-56.

Tadros, T. F. (2010). Rheology of dispersions: Principles and applications.

Tadros, T. F. (Ed.). (2013). Emulsion formation and stability. John Wiley & Sons.

Van Aken, G. A., & van Vliet, T. (2002). Flow-induced coalescence in protein-stabilized highly concentrated emulsions: Role of shear-resisting connections between the droplets. Langmuir, 18(20), 7364-7370.

Vladisavljevic, G. T., Surh, J., & McClements, J. D. (2006). Effect of emulsifier type on droplet disruption in repeated Shirasu porous glass membrane homogenization. Langmuir, 22(10), 4526-4533.

Walstra, P. (1993). Principles of emulsion formation. Chemical Engineering Science, 48(2), 333-349.

Walstra, P. (2002). Physical chemistry of foods. CRC Press.

Weers, J.G. (1998) In Binks, B. P. (Ed.), Modern aspects of emulsion science. Royal Society of Chemistry.

Whitehurst, R. J. (Ed.). (2008). Emulsifiers in food technology. John Wiley & Sons.

Wooster, T. J., Golding, M., & Sanguansri, P. (2008). Impact of oil type on nanoemulsion formation and Ostwald ripening stability. Langmuir, 24(22), 12758-12765.

Yuan, Q., Williams, R. A., & Biggs, S. (2009). Surfactant selection for accurate size control of microcapsules using membrane emulsification. Colloids and Surfaces A: Physicochemical and Engineering Aspects, 347(1), 97-103.

Zhou, Q. Z., Ma, G. H., & Su, Z. G. (2009). Effect of membrane parameters on the size and uniformity in preparing agarose beads by premix membrane emulsification. Journal of membrane science, 326(2), 694-700.

Chapter 2: Physical characterization of eco-friendly O/W emulsions developed through a strategy based on product engineering principles.

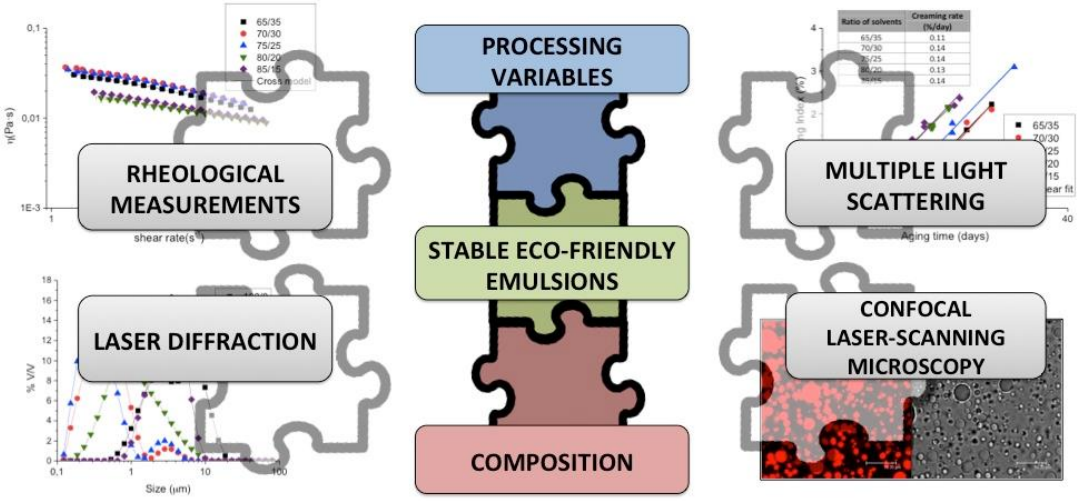

Abstract

Many traditional industrial products are being gradually replaced by environmental friendly alternatives. N,N-dimethyldecanamide and D-limonene are solvents that fulfil the requirements to be considered green solvents and may find application in agrochemicals. This contribution deals with the study of emulsions formulated with a mixture of these solvents and an eco-friendly emulsifier. The procedure followed for the development of these formulations was based on the application of product design principles. This led to the optimum homogenization rate and subsequently to the optimum ratio of solvents. The combination of different techniques (Rheology, Laser Diffraction, Confocal Laser-Scanning Microscopy and Multiple Light Scattering) was demonstrated to be a powerful tool to assist in the prediction of the emulsions destabilisation process. Thus, we found that the optimum ratio of solvents was 75/25 (N,N-dimethyldecanamide/D-limonene) on account of the lack of coalescence and of a low creaming rate.

2.1. Introduction

Emulsion is one of the most common formulation types for agricultural pesticides. This formulation type allows the pesticides to be easy to use, transport and mix[1], which contributes an added-value for a new product. Traditionally, more than 25% of all pesticides contain high concentrations of organic solvents, which represent a fire hazard, may also be toxic and contribute to atmospheric volatile compound emissions[2]. Thus, many of the classical solvents are being gradually replaced by the so-called 'green' solvents such as fatty acid dimethylamides and D-limonene. Fatty acid dimethylamides

(FAD) are solvents that fulfill the requirements to be considered green solvents and may find application in agrochemicals[3].

D-limonene, a naturally occurring hydrocarbon, is a cyclic monoterpene, which is commonly found in the rinds of citrus fruits such as grapefruit, lemon, lime, and in particular, oranges. D-limonene exhibits good biodegradability, hence it may be proposed as an interesting alternative to organic solvents[4, 5]. These solvents can meet the ever-increasing safety and environmental demands of the 21st Century.

N,N-dymethilamide is partially soluble in water, which may provokes some problems of the emulsion stability such as Ostwald ripening. A possible solution to this problem may be the addition of a second disperse phase component such as D-limonene, which is rather insoluble in the continuous phase. In addition, the presence of a surfactant helps to retard the destabilizing process and ensures long-term stability.

Ethoxylated glycerine esters are also eco-friendly and nontoxic[6], hence their consideration as green surfactants. Their use in detergents and personal care products is disclosed in several patents[7, 8].

In order to improve the emulsions stability, it is of prime importance to detect destabilization processes at an early stage to shorten the aging test. The rheology of emulsions from both a fundamental and an applied point of view is an important tool to detect the various destabilization processes that occur in emulsions. For instance, measurements of the viscosity at very low stresses may be quite suitable in order to predict creaming[9]. On the other hand, laser diffraction is the best method to characterize droplet sizes distribution (DSD) and coalescence process. Besides, the

technique of Multiple Light Scattering (MLS) is able to characterize droplet or aggregate size variation and droplet/aggregate migration as a function of aging time[10].

This work expects to show that the combined use of different techniques such as rheology, laser diffraction, and multiple light scattering provide very interesting information at an early stage about the mechanisms of destabilization occurring in emulsions.

The main objective of this work was the study of the influence of the ratio of a mixture of green solvents (N,N-dimethyldecanamide and D-limonene) on the physical stability of slightly concentrated O/W emulsions formulated with these eco-friendly solvents and a polyoxyethylene glycerol ester as emulsifier. These emulsions may be used as matrices for incorporation of active agrochemical ingredients. This work is a contribution to the development of new products, which may fulfill the customers' needs as well as the related industries' requirements. This is the one of the foundations of the so-called chemical product design and engineering[11]. On top of that, the overall goal of this project is under the frame of sustainable chemical engineering insofar as applications of bio-based chemicals are explored[12]. Also, according to this principle, a specific strategy was followed considering the emulsion formulation and the reduction of energy input in order to obtain fine stable emulsions[13].

2.2. Materials and methods.

2.2.1.Materials

N,N Dimethyl Decanamide (Agnique AMD-10^{TM}) was kindly provided by BASF. D-Limonene was supplied by Sigma Chemical Company. The emulsifier used was a nonionic surfactant derived from cocoa oil. Namely, a polyoxyethylene glycerol fatty acid ester,

Glycereth-17 Cocoate (HLB:13), received as a gift from KAO, was selected. Its trade name is Levenol C-201^{TM}. RD antifoam emulsion (DOW CORNING®) was used as antifoaming agent. This commercial product consists of an aqueous solution containing Polydimethyl siloxane (<10 %w/w) and Dimethyl siloxane, hydroxyl-terminated (<10 %w/w). Deionized water was used for the preparation of all emulsions.

2.2.2.Emulsion development

In the preliminaries studies emulsions containing 3 wt% Levenol C-201 as emulsifier, 0.1 wt% antifoam emulsion and 30 wt% solvent(s) were prepared. The ratio of solvents studied were 100/0, 75/25, 50/50, 25/75 and 0/100 of AMD-10/D-limonene. These O/W emulsions were carried out using a rotor-stator homogenizer (Silverson L5M), equipped with a mesh screen, at different homogenization rates (7000, 6000, 5000, 4000 and 3000 rpm) during 60 seconds.

When focusing on ratio of solvents, homogenization rate was fixed at 6000 rpm during 60 s in the emulsions with the following new AMD-10/D-limonene ratios: 65/35, 70/30, 80/20, 85/15.

2.2.3.Interface tension measurements

Interface tension measurements were performed with a drop pro-file analysis tensiometer (CAM200, KSV, Finland). The drop was formed inside a thermostated cuvette at 20ºC and controlled using a custom-built control unit consisting of a syringe with a piston that is driven by a stepper motor. The control procedure was as follows: once the drop was formed the contour of the drop was acquired and then the drop initial area was calculated. Every 10 s the area was calculated and the actual and initial values

were compared. If the values differed then the stepper motor drove the piston in the respective direction to correct the difference.

2.2.4.Droplet size distribution measurements.

Size distribution of oil droplets were determined by laser diffraction using Mastersizer X (Malvern, Worcestershire, United Kingdom). All measurements were done for three times for each emulsion. These measurements were carried out after 1, 3, 13, 21, 40 days aging time to analyze likely coalescence effects.

The mean droplet diameter was expressed as Sauter diameter (D[3,2]) and volume mean diameter (D[4,3]).

$$D[M,N] = \left[\frac{\int D^M n(D)dD}{\int D^N n(D)dD}\right]^{\frac{1}{M-N}} \text{ (Eq 1)}$$

The uniformity is an index of polydispersity of the different droplets sizes, defined by the following expression:

$$U = \frac{\sum V_i |d(v,0.5) - d_i|}{d(v,0.5)\sum V_i} \text{ (Eq 2)}$$

Where d(v,0.5) is the median for the distribution, and V_i is the volume of droplets with a diameter d_i.

2.2.5.Rheological measurements.

Rheological experiments were conducted with a Haake MARS controlled-stress rheometer (Thermo-Scientific, Germany), equipped with a sand-blasted coaxial cylinder Z-20 (sample volume: 8.2 mL, Re/Ri =1.085, Ri= 1 cm) to avoid slip effects. Flow curves were carried out from 0.05 Pa to 1 Pa at 20ºC. Flow curves were carried out after 1, 3, 13, 21 and 40 days aging time to follow the effect of aging time. All measurements were

repeated 3 times with each emulsion. Samples were taken at about 2 cm from the upper part of the container. Sampling from the top part of the container in contact with air was avoided.

Rheological measurements were carried out for the 85/15, 80/20, 75/25, 70/30 and 65/35 emulsions.

2.2.6.Multiple light scattering

Multiple light scattering measurements with a Turbiscan Lab Expert were used in order to study the destabilization of the emulsions. Measurements were carried out until 40 days at 20 ºC to determine the predominant mechanism of destabilization in each emulsion as well as the kinetics of the destabilization process. Multiple light scattering is a sensitive and non-intrusive technique to monitor physical stability of emulsions[14, 15] and more complex systems such as suspoemulsions[16].

To characterize the creaming process, it is used the creaming index (CI)[17]:

$$CI = 100 \cdot \frac{H_S}{H_E} \text{ (Eq 3)}$$

Where, H_E is the total height of the emulsion and H_S is the height of the serum layer.

Multiple light scattering measurements in the middle zone of the measuring cell also allowed the evolution of a mean droplet diameter with aging to be monitored.

2.2.7.Microscopic observation.

The microstructure of some emulsions was observed using a confocal laser-scanning microscope (CLSM) (Leica TCS-SP2).

For CLSM microscopy, a proper amount of emulsion was placed in a test tube and subsequently Nile red solution (1 mM in DMSO) were added and mixed thoroughly. That solution is selective to the AMD solvent. The mixture was dropped on a microscope slide, which was covered with a cover slip and observed under the microscope with 100x oil immersion objective lens. The samples were excited at 488 nm. The emission was recorded at 500-600 nm.

2.3. Results and discussion

Exploring the composition and homogenization process

Figure 2.1 shows the droplet size distribution of the emulsions with different ratios of solvents processed at the minimum speed studied (3000 rpm). This was chosen to assess if a low-energy input would yield emulsions with reasonable mean diameters and physical stability. Firstly, it should be stated that no result for the emulsion with D-limonene as the unique solvent is shown because D-limonene could not be emulsified under this processing condition. D-limonene is a strongly non-polar solvent possessing a high interfacial tension (Table 2.1).

Table 2.1.Values of interfacial tension for different ratios of solvents and water at 20ºC.

Ratio of solvents	Interfacial tension (mN/m)
0/100	40.0±1.3
1/99	27.3±0.8
5/95	17.5±0.7
10/90	14.1±0.7
25/75	7.0±0.4
50/50	3.5±0.3
75/25	1.6±0.1
100/0	1.0±0.1

This may be a disadvantage during the emulsification process, since lower interfacial tension results in higher ability to break into droplets [18]. Table 2.1 also shows the interfacial tensions of different mixtures of AMD-10/D-limonene and water. An increase in AMD-10 content of the solvent mixture provoked a progressive decrease of the interfacial tension, such that the lowest interfacial tension was reached by pure AMD-10. However, this extremely low interfacial tension led to an emulsion showing a bimodal droplet size distribution with a high polydispersity (Figure 2.1), that resulted in high values of the uniformity parameter (table 2.2). In addition AMD-10 is a slightly polar solvent and partially soluble in water (340 mg/L at 20 °C). The use of partially water-soluble solvents (as the dispersed phase in emulsions) may specially lead to destabilization of emulsions by the Ostwald ripening phenomenon [17,19]. In addition oil droplet flocculation, creaming and coalescence may also take place.

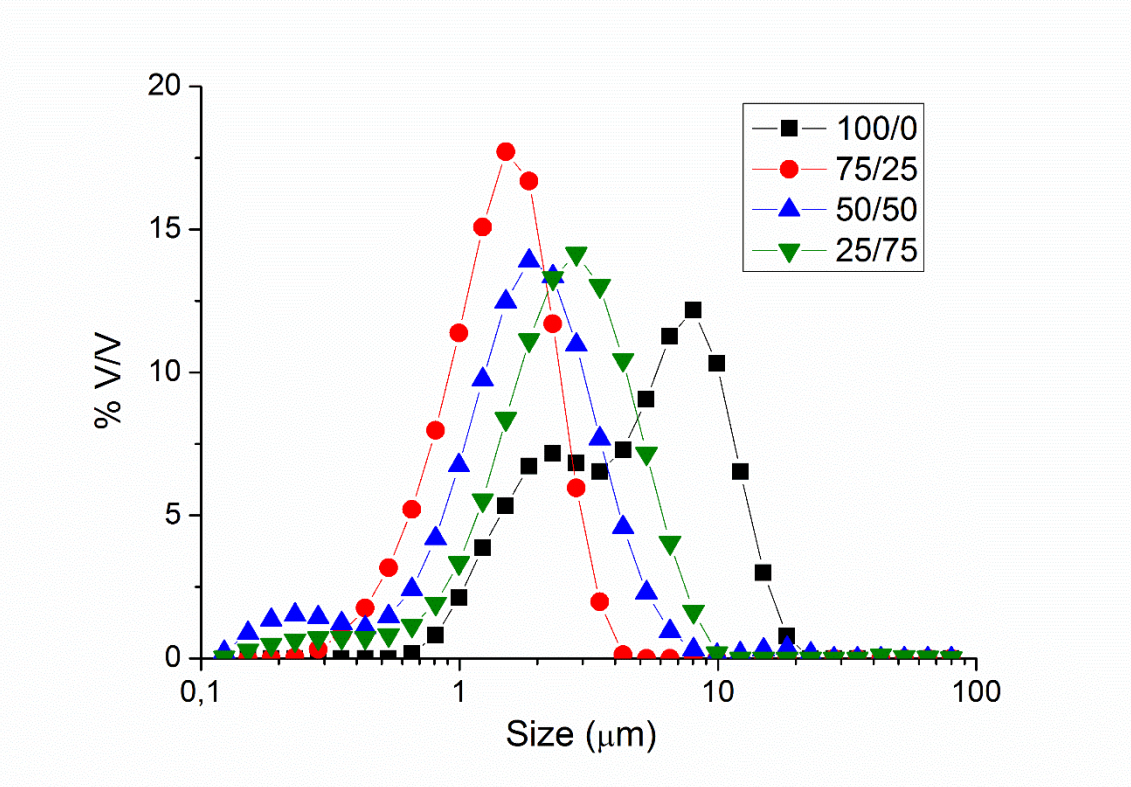

Figure 2.1. Droplet size distribution for the 100/0, 75/25, 50/50 and 25/75 emulsions processed at 3000 rpm. Aging time: 1 day. Tª=20 ºC.

Table 2. Values of Sauter diameter and Uniformity for all emulsions studied.

Standard deviation of the mean (3 replicates) for D[3,2]<5%

Standard deviation of the mean (3 replicates) for Uniformity<5%

Ratio of solvents	Homogenization rate (rpm)									
	7000		6000		5000		4000		3000	
	D[3,2] (μm)	*Uniformity (·10^{-1})*	*D[3,2] (μm)*	*Uniformity (·10^{-1})*	*D[3,2] (μm)*	*Uniformity (·10^{-1})*	*D[3,2] (μm)*	*Uniformity (·10^{-1})*	*D[3,2] (μm)*	*Uniformity (·10^{-1})*
100/0	2.72	5.70	3.09	7.29	1.78	3.93	3.42	4.68	3.75	6.02
75/25	0.33	9.26	0.35	7.54	0.47	7.18	0.73	4.34	1.07	3.79
50/50	0.27	11.01	0.29	9.68	0.34	8.72	0.64	7.80	1.05	5.16
25/75	0.6	9.87	0.72	8.87	1.02	7.17	1.57	4.53	1.55	4.96
0/100	1.83	3.77	2.43	4.10	2.50	5.03	3.15	4.57	-	-

Enhanced droplet size distributions were observed when both solvents were used, congruently with the controlled reduction of interfacial tensions achieved. It is worth noting that the addition of just 1 wt% of AMD-10 to D-limonene reduced interfacial tension by 33% (Table 2.1). This could be due to the fact that AMD-10 was able to migrate to the interface. Thus, droplets could be formed by both solvents distributed according to the solvents' concentration gradient. In this way, AMD-10 would tend to stay nearest the interface and limonene in the core of droplets, which could be similar to a "core-shell" model [20,21].

In figure 2.2a, the creaming index was plotted as a function of aging time at different ratios of solvents for the emulsion processed at 3000 rpm, which allowed the kinetics of the destabilization process by creaming to be analysed and quantified.

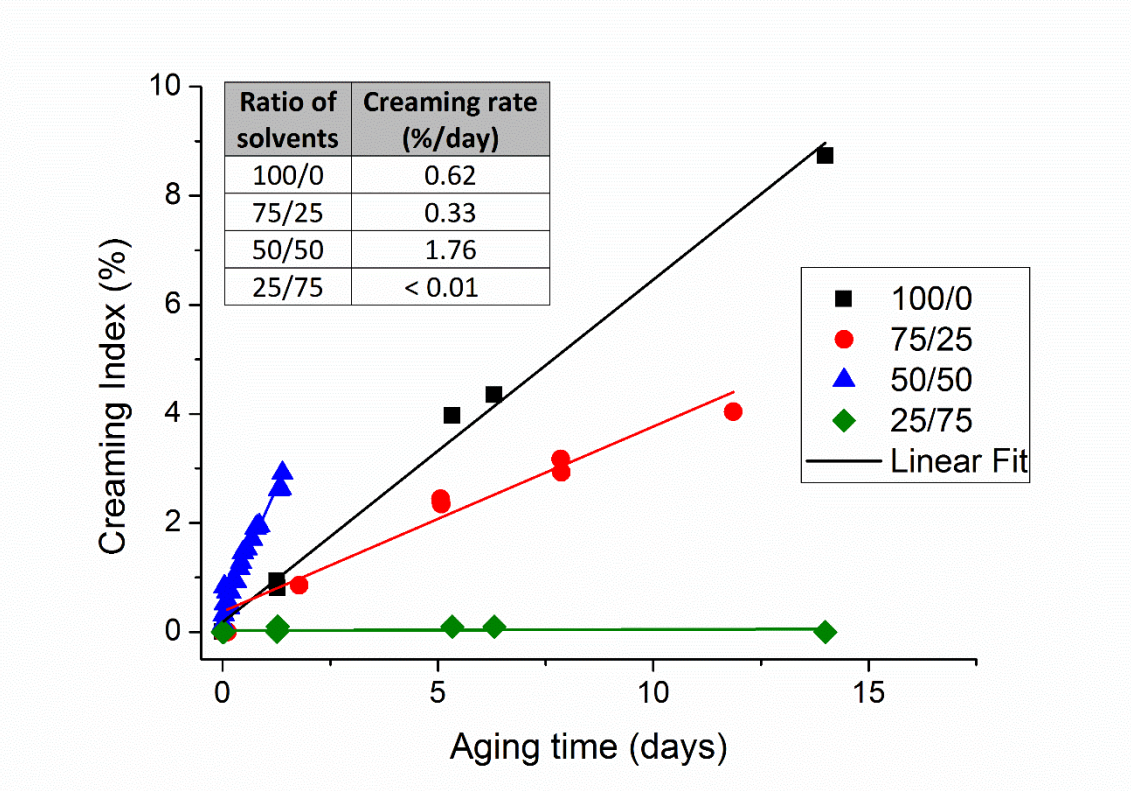

Figure 2.2a. Creaming index as a function of the aging time for emulsions processed at 3000 rpm. Samples kept under storage at 20ºC. Note: the data for 50/50 composition is not shown for aging time later than 3 days since emulsion phase separation occurred. It precludes further creaming measurements.

Firstly, it should be noted that 25/75 emulsion did not show destabilization by creaming. However, emulsions with higher AMD-10/D-limonene ratios showed a linear dependence of the creaming index with aging time in absence of a delay time for creaming. The slope of the linear region is directly related to the kinetics of the

destabilization process, which is called the 'creaming rate'. The 75/25 emulsion showed lower creaming rate than both 50/50 and 100/0 emulsions (see the inset of figure 2.2a).

Figure 2.2b shows the increase of droplet diameter from the diameter at time zero as a function of aging time for a homogenisation rate of 3000 rpm.

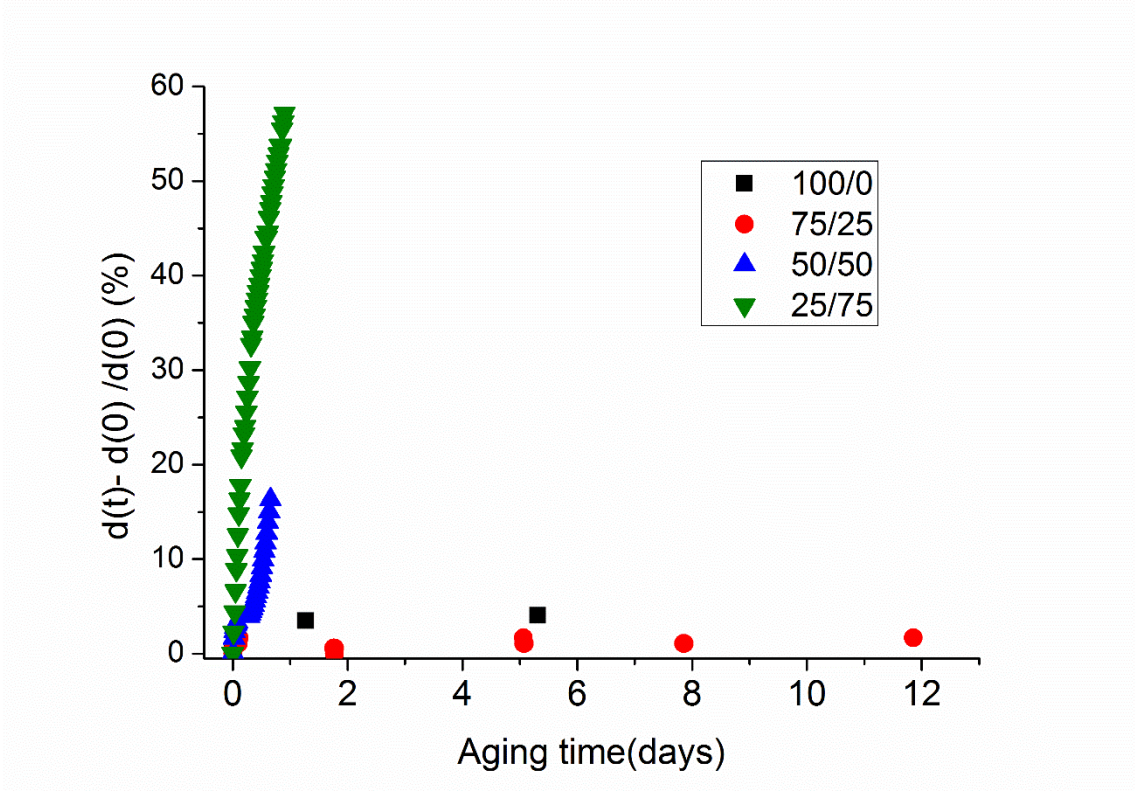

Figure 2.2b. Increase of droplet diameter from the diameter at time zero as a function of aging time for a homogenisation rate of 3000 rpm. Samples kept under storage at at 20ºC.

This plot allows for detecting flocculation and/or coalescence phenomena. On the one hand, an increase of droplet size over time was detected for the 50/50 and 25/75 emulsions. On the other hand, the emulsions without D-limonene or with lower contents of this (100/0 and 75/25) did not undergo these destabilisation phenomena as demonstrated by the fact that droplet diameter did not show any significant changes with aging time.

An overall analysis of the MLS results allows us to conclude that although the 25/75 emulsion showed the best results against destabilization by creaming, it underwent immediate destabilization by flocculation and/or coalescence. However, it is important to clarify that multiple light scattering technique does not distinguish by itself between flocculation and coalescence since both mechanisms provoke in this case an increase of backscattering in the middle zone of the measuring cell. By contrast, creaming process involves a decrease of backscattering in the low zone of the measuring cell, although this was not observed. In addition, creaming was not detected by naked eye. A tentative explanation may be that that creaming is covered up by flocculation and/or coalescence.

Hence, the 75/25 emulsion showed the best physical stability results for the homogenisation rate of 3000 rpm.

On account of the poor results obtained with the lowest energy input provided by 3000 rpm homogenization rate, this was increased up to 7000 rpm. Sauter diameter and uniformity values obtained at 4000 rpm, 5000 rpm, 6000rpm and 7000 rpm are shown in table 2.2. Figure 2.3 shows by way of example the droplet size distributions of emulsions prepared with different ratios of solvents and processed at 6000 rpm.

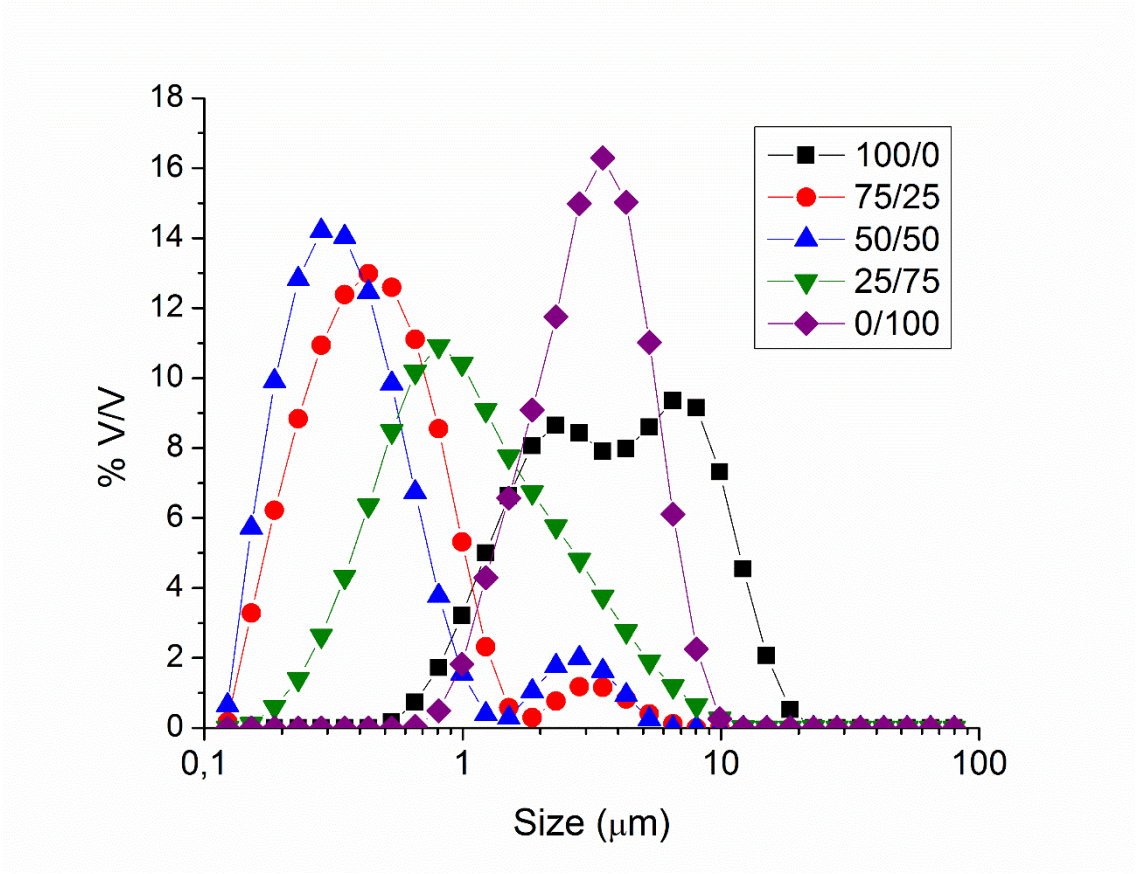

Figure 2.3. Droplet size distribution for the emulsions processed at 6000 rpm. Aging time: 1 day. T=20ºC

It was observed that the use of pure solvents yielded macroemulsions with Sauter mean diameters above 1 micron. However, the use of solvent mixtures caused a decrease of droplet size to submicron values (table 2.2). Furthermore, the ratio of solvents determined the final size distribution of the emulsion. Thus, the lower Sauter diameters were found for 50/50 emulsions, 270 nm being the lowest value reached. Despite this, it should be noted that higher contents of AMD-10 provoked bimodal distributions with a second population above 1 micron (centred around 3 microns). The occurrence of the second population of droplets may be related to a re-coalescence phenomenon induced by an excess of mechanical energy input during the emulsification process. Re-coalescence phenomenon is due to the fact that emulsion droplets are subjected to

excessive kinetic energy as a result of high-intensity turbulence in emulsification systems, which in turn yields the partial rupture of the interface of some droplets [22]. This is consistent with the fact that the appearance of this second peak occurred only for emulsions processed above 5000 rpm.

The lower values of the Sauter mean droplet size obtained for 50/50 emulsions for all homogenisation rates studied were counterbalanced by the lower polydispersity of emulsions with the ratio of solvents at 75/25, as indicated by the uniformity values obtained. McClements stated that an increase of polydispersity determines the stability of the emulsion as it provokes an increase of creaming rate due to higher values of the effective packing parameter [23].

In figure 2.4a, the creaming index was plotted as a function of aging time at different ratios of solvents for emulsions processed at 6000 and 7000 rpm.

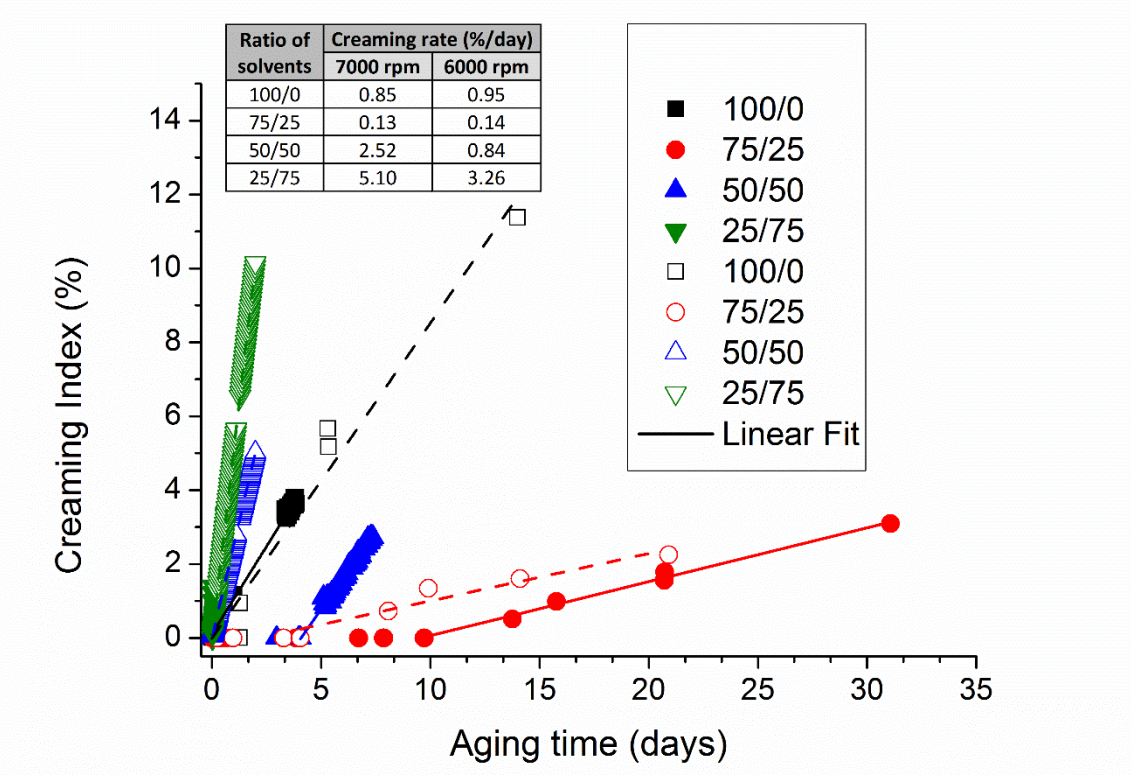

Figure 2.4a. Creaming index as a function of aging time for the emulsions 100/0, 75/25, 50/50 and 25/75 processed at 6000 rpm (closed symbols) and 7000 rpm (open symbols). Continuous lines illustrate data fitting to a linear fit for the emulsions processed at 6000 rpm and dash illustrate data fitting to a linear fit for the emulsions processed at 7000 rpm.

The 75/25 emulsion showed a slower creaming rate and greater delay time for creaming for both homogenization rates (see the inset of figure 2.4a). This fact indicates that emulsions with this ratio of solvents exhibited better physical stability against creaming as the results for emulsion processed at 3000 rpm had already pointed. However, the emulsions processed at 6000 and 7000 rpm showed greater delay time for creaming and lower rate of creaming than those processed at 3000 rpm (see figures 2.2a and 2.3). This is related to larger droplet sizes favouring destabilization by creaming [17]. In addition, the emulsion processed at 6000 rpm showed higher delay time for creaming than that processed at 7000 rpm. The latter emulsion was slightly over-processed since it showed a more noticeable second peak in DSD (recoalescence), which resulted in a higher uniformity value (table 2.2).

Figure 2.4b shows the relative increase of droplet diameter from the diameter at time zero as a function of aging time for homogenisation rates of 6000 and 7000 rpm.

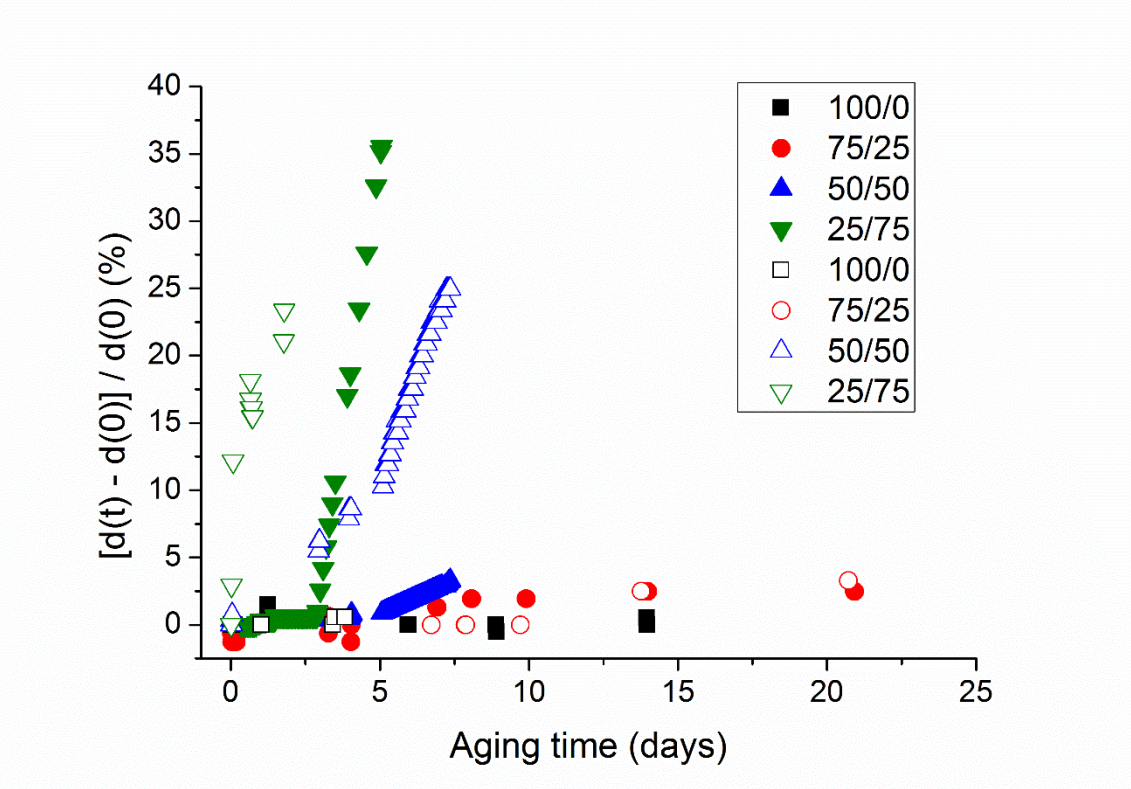

Figure 2.4b. Increase of droplet diameter from the diameter at time zero as a function of aging time for emulsions 100/0, 75/25, 50/50, 25/75 processed at 6000 rpm (closed symbols) and 7000 rpm (open symbols).

Firstly, it should be noted that both 25/75 and 50/50 emulsions underwent an increase of droplet size with aging time caused by flocculation and/or coalescence. In contrast, the 100/0 and 75/25 emulsions processed at both homogenisation rates (6000 rpm and 7000 rpm) did not exhibit destabilization by flocculation and/or coalescence for the test time.

Taking into account the above results, we concluded that the emulsion formulated with a 75/25 ratio of solvents and prepared at 6000 rpm provided the best stability results for the test time. For this reason, it was taken as a starting point for further analysis for optimising the formulation.

Focusing on ratio of solvents

Figure 2.5 shows the DSD of emulsions with different solvent ratios, around the 75/25 value, processed at 6000 rpm.

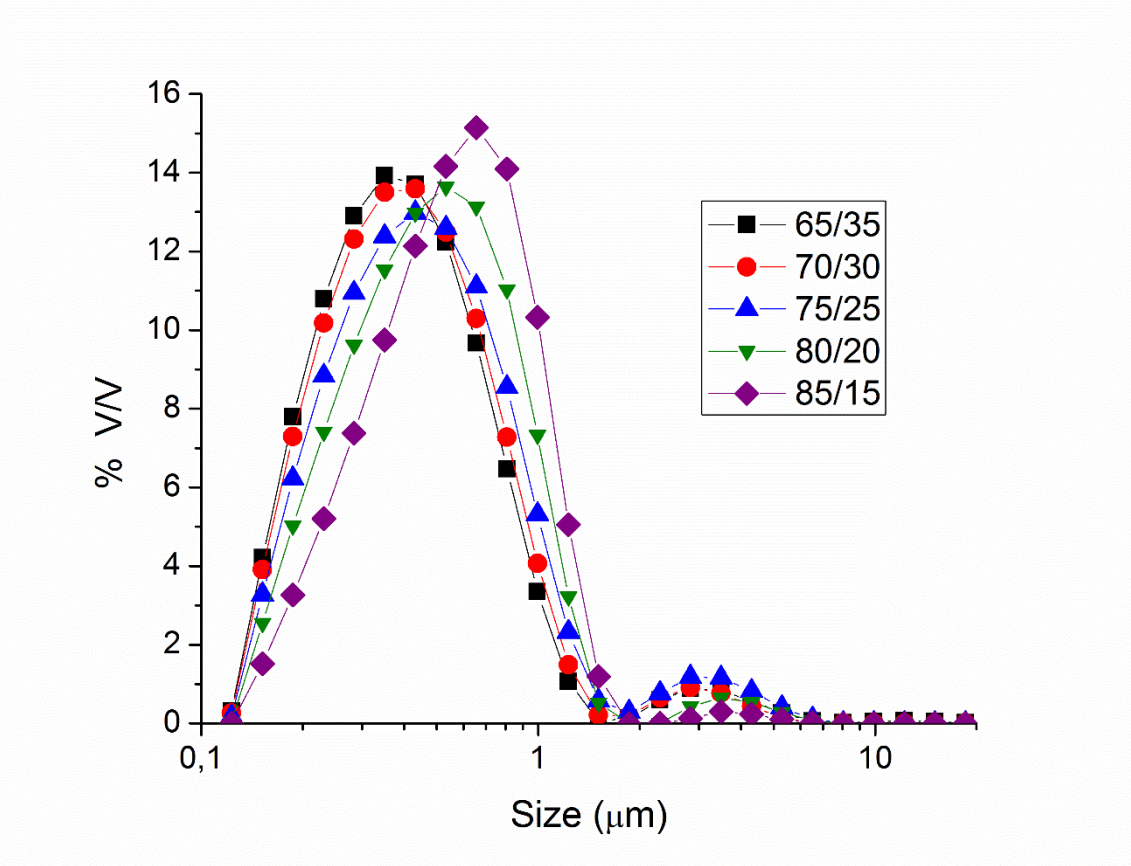

Figure 2.5. Droplet size distribution of 65/35, 70/30, 75/25, 80/20 and 85/15 emulsions. Aging time: 1 day. T=20ºC

All emulsions studied showed bimodal distributions with the majority of the population below one micron and a second peak at higher sizes as a consequence of the aforementioned recoalescence phenomenon induced by an excess of mechanical energy-input. Moreover, an increase of the AMD-10 content provoked the distributions to shift towards greater droplet sizes. Table 2.3 shows the values of the Sauter and volumetric mean diameters (D[3,2] and D[4,3]). Sauter mean diameter values ranged

from 0.31 μm to 0.42 μm and volumetric mean diameters varied between 0.48 μm and 0.57 μm.

Table 2.3. Sauter and volumetric mean diameters for 65/35, 70/30, 75/25, 80/20 and 85/15 emulsions.

Standard deviation of the mean (3 replicates) for D[3,2]<4%

Standard deviation of the mean (3 replicates) for D[4,3]<6%

Ratio of solvents	D[3,2] (μm)	D[4,3] (μm)
65/35	0.31	0.50
70/30	0.32	0.48
75/25	0.35	0.57
80/20	0.37	0.54
85/15	0.42	0.57

Figure 2.6 shows the flow properties for 1 day-aged emulsions studied as a function of the ratio of solvents. All the emulsions exhibited a trend to reach a Newtonian region at low-shear rate regime, which is defined by the zero-shear viscosity, (η_0). This range is followed by a slight decrease in viscosity (shear-thinning behaviour) above a critical shear rate. Fig. 6 also illustrates the fitting quality of the results obtained to the Cross model ($R^2 > 0.999$).

$$\eta = \frac{\eta_0}{1+\left(\frac{\dot{\gamma}}{\dot{\gamma}_C}\right)^{1-n}} \text{ (Eq 4)}$$

$\dot{\gamma}_c$ is related to the critical the shear rate for the onset of shear-thinning response, η_0 stands for the zero-shear viscosity and (1-n) is a parameter related to the slope of the power-law region; n being the so-called flow index. For shear thinning materials, 0 < n <1. A solid material would show n = 0, while a Newtonian liquid would show n = 1.

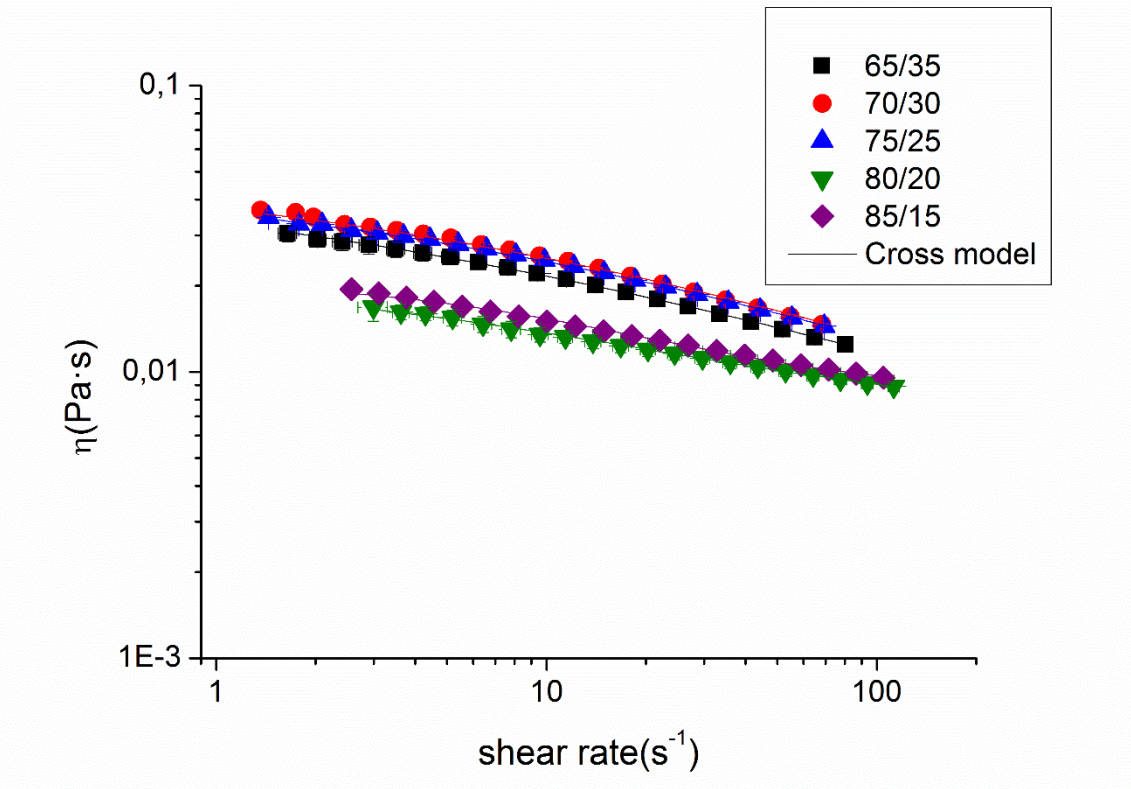

Figure 2.6. Flow curves for the studied emulsions as a function of ratio of solvents for 1 day aging time at 20ºC. Continuous lines illustrate data fitting to the Cross model.

Table 2.4. Flow curves fitting parameters for the Cross model for studied emulsions as a function of ratio of solvents at 1 day of aging time.

Standard deviation of the mean (3 replicates) for η_0<10%

Standard deviation of the mean (3 replicates) for $\dot{\gamma}_c$<10%

Standard deviation of the mean (3 replicates) for 1-n<10%

Ratio of solvents	η_0 (Pa·s)	$\dot{g}_c$ (s^{-1})	1-n
65/35	0.053	3.12	0.43
70/30	0.053	7.82	0.43
75/25	0.050	8.73	0.43
80/20	0.034	1.27	0.41
85/15	0.034	3.12	0.41

The values of these parameters are shown in Table 2.4 as a function of the ratio of solvents. Zero-shear viscosity of the three emulsions studied with higher limonene content showed no significant differences. However, two levels of zero-shear viscosity values were observed, 75/25 being the key ratio of solvents. In fact, a stepwise decrease in zero-shear viscosity with ratio of solvents was observed from 75/25 to 80/20 and 80/15 emulsions. This is consistent with the slightly higher Sauter diameters found for the high AMD-10 content emulsions. On the other hand, the higher zero-shear viscosities of emulsions with a solvent ratio lower than 75/25 may be attributed to the slightly lower Sauter diameters as well as to a flocculation process leading to the onset of some creaming for emulsions aged for 1 day. Greater tendency to flocculate has been previously associated to finer emulsions by Pal, and Barnes [24,25].

These authors attributed the trend to the flocculation to two different mechanisms: the occurrence of Brownian motion between droplets, and the fact that the droplets are subject to dominant Van der Waals attraction forces. This interpretation is strengthened by the fact that no significant differences of DSD obtained by laser diffraction were found. This may be explained by taking into account that weakly flocculated droplets are likely disrupted due to dilution and stirring during measurement carried out by laser diffraction [26].

Figure 2.7 shows the CLSM micrographs obtained for the 75/25 emulsion.

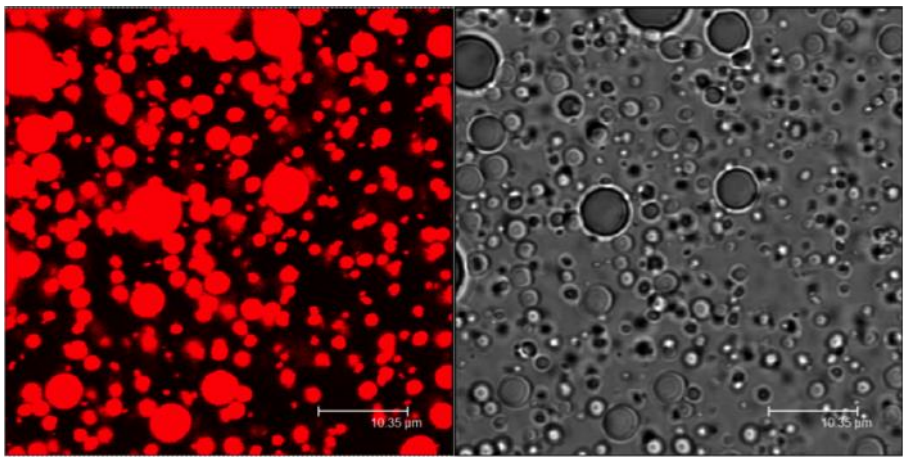

Figure 7.CLSM microphotographs for emulsion 75/25 at 1 day of aging time.

Droplet sizes observed are consistent with the results obtained by laser diffraction. Moreover, micrographs reveal the existence of flocs as commented in the previous section. It should be noted that all the droplets are stained with a fluorophore selective for AMD-10 solvent. This points out that the dispersed phase consisted of a mixture of both solvents. However, this does not exclude the fact that there may be a concentration gradient within the droplet, as previously explained.

Figure 2.8a shows the volumetric mean diameter as a function of both the ratio of solvents and aging time.

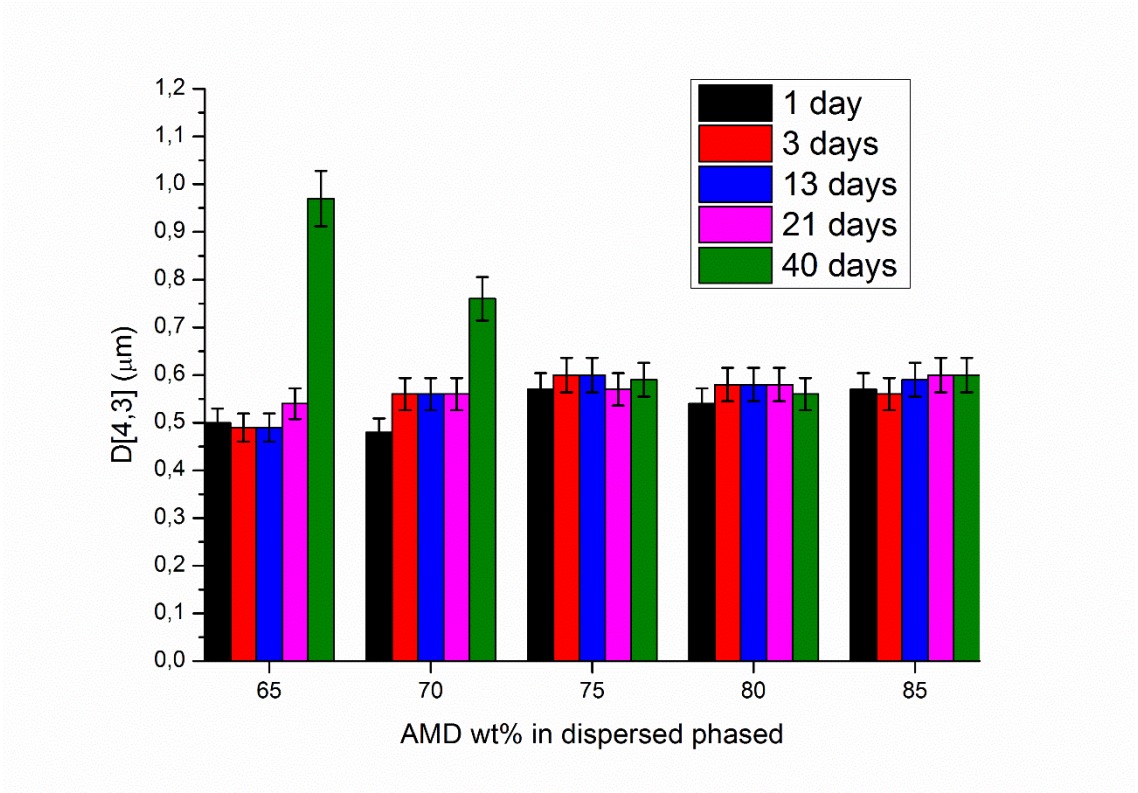

Figure 2.8a. Volumetric mean diameter as a function of aging time for the emulsions 65/35, 70/30, 75/25, 80/20 and 85/15.

Palazolo [26] previously stated that the volumetric mean diameter allows for detecting coalescence and the flocculation process with more sensitivity than the Sauter mean diameter. Thus, the 85/15, 80/20 and 75/25 emulsions did not show any significant changes of droplet sizes. By contrast, for emulsions containing less AMD-10, substantial changes of droplet size were observed, increasing by 94% for the 65/35 emulsion and by 58% for the 70/30 emulsion. This increase may indicate the existence of a destabilization phenomenon or coalescence by Ostwald ripening. The increase of volumetric mean diameter with time cannot be attributed to a flocculation process, since flocs are disrupted under the action of stirring and pumping during laser diffraction measurement.

Figure 2.8b shows the droplet size distributions for the 65/35 and 70/30 emulsions at 1 day and 40 days after preparation.

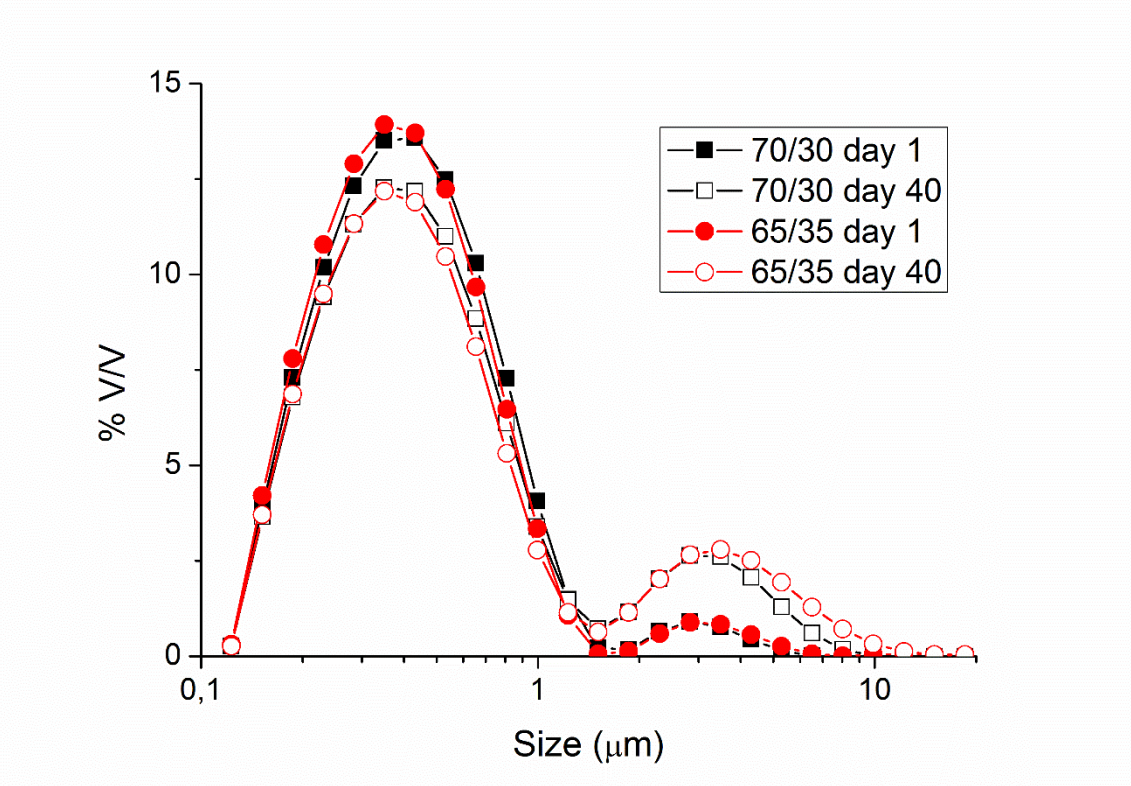

Figure 2.8b. Droplet size distributions for the emulsions 65/35 and 70/30 at 1 day and 40 days after preparation. Emulsions kept under storage at 20°C.

These distributions allow an increase of the second peak with ageing time to be detected, which resulted in a reduction of the population with smaller size. This usually points to the occurrence of a destabilization process by coalescence discarding an Ostwald ripening phenomenon, as the latter would lead to a shift of the DSD toward larger sizes without changing their shape. For Ostwald ripening the particle size distribution should attain a specific time-independent form that moves up the size axis with time, whereas with coalescence a bi-modal distribution is usually observed [17, 27].

Figures 2.9 a, b, c, d and e show the flow curves as a function of ageing time for all emulsions studied.

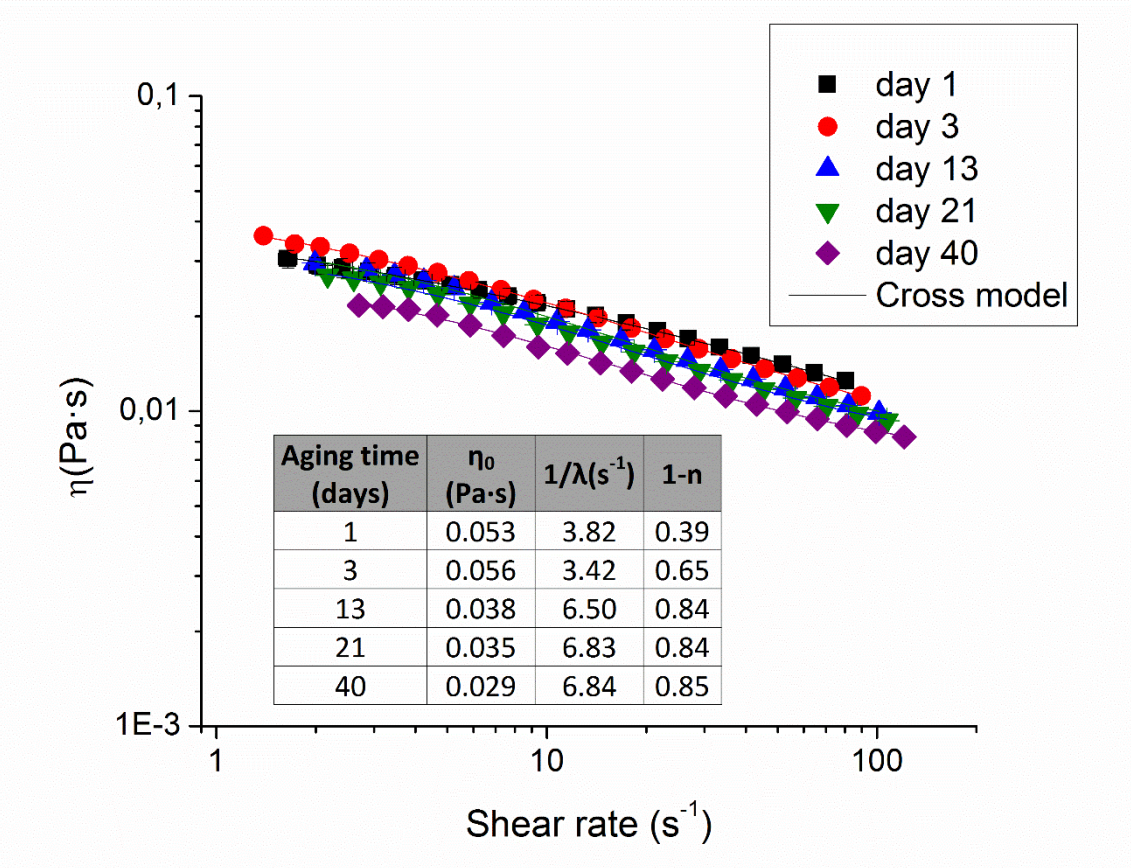

Aging time (days)	η_0 (Pa·s)	$1/\lambda(s^{-1})$	1-n
1	0.053	3.82	0.39
3	0.056	3.42	0.65
13	0.038	6.50	0.84
21	0.035	6.83	0.84
40	0.029	6.84	0.85

Figure 2.9.a. Flow curves as a function of aging time for 65/35 emulsion. Continuous line illustrate data fitting to the Cross model. Tables inset show the flow curve fitting parameters.

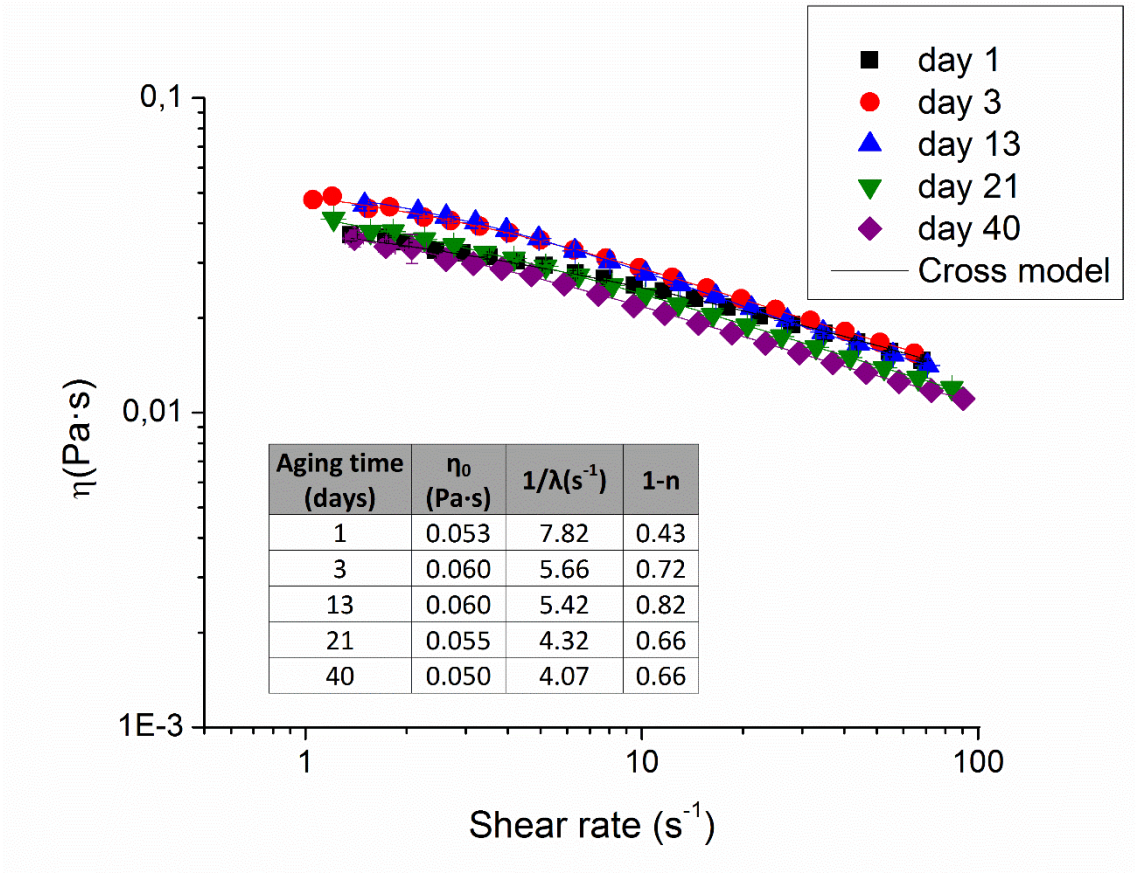

Aging time (days)	η_0 (Pa·s)	$1/\lambda(s^{-1})$	1-n
1	0.053	7.82	0.43
3	0.060	5.66	0.72
13	0.060	5.42	0.82
21	0.055	4.32	0.66
40	0.050	4.07	0.66

Figure 2.9.b.Flow curves as a function of aging time for 70/30 emulsion. Continuous line illustrate data fitting to the Cross model. Tables inset show the flow curve fitting parameters.

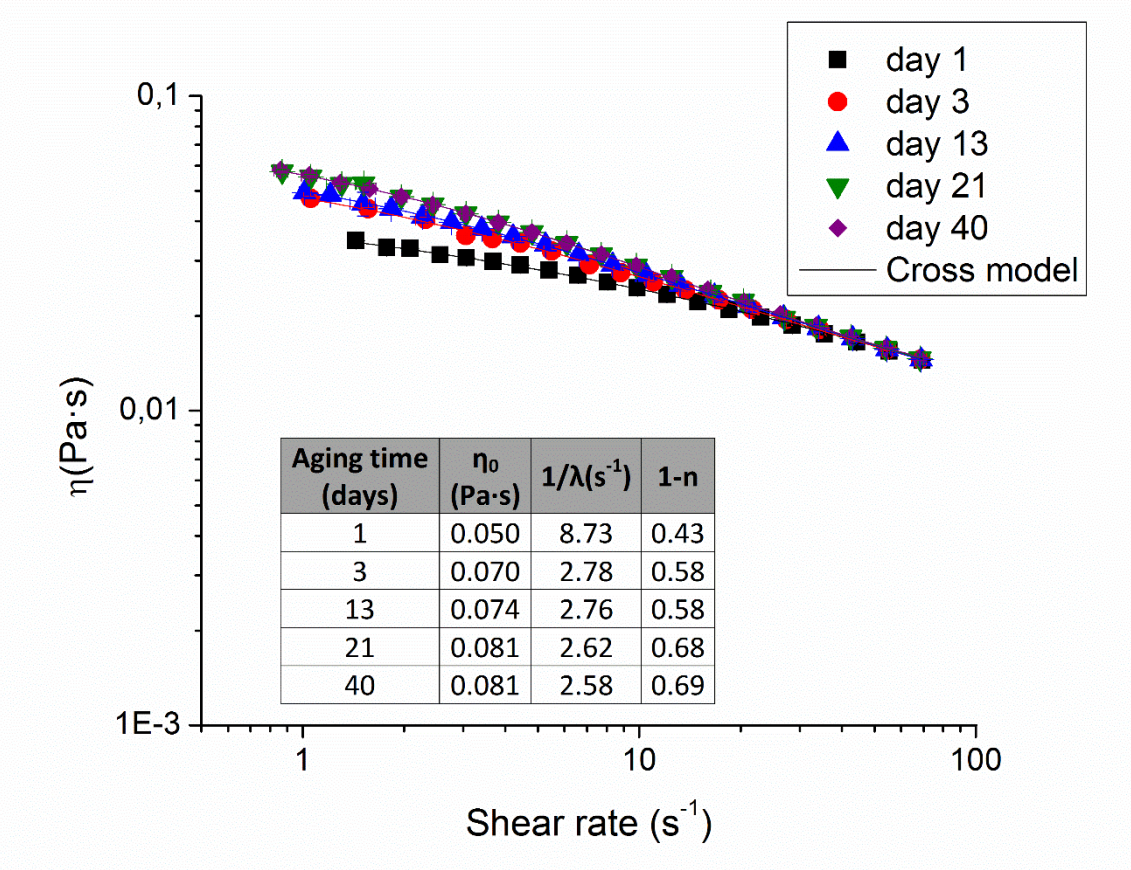

Aging time (days)	η_0 (Pa·s)	$1/\lambda(s^{-1})$	1-n
1	0.050	8.73	0.43
3	0.070	2.78	0.58
13	0.074	2.76	0.58
21	0.081	2.62	0.68
40	0.081	2.58	0.69

Figure 2.9.c. Flow curves as a function of aging time for 75/25 emulsion. Continuous line illustrate data fitting to the Cross model. Tables inset show the flow curve fitting parameters.

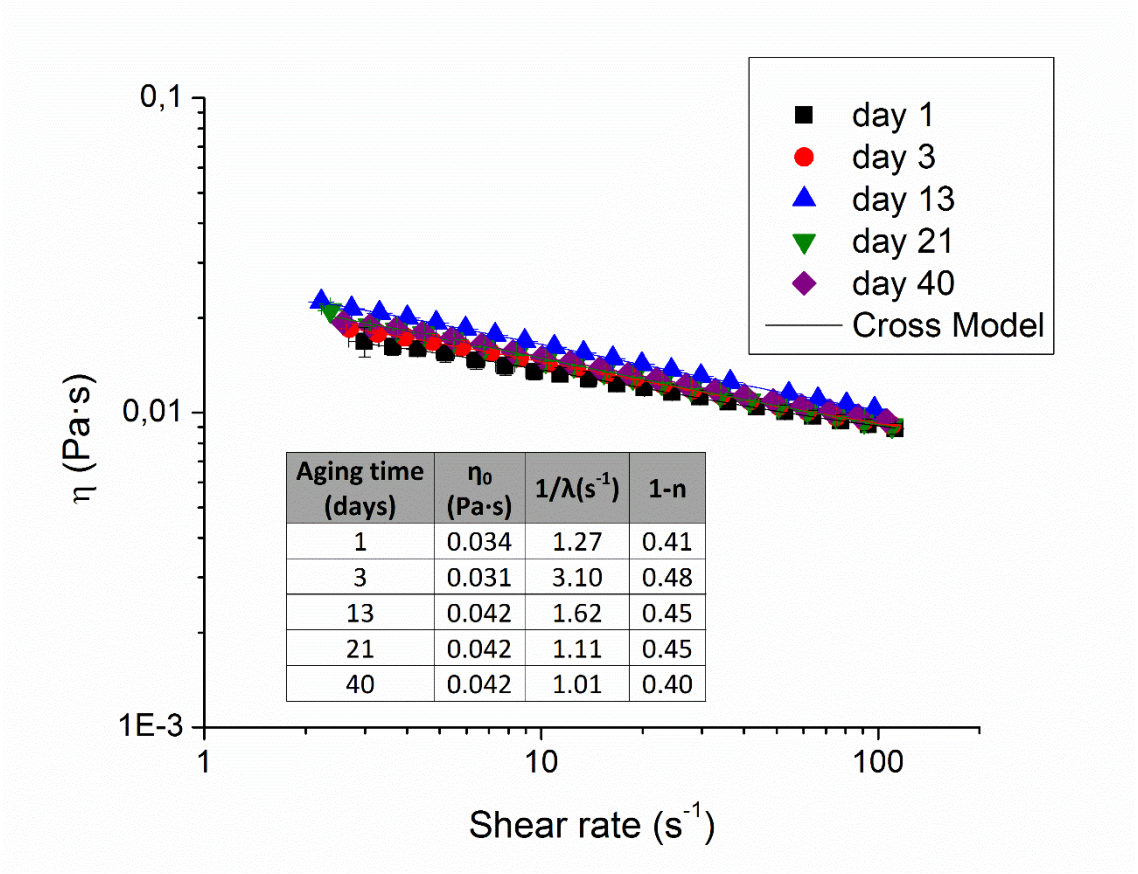

Aging time (days)	η_0 (Pa·s)	$1/\lambda(s^{-1})$	1-n
1	0.034	1.27	0.41
3	0.031	3.10	0.48
13	0.042	1.62	0.45
21	0.042	1.11	0.45
40	0.042	1.01	0.40

Figure 2.9.d. Flow curves as a function of aging time for 80/20 emulsion. Continuous line illustrate data fitting to the Cross model. Tables inset show the flow curve fitting parameters.

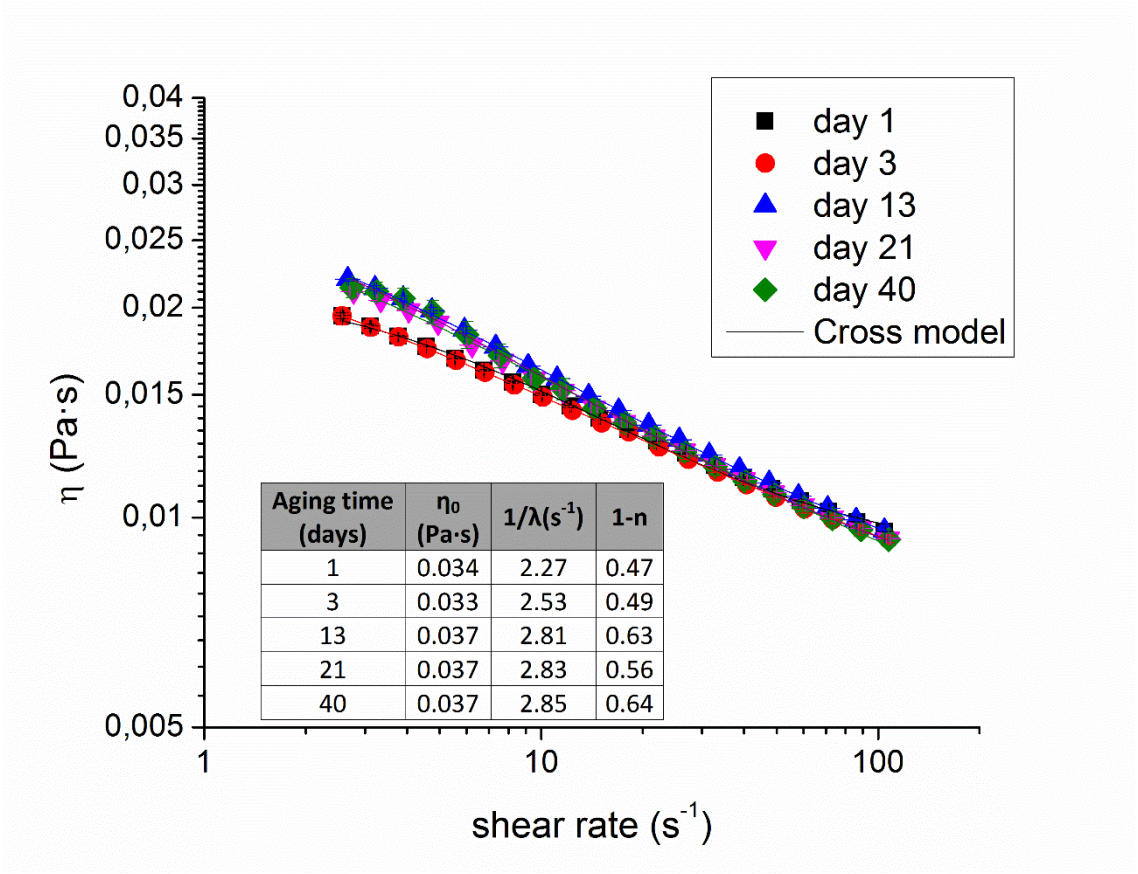

Figure 2.9.e. Flow curves as a function of aging time for 85/15 emulsion. Continuous line illustrate data fitting to the Cross model. Tables inset show the flow curve fitting parameters.

All emulsions exhibited a trend to reach a Newtonian region at low-shear rate regime, followed by a slight decrease in viscosity (shear-thinning behaviour) above a critical shear rate. This behaviour could be fairly well fitted to the Cross model with a R-square greater than 0.999. The fitting parameters are shown in the tables inset in the figures. The 65/35 emulsion showed a steady decrease in zero-shear viscosity with aging time, which is a clear indication of coalescence as confirmed by the significant increase of volumetric mean diameter from 21 ageing days on (figures 2.8a & 2.9a). The decrease of zero shear viscosity with time has been previously to an increase of average droplet size [23]. A slight increase of AMD-10/D-limonene ratio to 70/30 initially provoked an incipient creaming effect as demonstrated by the rise of both zero shear viscosity and

shear-thinning slope [28]. After that, coalescence became dominant as revealed by the steady drop of zero shear viscosity at longer ageing times (figure 2.9b).

An increase of zero shear viscosity was also detected for the 75/25, 80/20 and 85/15 emulsions as shown in figures 2.9c, 2.9d and 2.9e, respectively. The increase of zero shear viscosity with aging time indicates a higher concentration of the dispersed phase in the upper part of the sample. This involves a destabilization process by incipient creaming and/or flocculation.

Figure 2.10a shows the creaming index as a function of aging time at different ratios of solvents. It should be noted that the slope of the linear region, directly related to the 'creaming rate', was not significantly different for all studied systems (see the inset of figure 2.10a). However, important changes of the delay time were found, in such a way that the most D-limonene-concentrated emulsions showed the higher values of that parameter. This is totally consistent with the result obtained from the different rheological and laser diffraction measurements.

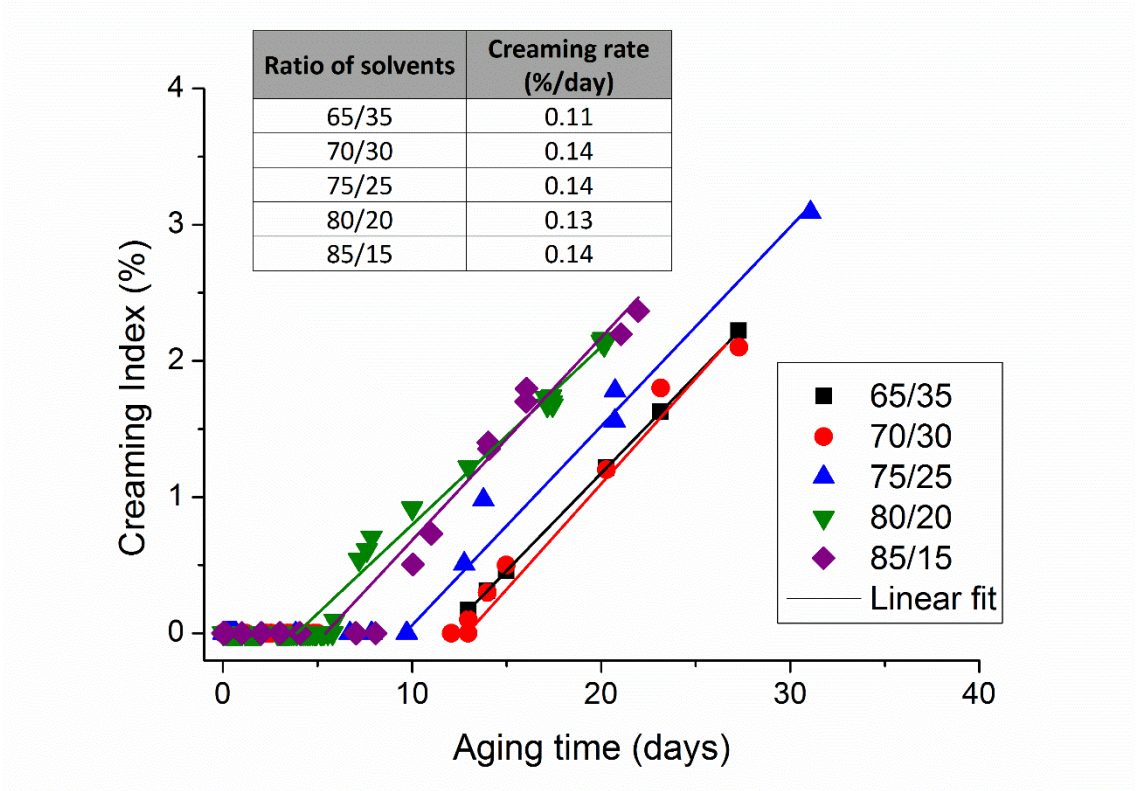

Figure 2.10a. Creaming Index as a function of aging time for studied emulsions.

Figure 10b shows the increase of droplet diameter from the diameter at time zero plotted as a function of ageing time for emulsions with the different ratios of solvents studied.

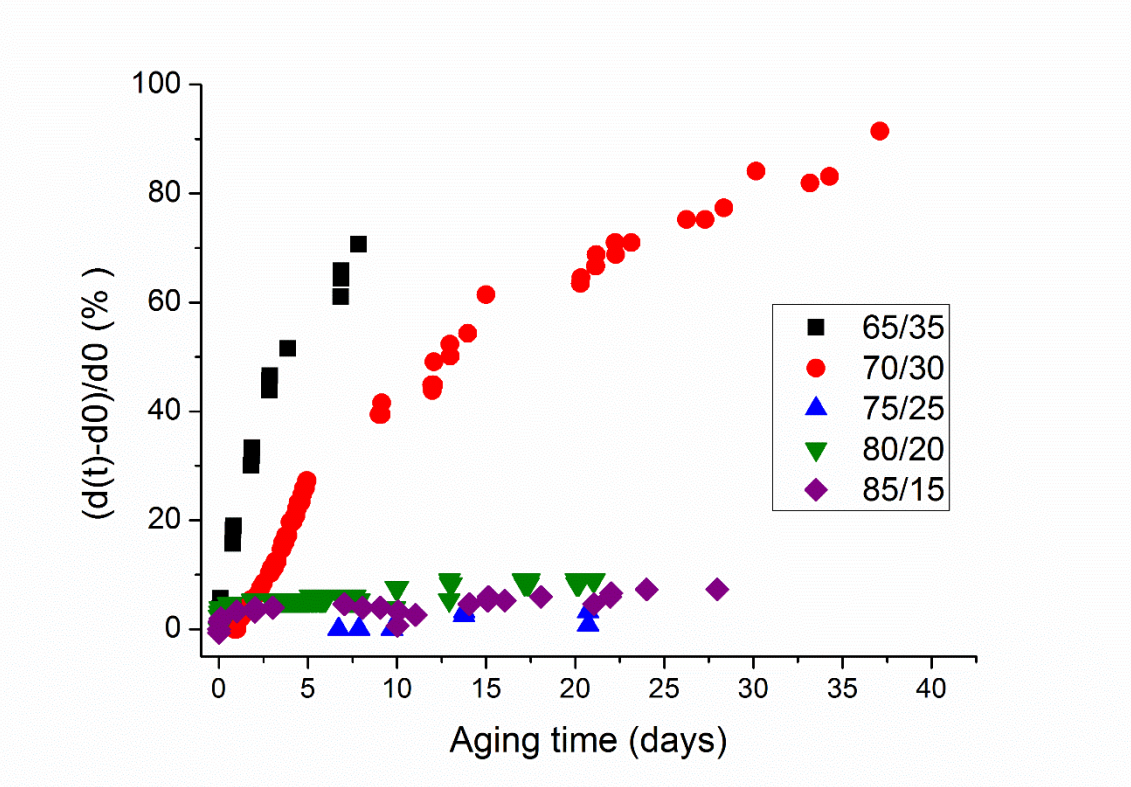

Figure 2.10b. Increase of droplet size diameter from the diameter at time zero as a function of aging time for studied emulsions.

No changes of droplet size emulsions associated with a coalescence phenomenon were detected for emulsions with less limonene content. By contrast, emulsions with higher limonene content exhibited significant changes of droplet size as a consequence of a destabilisation process by coalescence. These results are consistent with results obtained in flow curves and laser diffraction. In spite of that, MLS is not able to differentiate between both coalescence and flocculation phenomena. As a result, the results obtained from the rest of the experimental techniques used reveals that changes of backscattering in the intermediate zone of the vial are essentially due to a coalescence phenomenon. It should be noted that this phenomenon is more pronounced in the emulsion with higher limonene content. This may be related to the interfacial properties of limonene and its behaviour at the interface.

Conclusions

The exploring analysis initially carried out showed the dependence of homogenization rate and the ratio of solvents on DSDs and emulsion stability. The use of mixtures of green solvents led to obtain emulsions with submicron droplet mean diameter above 5000 rpm. In addition, the results of this preliminary study allowed an adequate homogenization rate to be fixed (6000 rpm) and laid the foundation for a further study of ratio of solvents. As a result of this study, an evolution of DSDs consistent with the occurrence of some coalescence was observed for emulsions with the higher content in D-limonene. However, emulsions containing high AMD-10/D-limonene ratio remained stable against coalescence. Coalescence information obtained by laser diffraction and multiple light scattering supported each other. In addition, the results provided by multiple light scattering revealed that 65/35 & 70/30 emulsions underwent not only coalescence but also creaming. Emulsion with 75/25 solvent ratio exhibited intermediate delay time for the onset of incipient creaming but it did not undergo coalescence. Rheology cleared up the destabilization mechanism for high-limonene content emulsions. First, creaming was dominant (increasing η_0) and later coalescence became predominant (decreasing η_0). From a methodological point of view, monitoring the cooperative information provided by rheology, laser diffraction, multiple light scattering and CSLM for a short aging time is a powerful tool to get a comprehensive panoramic view of the destabilization mechanism and kinetics of emulsions, especially when several mechanisms are simultaneously taking place.

References

1. Hill RL. Detergents in agrochemical and pesticide applications. In: Zoller U. Handbook of detergents Part E: Applications. Boca Raton: Taylor & Francis Group. 2009: 302-329.

2. Hofer R, Bigorra J. Green chemistry- a sustainable solution for industrial specialties applications. Green Chemistry. 2007, 9:203-212.

3. Bigorra J. Innovative solvents based on renewable raw materials. In: Proceedings of 40th Annual Meeting of CED. Barcelona, Spain. 2010.

4. Medvedovici A, Udrescu S, David V. Use of a green (bio) solvent – limonene – as extractant and immiscible diluent for large volume injection in the RPLC-tandem MS assay of statins and related metabolites in human plasma. Biomedical Chromatography. 2012; 27: 48-57.

5. Walter J. Metabolism of Terpenoids in Animal Models and Humans. In: Handbook of essential oils: Science, Technology and Applications. Boca Raton. CRC Press. 2010: 209-232.

6. Castán P, González X. Skin properties of glycerine polyethoxylene esters. Proceedings of 40th Annual Meeting of CED.2003; 33: 325-338.

7. Lutz, PJ. Ca. Patents Applications.CA 2537554 A1 20060822, 2006.

8. Denolle Y, Seita V, Delaire V. (2011). European Patents and Applications. EP 2368971 A1 20110928, 2011.

9. Tadros ThF. Rheology of Dispersions. Principles and Applications. Weinheim, Germany: Wiley-VCH, 2010.

10. Mengual O, Meunier G, Cayré I, Puech K, Snabre P. Turbiscan MA 2000 : multiple light scattering measurement for concentrated emulsion and suspensión instability analysis. Talanta. 1999; 50: 445-456.

11. Cussler EL, Moggridge GD. Chemical Product Design (2nd Edition). Cambridge University Press. 2011.

12. Brökel U. Meier W. Wagner G. Introduction. In: Brökel U. Meier W. Wagner G. Product Design and Engineering. Volume 1: Basics and Technologies. Weinheim: Wiley-VCH.2007:1-3.

13. Cuéllar I, Bullóna J, Forgarini A.M, Cárdenas A, Briceño M.I. More efficient preparation of parenteral emulsions or how to improve a pharmaceutical recipe by formulation engineering. Chemical Engineering Science. 2005; 60: 2127 – 2134.

14. Allende D, Cambiella A, Benito JM, Pazos C, Coca J. Destabilization-enhanced centrifugation of metalworking oil-in-water emulsions: Effect of demulsifying agents. Chemical Engineering & Technology. 2008; 31: 1007-1014.

15. Camino NA, Sanchez CC, Patino JMR, Pilosof AMR. Hydroxypropylmethylcellulose-beta-lactoglobulin mixtures at the oil-water interface. Bulk, interfacial and emulsification behavior as affected by pH. Food Hydrocolloids. 2012; 27: 464-474.

16. Santos J, Trujillo LA, Calero N, Alfaro MC, Muñoz J. Physical Characterization of a Commercial Suspoemulsion as a Reference for the Development of Suspoemulsions. Chemical Engineering and Technology. 2013; 11: 1-9.

17. McClements DJ. Critical review of techniques and methodologies for characterization of emulsion stability. Critical Reviews in Food Science and Nutrition. 2007; 47: 611-649.

18. Dickinson E. Hydrocolloids at interfaces and the influence on the properties of dispersed systems. Food Hydrocolloids. 2003; 17: 25-39.

19. Tadros ThF. Emulsion Science and Technology. Weinheim, Germany: Wiley-VCH, 2009.

20. Lee JM, Lim KH. Electroconductometric determination of completely engulfing Maxwell type three phase emulsions. Journal of Industrial and Engineering Chemistry. 2003; 9: 248-253.

21. Pal R. Rheology of particulate dispersions and composites. Boca Raton: CRC Press, 2007.

22. Jafari SM, He Y, Bhandari B. Re-coalescence of emulsion droplets during high-energy emulsification. Food Hydrocolloids. 2008; 22: 1191–1202

23. McClements DJ. Food Emulsions: Principles, Practice, and Techniques. Boca Raton: CRC Press, 2005.

24. Pal R. Effect of droplet size on the rheology of emulsions. AICHE Journal, 1996; 92: 3181-3190.

25. Barnes HA. Rheology of emulsions- a review. Colloid Surface A. 1994; 91 : 89-95.

26. Palazolo GG, Sorgentini DA, Wagner JR. Coalescence and flocculation in o/w emulsions of native and denatured whey soy proteins in comparison with soy protein isolates. Food Hydrocolloids. 2005; 19: 595-604.

27. Weers JG. Ostwald ripening in emulsions. In Binks (Ed.), Modern Aspects of Emulsions Science, Cambridge, UK. 1998: 292-327.

28. Calero N, Muñoz J, Cox P W, Heuer A, Guerrero A. Influence of chitosan concentration on the stability, microstructure and rheological properties of O/W

emulsions formulated with high-oleic sunflower oil and potato protein. Food Hydrocolloids. 2013; 30: 152-162.

Chapter 3: Influence of the concentration of a polyoxyethylene glycerol ester on the physical stability of submicron emulsions

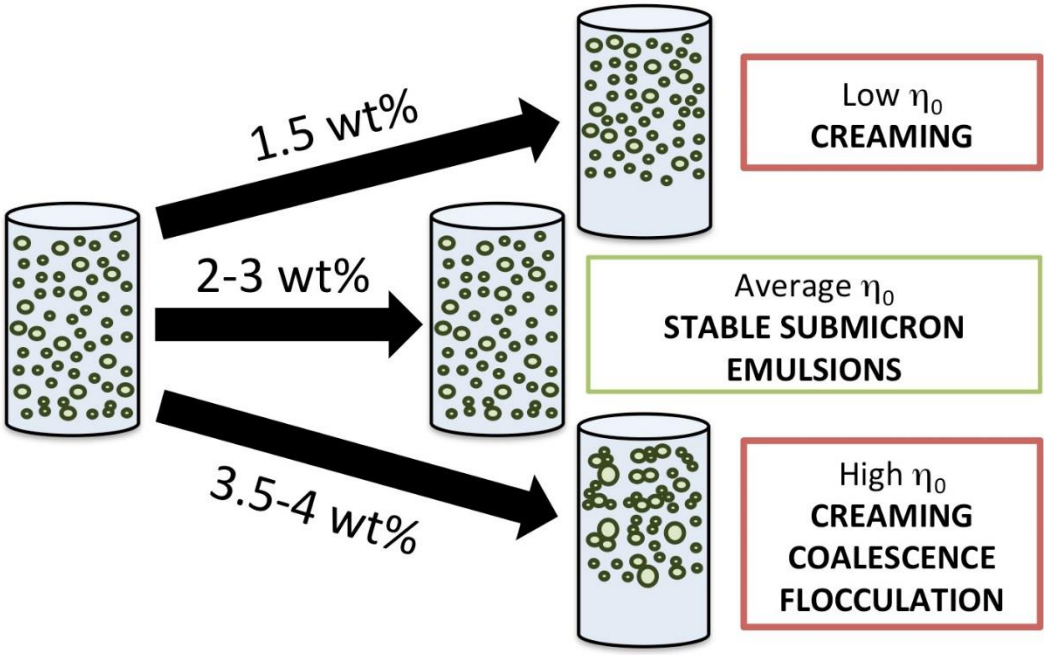

Abstract

The chemistry and technology of agrochemical products has undergone extensive changes over the last 20 years. The new formulations and ingredients should meet the needs of the agrochemical industry for products having greater safety to the user and much lower environmentally impact maintaining the same performance targets. A recent trend involves the use of the emulsion format for agrochemicals, which provides a more efficient performance than those conventionally used. Furthermore, the production of submicron stable emulsion is a key achievement especially for this product.

This study has been focused on the development of fine emulsions containing ecofriendly ingredients, such as surfactants and green solvents. It has been proven that the optimal surfactant concentration not only may lead to emulsions with submicron droplet sizes but also may prevent the typical destabilization process occurring in these formulations. In this particular case, it has been demonstrated that 3wt% surfactant concentration is adequate for three reasons: a) allowing the lowest droplet size to be achieved, b) providing the sufficient viscosity to prevent creaming and c) not being an excess of surfactant that leads to depletion flocculation.

3.1. Introduction

Emulsion science and technology has been used for many years to create a diverse range of commercial products, including pharmaceuticals, foods, agrochemicals, lubricants, personal care products, and cosmetics. Production of emulsion-based systems with specific physicochemical and functional properties often requires tight control over the

particle size distribution (McClements, 2005). Type and concentration of emulsifier play an important role in the droplet size distribution (DSD).

The interest in submicron emulsions has increased in recent years due to their very small droplet size and high stability and their applications in many industrial fields such as personal care and cosmetics, health care, pharmaceuticals, and agrochemicals. (Schultz et al, 2000; Sonneville et al, 2004; Leal-Calderon et al., 2007; McClements, 2005; Tadros, 2009). These emulsions whose range in the DSD falls typically of 100-500 nm are also sometimes referred to as ultrafine emulsions (Nakajima, 1997) ,mini-emulsions (El-Aasser et al, 2004) and nanoemulsions (Ying Tang et al, 2013). In addition, submicron emulsions can be prepared by reasonable surfactant concentrations (less than 10%), that may fulfil the requirements of a bio-based society (Brockel et al, 2007).

There is a need to replace the traditional organic solvents by more environmentally favorable solvents (Anastas and Warner, 1998.) Consequently, the renewed interest in search of appropriate greener and alternative solvents to be used in emulsions has grown enormously (Sheldon, 2005). Fatty acid dimethylamides (FAD) are among green solvents that can find applications in agrochemicals (Hofer and Bigorra, 2007). N,N-dimethyldecanamide (DMA-10) is considered a safe biosolvent, according to the Environmental Protection Agency. Therefore, it is a great solvent for agrochemical use due to the lack of risk to the farmer. The fact of satisfying the needs of customers is the basic principle of the product design (Brokel, 2007).

D-limonene, a naturally occurring hydrocarbon, is a cyclic monoterpene, which is commonly found in the rinds of citrus fruits such as grapefruit, lemon, lime, and in particular, oranges. D-limonene exhibits good biodegradability, hence it may be proposed as an interesting alternative to organic solvents (Walter, 2010 and

Medvedovici et al, 2012). These solvents can meet the ever-increasing safety and environmental demands of the 21st Century.

Environmentally friendly surfactants have attracted significant interest recently. Polyoxyethylene glycerol esters derived from cocoa oil are non-ionic surfactants obtained from a renewable source which fulfil the environmental and toxicological requirements to be used as ecofriendly foaming and/or emulsifying agents, hence their consideration as green surfactants (Castán and González, 2003). Their use in detergents and personal care products is disclosed in several patents (Lutz, 2006; Denolle,2011). Levenol C-201 was selected as emulsifier due to its great superficial and interfacial properties. Furthermore, α-pinene emulsions with Levenol C-201 showed better stability than emulsions containing its counterpart Levenol H&B (Trujillo-Cayado, 2014a, 2014b)

The main objective of this work was the study of the influence of the surfactant concentration (polyoxyethylene glycerol ester) on the physical stability of slightly concentrated O/W emulsions formulated with a mixture of green solvents (N,N-dimethyldecanamide and D-limonene). The optimum ratio of these solvents was previously studied by Santos et al, 2014. A further goal was to achieve stable fine emulsions which may be used as matrices for incorporation of active agrochemical ingredients. According to a recent study (Santos et al, 2014), the same strategy was followed considering the combination of different techniques, which was proven to be a powerful tool to provide very interesting information at an early stage about the mechanisms of destabilization occurring in emulsions.

3.2. Materials and methods

3.2.1. Materials

N,N Dimethyl Decanamide (Agnique AMD-10^{TM}) was kindly provided by BASF. D-Limonene was supplied by Sigma Chemical Company. The emulsifier used was a nonionic surfactant derived from cocoa oil. Namely, a polyoxyethylene glycerol fatty acid ester, Glycereth-17 Cocoate (HLB:13), received as a gift from KAO, was selected. Its trade name is Levenol C-201^{TM}. The safety data sheet provided by the supplier reports a value for oral toxicity (LD50) higher than 5000 mg/kg of animal in tests carried out with rats. It is interestingly to note that this value would be 3000 mg/kg for salt (Hollinger, 2005).

RD antifoam emulsion (DOW CORNING®) was used as antifoaming agent. This commercial product consists of an aqueous solution containing Polydimethyl siloxane (<10 %w/w) and Dimethyl siloxane, hydroxyl-terminated (<10 %w/w). Deionized water was used for the preparation of all emulsions.

3.2.2. Submicron emulsion development.

Emulsions containing 0.1 wt% antifoam emulsion, a variable surfactant concentration and 30 wt% mixture of solvents (75wt% AMD-10/25wt% D-Limonene) were prepared. The optimum ratio of solvents was previously studied by Santos, 2014. The surfactant concentrations studied were 1.5, 2, 2.5, 3, 3.5 and 4wt%. These O/W emulsions were carried out using a rotor-stator homogenizer (Silverson L5M), equipped with a mesh screen at 6000 rpm during 60 seconds.

3.2.3. Droplet size distribution measurements.

Size distribution of oil droplets was determined by laser diffraction using Mastersizer X (Malvern, Worcestershire, United Kingdom). All measurements were repeated 3 times

with each emulsion. These measurements were carried out after 1, 3, 13, 21, 40 days aging time to analyze likely coalescence effects.

The mean droplet diameter was expressed as Sauter diameter (D[3,2]) and volume mean diameter (D[4,3]).

$$D[M,N] = \left[\frac{\int D^M n(D)dD}{\int D^N n(D)dD}\right]^{\frac{1}{M-N}} \text{ (Eq 1)}$$

3.2.4. Rheological measurements.

Rheological experiments were conducted with a Haake MARS controlled-stress rheometer (Thermo-Scientific, Germany), equipped with a sand-blasted coaxial cylinder Z-20 (sample volume: 8.2 mL, Re/Ri =1.085, Ri= 1 cm) to avoid slip effects. Flow curves were carried out from 0.05 Pa to 1 Pa at 20°C. Flow curves were carried out after 1, 3, 13, 21 and 40 days to check the effect of aging time. All measurements were repeated 3 times with each emulsion. Samples were taken at about 2 cm from the upper part of the container. Sampling from the top part of the container in contact with air was avoided.

3.2.5. Multiple light scattering

Multiple light scattering measurements with a Turbiscan Lab Expert were used in order to study the destabilization of the emulsions. Measurements were carried out until 40 days at 20°C to determine the predominant mechanism of destabilization in each emulsion as well as the kinetics of the destabilization process. Multiple light scattering is a sensitive and non-intrusive technique to monitor physical stability of emulsions

(Allende et al, 2008 and Camino et al, 2012) and more complex systems such as suspoemulsions (Santos et al, 2013).

Multiple light scattering measurements in the middle zone of the measuring cell also allowed the evolution of a mean droplet diameter with aging to be monitored.

3.2.6 Viscosity of the continuous phase.

The viscosity of continuous phases solutions (from 2.14 wt% to 5.71 wt%) were measured with an Ubbelohde glass capillary viscometer. A volume of solution was pipetted into the capillary viscometer, which was equilibrated at 20°C in a water bath for 30 minutes prior to measurements. All the measurements were performed at 20^{o}C ± 0.1^{o}C and the result is the average of five measurements. Viscosity is obtained from the following equation:

$$h = C \times r \times t \quad \text{(Eq 2)}$$

where η is the viscosity of the continuous phase, *C* is a constant that depends of the glass capillary, ρ is the density of the continuous phase and t is the time.

3.3. Results and discussion

Figure 3.1 shows the droplet size distribution of the emulsions with different concentration of surfactant. All emulsions studied showed two populations of droplets except for emulsion with 1.5 % surfactant. The first peak is below 1 micron and the second population is centred about three microns. This second peak is probably due to recoalescence phenomenon induced by an excess of mechanical energy-input. (Jafari et al, 2008; Santos et al, 2014)

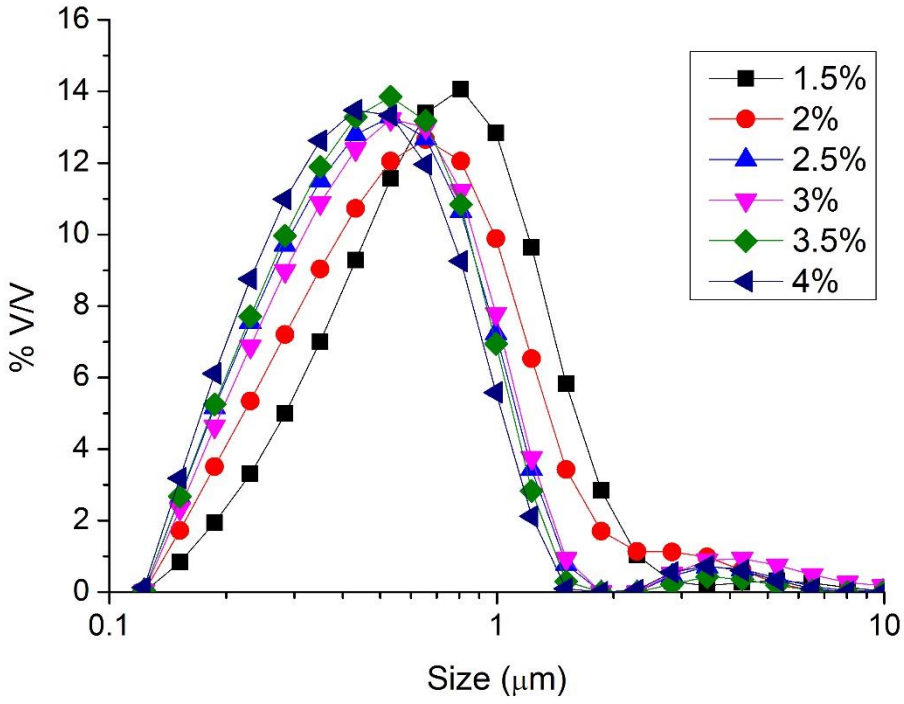

Figure 3.1. Droplet size distribution for emulsions containing 1.5, 2, 2.5, 3, 3.5 and 4 wt% of surfactant.

A decrease of the surfactant content provoked the distributions to shift towards greater droplet sizes. This fact is more pronounced for the emulsion containing 1.5wt% of surfactant. In the range 1.5-2.0 wt%, the surfactant available was not enough to achieve the minimum droplet size that can be obtained by these operating conditions.

Sauter and volumetric diameters for all emulsions are shown in table 3.1. All emulsions possess submicron mean diameters. It could be due to the low interfacial tension providing by the mixture of these solvents as reported by Santos et al, 2014. The Sauter and volumetric mean diameters levelled off for surfactant concentrations above 2.5 wt%.

Table 3.1. Sauter and volumetric diameters for the studied emulsions as a function of surfactant concentration for 1 day aging time.

wt% Surfactant	**$D_{3.2}$ (μm)**	**$D_{4.3}$ (μm)**
1.5	0.51	0.75
2	0.39	0.58

2.5	0.37	0.57
3	0.35	0.57
3.5	0.36	0.56
4	0.36	0.57

Figure 3.2 shows the flow properties for 1 day-aged emulsions studied as a function of surfactant concentration. All the emulsions exhibited a trend to reach a Newtonian region at low-shear rate regime, which is defined by the zero-shear viscosity, (η_0). This range is followed by a slight decrease in viscosity (shear-thinning behaviour) above a critical shear rate. Fig. 2 also illustrates the fitting quality of the results obtained to the Cross model ($R^2 > 0.999$).

$$\eta = \frac{\eta_0}{1+\left(\frac{\dot{\gamma}}{\dot{\gamma}_c}\right)^{1-n}} \text{ (Eq 3)}$$

$\dot{\gamma}_c$ is related to the critical shear rate for the onset of shear-thinning response, η_0 stands for the zero-shear viscosity and (1-n) is a parameter related to the slope of the power-law region; n being the so-called flow index. For shear thinning materials, $0 < n < 1$. A solid material would show n = 0, while a Newtonian liquid would show n = 1.

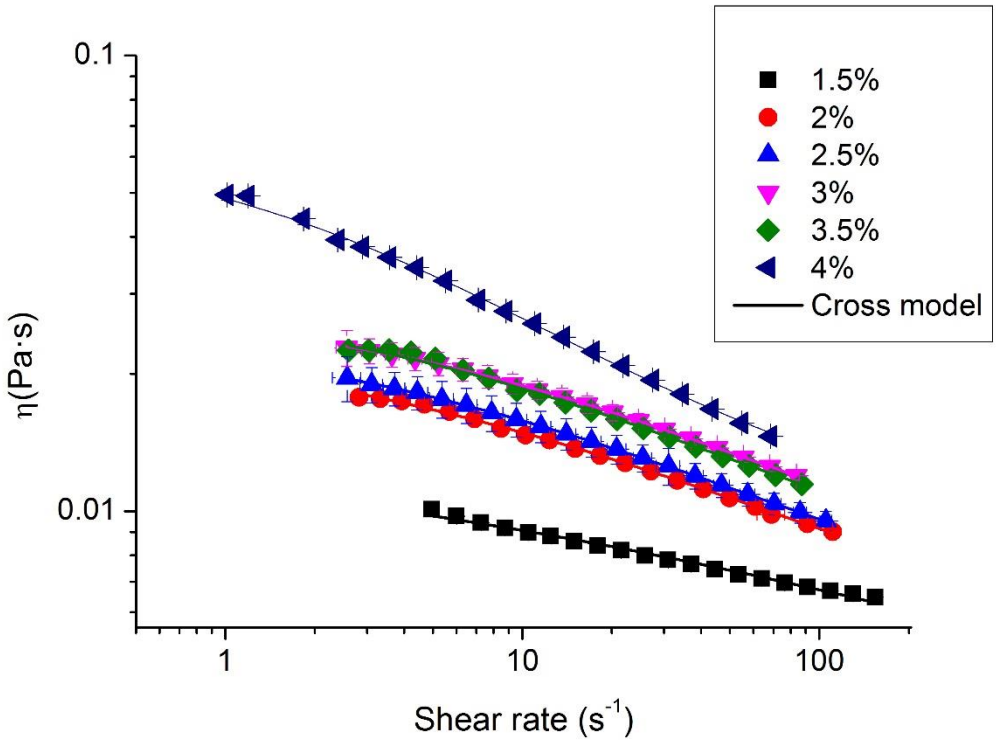

Figure 3.2. Flow curves for the studied emulsions as a function of surfactant concentration for 1 day aging time at 20°C. Continuous lines illustrate data fitting to the Cross model.

The values of these parameters are shown in Table 3.2 as a function of the concentration of surfactant. The emulsion at a low surfactant concentration of 1.5 wt% showed the lowest Zero-shear viscosity. It is related to the fact that this emulsion showed the higher Sauter diameter. Zero-shear viscosity for the emulsions containing from 2%wt to 3.5%wt showed no significant differences, even though a slight tendency to increase with surfactant concentration may be observed. This is supported by the fact that these emulsions showed similar Sauter diameter values.

Table 3.2. Flow curves fitting parameters for the Cross model for studied emulsions as a function of surfactant concentration at 1 day of aging time.

Standard deviation of the mean (3 replicates) for η_0<8%

Standard deviation of the mean (3 replicates) for $\dot{g}_c$<10%

Standard deviation of the mean (3 replicates) for 1-n<10%

wt% Surfactant	η_0 (mPa·s)	$\dot{\gamma}_c$ (s^{-1})	n
1.5	15	25	0.70
2	24	12.5	0.57
2.5	26	12.5	0.57
3	29	16.7	0.40
3.5	30	12.5	0.40
4	66	3.12	0.30

A sudden increase in the zero-shear viscosity of the emulsion upon increasing the surfactant concentration from 3.5 wt% to 4 wt% was observed. Given that DSD did not change between 3.5 wt% and 4 wt% surfactant, this rheological change could be produced by either, an enhanced viscosity of the continuous phase (due to increasing interactions among micelles), or the occurrence of a stronger oil network due to depletion flocculation (Palazolo et al, 2005; Manoj et al, 1998).

Table 3.3 shows the viscosity of the continuous phase prior emulsification. It is seen that increasing surfactant concentration from 5 wt% to 5.71 wt% provokes viscosity to increase from 12.89 to 17.93 mPa·s. Nonetheless, the increase in the viscosity of emulsions from 3.5wt% surfactant concentration to 4 wt% is about 120%. Hence, the marked increase of the viscosity of the emulsions is more influenced by a depletion flocculation phenomenon than to the viscosity of the continuous phase.

Table 3.3. Continuous phase density and viscosity values at 20^{o}C.

Note: These surfactant concentrations in the continuous phase are 1.5, 2, 2.5, 3, 3.5 and 4wt% in emulsions.

Levenol C-201 concentration in continuos phase (wt%)	ρ_{20^oC} (kg/m^3)	η_{20^oC} (mPa·s)
2.14	1.0013 ± 0.0001	2.03 ± <0.01
2.86	1.0017 ± 0.0001	2.84 ± 0.01
3.57	1.0022 ± 0.0001	4.04 ± 0.02
4.29	1.0027 ± 0.0001	5.58 ± 0.05
5.00	1.0031 ± 0.0001	12.89 ± 0.02
5.71	1.0036 ± 0.0001	17.93 ± 0.08

Therefore, it indicates that the critical surfactant concentration at which depletion flocculation of droplets occurs lies somewhere between 3.5 and 4wt%. Nowadays it is well established that in presence of high concentration of surfactant or polymer, the micelles can play an important role in the stability of the emulsions (Dickinson et al, 1997). After interface saturation by the adsorbed surfactant, micelles do not adsorb on the surfactant coated surface, and they can cause attraction between drops by a depletion mechanism. Thus, when two droplets approach in a solution of non-adsorbing micelles, the latter are expelled from the gap, generating a local region with almost pure solvent. The osmotic pressure in the liquid surrounding the particle pair exceeds that between the drops and consequently forces the droplets to aggregate. (Napper, 1983). The depletion flocculation could lead to a creaming and/or coalescence process.

This tendency is also showed in the critical shear rate. Nevertheless, the flow index decreases with the concentration of surfactant. This is due to the increase of the shear thinning character of emulsions. The emulsion with lowest surfactant concentration is only slightly shear thinning, whereas emulsions with higher surfactant concentrations are more shear thinning in nature.

Figure 3.3a and b show the results of the physical stability study performed at room temperature by a multiple light scattering technique. Figure 3.3a shows a plot of

backscattering versus container height of the sample at room temperature for 1.5wt% emulsion by way of example. This figure also includes an inset where backscattering is plotted versus container height in reference mode (enlargement of backscattering of the lower zone of the vial that contained the sample) to display higher resolution of backscattering changes. 2, 2.5, 3 and 3.5% emulsions showed the same behaviour.

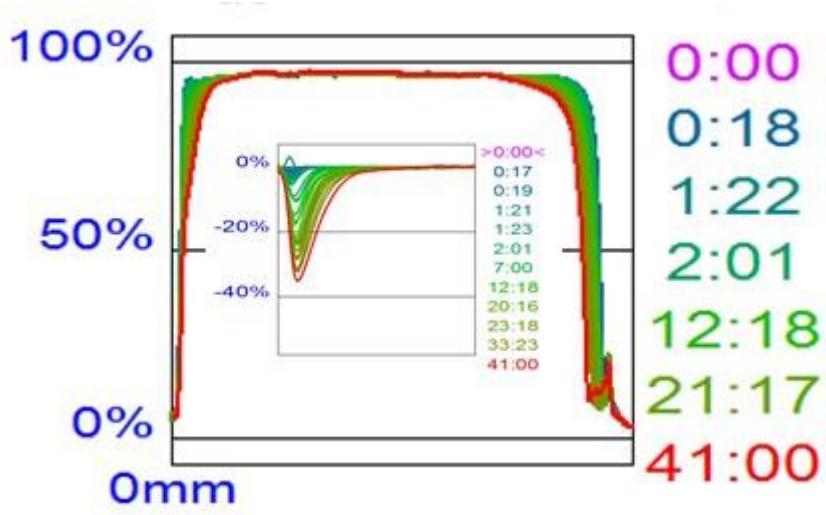

Figure 3.3a. Backscattering versus measuring cell height as a function of aging time in normal (main figures) and reference mode (insets) for 1.5wt% emulsion at 25°C. Note: the insets illustrate DBS values at the bottom of the measuring cell.

A backscattering decrease in the lower and higher zones of the vial was observed whereas it remained nearly constant in the intermediate zone. The drop in backscattering observed at the bottom of the measuring cell clearly indicated the occurrence of a destabilization mechanism by creaming, in that the dispersed phase possessed a lower density than the continuous phase (McClements, 2005). Thus all emulsions presented creaming process but in different degree.

The fact that the backscattering remained nearly constant in the intermediate zone suggests that destabilization mechanisms such as flocculation and coalescence were not

much significant for these emulsions. Nevertheless, with regards to the backscattering decrease observed at the top of the measuring cell, we think it may be attributed to the occurrence of some coalescence as a consequence of the migration of small droplets to the top (Mengual et al, 1999).

Figure 3.3b shows backscattering (BS) as a function of the measuring cell height of the 4wt% emulsion. Their reference mode plot was also included. On the contrary to the other emulsions, the backscattering increases with aging time in the middle zone of the vial. This fact suggest that a significant flocculation and/or coalescence process is taking place. In addition, a decrease in BS in the low zone of the vial is also observed. However, this decrease is cover up later by the increase of BS in the whole measuring cell (see figure 3.3b). This fact could be due to the coalescence and/or flocculation is more accused than the creaming.

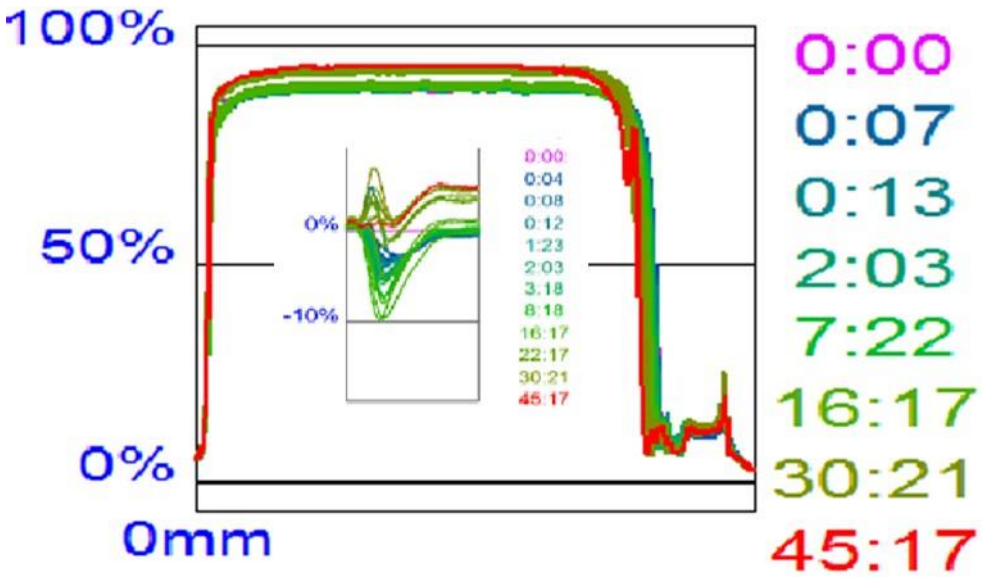

Figure 3.3b. Backscattering versus measuring cell height as a function of aging time in normal (main figures) and reference mode (insets) for 4wt% emulsion at 25^{o}C. Note: the insets illustrate DBS values at the bottom of the measuring cell.

Figure 3.4a shows the variation of BS in the low zone of the measuring cell as a function of aging time, which is related to the creaming process. The results for 4wt% emulsion were only shown until day 14 because later creaming is covered up by flocculation and coalescence (see inset fig 3.3b).

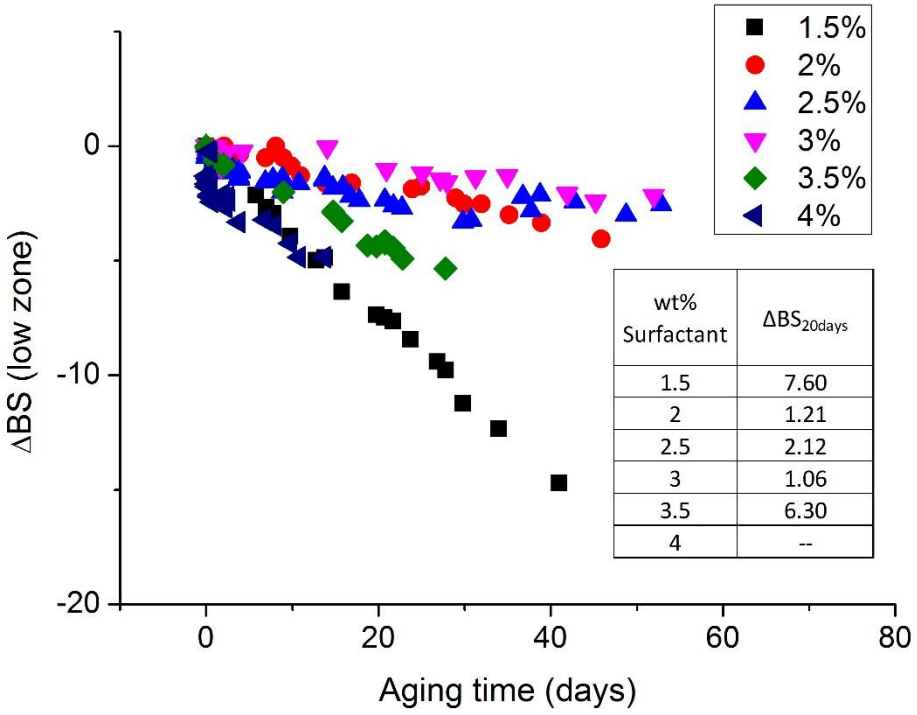

Figure 3.4a. Variation of the BS in the low zone of the measuring cell as a function of aging time for studied emulsions at 25°C.

2, 2.5 and 3wt% emulsions underwent slight changes of BS in the low zone of the measuring cell while 1.5wt% and 4wt% emulsion showed the greatest increase of BS. Emulsion containing lowest concentration of surfactant showed a higher trend to creaming as a consequence of the Stokes law since its continuous phase possesses the lowest viscosity. In addition 1.5wt% showed the highest Sauter diameter, therefore it led to accelerate the creaming process. As previously mentioned, emulsion 4% underwent depletion flocculation as destabilisation mechanism. These flocs may also accelerate the creaming process, which provokes higher changes of BS in the lower zone of measuring cell.

Figure 3.4b shows the increase of droplet diameter from the diameter at time zero in the middle part of the measuring cell plotted as a function of aging time for emulsions with different surfactant concentration. No changes of droplet size emulsions associated with a coalescence/flocculation phenomenon were detected for emulsions with containing less than 3.5wt% of surfactant. By contrast, the emulsion with higher surfactant content exhibited significant changes of droplet size as a consequence of a destabilisation process by coalescence/flocculation.

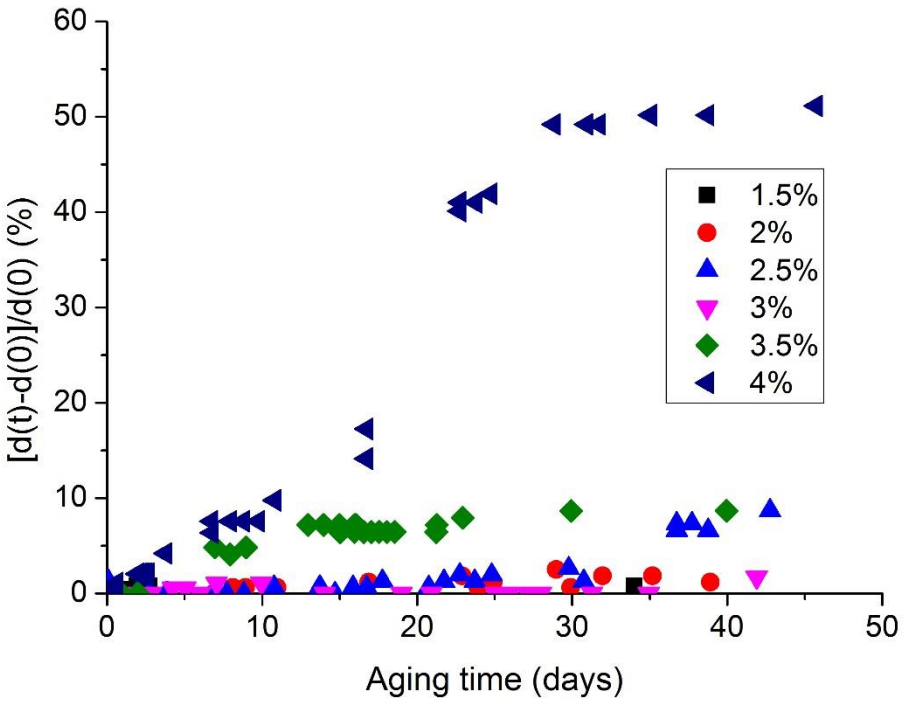

Figure 3.4b. Increase of droplet size diameter from the diameter at time zero as a function of aging time for studied emulsions.

Emulsions with higher surfactant concentration underwent a destabilisation process by coalescence/flocculation and by creaming. By contrast, an incipient creaming process was detected for the emulsions with surfactant concentration between 2 and 3wt%. The

emulsion with 3wt% of surfactant exhibited the lowest increment of BS at 20 days of aging time (see table inset figure 3.4a).

Figure 3.5a shows the volumetric mean diameter as a function of both surfactant concentration and aging time. Palazolo (2005) previously postulated that the volumetric mean diameter allows for detecting coalescence process with more sensitivity than the Sauter mean diameter. Thus, the emulsions containing 2, 2.5 and 3%wt of surfactant did not show any significant changes of droplet sizes. By contrast, some changes of droplet size were observed for emulsions containing more than 3wt% or less than 2wt%. A slightly change was detected for both 1.5 and 3.5 emulsions while a substantial change was found for the 4wt% emulsion. This increase may indicate the occurrence of a destabilization phenomenon by coalescence or Ostwald ripening.

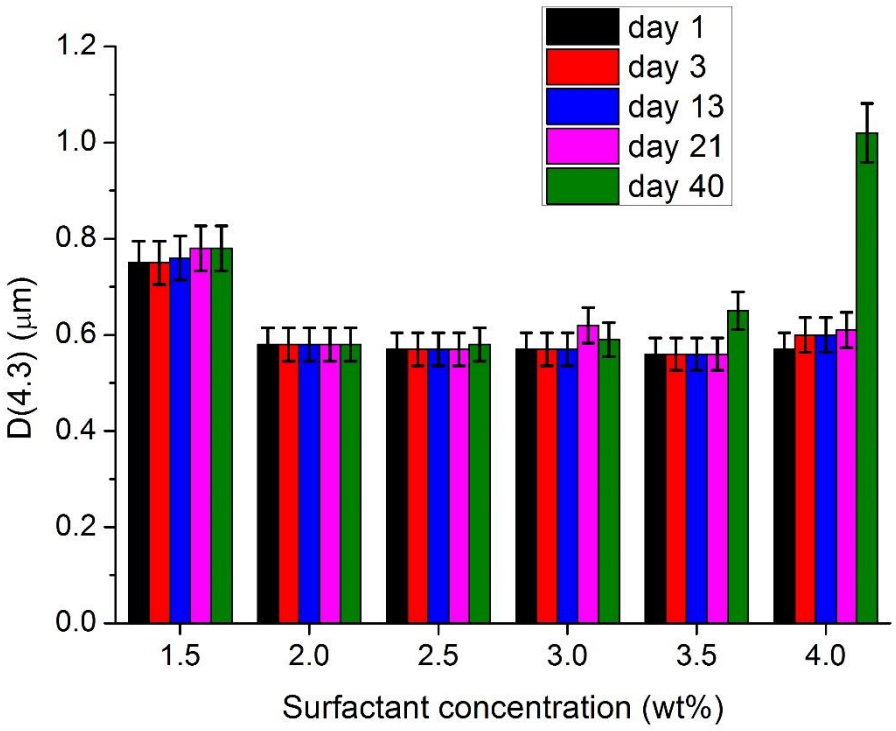

Figure 3.5a. Volumetric mean diameter as a function of aging time for the emulsions 1.5, 2, 2.5,3, 3.5 and 4wt%.

In the case of 1.5wt% the increase of droplet size could be due to a destabilisation phenomenon by coalescence. Coalescence becomes more important when drops are not fully covered with surfactant, as manifested by an increase of mean droplet size with time. (Nazarzadeh et al, 2013). This increasing could lead to a oiling off process which was observed by MLS.

In addition, the increase of the droplet size in 3.5wt% emulsion could be attributed to a coalescence mechanism induced by a flocculation and/or creaming process previously mentioned since coalescence tends to occur after the droplets have been in contact for extended periods such as in a cream layer or in a floc (McClements, 2007).

Moreover, emulsion with 4% showed the highest change of droplet size, which could be due to the destabilisation process by flocculation from the moment of its preparation.

Figure 5.5b shows the droplet size distributions for the 4wt% emulsion at different aging time by way of example. The emulsions which showed increased of the size of droplets followed the same trend: an increase of the second peak with aging time was detected, which resulted in a reduction of the population with smaller size. This usually points to the occurrence of a destabilization process by coalescence discarding an Ostwald ripening phenomenon, as the latter would lead to a shift of the DSD toward larger sizes without changing their shape (Santos et al, 2014). For Ostwald ripening the particle size distribution should attain a specific time-independent form that moves up the size axis with time, whereas with coalescence a bi-modal distribution is usually observed (McClements, 2007; Weers, 1998)

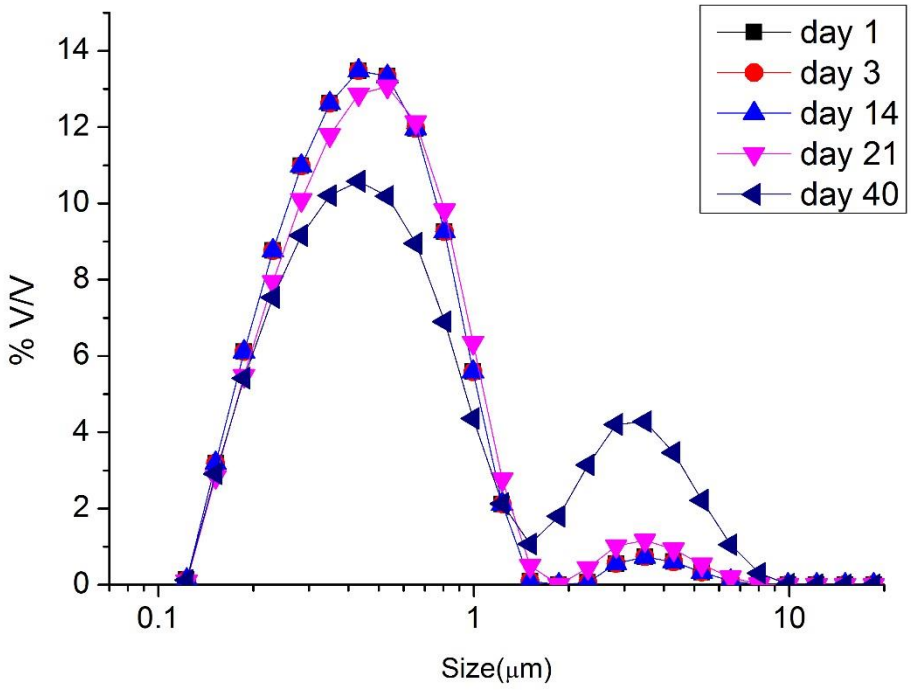

Figure 3.5b. Droplet size distributions for the emulsions containing 4wt% of surfactant as a function of aging time. Emulsions kept under storage at 20°C.

Figure 3.6 shows the zero shear viscosity at different aging times for all emulsions. As all emulsions exhibited a trend to reach a Newtonian region at low-shear rate regime, followed by a slight decrease in viscosity (shear-thinning behaviour) above a critical shear rate, it has fairly well fitted to the Cross model with a R-square greater than 0.999. The showed zero shear viscosity is a fitting parameter of this model.

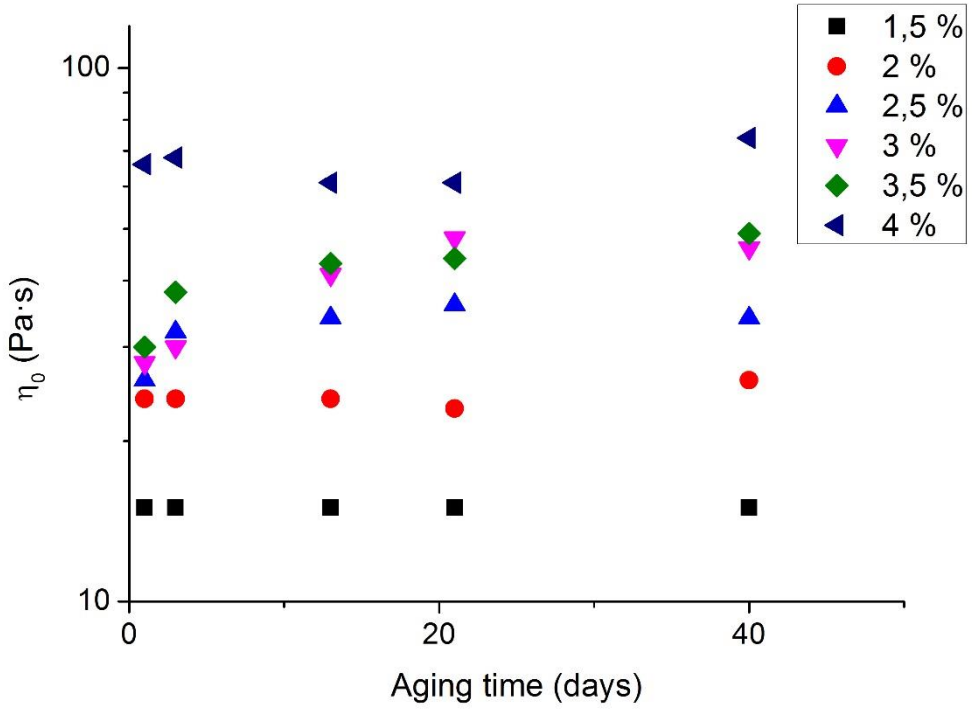

Figure 3.6. Zero-shear viscosity as a function of aging time for the studied emulsions. Note: Standard deviation of the mean (3 replicates) for η_0<8%.

Emulsion 1.5wt% did not show any significant changes, which may be due to a lack of sensibility of the measurements since the value of the zero shear viscosity is very low to be measured in the rheometer. The presence of two opposing mechanisms such as coalescence and creaming/flocculation may be related to this fact. Coalescence would provoke a decrease in the zero shear viscosity and creaming/flocculation, an increase. Hence, the zero shear viscosity may level off. This latter case supports the results obtained by MLS and Laser Diffraction.

On the contrary, the zero shear viscosity increases slightly with the aging time for the emulsions 2wt%, 2.5wt%, 3wt% and 3.5wt%. This fact is related to an incipient flocculation and/or incipient creaming. 2wt%, 2.5wt% and 3wt% exhibited creaming

process in MLS measurements whereas 3.5wt% showed creaming and coalescence/flocculation.

In addition, zero shear viscosity decreases slightly from day 3 to day 21 for the 4wt% emulsion, which is an indication of an increase of droplet size. However, an increase of zero shear viscosity was detected from day 21 to day 40. (McClements, 2005). These opposed trends could be explained by the existence of two different destabilization processes. Coalescence and creaming/flocculation could be simultaneously coexisting. The increase of η_0 is related to flocculation or/and creaming whereas its decrease is related to a coalescence process. The previous coalescence could accelerate the rate of possible flocculation and/or creaming. These results supports the MLS and laser diffraction measurements.

Conclusions

The influence in DSD, rheological properties and physical stability in the range of 2-3 wt% was not really significant. However, 1.5wt% of surfactant is not enough to cover the surface of the interface and it led to higher Sauter and volumetric mean diameters. Consequently, this emulsion has the lowest zero-shear viscosity and the highest flow index.

Emulsion containing above 3.5wt% of surfactant showed an accused depletion flocculation process since its preparation. The combination of measurements of laser diffraction, flow curves and multiple light scattering at different aging times showed the destabilization phenomenon in the emulsions in short period of time. These techniques have complemented each other leading to the conclusions:

- 1.5 wt% emulsion showed creaming as a predominant mechanism.

- 2-3 wt% emulsions exhibited low creaming rates being 3wt% emulsion which showed the greatest stability.
- 3.5-4 wt% emulsion showed flocculation, creaming and coalescence. 4wt% emulsion showed the major increase in the droplet size due to the depletion flocculation showed since its preparation.

The emulsions in the range 2-3wt% were highly stable and this excellent result can be explained by considering that the emulsion prepared at intermediate surfactant concentrations showed enough viscosity to prevent creaming and cover the interface. Also, it is not excessive surfactant concentration that may lead to a depletion flocculation process.

References

Allende, D., Cambiella, A., Benito, J.M., Pazos, C., Coca, J., 2008. Destabilization-enhanced centrifugation of metalworking oil-in-water emulsions: Effect of demulsifying agents. Chem. Eng. Technol. 31, 1007-1014.

Anastas, P. T., and Warner, J. C., 1998. Green Chemistry: Theory and Practice, Oxford University Press, New York, 30.

Brökel U., Meier W., Wagner G., 2007.Introduction. In: Brökel U., Meier W., Wagner G., Product Design and Engineering. Volume 1: Basics and Technologies. Weinheim: Wiley-VCH.1-3.

Camino, N.A, Carrera, C., Patino, J.M.R., Pilosof, A.M.R., 2012. Hydroxypropylmethylcellulose-beta-lactoglobulin mixtures at the oil-water interface. Bulk, interfacial and emulsification behavior as affected by pH. Food Hydrocolloid. 27, 464-474.

Castán, P., González, X., 2003. Skin properties of glycerine polyethoxylene esters. Proceedings of 40th Annual Meeting of CED. 33, 325-338.

Denolle, Y., Seita, V., Delaire, V., 2011. Eur. Pat. Appl., EP 2368971 A1 20110928, 2011.

Dickinson, E., Golding, M., & Povey, M. J., 1997. Creaming and flocculation of oil-in-water emulsions containing sodium caseinate. . J. Colloid Interface Sci. 185(2), 515-529.

EI-Aasser, M. S., & Sudol, E. D., 2004. Miniemulsions: overview of research and applications. J. Coat. Technol. Res. 1(1), 20-31.

Hofer, R., Bigorra, J., 2007. Green Chem. 9, 203-212

Hollinger, M.A., 2005. Introduction to Pharmacology, Third Edition, CRC Press.

Jafari, S.M., He, Y., Bhandari, B., 2008. Re-coalescence of emulsion droplets during high-energy emulsification. Food Hydrocolloid. 22, 1191– 1202.

Leal-Calderon, F., Schmitt, V., & Bibette, J., 2007. Emulsion science: basic principles. Springer.

Lutz, P.J.,2006. Ca. Pat. Appl., CA 2537554 A1 20060822.

Manoj, P., Watson, A.D., Hibberd, D.J., Fillery-Travis, A.J., Robins, M.M., 1998. Characterization of a depletion-flocculated polydisperse emulsion. II. Steady-state rheological investigations. J. Colloid Interface Sci. 207 (2), 294-302

McClements D.J., 2005. Food Emulsions: Principles, Practice, and Techniques. Boca Raton: CRC Press.

McClements, D.J., 2007. Critical review of techniques and methodologies for characterization of emulsion stability. Crit. Rev. Food Sci. Nutr. 47, 611-649.

Medvedovici, A., Udrescu, S., David, V., 2012. Use of a green (bio) solvent – limonene – as extractant and immiscible diluent for large volume injection in the RPLC-tandem MS assay of statins and related metabolites in human plasma. Biomedical Chromatography.27: 48-57.

Mengual, O., Meunier, G., Cayré, I., Puech, K., Snabre, P., 1999. Turbiscan MA 2000: multiple light scattering measurement for concentrated emulsion and suspension instability analysis. Talanta. 50: 445-456.

Nakajima, H., 1997. Microemulsions in cosmetics. Surfactant science series,CRC Press. 66, 175-197.

Napper, D. H., 1983. Polymeric stabilization of colloidal dispersions (Vol. 7). London: Academic Press.

Nazarzadeh, E., Anthonypillai, T., & Sajjadi, S., 2013. On the growth mechanisms of nanoemulsions. J. Colloid Interface Sci.397, 154-162.

Palazolo, G. G., Sorgentini, D. A., & Wagner, J. R., 2005. Coalescence and flocculation in o/w emulsions of native and denatured whey soy proteins in comparison with soy protein isolates. Food Hydrocolloid. 19(3), 595-604

Santos, J., Trujillo, L.A., Calero, N., Alfaro, M.C., Muñoz, J., 2013.Physical Characterization of a Commercial Suspoemulsion as a Reference for the Development of Suspoemulsions. Chem. Eng. Technol. 11, 1-9

Santos, J., Trujillo-Cayado, L. A., Calero, N., & Muñoz, J., 2014. Physical characterization of eco-friendly O/W emulsions developed through a strategy based on product engineering principles. AIChE J. 7, 2644-2653.

Schultz, S., Wagner, G., Urban, K., & Ulrich, J.,2004. High-Pressure Homogenization as a Process for Emulsion Formation. Chem. Eng. Technol. 27(4), 361-368.

Sheldon, R. A., 2005. Green solvents for sustainable organic synthesis: state of the art. Green Chem. 7(5), 267-278.

Sonneville-Aubrun, O., Simonnet, J. T., & L'alloret, F., 2004. Nanoemulsions: a new vehicle for skincare products. Adv Colloid Interfac.108, 145-149.

Tadros, T.F., 2009. Colloids in Agrochemicals. Wiley.

Trujillo-Cayado, L. A., Ramírez, P., Pérez-Mosqueda, L. M., Alfaro, M. C., & Munoz, J., 2014a. Surface and foaming properties of polyoxyethylene glycerol ester surfactants. Colloid Surface A. 458, 195-202.

Trujillo-Cayado, L. A., Ramírez, P., Alfaro, M. C., Ruíz, M., & Muñoz, J., 2014b. Adsorption at the biocompatible α-pinene–water interface and emulsifying properties of two eco-friendly surfactants. Colloid Surface B. 122, 623-629.

Tang, S. Y., Shridharan, P., & Sivakumar, M., 2013. Impact of process parameters in the generation of novel aspirin nanoemulsions–comparative studies between ultrasound cavitation and microfluidizer. Ultrason. Sonochem., 20(1), 485-497.

Walter J., 2010. Metabolism of Terpenoids in Animal Models and Humans. In: Handbook of essential oils: Science, Technology and Applications. Boca Raton. CRC Press. 209-232.

Weers J.G., 1998. Ostwald ripening in emulsions. In Binks (Ed.), Modern Aspects of Emulsions Science, Cambridge, UK. 292-327.

Chapter 4: Controlled production of eco-friendly emulsions using direct and premix membrane emulsification

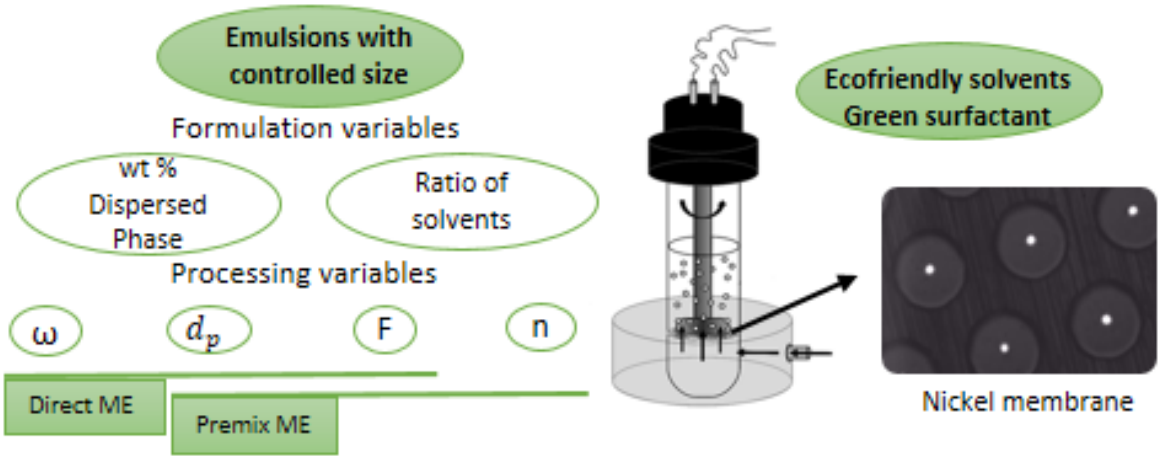

Abstract

Eco-friendly O/W emulsions were produced by membrane emulsification using nickel membrane consisting of hexagonal arrays of cylindrical pores of 10 or 20 μm diameter and 200 μm spacing. The dispersed phase was a mixture of N,N-dimethyldecanamide (AMD-10) and d-limonene containing 0-35 wt% AMD-10 in the dispersed phase and the continuous aqueous phase was 3 wt% polyoxyethylene glycerol fatty acid ester (Levenol® C-201). In direct membrane emulsification, the droplet-to-pore size ratio was 1.5-4.6 and the most uniform droplets were obtained with pure d-limonene at a stirrer speed of 620 rpm, corresponding to the peak shear stress on the membrane surface of 7 Pa. In premix membrane emulsification, the median droplet diameter decreased with increasing the transmembrane flux and was smaller than the pore size at the flux above 2000 L m^{-2} h^{-1}. The droplet size was about 6 μm after two passes through the membrane with a pore diameter of either 10 or 20 μm. The viscosity of emulsions with 30 wt% was not influenced by the shear rate but an emulsion with a dispersed phase content of 40 wt% showed shear thinning behaviour and viscoelastic properties. The produced emulsions can be used as environmentally friendly matrices for incorporation of agrochemical actives.

4.1.Introduction

The task of product engineering is to design products of desirable features for given applications. All properties are the result of certain physical and chemical characteristics of the product, which are determined by the choice of the formulation and processing conditions. Many important properties of emulsions are largely determined by structural parameters such as volume ratio of the phases, particle size distribution and

mean particle size (Schubert et al., 2003). Production of emulsion-based systems with specific physicochemical and functional properties often requires control over the particle size distribution (PSD) (McClements, 2005, Santos et al., 2011).

Conventional emulsification devices such as colloid mills, rotor-stator mixers, high-pressure homogenizers and ultrasonic homogenizers offer limited flexibility in terms of PSD. Recently, membrane emulsification (ME) has received much attention due to its ability to control the mean droplet size over a wide range together with the ability to provide a narrow size distribution (Kosvintsev et al., 2005). Low energy consumption lies at the heart of sustainable and socially responsible society (Cussler and Moggridge, 2011). The reduction in energy requirements by using ME is very significant. In addition, the ability to form uniform dispersions in a technique that can be scaled from small scale to industrial production makes the process very attractive (Peng and Williams, 1998).

Two main types of ME processes have been developed: direct ME involving the permeation of pure dispersed phase through a microporous membrane into agitating or recirculating continuous phase and premix ME involving the passage of previously prepared coarse emulsion through the membrane (Charcosset et al., 2004). Premix ME provides several advantages over direct ME: (i) the dispersed phase flux is higher, so the time required for the production is very short; (ii) the mean droplet-to-pore size ratios are smaller than in direct ME. In direct ME, the mean droplet-to-pore size ratio can range between 2 and 50 (Ma, 2003, Yuan et al., 2009, Zhou et al., 2009), but it is often below 10. In premix ME, the mean droplet-to-pore size ratio is typically between 0.6 and 2 (Vladisavljević et al., 2006); (iii) the process parameters are easier to control than in

direct ME. One of the disadvantages of premix ME is a higher emulsion polydispersity compared to direct ME.

Premix ME has been applied using a wide range of membranes, such as Shirasu Porous Glass (SPG) membrane (Suzuki et al., 1996), polycarbonate (Yafei et al., 2009), nylon and nitrocellulose polymeric membranes (Ramakrishnan et al., 2012), and nickel microsieves with rectangular and square membranes (Nazir et al., 2011, 2013). Typical laboratory devices for ME are SPG micro kits (Kukizaki and Goto, 2007) and Micropore Dispersion Cell (MDC) (Kosvintsev et al., 2005). Although MDC has been widely used in direct ME, so far there are no published studies on premix ME in MDC.

In recent years, there has been an increasing interest in using the so-called green solvents due to the need to replace traditional petrochemical organic solvents by more environmentally friendly solvents derived from agricultural crops (Anastas and Wagner, 1998). N,N-dimethyldecanamide (AMD-10) is considered as a safe biosolvent, according to the Environmental Protection Agency in 2005 and has excellent solubilizing properties towards agrochemical actives. Therefore, AMD-10 is a suitable solvent for agrochemical use (Hofer and Bigorra, 2007), that imposes minimal risk to the farmers while satisfying the needs of customers, which is a principal aim of the product design (Brokel et al., 2007).

D-limonene, a naturally occurring hydrocarbon, is a cyclic monoterpene, which is commonly found in the rinds of citrus fruits such as grapefruit, lemon, lime, and in particular, oranges. D-limonene exhibits good biodegradability, hence it may be used as a direct substitute for toxic organic solvents (Walter, 2010, Medvedovici et al., 2012). These two solvents can meet the ever-increasing performance, safety and

environmental demands of 21st century solvents. In this study, mixtures of d-limonene and AMD-10 will be used as a dispersed phase. The use of these solvent blends as a dispersed phase instead of common organic solvents and vegetable oils could represent a challenge for the size control in ME, due to their distinct physical properties, such as low viscosity and low interfacial tension and a medium solubility in water of AMD-10 (340 mg L^{-1}).

In addition, environmentally friendly surfactants have also attracted significant interest recently. Polyoxyethylene glycerol esters derived from cocoa oil are non-ionic surfactants obtained from a renewable source, which fulfil the environmental and toxicological requirements for eco-friendly foaming and/or emulsifying agents (Castán and González, 2003). Their use as green surfactants in detergents and personal care products is disclosed in several patents (Lutz, 2006; Denolle, 2011). Levenol ® C-201 and Levenol ® H&B are commercial polyoxyethylene glycerol esters. The former was found to be more surface active at the biocompatible α-pinene/water interface than Levenol H&B, its counterpart with a lower number of oxyethylene groups (Trujillo-Cayado et al., 2014a and 2014b).

The main objective of this work was to produce O/W eco-friendly emulsions with a controlled mean droplet size using ME. For the first time, premix ME has been performed in a Micropore Dispersion Cell (MDS) using micro-engineered membranes with circular pores. The operation procedure, formulation, pore size, and process parameters were optimized in order to obtain finer emulsions with low energy inputs. These emulsions may be used as matrices for incorporation of active agrochemical ingredients. This study is a contribution towards the development of new emulsion

products, which may fulfil the customers' needs as well as the requirements of the related industries.

4.2. Materials and methods.

4.2.1. Materials

N,N Dimethyl Decanamide (Agnique AMD-10^{TM}) was kindly provided by BASF. D-Limonene was supplied by Sigma Chemical Company. The dispersed phase was a mixture of AMD-10 and d-limonene containing 0, 25, or 35 wt% of AMD-10. The dispersed phase content in the prepared emulsions was 30 wt% in all experiments except those reported in Figure 8, where it was 5-40 wt %.

The continuous phase was 3 wt% Levenol ® C-201 and 0.1 wt% antifoam agent dissolved in deionized water. Levenol ® C-201 is a nonionic surfactant derived from cocoa oil, received as a gift from KAO Chemicals. It is a trade name of glycereth-17 cocoate (HLB:13), which is an ester of coconut acid and a polyethylene glycol ether of glycerin containing an average of 17 ethylene oxide units per molecule. RD antifoam emulsion (DOW CORNING®) was used as antifoaming agent. This commercial product consists of an aqueous solution containing polydimethyl siloxane (<10 wt%) and dimethyl siloxane, hydroxyl-terminated (<10 wt%).

4.2.2 Membrane and membrane module

The emulsions were obtained using a Micropore Dispersion Cell (MDS), a stirred cell with a flat disc membrane under the paddle stirrer shown in Figure 1. Both stirred cell and membranes were supplied by Micropore Technologies Ltd. (Loughborough, UK). The agitator was driven by a 24 V DC motor (INSTEK Model PR 3060) and paddle rotation speed was controlled by the applied voltage.

The membranes used were nickel membranes containing uniform cylindrical pores with a diameter of d_p= 10 µm or d_p= 20 µm and a spacing of L= 200 µm. The membranes were fabricated by the LIGA process, which involves galvanic deposition of nickel onto a template formed by photolithography and etching. Perfectly ordered hexagonal arrays of pores with one pore at the centre of each hexagonal cell can be seen on the micrographs in Figure 2.

The porosity of a membrane with regular hexagonal pore array is given by:

$$\varepsilon = \frac{\pi}{2\sqrt{3}}\left(\frac{d_p}{L}\right)^2 \qquad (1)$$

For the membranes used in this work, the porosity calculated from Eq. (1) is 0.26% and 0.90% for d_p= 10 and 20 µm, respectively. The effective cross-sectional area of the whole membrane is 8.5 cm^2, which is significantly greater than 1.4 cm^2, which was the membrane area used in previous premix ME studies with microsieve membranes (Nazir et al., 2011, 2013).

4.2.3. Emulsion production

4.2.3.1. Direct membrane emulsification

Dispersed phase was injected through the membrane using a syringe pump (Secondary Dual Pump, World Precision Instruments, Sarasota, Florida) at the constant flow rate of 110-910 mL h^{-1}, corresponding to the dispersed phase flux of 129-1070 L m^{-2} h^{-1} (See Figure 4.1A). The stirring speed was fixed at 400-1200 rpm. Once the desired amount of oil had passed though the membrane, both the pump and the agitator were switched off and the droplets were collected and analyzed. The membrane was cleaned with 4 M

NaOH in an ultrasonic bath for 5 min followed by treatment in 2 wt% citric acid for 5 min.

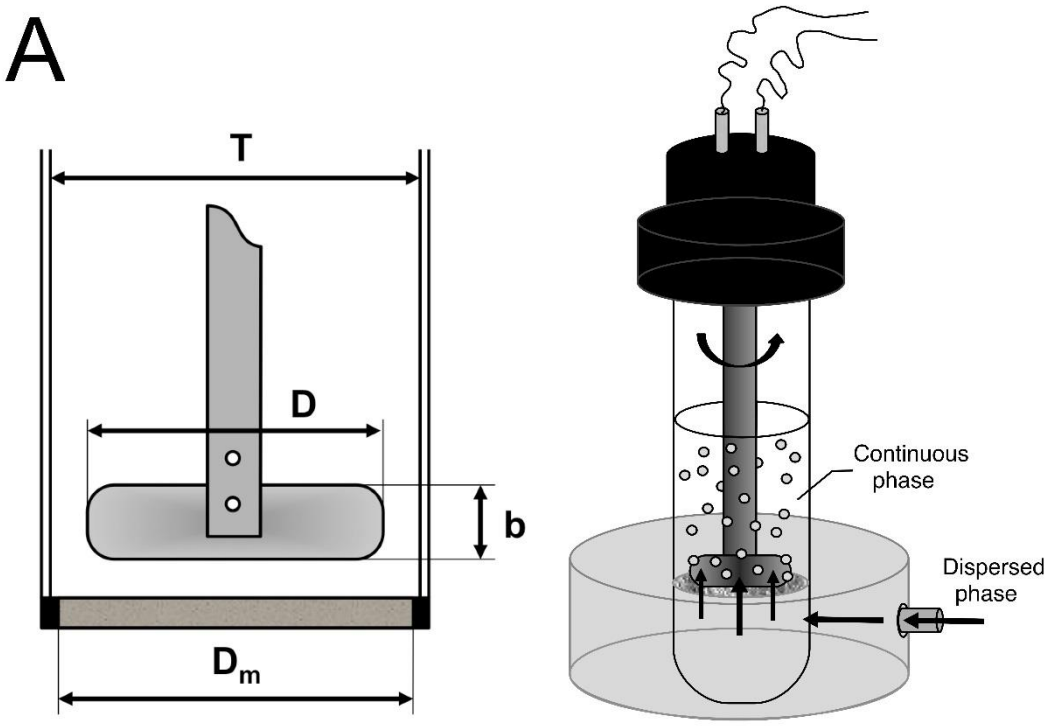

Figure 4.1. A) Schematic illustration of Dispersion Cell with simple paddle stirrer above a flat-disc membrane (b= 11 mm, D= 30 mm, D_m= 32 mm, and T= 37 mm) used in direct ME.

4.2.3.2. Premix membrane emulsification

The mixture of solvents and the continuous phase was first premixed for one minute using a magnetic bar to produce a coarse emulsion with large droplets. This coarse emulsion was then injected 1-3 times through the membrane using a syringe pump (Model 11 Plus, Harvard Apparatus) at the constant flow rate of 110-910 mL h^{-1}, corresponding to the flux of 129-1070 L m^{-2} h^{-1} (See figure 4.1B). The membrane was not cleaned between the passes. The emulsion samples obtained after each pass were collected and analysed.

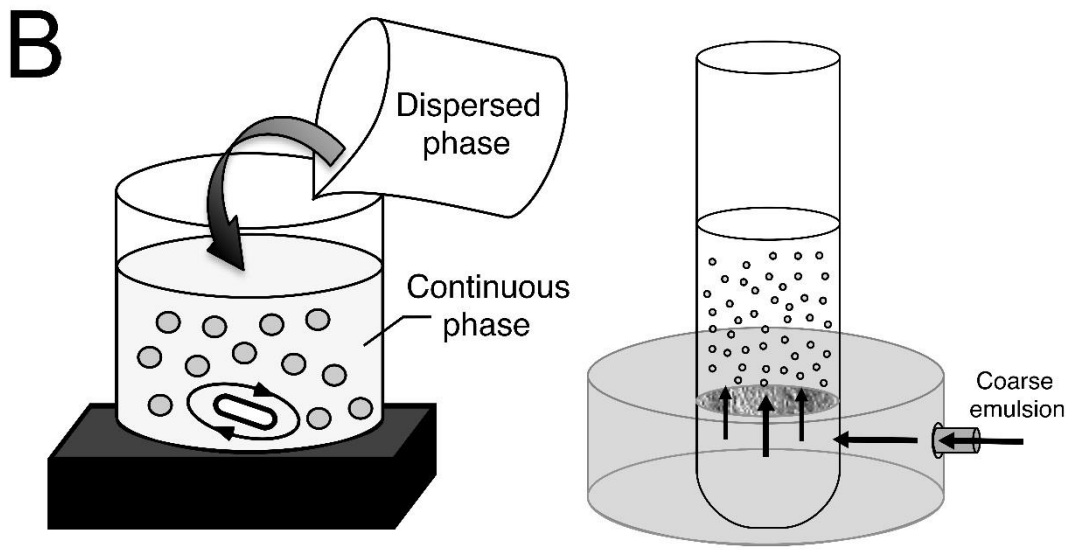

Figure 4.1.B) Schematic illustration of the premix ME process used. The coarse emulsion was prepared by magnetic stirrer and injected through the membrane without stirring.

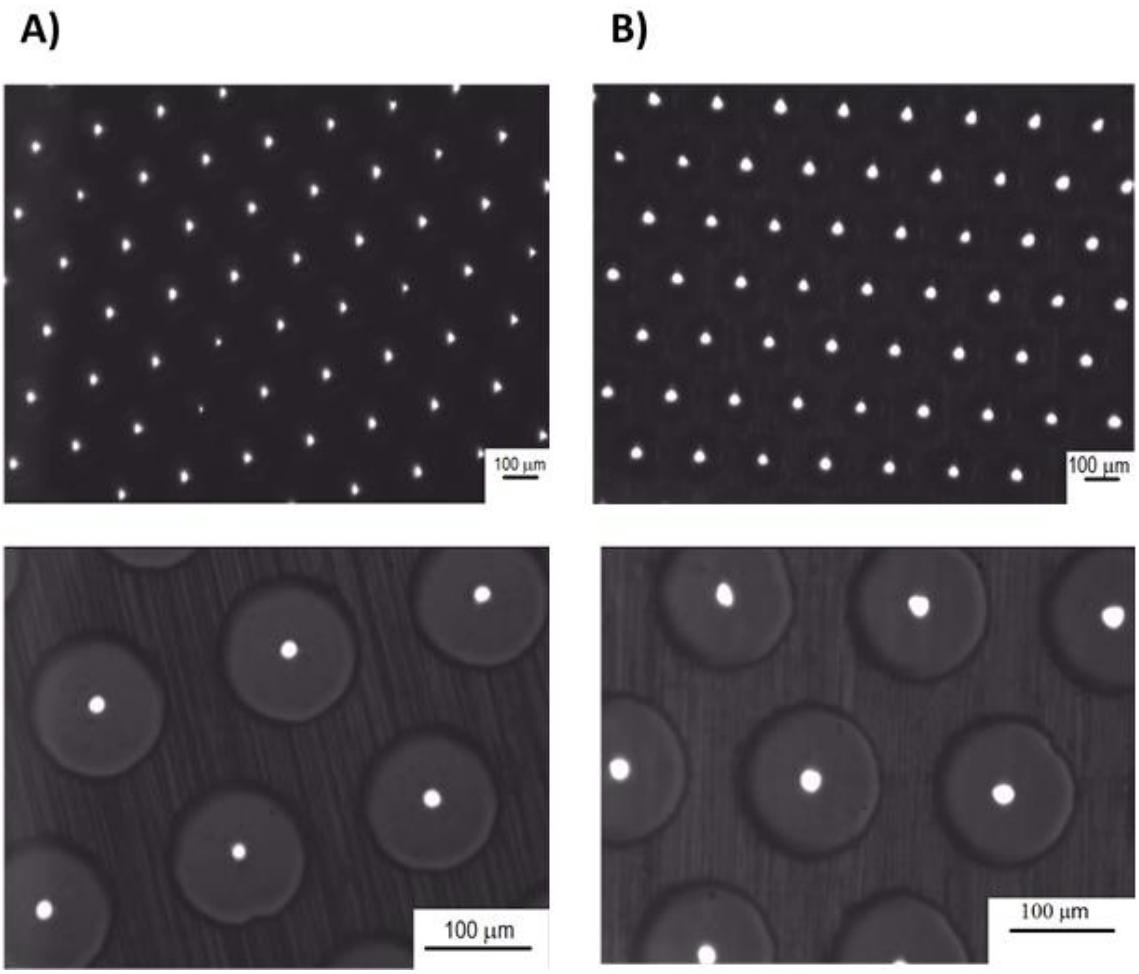

Figure 4.2. Photomicrographs of the membranes used in this work taken at two different magnifications: A) 10 µm pore size membrane and B) 20 µm pore size membrane.

4.2.4. Droplet size distribution measurements

PSD of oil droplets was determined by static laser light scattering (laser diffraction) using Mastersizer 2000 (Malvern, Worcestershire, United Kingdom). All measurements were repeated three times for each sample.

The mean droplet diameter was expressed as the volume median diameter d(v,0.5), which is the diameter corresponding to 50 vol% on the cumulative distribution curve. The relative span of a drop size distribution was used to express the degree of drop size uniformity (see Eq. 2).

$$span = \frac{[d(v,0.9) - d(v,0.1)]}{d(v,0.5)} \quad (2)$$

4.2.5. Rheological measurements

Rheological experiments were conducted with AR 1000 controlled-stress rheometer (TA instruments, USA), equipped with a cone-plate of 60 mm diameter and 1 degree. Flow curves were generated from 0.05 Pa to 1 Pa at 20°C. Small amplitude oscillatory shear tests were carried out for the emulsion containing 40 wt % of dispersed phase. The frequency sweep was carried out in the 20-0.5 rad s^{-1} angular frequency range at shear stress amplitude of 0.05 Pa. This was previously determined by conducting oscillatory stress sweeps at three different frequencies, namely 0.63 rad s^{-1}, 6.3 rad $s^{-1}$and 18.9 rad s^{-1}. All measurements were repeated 3 times with each emulsion. Sampling from the top part of the container in contact with air was avoided.

4.3. Results and discussion

4.3.1. Reproducibility of experimental data

Figure 4.3 shows PSD curves for the emulsions prepared using direct ME with 10 μm membrane (Fig. 4.3.A) and premix ME with 20 μm membrane (Fig. 4.3.B). In each case, the dispersed phase contained 25 wt% AMD-10 and 75 wt% d-limonene. Replicated runs 1, 2 and 3 in Fig. 4.3.A were performed on the same day, while run 4 was done in two days, after several other experiments had been performed in the meantime. PSD for all replicates was very similar, which indicates that the membrane cleaning procedure was robust and successful. The average D(v,0.5) value was (28.79 ± 1.37) μm and span was 1.35 ± 0.03, where the error margins were calculated as one standard deviation away from the mean. There is no difference between a new and used membrane provided that a new membrane was treated with a wetting agent to render the surface hydrophilic (Fig. 4.3.A). The new membrane that was not treated with wetting agent exhibited the broadest particle size distribution in Fig. 4.3.A.

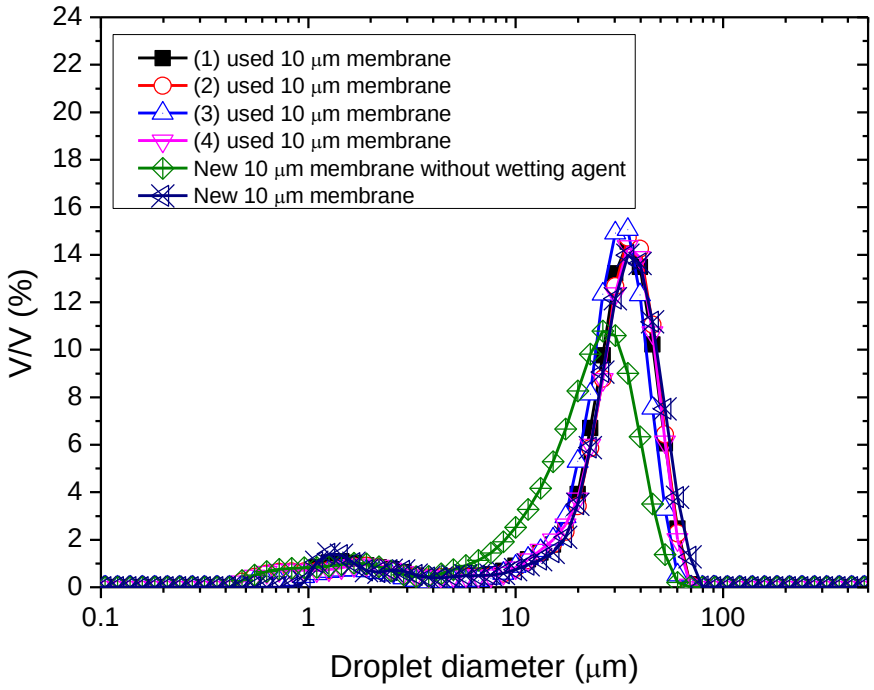

Figure 4.3.A. Particle size distribution for different replicates: 25/75 emulsion produced using direct ME at 850 rpm and 600 L m^{-2} h^{-1} with a 10 μm membrane.

In addition, PSD for the emulsions prepared by premix ME did not change substantially in the experiments repeated 3 times under constant experimental conditions (Fig 4.3.B). The average D(v,0.5) value was (23.16 ± 1.85) μm and span was 1.78 ± 0.09. The reproducibility of the results in direct ME was better than that in the premix process, probably because the PSD of the coarse emulsion was not exactly the same in all premix ME runs. In both processes, bimodal distributions were obtained and PSD was more uniform in the samples prepared by direct ME.

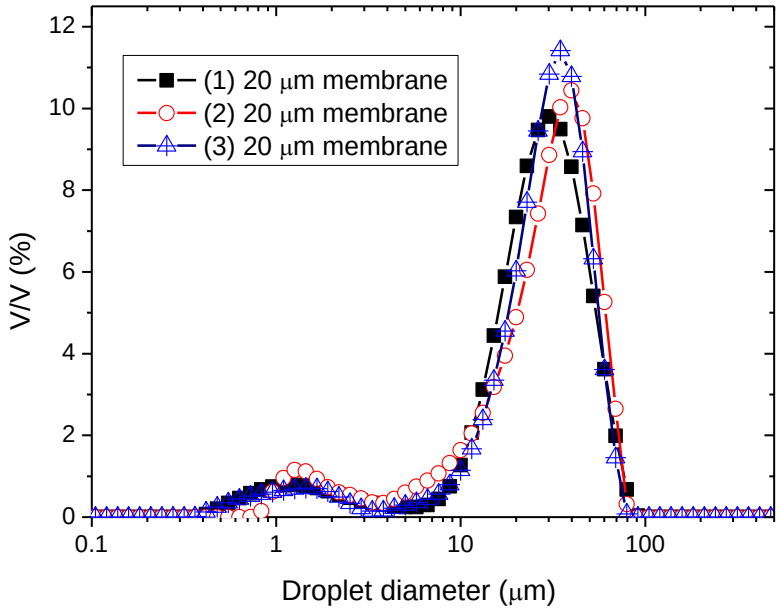

Figure 4.3.B. Particle size distribution for different replicates: 25/75 emulsion produced using single-pass premix ME process at 706 L m^{-2} h^{-1} with a 20 μm membrane.

3.2 Laser diffraction measurements

3.2.1. Direct Membrane Emulsification

Figure 4.4 shows PSD for the emulsions prepared by direct ME at 620 rpm and 600 L m^{-2} h^{-1} with a 10 μm and 20 μm membrane as a function of the solvent ratio in the dispersed phase. An increase in the content of AMD-10 in the dispersed phase caused a shift of the distribution towards smaller droplet sizes and the distribution became wider, as evidenced by higher span values (Table 4.1). This could be due to the low interfacial tension of the solvent blends compared to pure d-limonene (Table 4.2). The interfacial tension force is the main force resisting the drag force and holding a growing droplet at the membrane surface. By decreasing the interfacial tension, the droplets detach sooner from the membrane surface and the resultant droplet size is smaller. In addition, AMD-

10 is more polar solvent than d-limonene (the solubility of AMD-10 and D-Limonene in water is 340 and 13.8 mg L^{-1}, respectively), which means that the solvent blends have a higher affinity towards the hydrophilic membrane surface than pure d-limonene. The PSD curves for pure limonene are monomodal, suggesting that the membrane was not wetted by pure d-limonene during emulsification. In addition, the impact of the pore size on the mean droplet size was very substantial for the pure limonene emulsions and negligible for the 25/75 emulsions. This may be related to the low interfacial tension of the mixture that is the crucial property to achieve low droplet size (Santos et al., 2014). The subsequent experiments will be done using the 25/75 solvent mixture which is a compromise between a need to obtain a narrow distribution and to replace as much d-limonene as possible by a cheaper AMD-10 solvent.

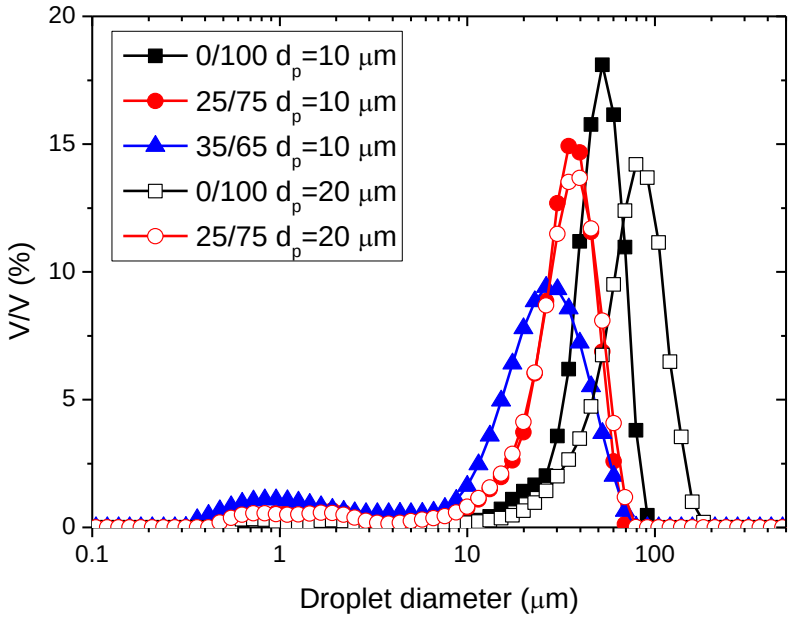

Figure 4.4. PSD for emulsions prepared by direct ME at 620 rpm and 600 L m^{-2} h^{-1} as a function of the pore size of the membrane and the ratio of solvents in the dispersed phase.

Table 4.1. The effect of the ratio of AMD-10 and d-limonene in the dispersed phase on D(v,0.5) and span for emulsions prepared by direct ME at 620 rpm and 600 L m^{-2} h^{-1}.

wt% AMD-10 in dispersed phase	10 µm membrane		20 µm membrane	
	D(v,0.5)	span	D(v,0.5)	span
0	45.5	0.9	69.3	1.1
25	30.4	1.2	30.9	1.2
35	21.7	1.8	-	-

Table 4.2. The equilibrium interfacial tension between the aqueous and oil phase for different solvent ratios in the absence and in the presence of the used surfactant at 20°C.

AMD-10/d-limonene mass ratio (wt/wt)	**Interfacial tension (mN/m)**	
	no surfactant	3 wt% Levenol ® C-201
0/100	40 ± 1.3	7 ± 0.5
25/75	7 ± 0.4	1 ± 0.1
35/65	4 ± 0.3	-

Figure 4.5 shows the effect of stirring speed on the droplet size distribution for 25/75 emulsions prepared with a 10 µm membrane at the oil flux of 600 L m^{-2} h^{-1}. The increase of stirring speed caused the PSD curves to shift toward smaller droplet sizes. In addition, the volume median diameter decreased with increasing the stirring speed (Fig. 4.6), which was due to an increase of the drag force acting on the droplets. The same stirring rate vs. droplet size relationship was reported by Kosvintsev et al. (2005) and Stillwell et al. (2007) for sunflower O/W emulsions. The droplet size showed large variations with stirring speed up to 620 rpm, corresponding to average shear stress at the membrane surface of 6.25 Pa. However, the effect was less pronounced at the higher stirring speeds, when the volume median diameter virtually reached its asymptotic value. Figure 6 also provides a comparison of experimental drop size and model prediction at different

stirring speeds. The shear-capillary model used in this work (see Appendix A) does not recognise the dispersed phase flux as having a contribution to the formed droplet size. Therefore, the model should represent the smallest droplet size that can be produced for a given set of operating conditions. It could explain why the model fits the experimental data best at high stirring speeds, where the droplet formation times are very short due to high drag forces exerted on the droplets by the stirrer (Dragosavac et al., 2008).

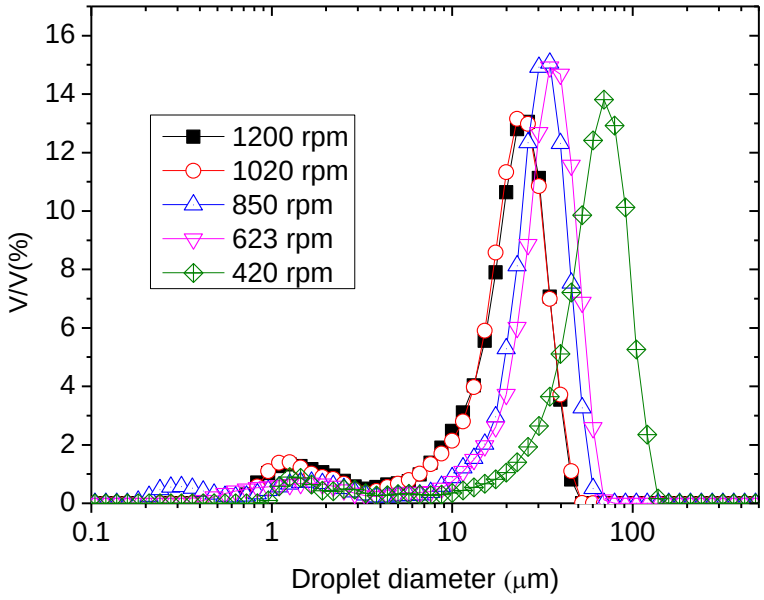

Figure 4.5. The effect of stirring speed on the PSD of 25/75 emulsions prepared by direct ME at 600 L m^{-2} h^{-1} with a 10 µm membrane.

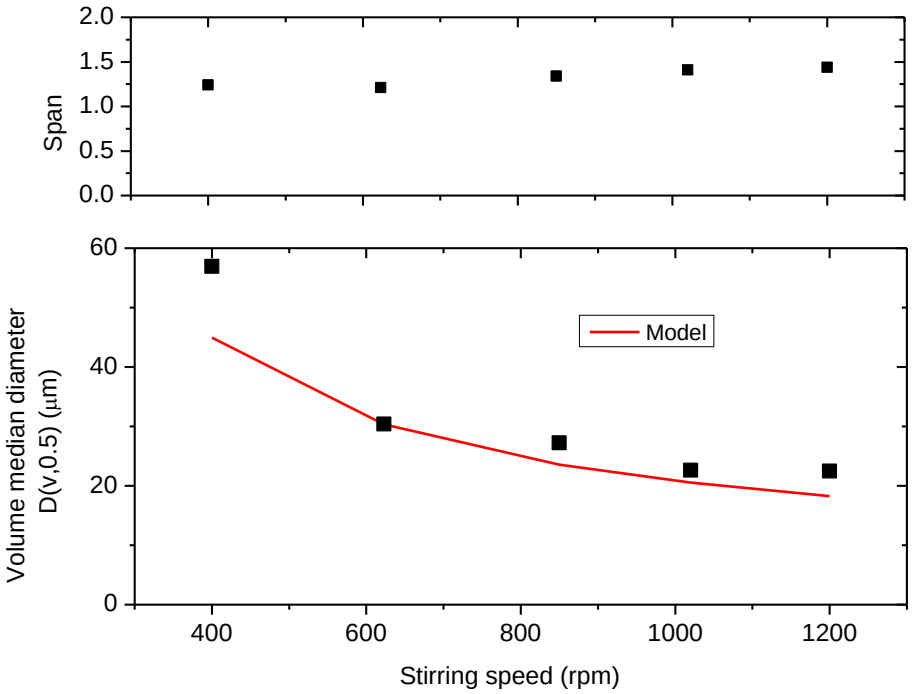

Figure 4.6. The volume median diameter, D(v, 0.5) and span of the emulsions prepared by direct ME at 600 L m^{-2} h^{-1} with a 10 µm membrane as a function of stirring speed. The predicted values are calculated using model presented in the appendix A.

Figure 4.6 also shows the influence of stirring speed on the span values for the emulsions prepared at 600 L m^{-2} h^{-1} with a 10 µm membrane. The higher span values obtained above 620 rpm could be attributed to more significant deformation of the droplets on the membrane surface before detachment due to high shearing, which can lead to more pronounced droplet interactions with the membrane surface and membrane wetting. The optimal rotational speed with regard to droplet size uniformity was 620 rpm, which corresponded to the peak shear stress on the membrane surface of 7 Pa.

Figure 4.7 shows A) D(v,0.5) and B) span as a function of transmembrane flux for the emulsions prepared with a 10 and 20 µm membrane. The rotational speed was kept at the optimal value of 620 rpm. For both pore sizes, an increase in the transmembrane flux led to an increase in the mean droplet size, while span did not show significant

variations. As the transmembrane flux is increased, the drop grows faster and the interface cannot be stabilised fast enough by adsorbed emulsifier molecules. In addition, at higher transmembrane fluxes a higher amount of oil will flow into the growing drop during pinch off. This effect was more significant up to 400 L h^{-1} m^{-2} and then the droplet size tended to stabilize, probably due to droplet-droplet interactions on the membrane surface that restricted further droplet growth (Egidi et al., 2008).

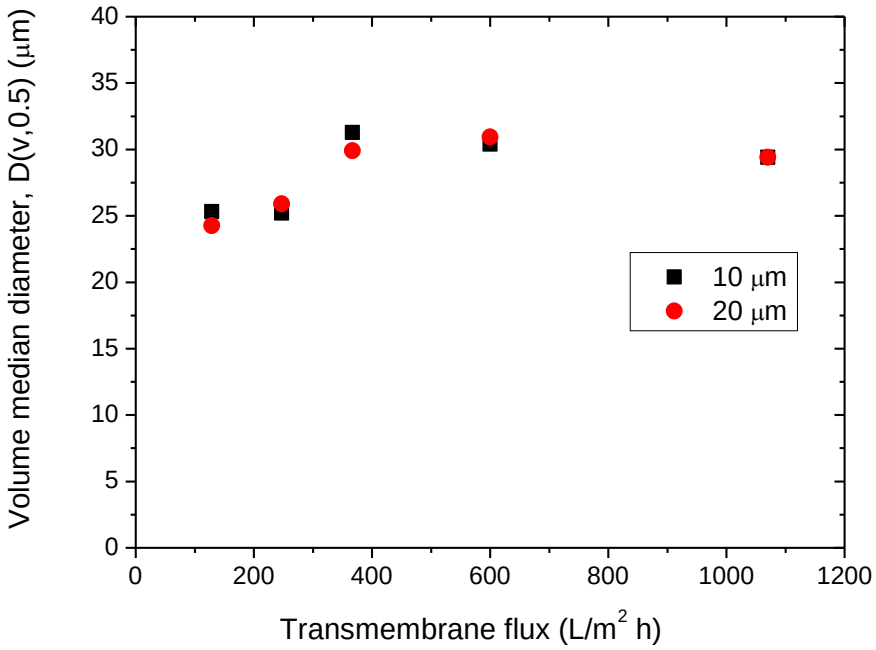

Figure 4.7.A. The effect of transmembrane flux on: Volume median diameter, D(v,0.5), for the emulsions processed by direct ME at 620 rpm with a 10 and 20 μm membrane.

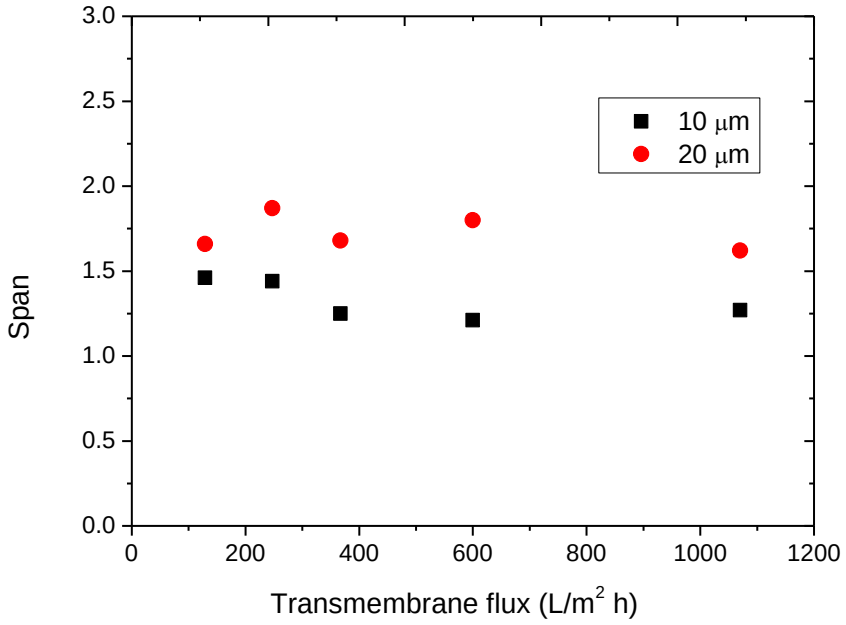

Figure 4.7.B. The effect of transmembrane flux on Span for the emulsions processed by direct ME at 620 rpm with a 10 and 20 μm membrane.

The influence of pore size on D(v,0.5) was insignificant for the emulsions containing AMD-10 in the dispersed phase. However, span increased with an increase in the pore size. Therefore, the optimum conditions for direct ME in this work were: a pore size of 10 μm, a transmembrane flux of 129 L m^{-2} h^{-1} and a stirrer speed of 620 rpm.

Figure 4.8 shows the effect of dispersed phase content on D(v,0.5) for 25/75 emulsions prepared by direct ME at 129 L m^{-2} h^{-1} and 620 rpm using a 10 μm membrane. The surfactant/oil ratio was kept at 0.10 (w/w) in all samples. The volume median diameter decreased with increasing the dispersed phase content in the emulsion. For a given surfactant/oil ratio (R=0.10), when the dispersed phase content is increased, the surfactant concentration in the continuous phase also increases, leading to the higher viscosity of the continuous phase, η_c. It has been reported that the viscosity of the continuous phase significantly affects the droplet size obtained in rotor stator homogenizers and in direct ME. It is stated that an increase in η_c will lead to an increase

of the drag force acting on the forming droplets at the same stirring speed producing smaller droplets (Vankova et al., 2007, Dragosavac et al., 2008).

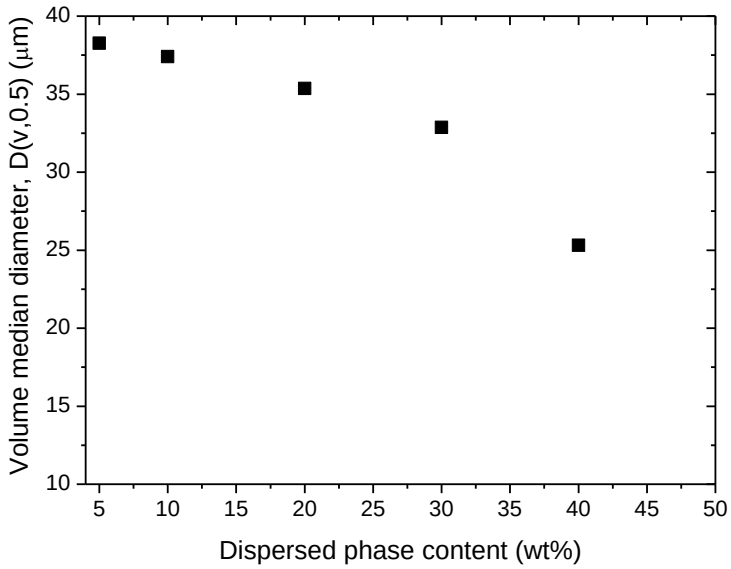

Figure 4.8. The effect of the dispersed phase content in the emulsions on the volume mean diameter, (D(v,0.5) in direct ME at 129 L m^{-2} h^{-1} and 620 rpm with 10 μm membrane. The surfactant/oil ratio was kept at 0.10 (w/w) in all samples.

3.2.2. Premix membrane emulsification

Figure 9A illustrates the effect of transmembrane flux on the PSD of emulsions produced by premix ME with a 10 μm membrane. Injection of pre-mix through the membrane led to reduction in the droplet size and modification of the PSD compared to that of the pre-mix.

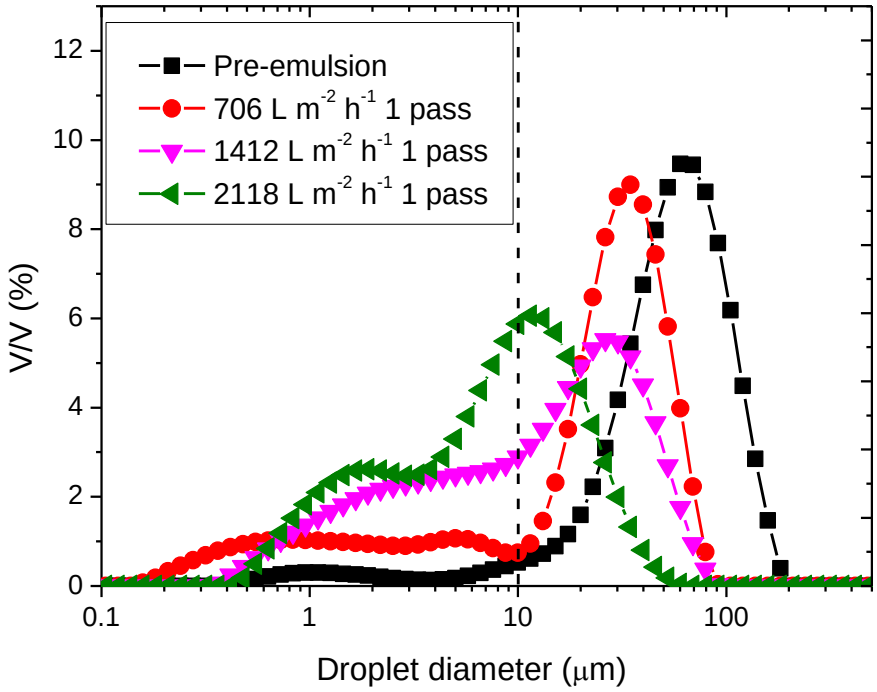

Figure 4.9.A. The effect of transmembrane flux on the PSD of the emulsions prepared by premix ME using a 10 μm membrane. The location of the dashed line corresponds to the membrane pore diameter.

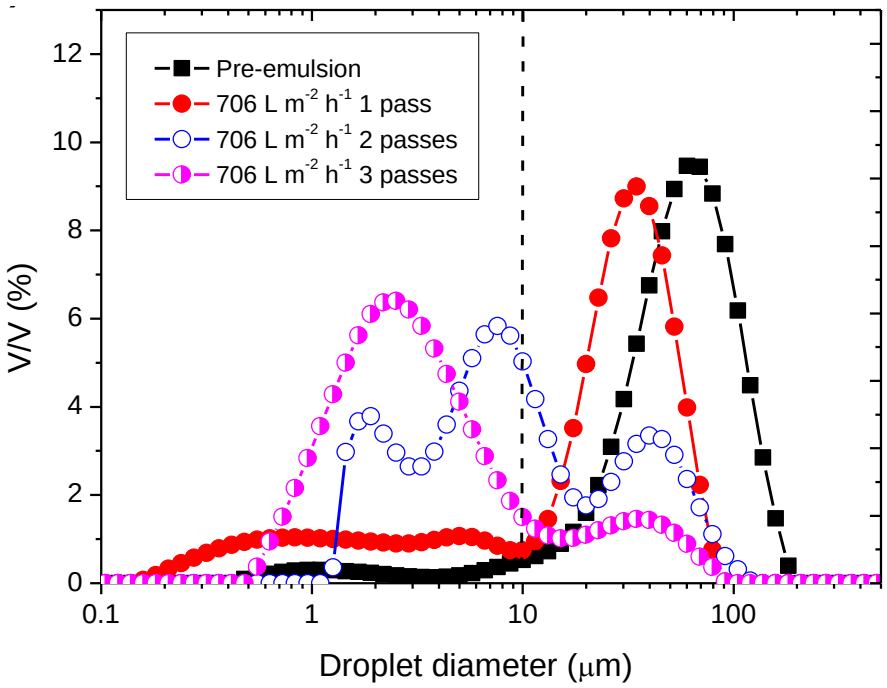

Figure 4.9.B. The effect of number of membrane passes on the PSD of the emulsions prepared by premix ME using a 10 μm membrane. The location of the dashed line corresponds to the membrane pore diameter.

An increase in the transmembrane flux caused a shift of the PSD curves towards lower droplet sizes. As a result of energy input brought by fluid flow, large oil drops in the coarse emulsion were deformed in the pores and broken up into smaller droplets (Van Aken, 2002). A reduction in drop size occurred as a result of various disruptive forces, such as shear and extensional forces, interfacial tension effects (Rayleigh and Laplace instabilities) and impact forces due to droplet-droplet and droplet-wall interactions (Vladisavljević et al., 2004 and 2006, Cheetangdee et al., 2011). Here, droplet-wall interactions are probably less significant than in SPG membrane, due to shorter pore lengths as a result of non-tortuous and non-interconnected pores and small membrane thickness. The wall shear stress τ_p in cylindrical non-tortuous pores with a diameter of d_p is given by (Vladisavljević et al., 2006b): $\tau_p = 8\eta_c J/(\varepsilon d_p)$, where ε is the membrane porosity defined by Eq. (1) and J is the transmembrane flux. Hence, τ_p increases with increasing J, which results in more intensive droplet break-up, as shown in Figs. 4.9 and 4.10. The droplet size can also be reduced by increasing number of passes through membrane, as shown in Figure 4.9.B, due to additional amount of energy added to the system (Vladisavljević et al., 2006). The same trend was observed in this work, although larger droplets were still present in the product emulsion after two passes (Fig. 4.9.B), probably due to partial droplet re-coalescence. Due to bimodal PSDs, the span values were 1.5-6 (the data not shown here). The fraction of larger droplets (d>10 μm) can be reduced by implementing three passes, as can be seen from the PSD curves at 706 L m^{-2} h^{-1} in Fig. 4.9.B.

Figure 4.10 shows the effect of transmembrane flux on the volume median diameter of the product emulsions after 1-3 membrane passes. The transmembrane pressure, Δp is equivalent to energy input per unit volume, E_V and can be expressed as follows:

$E_V = \Delta p = J(R_m + R_f)$, where R_m and R_f is the hydraulic resistance of the clean membrane and fouling layer, respectively. The fouling resistance occurs due to accumulation of oil drops on the upstream side of the membrane (external fouling) and inside the pores (internal fouling) (Vladisavljevic et al., 2004). The mean Sauter diameter of an emulsion produced in mechanical emulsification device exponentially decreases with increasing energy input per unit volume (Karbstein and Schubert, 1995): $D_{3,2} = CE_V^{-b}$, where C and b are constants whose values depend on the physical properties of the phases. If the total hydraulic resistance is constant, the above equation can be simplified to $D_{3,2} \propto J^{-b}$. Therefore, the higher the flux, the lower the resultant droplet size, which agrees with the results in Fig. 4.10. The same behaviour was observed by Suzuki et al. (1996 and 1998) in premix ME with SPG and PTFE membranes.

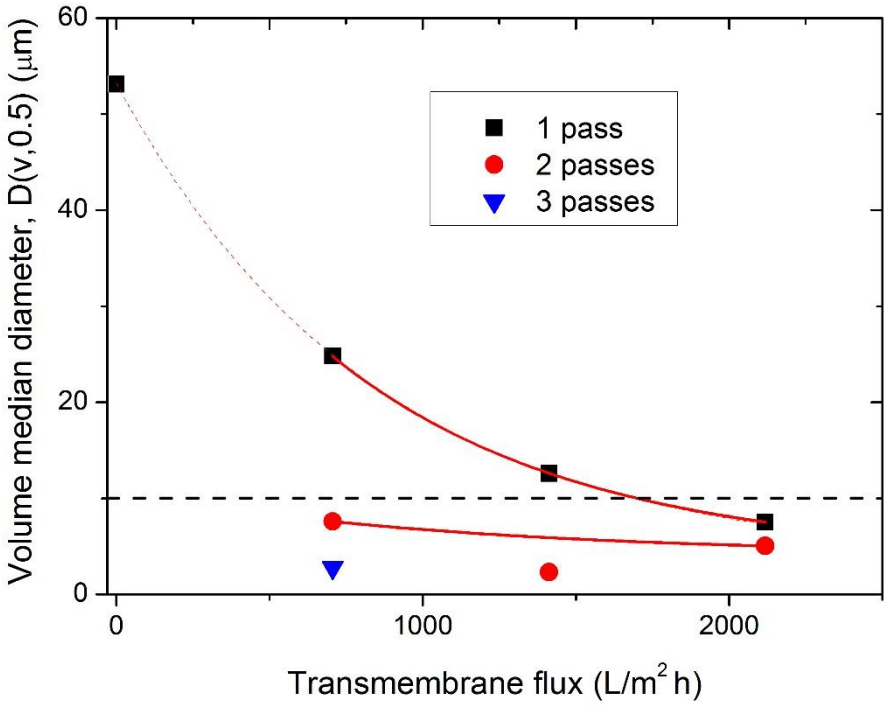

Figure 4.10. The effect of transmembrane flux and number of passes through the 10 µm membrane on the volume median diameter of emulsions prepared by premix ME.

D(v,0.5) was less than 10 µm (the pore size) after two passes through the membrane irrespective of the flux and even after a single pass at the flux of 2118 L m^{-2} h^{-1}. Large droplets of a pre-mix are squeezed as they pass through the pores due to elongational forces. At high flux values, a deformed droplet remains elongated after it exits the pore, due to high velocity of the continuous phase relative to that of the dispersed phase (van der Zwan et al., 2006). The resulting long droplet filament is subjected to Plateau-Rayleigh instability due to perturbations on its interface, which leads to jet fragmentation into very fine droplets, typically smaller than the pore size. At low fluxes, a squeezed droplet re-emerges on the downstream side of the membrane acquiring a dumbbell shape. The droplet does not form a long cylinder, since the flow rate of the continuous phase is insufficient and thus, Plateau-Rayleigh instability is not relevant (van der Zwan et al., 2006). The droplet is disrupted due to Laplace instability caused by the difference in capillary pressure between the dispersed phase in the neck region inside the pore and the dispersed phase before and after the pore (in hemispherical ends).

Figures 4.11.A and 4.11.B show the effect of transmembrane flux and number of passes through the membrane, respectively, on the PSD for emulsions prepared using a 20 µm membrane. As expected, the smallest droplets were obtained after two passes at 2118 L m^{-2} h^{-1} (due to the highest energy input) and the biggest droplets were produced at 350 L m^{-2} h^{-1} after single pass.

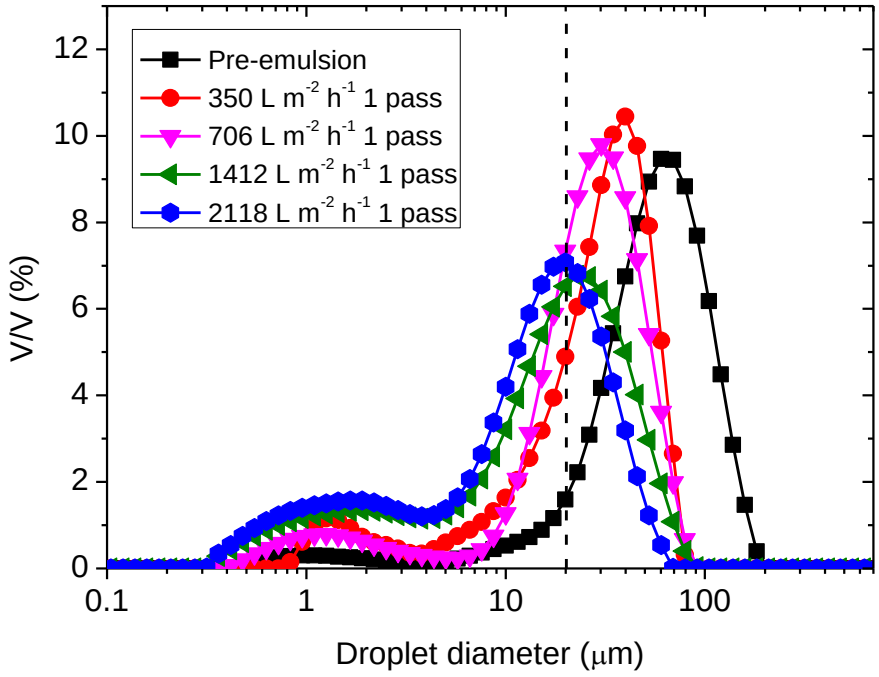

Figure 4.11.A. The effect of transmembrane flux on the PSD of emulsions obtained by premix ME with the 20 μm pore size membrane.

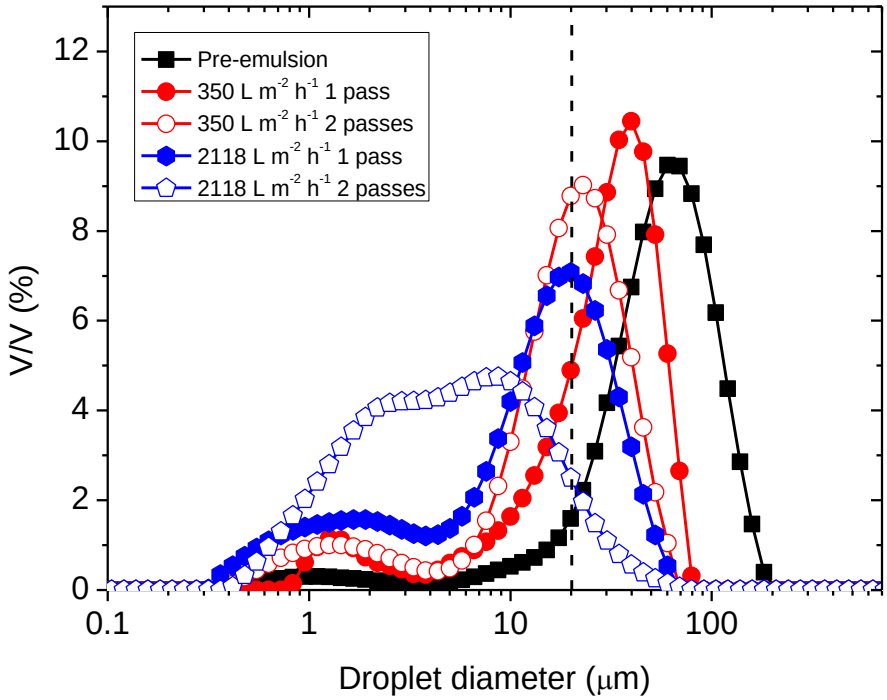

Figure 4.11.B. The effect of number of passes through the membrane on the PSD of emulsions obtained by premix ME with the 20 μm pore size membrane.

Figure 4.12 shows the effect of transmembrane flux and number of passes on for the 20 µm pore size. The D(v,0.5) value after first pass at 2118 L m^{-2} h^{-1} was 15 µm and was higher than that for the 10 µm pore size. At the constant flux, flow velocity in the membrane pores is lower for larger pores, due to 3.5 times higher membrane porosity, leading to less intensive droplet break-up. The volume median diameter after two passes levelled off at about 6 µm and was similar to the limiting D(v,0.5) value for the 10 µm pore size after two passes. However, span values for 20 µm pore size membrane were lower than those for the 10 µm pore size (data not shown). Therefore, in premix ME more uniform emulsion droplets were produced with the higher pore size, as opposed to direct ME.

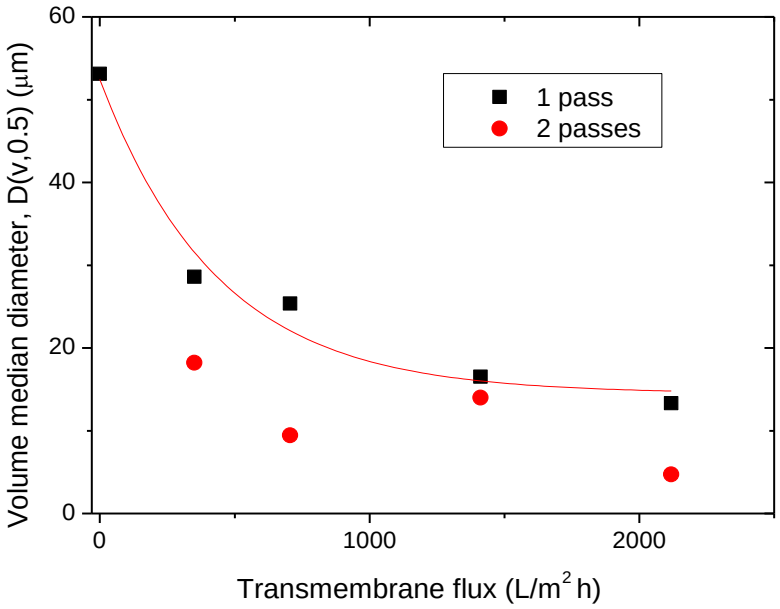

Figure 4.12. The effect of transmembrane flux and number of passes through the membrane on D(v,0.5) for emulsions obtained by premix ME using the 20 µm pore size membrane.

4.3.3. Rheological measurements

Figures 4.13A and 4.13B show flow properties of 30 wt% emulsions prepared by direct and premix ME, respectively, as a function of transmembrane flux and number of passes.

In both cases, the pore size of the membrane was 10 µm. All samples with 30% dispersed phase exhibited Newtonian behaviour with the flow curves fitting fairly well to the Newtonian law. Hence, viscosities of these emulsions are not influenced by shear rate.

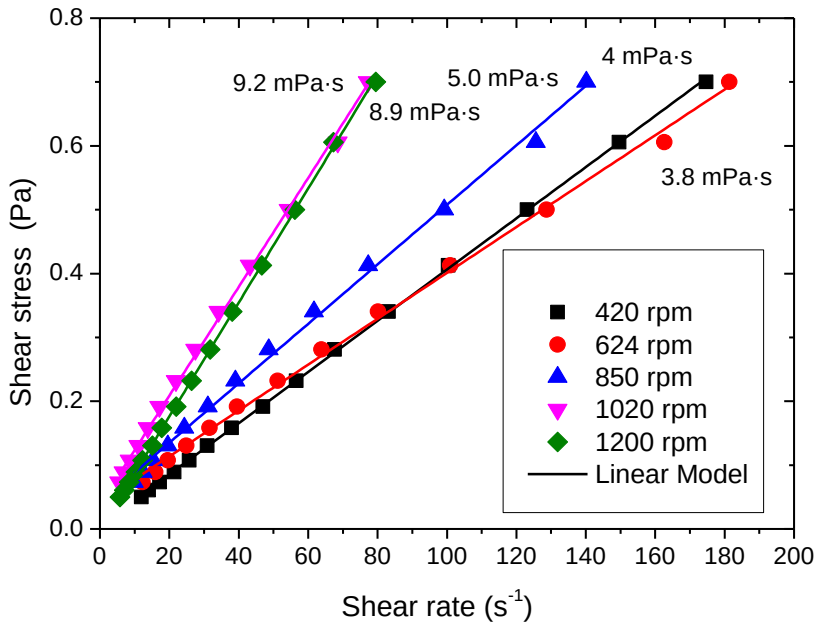

Figure 4.13A. Flow curves for emulsions produced by direct ME at 600 L m^{-2} h^{-1} with the 10 µm membrane as a function of stirring speed. Continuous lines illustrate data fitting to the linear regression.

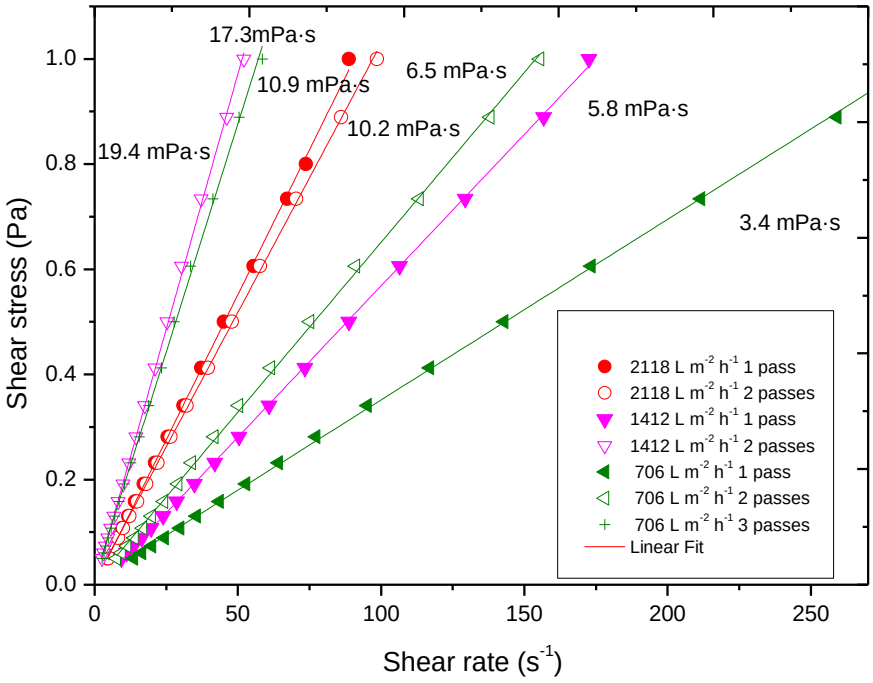

Figure 4.13.B. Flow curves for emulsions produced by premix ME with the 10 µm membrane as a function of transmembrane flux. Continuous lines illustrate data fitting to the linear regression.

Increasing the stirring speed increases the viscosity of the samples, which supports laser diffraction results. An increase of transmembrane flux and number of passes led to an increase of viscosity. In addition, the emulsions prepared by premix ME showed higher viscosities than the ones obtained by direct process. These results are in good correlation with the mean droplet diameters observed by laser diffraction. Clearly, emulsions with a dispersed phase content of 30 wt% did not possess enough internal structure to show shear thinning behaviour or viscoelastic properties.

By contrast, an emulsion with a dispersed phase content of 40 wt% exhibited shear thinning behaviour and viscoelastic properties. Measurable viscoelastic responses could not be obtained below 40 wt% dispersed phase. Figure 4.13.C shows mechanical

spectrum of a 40 wt% emulsion produced by direct ME at 620 rpm and 129 L m^{-2} h^{-1}. The loss modulus G'' was higher than the storage modulus G' at every frequency. This behaviour is typical in viscoelastic liquids (tan δ <1) (Mezger, 2006). Emulsions with viscoelastic properties usually show better stabilities against creaming than the non-viscoelastic emulsions (Barnes, 1994).

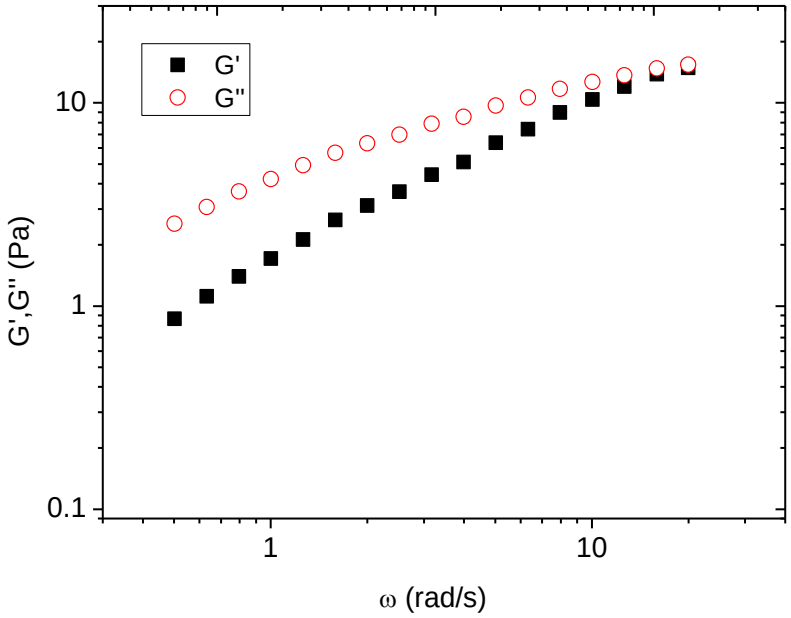

Figure 4.13.C. Mechanical spectra for 40 wt% emulsion produced by direct ME at 129 L m^{-2} h^{-1} and 620 rpm with 10 µm membrane.

Conclusions

The production of eco-friendly emulsions with a median droplet diameter ranging from 21 to 69 µm has been demonstrated using direct and premix membrane emulsification (ME) in a simple paddle-bladed stirred cell. An increase of the content of AMD-10 solvent in the dispersed phase caused a decrease in the mean droplet size and deterioration of the droplet size distribution, probably due to lower interfacial tension and higher polarity of the solvent blend compared to pure d-limonene. In direct ME, the mean

droplet size decreased with increasing the stirring speed and decreasing the transmembrane flux. The droplet-to-pore size ratio was 2.2-4.6 and 1.5-3.5 for the membrane with a pore size of 10 and 20 μm, respectively. The minimum droplet-to-pore size ratio of 1.5 was smaller than 3 reported in direct ME with SPG membrane, probably due to very low interfacial tension of 1 mN/m when 25/75 solvent mixture was used. The most uniform droplets were obtained at at the flux of 600 L m^{-2} h^{-1} and the stirrer speed of 620 rpm, which corresponded to the peak shear stress on the membrane surface of 7 Pa. For a constant surfactant/oil ratio (*R*) of 0.10, the mean droplet size decreased with increasing the dispersed phase content in the emulsion.

In premix ME, the mean droplet size exponentially decreased with increasing transmembrane flux from an initial value greater than 50 μm in a pre-mix to a final value lower than the pore size in the emulsions processed at the flux above 2000 L m^{-2} h^{-1}. The mean droplet size was additionally reduced using two or three passes through the membrane, but the particle size distribution was relatively broad. A lower transmembrane flux and smaller number of passes were needed to achieve the same droplet size reduction as with SPG membrane of the same pore size, probably due to smaller interfacial tension in this work. The effect of pore size on the mean droplet size was more pronounced in premix than in direct ME. This work demonstrates that premix ME with only two passes through nickel micro-engineered membrane enables to obtain O/W emulsions with very small mean droplet sizes compared to the pore size. The mean droplet size lower than 6 μm was achieved using both 10 and 20 μm membrane, but more uniform droplets were obtained with a 20 μm membrane.

O/W emulsions with a dispersed phase content of 40 wt% showed viscoelastic properties, due to structuration in the emulsion. On the other hand, O/W emulsions with a dispersed phase content of 30 wt% exhibited Newtonian behaviour with the viscosity values in a good correlation with the mean droplet sizes.

Appendix A

For predicting the drop size of the dispersed phase, a force-balance model (Dragosavac et al., 2008) has been used here.

The shear stress τ at the membrane surface varies with the radial distance from the stirrer axis, r, according to the equations (Nagata, 1975):

For $r < r_{trans}$ $$\tau = 0.825\,\eta_c \omega r \frac{1}{\delta} \quad (3)$$

For $r > r_{trans}$ $$\tau = 0.825\,\eta_c \omega r_{trans} \left(\frac{r_{trans}}{r}\right)^{0.6} \frac{1}{\delta} \quad (4)$$

where r_{trans} is the transitional radius, i.e. the radial distance where the shear stress is greatest:

$$\mathrm{r_{trans}} = 1.23\frac{D}{2}\left(0.57 + 0.35\,\frac{D}{T}\right)\left(\frac{b}{T}\right)^{0.036} n_b^{0.116}\,\frac{Re}{1000 + 1.43\,Re} \quad (5)$$

Here, D is the stirrer diameter, T is the cell diameter, b is the blade height, and n_b is the number of impeller blades (Fig. 1A). The rotating Reynolds number is given by: Re = $\omega\rho_c D^2/(2\pi\eta_c)$, where ρ_c and η_c is the continuous phase density and viscosity, respectively, and ω is the angular velocity.

The boundary layer thickness, δ, is defined by the equation (Landau and Lifshitz, 1959):

$$\delta = \sqrt{\eta_c/(\rho_c \omega)} \quad (6)$$

The local shear stresses on the membrane surface are plotted in Figure 4.14. The maximum shear stress τ_{max} is expressed by putting $r = r_{trans}$ in Eq. (3):

$$\tau_{max} = 0.825\,\eta_c \omega r_{trans} \frac{1}{\delta} \qquad (7)$$

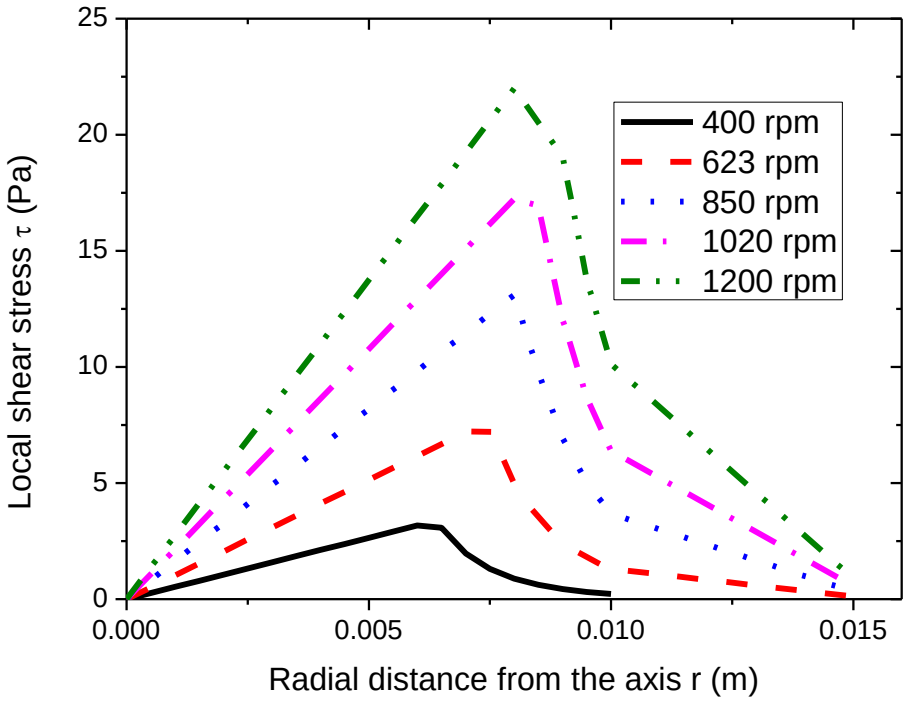

Figure 4.14. The variation of local shear stress over the membrane surface at different stirrer speeds for 30% emulsion, calculating using Eq. (3) or Eq. (4).

The droplet diameter, x, can be predicted from a simple force balance on a droplet at pinch-off: $F_d = F_{ca}$, where F_{ca} and F_d are the capillary and drag force, respectively (Kosvintsev et al., 2005):

$$F_{ca} = \pi d_p \gamma \qquad (8)$$

$$F_d = 9\pi\tau x \sqrt{-r_p^2 + \left(\frac{x}{2}\right)^2} \qquad (9)$$

r_p is the pore radius and γ is the interfacial tension. Solving Eqs. (8) and (9) for x gives the equation for the drop diameter (Kosvintsev et al., 2005 and Stillwell et al., 2007):

$$x = \frac{\sqrt{18\tau^2 r_p^2 + 2\sqrt{81\tau^4 r_p^4 + 4r_p^2\tau^2\gamma^2}}}{3\tau} \qquad (10)$$

Since the pressure on the surface of the membrane is lowest at $\tau=\tau_{max}$, the majority of the drops will be formed near the transitional radius and thus τ_{max} from Eq. (7) will be used instead of τ in Eq. (10).

References

Anastas, P. T., & Warner, J. C. Green Chemistry: Theory and Practice, Oxford University Press, New York, 1998.

Barnes, H. A. (1994). Rheology of emulsions—a review. Colloids and Surfaces A: Physicochemical and Engineering Aspects, 91, 89-95.

Brokel, U., Meier, W., & Wagner, G. Introduction. In: Brokel, U., Meier, W., & Wagner, G, editors. Product Design and Engineering. Vol. 1: Basics and Technologies. Weinheim: Wiley-VCH, 2007:1–3.

Castán, P., & González, X. Skin properties of glycerine polyethoxylene esters. In: Proceedings of 40th Annual Meeting of CED, Vol. 33. 2003:325–338.

Charcosset, C., Limayem, I., & Fessi, H. (2004). The membrane emulsification process—a review. Journal of chemical technology and biotechnology, 79(3), 209-218.

Cheetangdee, N., & Fukada, K. (2012). Protein stabilized oil-in-water emulsions modified by uniformity of size by premix membrane extrusion and their colloidal stability. Colloids and Surfaces A: Physicochemical and Engineering Aspects, 403, 54-61.

Cussler, E.L., & Moggridge, G.D. Chemical Product Design, 2nd ed. Cambridge, UK: Cambridge University Press, 2011.

Denolle, Y., Seita, V., & Delaire V. European Patents and Applications. EP 2368971 A1 20110928, 2011.

Dos Santos, R. G., Bannwart, A. C., Briceno, M. I., & Loh, W. (2011). Physico-chemical properties of heavy crude oil-in-water emulsions stabilized by mixtures of ionic and non-ionic ethoxylated nonylphenol surfactants and medium chain alcohols. Chemical Engineering Research and Design, 89(7), 957-967.

Dragosavac, M. M., Sovilj, M. N., Kosvintsev, S. R., Holdich, R. G., & Vladisavljević, G. T. (2008). Controlled production of oil-in-water emulsions containing unrefined pumpkin seed oil using stirred cell membrane emulsification. Journal of Membrane Science, 322(1), 178-188.

Egidi, E., Gasparini, G., Holdich, R. G., Vladisavljević, G. T., & Kosvintsev, S. R. (2008) Membrane emulsification using membranes of regular pore spacing: Droplet size and uniformity in the presence of surface shear. Journal of Membrane Science, 323(2), 414-420

Höfer, R., & Bigorra, J. (2007). Green chemistry—a sustainable solution for industrial specialties applications. Green Chemistry, 9(3), 203-212.

Karbstein, H., & Schubert, H. (1995). Developments in the continuous mechanical production of oil-in-water macro-emulsions. Chemical Engineering and Processing, 34(3), 205-211.

Kosvintsev, S. R., Gasparini, G., Holdich, R. G., Cumming, I. W., & Stillwell, M. T. (2005). Liquid-liquid membrane dispersion in a stirred cell with and without controlled shear. Industrial & Engineering Chemistry Research, 44(24), 9323-9330.

Kukizaki, M., & Goto, M. (2007). Preparation and evaluation of uniformly sized solid lipid microcapsules using membrane emulsification. Colloids and Surfaces A: Physicochemical and Engineering Aspects, 293(1-3), 87-94.

Landau, L. D., & Lifshitz, E. M. (1959). Fluid mechanics, 1959. Course of Theoretical Physics.

Lutz, P.J. Ca. Patents Applications.CA 2537554 A1 20060822, 2006.

Ma, G. (2003). Control of polymer particle size using porous glass membrane emulsification: A review. China Particuology, 1(3), 105-114.

McClements, D. J. Food Emulsions: Principles, Practice, and Techniques. Boca Raton: CRC Press, 2005.

Medvedovici, A., Udrescu, S., & David, V. (2013). Use of a green (bio) solvent–limonene–as extractant and immiscible diluent for large volume injection in the RPLC-tandem MS assay of statins and related metabolites in human plasma. Biomedical Chromatography, 27(1), 48-57.

Mezger, T. G. (2006). The rheology handbook: for users of rotational and oscillatory rheometers. Vincentz Network GmbH & Co KG.

Nagata, S. (1975). Mixing: principles and applications (Vol. 44). Tokyo: Kodansha.

Nazir, A., Schroën, K., & Boom, R. (2011). High-throughput premix membrane emulsification using nickel sieves having straight-through pores. Journal of Membrane Science, 383(1), 116-123.

Nazir, A., Schroën, K., & Boom, R. (2013). The effect of pore geometry on premix membrane emulsification using nickel sieves having uniform pores. Chemical Engineering Science, 93, 173-180.

Peng, S. J., & Williams, R. A. (1998). Controlled production of emulsions using a crossflow membrane: Part I: Droplet formation from a single pore. Chemical Engineering Research and Design, 76(8), 894-901.

Ramakrishnan, S., Ferrando, M., Aceña-Muñoz, L., De Lamo-Castellví, S., & Güell, C. (2013). Fish oil microcapsules from O/W emulsions produced by premix membrane emulsification. Food and Bioprocess Technology, 6(11), 3088-3101.

Santos, J., Trujillo-Cayado, L. A., Calero, N., & Muñoz, J. (2014). Physical characterization of eco-friendly O/W emulsions developed through a strategy based on product engineering principles. AIChE Journal. 60(7), 2644-2653.

Schubert, H., Ax, K., & Behrend, O. (2003). Product engineering of dispersed systems. Trends in Food Science & Technology, 14(1), 9-16.

Stillwell, M. T., Holdich, R. G., Kosvintsev, S. R., Gasparini, G., & Cumming, I. W. (2007). Stirred cell membrane emulsification and factors influencing dispersion drop size and uniformity. Industrial & Engineering Chemistry Research, 46(3), 965-972.

Suzuki, K., Fujiki, I., & Hagura, Y. (1998). Preparation of Corn Oil/Water and Water/Corn Oil Emulsions Using PTFE Membranes. Food Science and Technology International, Tokyo, 4(2), 164-167.

Suzuki, K., Shuto, I., & Hagura, Y. (1996). Characteristics of the Membrane Emulsification Method Combined with Preliminary Emulsification for Preparing Corn Oil-in-Water Emulsions. Food Science and Technology International, Tokyo, 2(1), 43-47.

Trujillo-Cayado, L. A., Ramírez, P., Pérez-Mosqueda, L. M., Alfaro, M. C., & Muñoz, J. (2014a). Surface and foaming properties of polyoxyethylene glycerol ester surfactants. Colloids and Surfaces A: Physicochemical and Engineering Aspects, 458(1), 195-202.

Trujillo-Cayado, L. A., Ramírez, Ruiz, M., Alfaro, M. C., & Muñoz, J. (2014b). Adsorption at the biocompatible -pinene–water interface and emulsifying properties of two eco-friendly surfactants. Colloids and Surfaces B: Biointerfaces, 122(1), 623-629

van Aken, G. A. (2002). Flow-induced coalescence in protein-stabilized highly concentrated emulsions. Langmuir, 18(7), 2549-2556.

van der Zwan, E., Schroen, K., van Dijke, K., & Boom, R. (2006). Visualization of droplet break-up in pre-mix membrane emulsification using microfluidic devices. Colloids and Surfaces A: Physicochemical and Engineering Aspects, 277(1-3), 223-229.

Vladisavljević, G. T., Shimizu, M., & Nakashima, T. (2004). Preparation of monodisperse multiple emulsions at high production rates by multi-stage premix membrane emulsification. Journal of Membrane Science, 244(1), 97-106.

Vladisavljević, G. T., Surh, J., & McClements, J. D. (2006). Effect of emulsifier type on droplet disruption in repeated Shirasu porous glass membrane homogenization. Langmuir, 22(10), 4526-4533.

Vladisavljević, G. T., Shimizu, M. & Nakashima, T. (2006b). Production of multiple emulsions for drug delivery systems by repeated SPG membrane homogenization: Influence of mean pore size, interfacial tension and continuous phase viscosity. Journal of Membrane Science, 284(1-2), 373-383.

Walter J. (2010). Metabolism of terpenoids in animal models and humans. In: Husnu Can Baser K, Buchbauer, G., editors. Handbook of essential oils: Science, Technology and Applications. Boca Raton: CRC Press, 209-232.

Yafei, W., Tao, Z., & Gang, H. (2006). Structural evolution of polymer-stabilized double emulsions. Langmuir, 22(1), 67-73.

Yuan, Q., Williams, R. A., & Biggs, S. (2009). Surfactant selection for accurate size control of microcapsules using membrane emulsification. Colloids and Surfaces A: Physicochemical and Engineering Aspects, 347(1), 97-103.

Zhou, Q. Z., Ma, G. H., & Su, Z. G. (2009). Effect of membrane parameters on the size and uniformity in preparing agarose beads by premix membrane emulsification. Journal of membrane science, 326(2), 694-700.

Vankova, N., Tcholakova, S., Denkov, N.D., Ivanov, I.B., Vulche, V.D. & Danner, T. (2007) Emulsification in turbulent flow. 1. Mean and maximum drop diameters in inertial and viscous regimes. J Colloid Interf Sci, 312: 363-380.

Chapter 5: Development of eco-friendly emulsions produced by microfluidization technique.

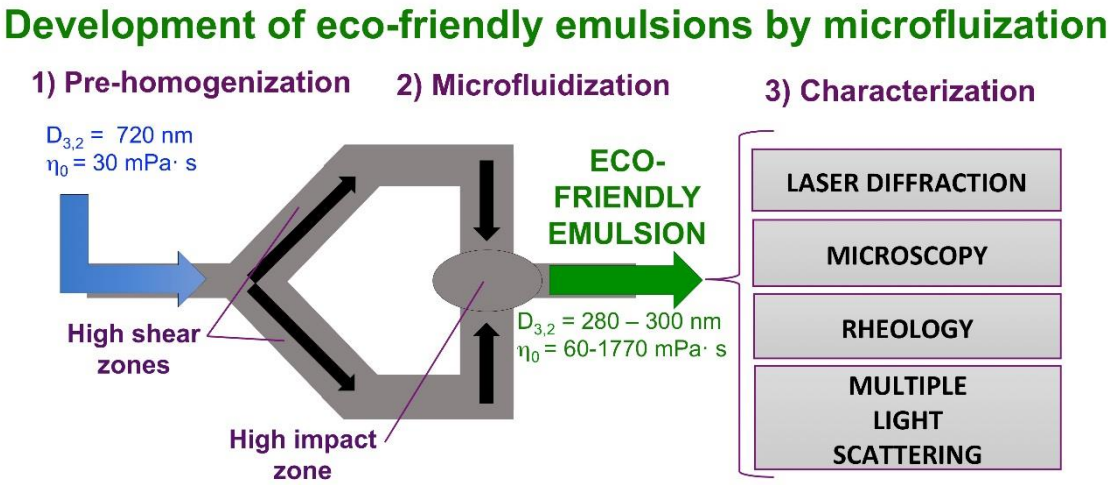

Abstract

Green solvents have recently attracted much attention due to the necessity of replacing traditional solvents. In this work, a mixture of eco-friendly solvents and a green surfactant have been utilized in emulsions with a potential use for agrochemicals. Results obtained show that the Microfluidizer® was capable of producing very fine nanoemulsions ($D_{3,2}$ = 280 nm).This contribution has demonstrated the significant role of the rheology to understand the destabilization processes which occur in emulsions with very similar DSD. Thus, we found the optimum homogenization pressure was 1034 bar (15000 psi) on account of the lack of creaming and of low coalescence.

5.1. Introduction

The task of product engineering is to produce products of a certain quality, i.e. with specific properties. All properties are the result of specific physical and chemical effects in the product, which are determined by the choice of the formulation and processing conditions. Many important properties of emulsions are largely influenced by structural parameters such as the volume ratio of the phases and particle size distribution.[1] The droplet size distribution (DSD) of the emulsions strongly depends on the emulsification method used.

Interest in submicron emulsions has increased recently due to their very small DSD, high stability, and their applications in many industrial fields such as personal care and cosmetics, health care, pharmaceuticals, and agrochemicals. [2,3] Emulsions whose average droplet size falls in the range of 100-500 nm could be considered as nanoemulsions.[4] In spite of the fact that submicron emulsions can be produced by

both low and high-energy methods, the latters generally more likely to be used in the industry due to their scale up and equipment availability. [5] Typically submicron emulsions are produced either by using a high-pressure valve homogenizer (HPVH) or a Microfluidizer. A piston pump and a narrow gap are the main parts in a HPVH. In the narrow gap there is a valve, which is able to arrive at homogenization pressure up to 150 MPa. Break-up of the droplets occurs in the region of the valve gap, and in the jet after the gap. By contrast, droplet break-up occurs in the Microfluidizer due to the impact of two impinging jets achieving similar pressures as those obtained in a HPVH. In this process, high turbulence and tremendous shearing action are created. Consequently, this forces flow stream to pass though well-defined microchannels. As a result, extraordinarily fine emulsions are created. In fact, it has been observed that emulsions produced by microfluidization possess narrower DSD to those prepared using a HPVH.[6,7] It is also shown that a continued increase in the homogenization pressure in the Microfluidizer provoked a decrease in droplet size.[8] However, this fact was not observed under all circumstances. Furthermore, microfluidization is unfavorable in some specific situations, such as higher pressures and longer emulsification times. This could lead to over-processing, namely the re-coalescence of emulsion droplets.[9,10] Although the effect of the homogenization pressure on droplet size is well known, there is no reported systematic study of the effect of homogenization pressure on rheology of submicron emulsions processed in microfluidizers and how this property affects the stability of these emulsions.

In recent years, there has been an increasing interest in using the so-called “green solvents” due to the need to replace traditional organic solvents by more environmentally favorable solvents.[11] N,N-dimethyldecanamide (AMD-10) is

considered a safe biosolvent, according to the Environmental Protection Agency. Therefore, it is a good solvent for agrochemical use due to the lack of risk to the farmer satisfying the needs of customers, which is the basic principle of the product design.[12,13] D-Limonene, the most common terpene used as a solvent, is an interesting bio-derived solvent that can be obtained from citrus rinds. This compound is an environmental friendly chemical, which can replace typical volatile organic compounds. Hence, D-limonene is considered as a good choice to be included as a solvent in the formulation of agrochemicals. [14,15] Furthermore, the mixture of AMD-10 and D-Limonene has been recently used in emulsions as a solvent by Santos et al, 2014.[16]

In addition, environmentally friendly surfactants have also recently attracted significant interest. Polyoxyethylene glycerol esters, which are non-ionic surfactants, have been considered adequate for designing ecological products due to the fact that they are completely innocuous for human skin and hair. [17] It has been used in detergents and personal care products.[18,19] One of these surfactants, namely Levenol C-201, possesses ecolabel (DID list: 2133). In addition, the interfacial properties at the air/water and □-pinene/water interface of these surfactants, namely the equilibrium adsorption, dynamic surface tension and interfacial rheology have been recently reported. [20,21]

The goal of this study was to investigate the influence of emulsification pressure on the rheological properties, DSD and the physical stability of O/W eco-friendly emulsions. This formulation not only contains two green solvents but also an ecofriendly surfactant

that satisfy the new needs of a bio-based society. This work could be considered the continuation of the previously reported article by Santos et al (2014).[16]

5.2. EXPERIMENTAL SECTION

5.2.1. Materials

N,N Dimethyl Decanamide (Agnique AMD-10^{TM}) and D-Limonene was kindly supplied by BASF and Sigma Chemical Company, respectively. A non-ionic surfactant derived from cocoa oil (polyoxyethylene glycerol fatty acid ester, Glycereth-17 Cocoate) was used as an emulsifier. Its trade name is Levenol C-201^{TM} and it was received as a gift from KAO. The safety data sheet provided by the supplier reports a value for oral toxicity (LD50) higher than 5000 mg/kg of animal in tests carried out with rats. It is interestingly to note that this value would be 3000 mg/kg for salt [22]. An antifoaming agent (RD antifoam emulsion, DOW CORNING) was used. All emulsions were prepared using deionized water.

5.2.2. Emulsion development

5.2.2.1. Coarse emulsion preparation.

The aqueous phase was a solution of deionized water, 0.1 wt% antifoam emulsion and 3 wt% of the green surfactant. The oil phase (30 wt%) consisted of a mixture of two eco-friendly solvents: AMD-10 and D-Limonene in a ratio of 75/25. This ratio of solvents was previously demonstrated to be optimum by Santos et al., 2014.[16]

The coarse emulsion was created using a rotor-stator homogenizer (Silverson L5M), equipped with a mesh screen, at 4000 rpm during 60 seconds.

5.2.2.2. Microfluidization

The coarse emulsion was passed through an air-driven microfluidizer (Model M-110P, Microfluidics, USA) operating from 5000 to 25000 psi (345-1724 bar). This equipment included a pneumatic pump, a filter, and an interaction chamber F12Y (Minimun internal dimension 75 µm).

Emulsions were homogenized at different pressures and they were named as table 5.1 shows.

Table 5.1. Relation between name of emulsion and pressure that emulsion were processed at.

Emulsion name	Pressure applied (psi)	Pressure applied (bar)
E1	5000	345
E2	10000	689
E3	15000	1034
E4	20000	1379
E5	25000	1724

The outflow sample tube of the microfluidizer was cooled with water at 15ºC in order to slow down the rise of temperature. For each pressure, a 250 g sample was prepared and passed through the microfluidizer at the set pressure for 1 cycle. Emulsions were prepared in duplicate

5.2.3 Droplet size distribution measurements.

Droplet size distributions and mean diameters of oil droplets were measured by the technique of laser diffraction (Mastersizer X, Malvern, Worcestershire, United Kingdom). All measurements were carried out in triplicate for each emulsion. The

influence of aging time on droplet size distributions were carried out 1, 3, 13, 21 and 40 days after preparation.

The mean droplet diameters were expressed as Sauter diameters ($D_{3,2}$) and volume mean diameter ($D_{4,3}$):

$$D_{3,2} = \sum_{i=1}^{N} n_i d_i^3 / \sum_{i=1}^{N} n_i d_i^2 \quad \text{Eq. (1)}$$

$$D_{4,3} = \sum_{i=1}^{N} n_i d_i^4 / \sum_{i=1}^{N} n_i d_i^3 \quad \text{Eq. (2)}$$

where d_i is the droplet diameter, N is the total number of droplets and n_i is the number of droplets having a diameter d_i.

5.2.5. Rheological measurements.

Rheological tests were performed with a controlled-stress rheometer (Haake MARS, Thermo-Scientific, Germany), equipped with a sand-blasted coaxial cylinder Z-20 (sample volume: 8.2 mL, R_e/R_i =1.085, R_i= 1 cm). Flow curves were carried out from 0.05 Pa to 2 Pa at 20 ºC. The results show the mean of three measurements done of emulsions aged for 1, 3, 13, 21 and 40 days.

5.2.6. Multiple light scattering

Multiple light scattering measurements were conducted with a Turbiscan Lab Expert until 40 days at 20 ºC. Multiple light scattering is a sensitive and non-intrusive tool to allow physical stability of complex fluids to be analysed.[23,24,25]

The creaming index (CI) [26] shown below was able to characterize the creaming phenomenon:

$$CI = \frac{H_S}{H_E} \cdot 100 \quad \text{Eq. (3)}$$

Where, H_E is the total height of the emulsion and H_S is the height of the serum layer.

Turbiscan stability index (TSI) is a parameter that can be used for the estimation of emulsion stability. In this study, it has been applied to study the coalescence phenomenon observed in the middle part of the measuring cell. When the TSI value increases, the stability of the system decreases. This index is a statistical factor and its value is given by the following equation [27,28]:

$$TSI = \sum_j \left| scan_{ref}(h_j) - scan_i(h_j) \right| \quad \text{Eq. (4)}$$

where $scan_{ref}$ and $scan_i$ are the initial backscattering value and the backscattering value at a given time, respectively. h_j is a given height in the measuring cell and TSI is the sum of all the scan differences in the intermediate zone of the measuring cell.

5.2.7. Microscopic observation.

The microstructure of emulsions was observed at room temperature using an optical microscope Axio Scope A1 (Carl Zeiss) with an AxioCam camera. Microphotographs were taken of all emulsions with a 40x objective and with via the contrast phase technique. All samples were diluted to 1:10 in distilled water in order to improve the view of droplets in the micrographs.

5.2.8. Statistical analysis.

Laser diffraction and rheological tests were carried out in triplicate, and the resulting data was analysed using one-way analysis of variance (ANOVA). This was carried out using Microsoft excel 2013. All statistical calculations were conducted at a significance level of p= 0.05.

5.3. Results and discussion

Figure 5.1 shows the droplet size distribution (DSD) for emulsions as a function of different emulsification processes: emulsion processed at 4000 rpm in rotor-stator (pre-emulsion or coarse emulsion) and the emulsions processed at different homogenization pressures (345-1724 bar) in the Microfluidizer. The coarse emulsion showed a monomodal DSD while all emulsions processed in the Microfluidizer showed two populations of droplets. An excess of mechanical energy-input is the reason for the appearance of droplets above 1 µm as previously reported.[16,29]

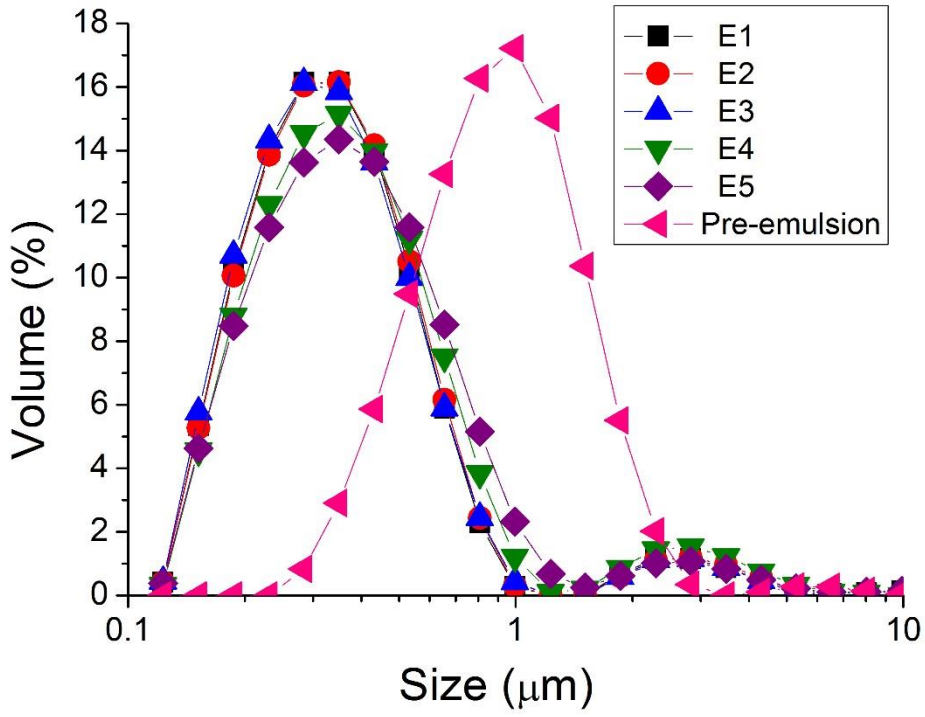

Figure 5.1. Droplet size distribution for pre-emulsion and emulsions processed in Microfluidizer at different pressures at one day of aging time.

In the Microfluidizer, the energy input can be increased by the operating pressure. The Sauter diameter of coarse emulsions was more than 700 nm but the Microfluidizer was able to reduce this emulsion size significantly (Table 5.2). All emulsions processed in the Microfluidizer showed submicron Sauter and volumetric diameters. Results of the

ANOVA test demonstrated that there are no significantly differences in the DSD of the emulsions processed in the Microfluidizer.

Table 5.2. Sauter and volumetric mean diameters for pre-emulsion and emulsions processed in Microfluidizer at different pressures one day after preparation.

Standard deviation of the mean (3 replicates) for $D_{3,2}$ < 4%

Standard deviation of the mean (3 replicates) for $D_{4,3}$ < 6%

Emulsion	$D_{3,2}$ (nm)	$D_{4,3}$ (nm)
E1	280	440
E2	280	430
E3	280	430
E4	290	430
E5	300	440
Pre-emulsion	730	930

Flow curves representing the viscosity, η, and dependence on the shear rate, $\dot{\gamma}$, for emulsions studied as a function of homogenization pressure after one day of aging time are shown in figure 5.2. These results fitted fairly well to the Cross model (R^2>0.999) (Eq 5).

$$\eta = \frac{\eta_0}{1+\left(\frac{\dot{\gamma}}{\dot{\gamma}_C}\right)^{1-n}} \qquad \text{Eq. (5)}$$

Where $\dot{\gamma}_c$ is related to the critical shear rate for the onset of shear-thinning response, η_0 stands for the zero-shear viscosity and (1-n) is a parameter related to the slope of the power-law region; n being the so-called “flow index”.

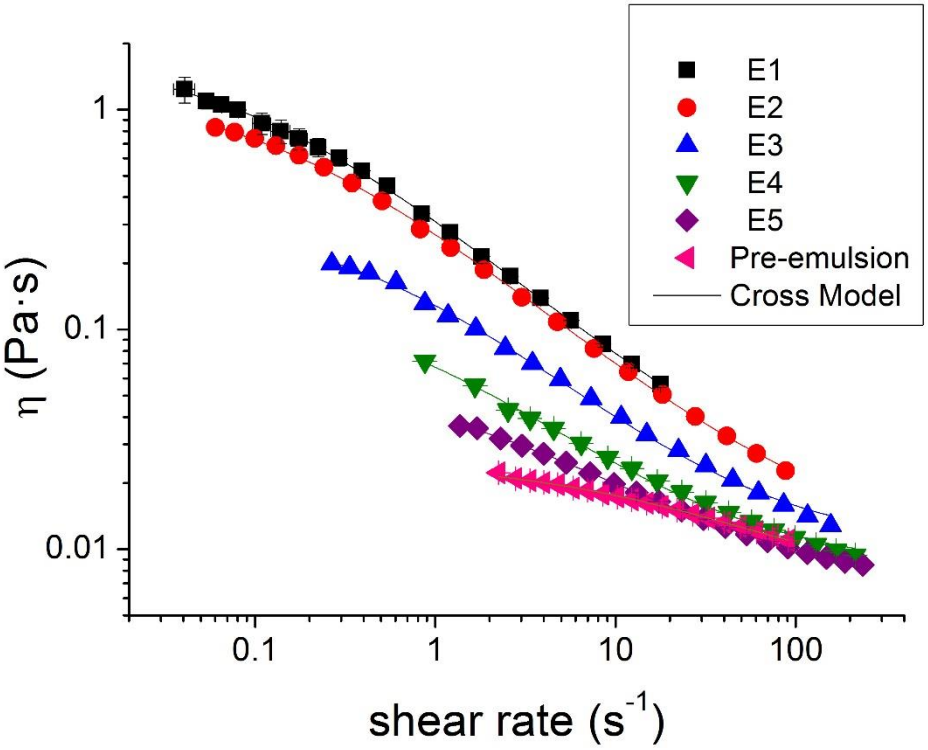

Figure 5.2. Flow curves for emulsions studied as a function of homogenization pressure for 1 day aging time at 20ºC. Continuous lines illustrate data fitting to the Cross model.

Table 5.3. Flow curves fitting parameters for the Cross model for studied emulsions as a function of surfactant concentration at 1 day of aging time.

Standard deviation of the mean (3 replicates) for η_0, η_∞ < 8%

Standard deviation of the mean (3 replicates) for $\dot{\gamma}_c$ < 10%

Standard deviation of the mean (3 replicates) for n < 10%

Emulsion	η_0 (Pa·s)	η_∞ (Pa·s)	$\dot{\gamma}_c$ (s^{-1})	n
Pre-emulsion	0.03	0.003	16.80	0.50
E1	1.77	0.013	0.11	0.28
E2	1.24	0.010	0.16	0.28
E3	0.33	0.008	0.46	0.28
E4	0.15	0.008	0.63	0.27

E5	0.06	0.006	2.04	0.31

The values of these parameters are shown in Table 5.3 as a function of the emulsion processing. Coarse emulsions showed very different fitting parameter values than the emulsions processed in the Microfluidizer: lower zero shear viscosity and shear thinning behavior. This is consistent with the different mean diameters between coarse emulsions and emulsions processed in the Microfluidizer. The droplet-size effect in the rheology is particularly important for fine dispersions with droplets considerably smaller than 1 μm.[30] In regards to the emulsions processed in the Microfluidizer at different pressures, an increase in pressure provoked a decrease in zero shear viscosity and an increase in critical shear rate. ANOVA tests demonstrated that there are significant differences in zero-shear viscosity and critical shear rates for the emulsions studied. Taking into account that emulsions processed in the Microfluidizer turned out to have the same mean diameters, the aforementioned difference in zero shear viscosity is due to a flocculation phenomenon.[31,32] An increase in the homogenization pressure probably broke some flocs and decreased the zero shear viscosity since interactions of oil phase/emulsifier and emulsifier/emulsifier are influenced by homogenization conditions. [33]

All emulsions processed in the Microfluidizer showed more shear-thinning behaviour than the coarse emulsion. It is related to the flocculation of microfluidized emulsions. Higher values of the slope of the viscosity versus shear rate plot point out more structured systems (aggregates of oil droplets). [34]

Figure 5.3 shows the Sauter and volumetric mean diameters as a function of the homogenization pressure for emulsions aged for 1 to 40 days. Taking into account the increase of $D_{3,2}$ and $D_{4,3}$ from day 1 to day 40 for the studied emulsions, the results obtained pointed out that the occurrence of some coalescence for emulsions developed in the 345-1379 bar range. By contrast, the E5 emulsion did not show any significant change of droplet sizes. It is noted that the emulsion that showed the highest value of zero shear viscosity increased the droplet size the most. It is consistent with the fact that coalescence tends to occur when droplets have been in contact for extended periods of time, i.e. in flocculated emulsions. This is the reason why the E5 emulsion did not show changes in droplet size with aging time.

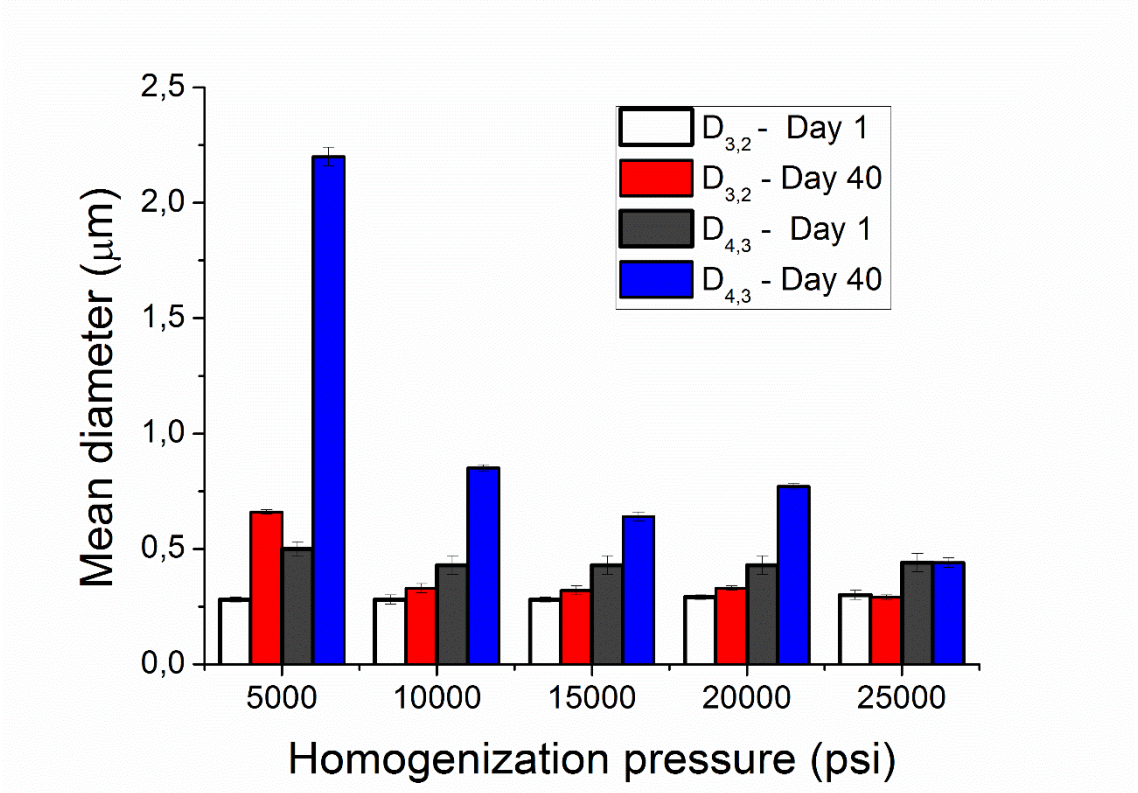

Figure 5.3. Sauter and volumetric mean diameters as a function of aging time for the emulsions processed at different pressures in Microfluidizer.

Additionally, figure 5.4.A and 5.4.B show the microphotographs at one day and 40 days of aging time for the E1 emulsion. Optical microscopy with a 40x objective does not possess enough resolution to an accurate analysis of droplets with diameters below 1 µm. However, bigger droplets were analysed by an image analysis software (MatLab). Mean radius at one day of aging time was 0.63 ± 0.06 µm and 1.91 ±0.63 µm at 40 days of aging time. Therefore, a clear coalescence phenomenon was clearly detected with aging time. This coalescence was also qualitatively supported by laser diffraction results.

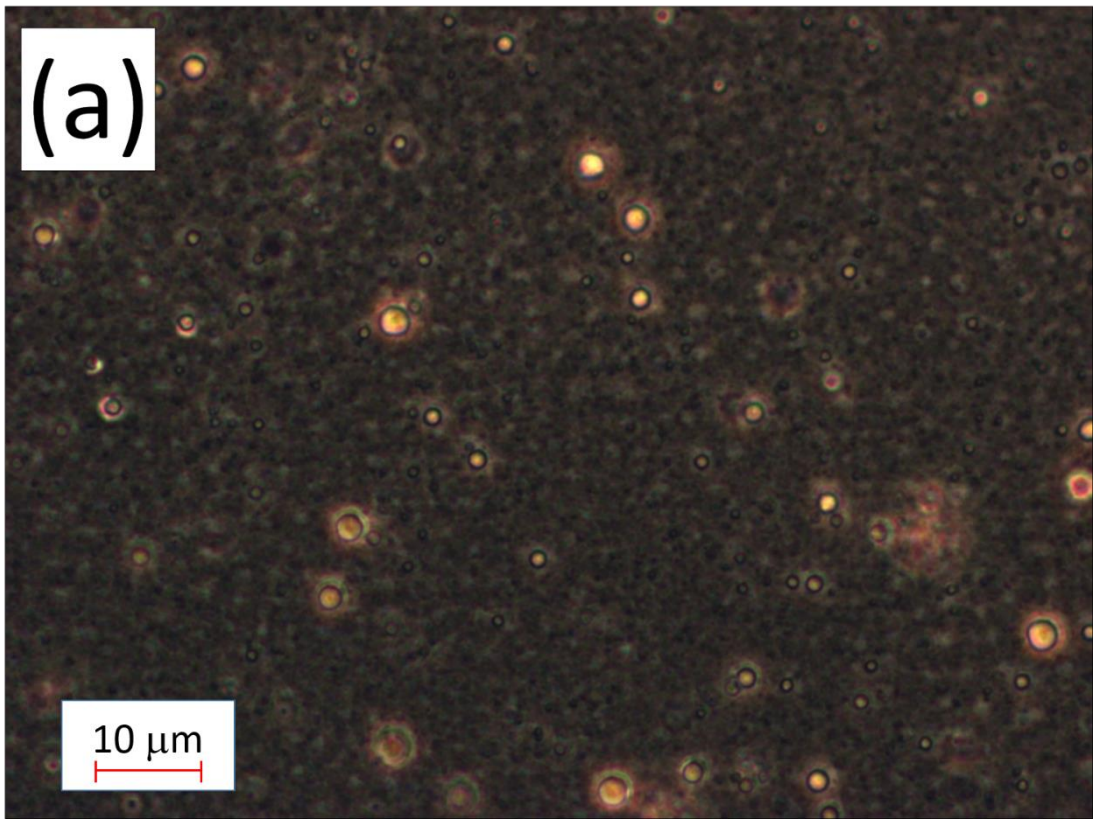

Figure 5.4.A. Photomicrograph for E1 emulsion at 1 day of aging time.

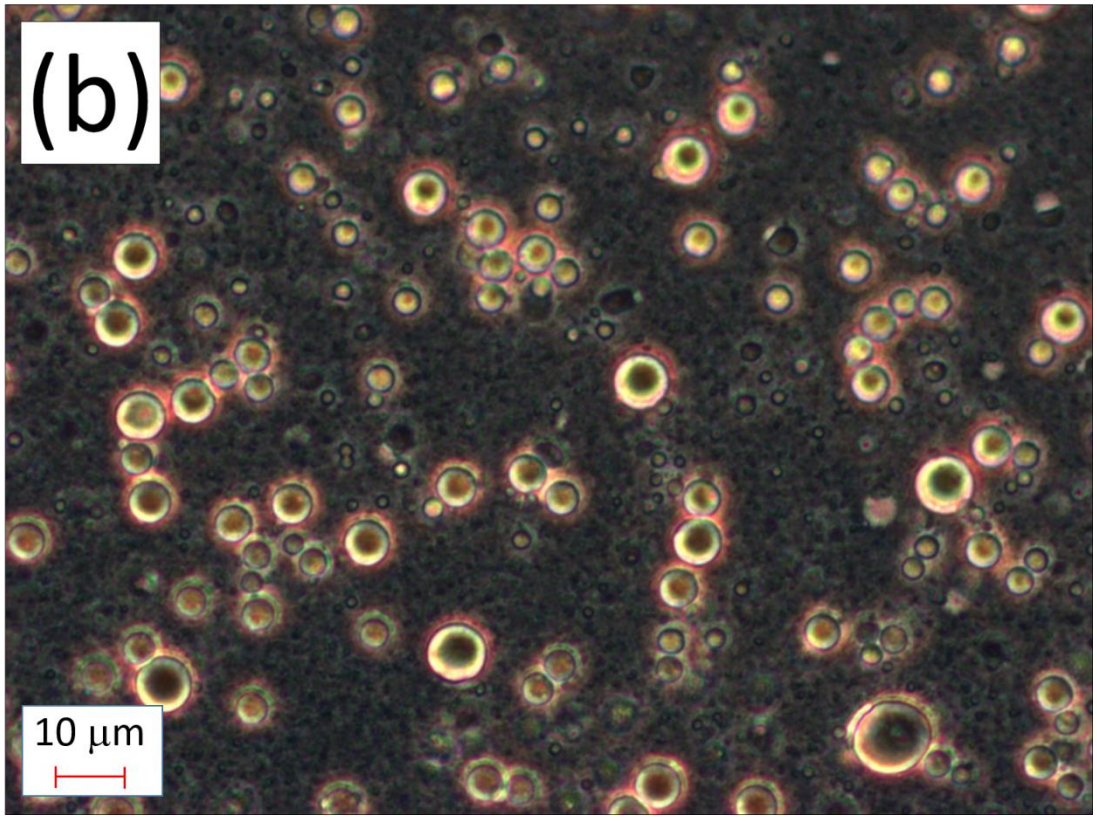

Figure 5.4.B. Photomicrograph for E1 emulsion at 40 days of aging time.

Figure 5.5 shows the zero shear viscosity as a function of aging time for emulsions processed in the Microfluidizer. A progressive increase of zero shear viscosity was detected for the E5 emulsion. In addition, an increase of zero shear viscosity from day 1 to day 3 was also detected for E1, E2 and E4 emulsions. The increase of zero shear viscosity with aging time indicated a destabilization process by incipient creaming and/or flocculation. However, a decrease in zero shear viscosity from day 3 to 40 for E1,E2 and E4 emulsions and a slight decrease in zero-shear viscosity for the E3 emulsion were detected. This fact pointed out a coalescence process that supports laser diffraction results (see figure 4.3). Thus, the incipient flocculation/creaming of E1,E2 and E4 emulsions have led to a coalescence phenomenon.

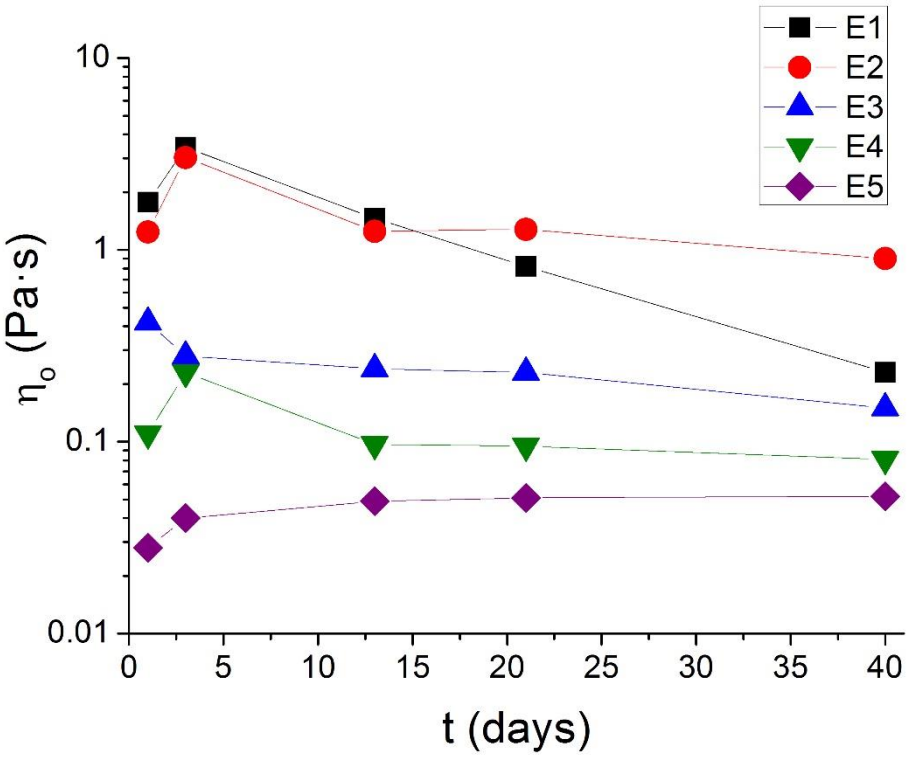

Figure 5.5. Zero-shear viscosity as a function of aging time for all the studied. emulsions. Note: Standard deviation of the mean (3 replicates) for η_0 < 8%.

Figure 5.6 shows the results of the physical stability study performed at 20 ºC by the multiple light scattering technique for E1 and E5 emulsions. Figure 5.6A shows a plot of backscattering (BS) versus height of the measuring cell at 20 ºC for E1 emulsion. This figure also includes an inset where backscattering is plotted versus the cell height measurement in order to display a higher resolution of backscattering changes. A backscattering increase in the lower and intermediate zones of the measuring cell was observed whereas it decreased in the upper zone. The fact that the backscattering increases in the lower and intermediate zone suggests that destabilization mechanisms such as flocculation and coalescence were significant for this emulsion. [25] Concerning the backscattering decrease observed at the top of the measuring cell, we think it may be attributed to the occurrence of some coalescence as a consequence of the migration

of bigger droplets to the top. This coalescence led to an oiling-off process. This behaviour was also shown by the E2 and E3 emulsions. This coalescence showed in MLS is the cause of the decrease of zero shear viscosity with aging time (fig 5.5). In addition, MLS supports laser diffraction results.

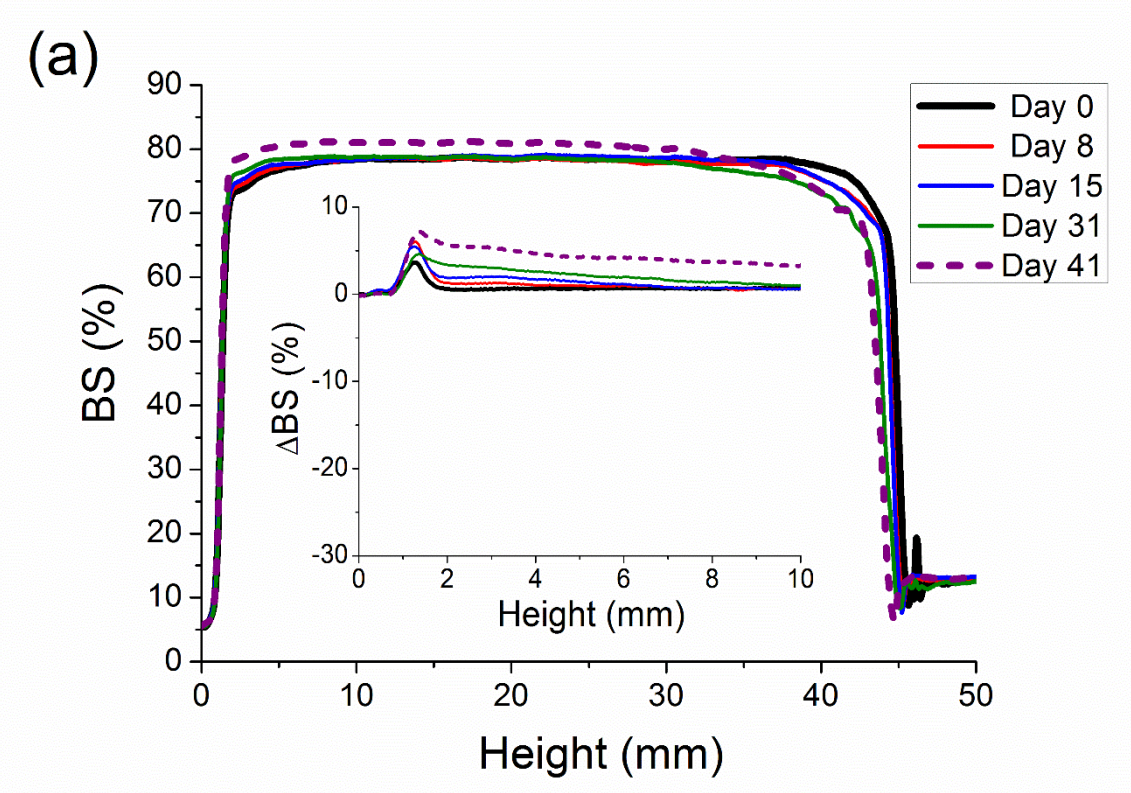

Figure 5.6a. Backscattering versus measuring cell height as a function of aging time in normal (main figures) and reference mode (insets) for E1 emulsion at 25°C. Note: the insets illustrate ΔBS values at the bottom of the measuring cell.

Figure 5.6b shows a plot of BS versus container height for the E5 emulsion. BS did not change in the intermediate zone for the E5 emulsion. This suggests that neither coalescence nor flocculation were taking place. Nevertheless, a decrease in BS in the bottom zone of the measuring cell was observed, which reveals the beginning of a creaming process. [34] This fact is consistent with the rheological results with aging time. With regards to the backscattering decrease observed at the top of the measuring cell,

we think it may be attributed to the aforementioned oiling-off. This behaviour is also observed in the E4 emulsion. However, this emulsion also showed a slight increase of the BS in the intermediate zone of the measuring cell due to coalescence as previously explained. This coalescence was also shown by mean of both rheological and laser diffraction techniques.

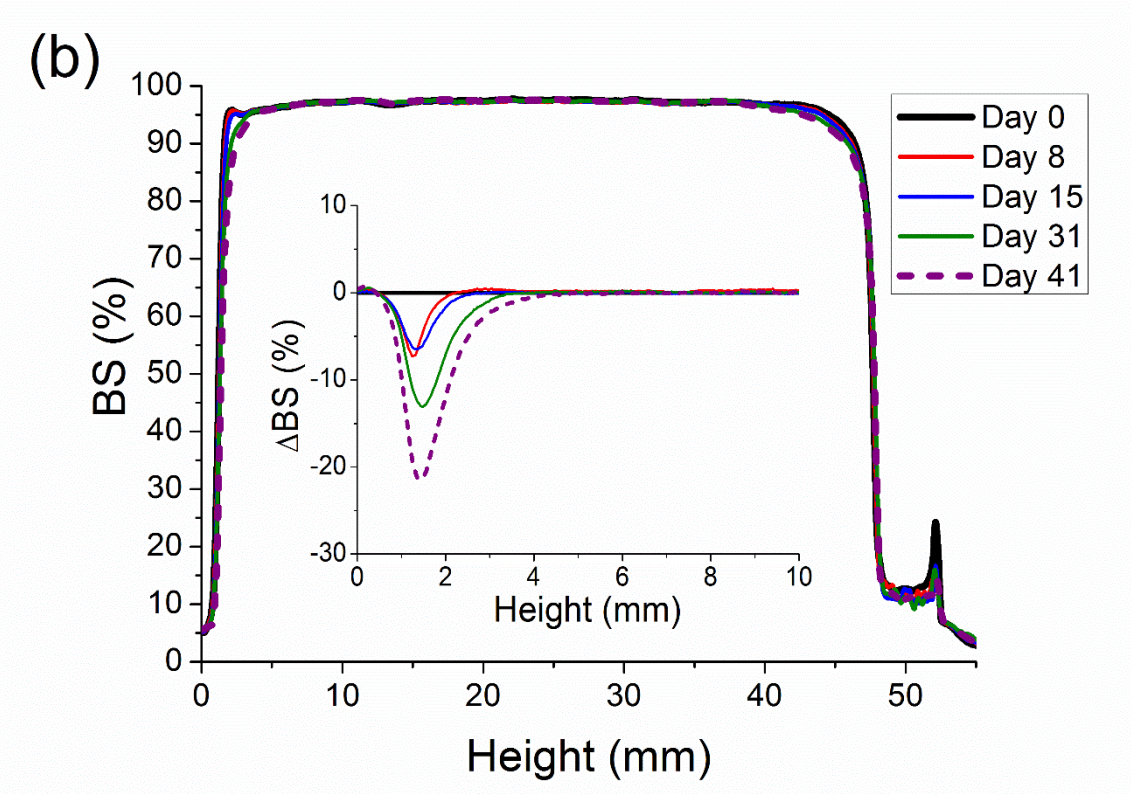

Figure 5.6b. Backscattering versus measuring cell height as a function of aging time in normal (main figures) and reference mode (insets) for E5 emulsion at 25°C. Note: the insets illustrate ΔBS values at the bottom of the measuring cell.

Figure 5.7.A shows the Turbiscan Stability Index (TSI) in the middle zone of the measuring cell for emulsions processed in Microfluidics at 40 days of aging time. Higher values of TSI in the middle zone are related to the coalescence and/or flocculation phenomena. The E1 emulsion exhibited the highest value of TSI while the E5 emulsion showed the lowest. The highest TSI values in the intermediate zone for the E1 and E2

emulsions confirmed they underwent a coalescence phenomenon, as experimentally checked by laser diffraction. The E3 and E4 emulsions did not show such high TSI values as compared to the E1 and E2 emulsions. Thus, the E5 emulsion showed the lowest value of TSI at 40 days of aging time, which supports the laser diffraction and rheology results.

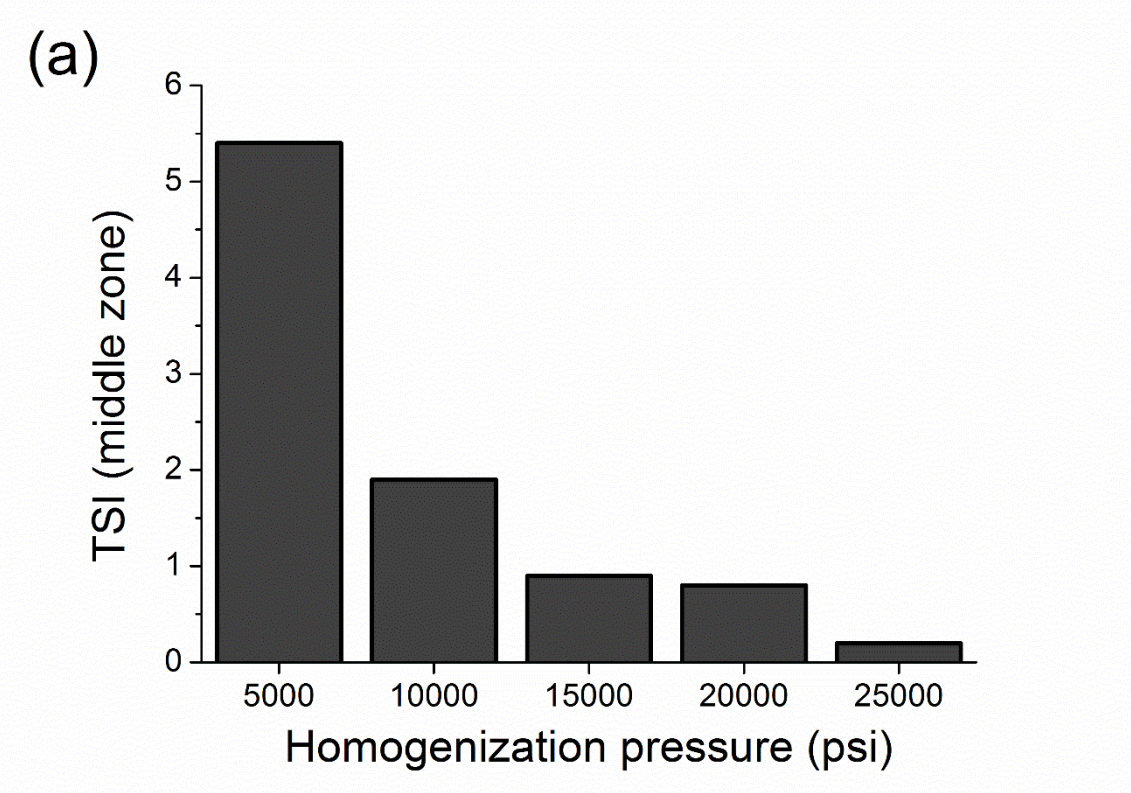

Figure 5.7a. Turbiscan Stability Index (TSI) in the middle zone of the measuring cell for studied emulsions at 40 day of aging time.

Figure 5.7.B shows the creaming index (CI) as a function of aging time for emulsions processed at different homogenization pressures. It should be stated that E1,E2 and E3 emulsions did not show creaming in MLS. By contrast, E4 and E5 emulsions showed an increase of CI with aging time. Moreover, the initial slope of the plot of CI versus time is related to the creaming rate (ω):

$$\omega = \frac{d(CI)}{dt}\,\frac{H_E}{100} \qquad \text{Eq. (6)}$$

Creaming rate values were very similar for these emulsions (see inset figure 7b). However, an increase of 7 days for delay time was found for the E4 emulsion in comparison with the E5 emulsion. This is explained by the difference of the zero shear viscosity of the emulsions at one day of aging time. Emulsions with lower viscosities tend to break up more quickly by creaming. [26]. Furthermore, the emulsion that showed an increase of zero shear viscosity with aging time (E5 emulsion) is the emulsion that present the lowest delay time for creaming. Hence, both techniques supports each other.

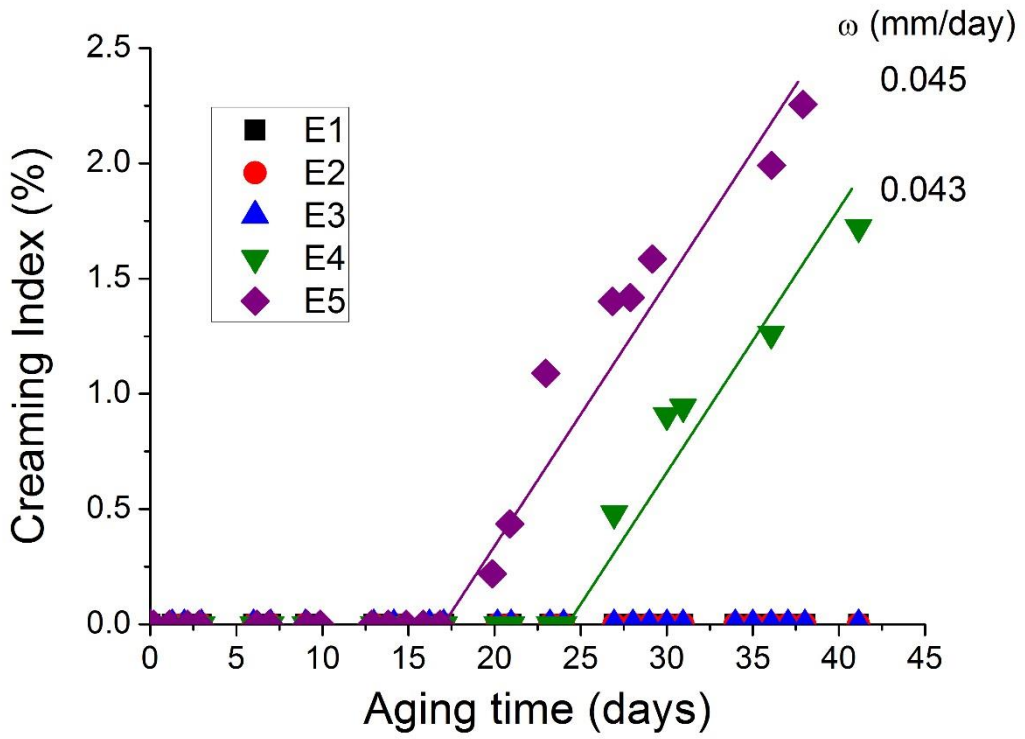

Figure 5.7b. Creaming Index as a function of aging time for studied emulsions.

5.4. Conclusions

Microfluidization was capable of producing nano-emulsions for the eco-friendly formulation studied, regardless of the homogenization pressure used. These emulsions

showed re-coalescence due to an over-processing undergone during their preparation. In spite of the fact that all microfluidized emulsions did not show significant changes in the DSD, these emulsions exhibited different values of zero shear viscosity. Emulsions processed at lower homogenization pressures showed higher values of zero shear viscosity; this is related to flocculated emulsions. This flocculation led to a coalescence process. Furthermore, slightly flocculated emulsions did not show an increase of the droplet size, but rather the creaming process took place. Consequently, moderate pressure of 1034 bar (15000 psi) responded better than higher or lower pressures due to the lack of creaming and a lower coalescence. Hence, Rheology was a relevant and decisive tool to allow us to understand why different destabilization mechanisms occur depending on homogenization pressure in emulsions with very similar DSD.

References

[1] H. Schubert, K. Ax, O. Behrend, *Trends. Food. Sci. Tech*. *14 (2003)* 9-16.

[2] S. Schultz, G. Wagner,K. Urban,J. Ulrich, *Chem. Eng. Technol*. *27(*2004*)* 361-368. DOI: 10.1002/ceat.200406111

[3] O. Sonneville-Aubrun, J.T. Simonnet, F. L'alloret, *Adv. Colloid. Interfac*. *108 (*2004*)* 145-149. DOI: 10.1016/j.cis.2003.10.026

[4] S.Y. Tang, P. Shridharan, M. Sivakumar, *Ultrason. Sonochem*. 20(2013) 485-497.DOI:10.1016/j.ultsonch.2012.04.005

[5] D.J. McClements, J. Rao, *Cri. Rev. Food. Sci*. *51 (*2011*)* 285-330. DOI: 10.1080/10408398.2011.559558.

[6] K.B. Strawbridge, E. Ray, F.R. Hallett, S.M. Tosh, D.G. Dalgleish, *J. Colloid. Interf. Sci. 171 (*1995*)* 392-398. DOI: 10.1006/jcis.1995.1195

[7] J.M. Perrier-Cornet, P. Marie, P. Gervais, *J. Food. Eng*. *66 (*2005*)* 211-217. DOI: 10.1016/j.jfoodeng.2004.03.008

[8] C. Qian, D.J. McClements, *Food. Hydrocoll*. *25(*2011*)* 1000-1008. DOI: 10.1016/2fj.foodhyd.2010.09.017

[9] S.M. Jafari, E. Assadpoor, Y. He, B. Bhandari, Food. Hydrocoll. *22(*2008) 1191-1202. DOI: 10.1016/j.foodhyd.2007.09.006

[10] S.M. Jafari, Y. He, B. Bhandari, *J. Food. Eng*. *82(*2007*)* 478-488. DOI: 10.1016/j.jfoodeng.2007.03.007

[11] P.T. Anastas, J.C. Warner, *Green Chemistry: Theory and Practice,* Oxford University Press, New York, 1998.

[12] R. Hofer, J. Bigorra. *Green. Chem*. *9 (*2007*)* 203-212. DOI: 10.1039/B606377B

[13] U. Brökel, W. Meier, G. Wagner, in: Product Design and Engineering. Volume 1: Basics and Technologies. Wiley-VCH, Weinheim, 2007.

[14] F.M. Kerton, *Alternative solvents for green chemistry,* Royal society of chemistry, Cambridge, 2009.

[15] L.M. Pérez-Mosqueda, P. Ramírez, L.A. Trujillo-Cayado, J. Santos, J. Muñoz, *Colloid. Surface. B. 123 (*2014*)*, 797-802. DOI: 10.1016/j.colsurfb.2014.10.022

[16] J. Santos, L.A. Trujillo-Cayado, N. Calero, J. Muñoz, *AIChE. J*. *60 (*2014*)* 2644-2653. DOI: 10.1002/aic.14460

[17] P. Castán, X. González, in: *Proceedings of 40th Annual Meeting of CED*. Barcelona, 2003, 325-338

[18] P.J. Lutz, *Ca. Pat. Appl*. (2006). CA 2537554 A1 20060822.

[19] Y. Denolle, V. Seita, V. Delaire, *Eur. Pat. Appl*. (2011). EP 2368971 A1 20110928.

[20] L.A. Trujillo-Cayado, P. Ramírez, M.C. Alfaro, M. Ruíz, J. Muñoz, *Colloid. Surface. B. 122 (*2014*)* 623–629. DOI: 10.1016/j.colsurfb.2014.07.041.

[21] L.A. Trujillo-Cayado, P. Ramírez, L.M. Pérez-Mosqueda, M.C. Alfaro, J. Muñoz, Colloid. Surface. A. 458(2014) 195-202. DOI: 10.1016/j.colsurfa.2014.02.009

[22] M.A. Hollinger, *Introduction to Pharmacology*, Third Edition, CRC Press, Boca Ratón, 2005.

[23] D. Allende, A. Cambiella, J.M. Benito, C. Pazos, J. Coca, *Chem. Eng. Technol*. *31 (*2008*)*1007–1014. DOI: 10.1002/ceat.200700018

[24] N.A. Camino, C.C. Sanchez, J.M.R. Patino, A.M.R. Pilosof, *Food. Hydrocoll*. *21 (*2011*)*, 1–11. DOI: 10.1016/j.foodhyd.2011.09.006

[25] J. Santos, L.A. Trujillo, N. Calero, M.C. Alfaro, J. Muñoz. *Chem. Eng. Technol*. *36 (*2013*)* 1–9. DOI: 10.1002/ceat.201300284

[26] D.J. McClements, *Crit. Rev. Food. Sci. Nutr*. 47 (2007) 611–649. DOI: 10.1080/10408390701289292

[27] C. Lesaint, W.R. Glomm, L.E. Lundgaard, J. Sjöblom. *Colloid. Surface. A. 352 (*2009*)* 63-69. DOI: 10.1016/j.colsurfa.2009.09.051

[28] L.M. Pérez-Mosqueda, L.A. Trujillo-Cayado, F. Carrillo, P. Ramírez, J. Muñoz, *Colloid. Surface. B*. 128 (2015) 127-131. DOI: 10.1016/j.colsurfb.2015.02.030

[29] S.M. Jafari, Y. He, B. Bhandari, *Food. Hydrocoll*. *22 (*2008*)* 1191– 1202. DOI: 10.1016/j.foodhyd.2007.09.006

[30] R. Pal. AICHE. J. *42 (*1996*)* 3181–3190. DOI: 10.1002/aic.690421119

[31] C. Puppo, F. Speroni, N. Chapleau, M. de Lamballerie, M.C. Añón, M Anton, *Food. Hydrocoll*. *19 (*2005*)* 289–296. DOI: 10.16/j.foodhyd.207.01.027

[32] H.A. Barnes, *Colloid. Surface. A*. 91 (1994) 89–95. DOI: 10.1016/0927-7757(93)02719-U

[33] J. Zhang, T.L. Peppard, G.A. Reineccius. *Flavour Fragr. J.* 30 (2015) 288–294. DOI: 10.1002/ffj.3244

[34] R. Pal, *Chem. Eng. Sci*. *52 (*1997*)* 1177-1187. DOI: 10.1016/S0009-2509(96)00451-4

[35] D.J. McClements, *Food Emulsions: Principles, Practice, and Techniques*, CRC Press, Boca Raton, 2005.

Chapter 6: Optimization of a Green Emulsion Stability by Tuning Homogenization Rate.

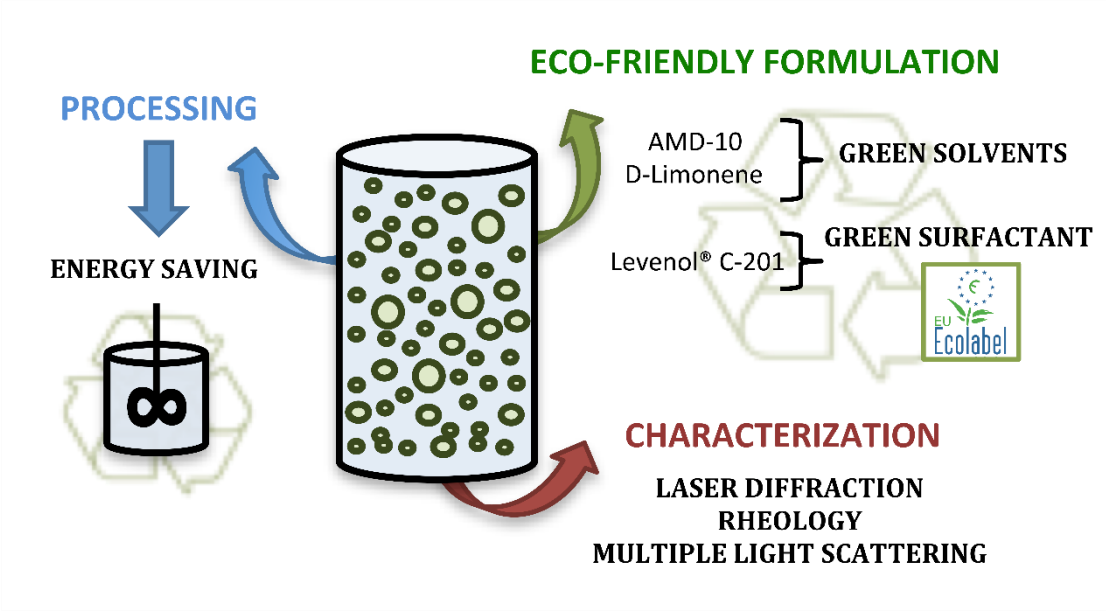

Abstract

Green chemistry raise the design of new products and processes that considers the reduction or removal of the use or production of hazardous substances. In this sense, this study has been focused on the development of the stable emulsions using ecofriendly ingredients and taking into account that energy requirements should be minimized. Physical stability of emulsions studied was explored by mean of a combination of different techniques such as laser diffraction, multiple light scattering and rheology. It has been proven that the coalescence process was detected not only from laser diffraction measurements but also from analysis of plateau modulus with aging time. This rheological parameter was also useful to distinguish between grades of flocculation. In addition, Turbiscan Stability Index showed that the stability enhanced at higher homogenization rates for 30 wt% emulsions, conversely for 40 wt% emulsions. The results obtained from the combination of different techniques used demonstrated that the most stable emulsion was achieved with 40 wt% dispersed phase using less energy input, which lies at the heart of sustainable society.

6.1. Introduction

Emulsions are thermodynamically unstable systems consisting of at least two immiscible fluids, one of which is dispersed in form of droplets in the other. Emulsions tend to break down over time due to a variety of physicochemical mechanisms, such as creaming, flocculation, coalescence and Ostwald ripening [1]. However, flocculation in emulsions sometimes could be desirable. Usually flocculated emulsions exhibit a highly shear-thinning behaviour and higher viscosity. This is due to the increase of droplet-droplet

interactions [2] .The higher viscosity created by a flocculated network has been reported to stabilize the emulsion temporarily against phase separation [3,4].

There are two different methods to prepare an emulsion, namely low-energy or high-energy methods. The second group is more likely to be use in the industry due to their scale-up and equipment availability. Rotor-stator devices, membranes, high-pressure homogenizers or Microfluidizer are common to use to prepare an emulsion. Energy dissipation required to achieve a mean droplet size of 0.5–100 μm using rotor-stator device typically range from 10^3 to 10^5 W/kg, while energy dissipation of high pressure homogenizers range about 10^8 and for ultrasonics about 10^9 W/kg [5]. Hence, the reduction in energy requirements by using a rotor-stator is very significant compared with other homogenization processes. Low energy consumption lies at the heart of sustainable and socially responsible society [6,7]. However, the energy input level of emulsification is not only related to create smaller droplets, but also may affect the aggregation of droplets [8].

In many emulsion applications such as cosmetics, foods, or paints, rheological properties have been of primary importance in the past 50 years. Many studies of the influence of aging time on zero shear viscosity and the viscoelastic functions to predict physical stability have been reported due to its direct relation with droplet size distribution and dispersed phase content [9,10] [11]

Researchers are engaged to explore new eco-friendly solvents for different applications due to the current trends in green chemistry and to replace the traditional organic solvents.[12] These new solvents must satisfy the customer requirements as well as they should derive from renewable resources. This study was focused on preparation of

emulsions containing eco-friendly solvents such as N,N-dimethyldecanamide and D-Limonene [13] and a green surfactant possessing an eco-label (DID list: 2133). In addition, the interfacial properties at the air/water and □-pinene/water interface of this surfactant, namely the equilibrium adsorption, dynamic surface tension and interfacial rheology have been recently reported. [14, 15] Apart from that, it is interesting to mark the role of a non-ionic surfactant improving the physical stability against flocculation and/or coalescence due a steric effect. This steric effect is based on the fact of the surfactants chains overlap with each other. [16]

The objective of the present work was to evaluate the influence of a processing parameter (homogenization rate) and a formulation parameter (dispersed phase content) on droplet size, stability and rheology of eco-friendly emulsions. This was based on the achievement of stable emulsions with submicron droplets modifying and controlling the formulation variables minimizing the energy required.

6.2. Materials and methods

6.2.1. Materials

N,N Dimethyl Decanamide (Agnique AMD-10^{TM}) and D-Limonene, was kindly supplied by BASF and Sigma Chemical Company respectively. A non-ionic surfactant derived from cocoa oil (polyoxyethylene glycerol fatty acid ester, Glycereth-17 Cocoate) was used as emulsifier. Its trade name is Levenol C-201^{TM} and it was received as a gift from KAO. An antifoaming agent (RD antifoam emulsion, DOW CORNING) was used. All emulsions were prepared using deionized water.

6.2.2. Emulsion preparation

The aqueous phase was a solution of deionized water, 0.1 wt% antifoam emulsion and 3 wt% of the green surfactant. The oil phase (30 wt% or 40 wt%) consisted of a mixture of two eco-friendly solvents: AMD-10 and D-Limonene in a ratio of 75/25. This ratio of solvents was previously demonstrated to be optimum by Santos et al., 2014.[17]

Emulsions were prepared using a rotor-stator homogenizer (Silverson L5M), equipped with a mesh screen, in the range 3000-8000 rpm during 60 seconds.

6.2.3 Droplet size distribution measurements.

Droplet size distributions and mean diameters of oil droplets were measured by laser diffraction technique (Mastersizer X, Malvern, Worcestershire, United Kingdom). All measurements were carried out in triplicate for each emulsion. The influence of aging time on droplet size distributions were carried out 1, 3, 13, 21 and 40 days after preparation.

The mean droplet diameters were expressed as Sauter diameter ($D_{3,2}$) and volume mean diameter ($D_{4,3}$):

$$D_{3,2} = \sum_{i=1}^{N} n_i d_i^{\,3} \Big/ \sum_{i=1}^{N} n_i d_i^{\,2} \qquad \text{Eq. (1)}$$

$$D_{4,3} = \sum_{i=1}^{N} n_i d_i^{\,4} \Big/ \sum_{i=1}^{N} n_i d_i^{\,3} \qquad \text{Eq. (2)}$$

where d_i is the droplet diameter, N is the total number of droplets and n_i is the number of droplets having a diameter d_i.

6.2.4. Rheological measurements.

Rheological tests were performed with a controlled-stress rheometer (Haake MARS, Thermo-Scientific, Germany). 30 wt% emulsions were measured using a sand-blasted

coaxial cylinder Z-20 (sample volume: 8.2 mL, R_e/R_i =1.085, R_i= 1 cm). Flow curves were carried out from 0.05 Pa to 2 Pa at 20 ºC. The results show the mean of three measurements done of emulsions aged for 1, 3, 13, 21 and 40 days.

40 wt% emulsions were measured using a sandblasted double-cone geometry (angle: 0.017 rad; diameter: 60 mm). Flow curves for 40 wt% emulsions processed above 5000 rpm were carried out from 0.05- 5 Pa.

6.2.5. Multiple light scattering

Multiple light scattering measurements were conducted with a Turbiscan Lab Expert until 30 days at 20 ºC. Multiple light scattering is a sensitive and non-intrusive tool to allow physical stability of complex fluids to be analysed.[18,19,20]

Turbiscan stability index (TSI) is a parameter that can be used for estimation of emulsion stability. This index is a statistical factor and its value is given by the following equation [21,22]:

$$TSI = \sum_j \left| scan_{ref}(h_j) - scan_i(h_j) \right| \qquad \text{Eq. (3)}$$

where $scan_{ref}$ and $scan_i$ are the initial backscattering value and the backscattering value at a given time, respectively, h_j is a given height in the measuring cell and TSI is the sum of all the scan differences in the measuring cell. When the TSI value increases the stability of the system decreases.

6.2.6. Statistical analysis.

Laser diffraction were carried out in triplicate, and the resulting data was analyzed using one-way analysis of variance (ANOVA). This was carried out using Microsoft excel 2013. All statistical calculations were conducted at a significance level of p= 0.05.

6.3. Results

Figure 6.1 shows the influence of homogenization rate on droplet size distribution (DSD) for a) 30 wt% emulsions and b) 40 wt% emulsions. The same trend in the DSD and Sauter diameter was observed for 30 wt% and 40 wt% emulsions: an increase of homogenization rate provoked a decrease in droplet sizes (Table 6.1). However, a strong influence of homogenization rate on DSD for 30 wt% emulsions was shown whereas only a slight influence was exhibited for 40 wt% emulsions. This fact was also observed in Sauter diameters, which decreased in a 69% for 30 wt% emulsions and only a 23% for 40 wt% emulsions from the lowest homogenization rate to the highest one. Results of the ANOVA test demonstrated that there are significantly differences in the Sauter diameters of the emulsions studied. The ratio oil/surfactant (R) has been fixed with the value of 0.1. As a consequence, an increase in the dispersed phase content increases the viscosity of the continuous phase ,η_c. An increase of η_c may provoke a change of regime of emulsification from inertial to viscous [23]. In the turbulent inertial regime, the drops are larger in diameter than the smallest turbulent eddies in the continuous phase, whereas in the turbulent viscous regime the drop diameter is smaller than the size of the smallest eddies. This fact can be the reason why smaller droplets were obtained in 40 wt% emulsions. Therefore, viscosity of the continuous phase could influence on the droplet size in emulsions processed in rotor stator devices.

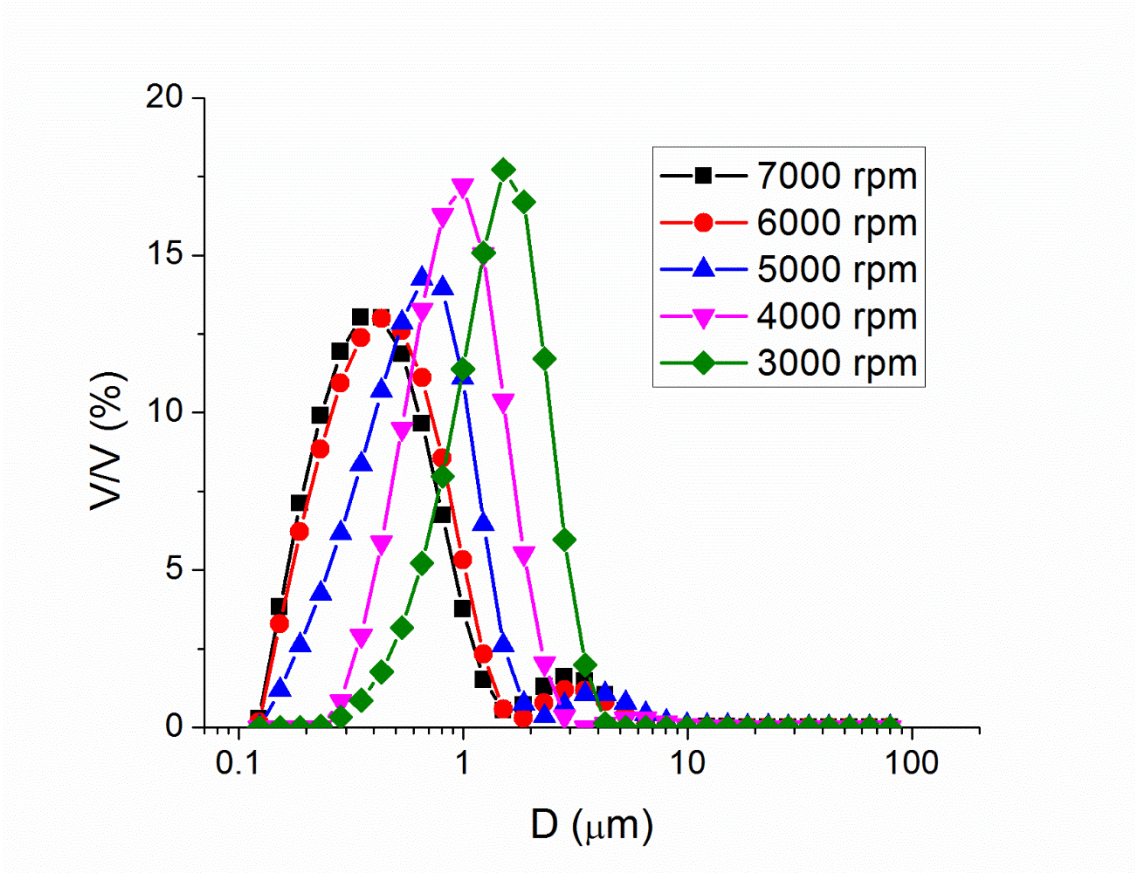

Figure 6.1a. Droplet size distribution for 30 wt% emulsions as a function of homogenization rate.

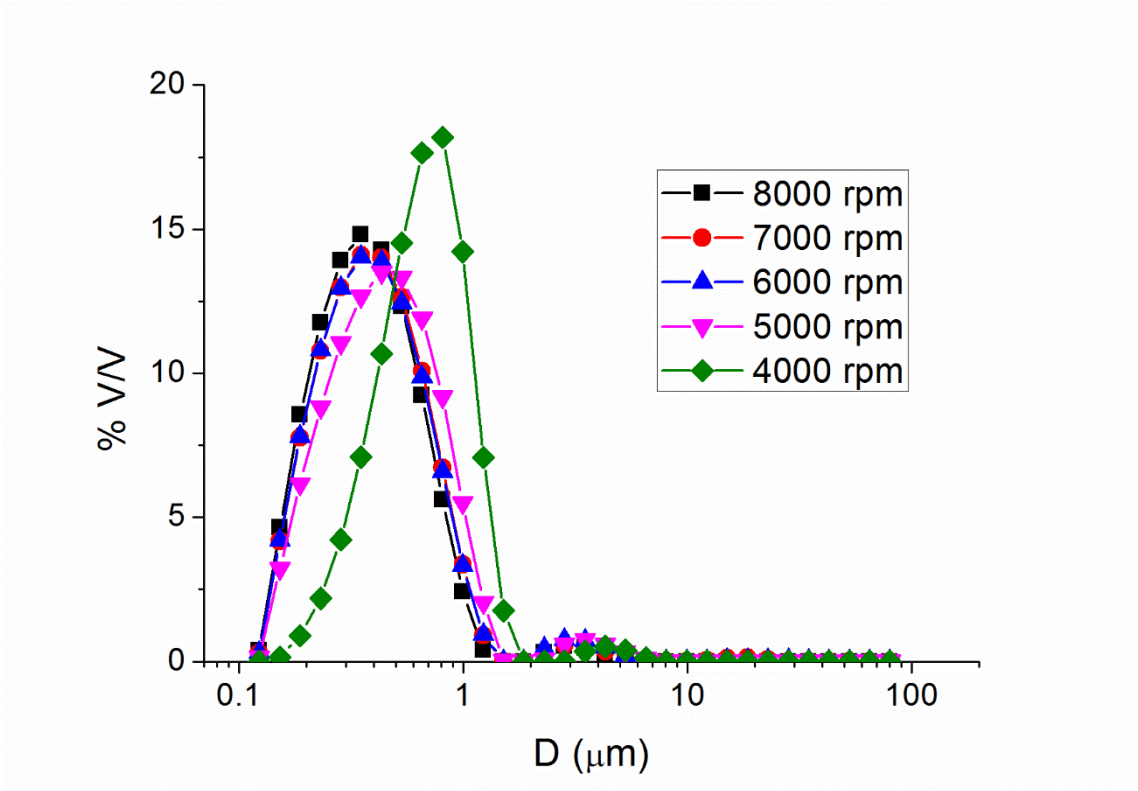

Figure 6.1b. Droplet size distribution for 40 wt% emulsions as a function of homogenization rate.

Table 6.1. Sauter diameter values for 30 wt% and 40 wt% emulsions processed at different homogenization rates at one day of aging time.

Homogenization rate	**30%**	**40%**
3000 rpm	1.07	-
4000 rpm	0.73	0.39
5000 rpm	0.47	0.34
6000 rpm	0.35	0.31
7000 rpm	0.33	0.31
8000 rpm	-	0.30

Figure 6.2 shows the influence of homogenization rate on flow properties for a) 30 wt% emulsions and b) 40 wt% emulsions. All emulsions exhibited shear-thinning behaviour, which fitted fairly well with Cross model (R^2>0.99). Fitting parameters for this model are shown in table 6.2. There is an increase in zero-shear viscosity (η_0) with homogenization rate for 30 wt% emulsions except for these processed at 7000 rpm. The increase of zero-shear viscosity with homogenization rate up to 6000 rpm is related to the reduction of droplet-size [2]. However, 7000 rpm did not follow this trend. This fact could be due to the break down of possible flocs, since 7000 and 6000 rpm emulsions showed the same DSD. In addition, emulsions with higher zero shear viscosity showed lower values of flow index. This means that these emulsions exhibited more shear thinning behaviour that

may be related to an increase of flocculation degree.[24] This phenomenon may explain the results obtained for 7000 and 6000 rpm emulsions previously mentioned.

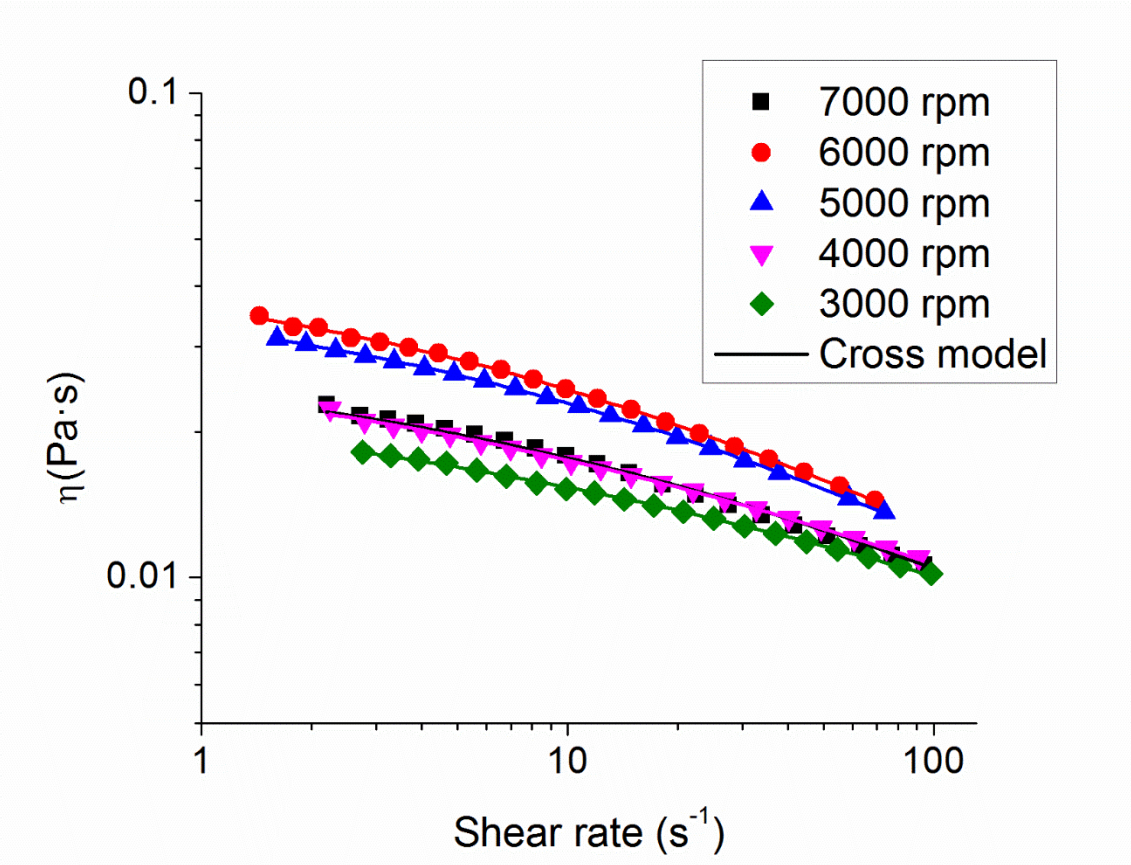

Figure 6.2.A. Flow curves for 30 wt% emulsions as a function of homogenization rate at 20°C.

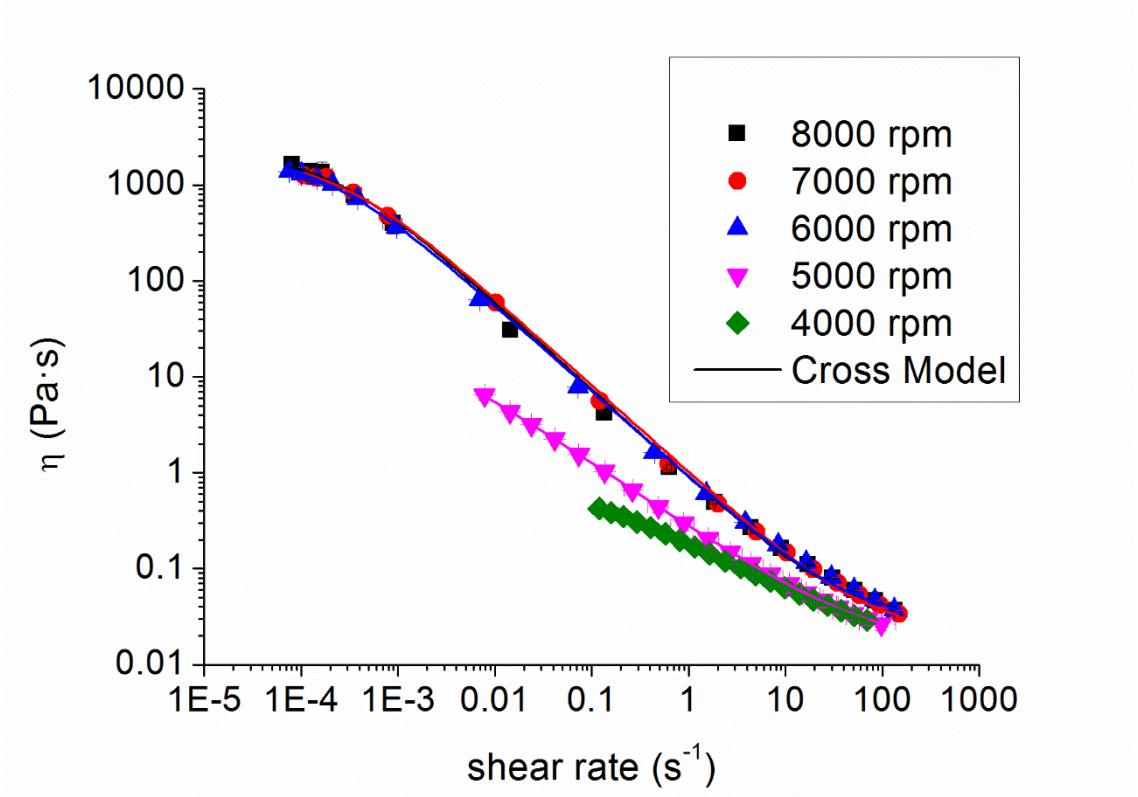

Figure 6.2.B. Flow curves for 40 %wt emulsions as a function of homogenization rate at 20°C.

Table 6.2. Fitting parameters to Cross model for the emulsions studied.

Homogenization rate (rpm)	***η₀ (Pa·s)***		***1/k (s⁻¹)***		***n***	
	30 wt%	***40 wt%***	***30 wt%***	***40 wt%***	***30 wt%***	***40 wt%***
8000	x	2200	x	4986	x	0.10
7000	0.030	1961	23	4152	0.57	0.09
6000	0.045	2074	11	5512	0.49	0.09
5000	0.041	49.9	14	2200	0.51	0.33
4000	0.032	1.2	17	28.7	0.60	0.45
3000	0.026	x	25	x	0.65	x

An increase of zero shear viscosity with homogenization rate was also observed in 40wt% emulsions but it did not vary significantly in the range from 6000 to 8000 rpm,

which was demonstrated by ANOVA test. An important increase of both zero shear viscosity and flow index was detected for emulsions processed from 5000 rpm to 6000 rpm. This fact is probably due to a flocculation process induced by homogenization conditions since droplets size were very similar as previously explained [24]. Flocculation tends to occur when the attractive interactions between droplets dominate the long-range repulsive interactions, but not the short-range repulsive interactions. Therefore, the droplets remain in close proximity to each other (flocculation), but not close enough to merge into each other (coalescence). Coalescence is defined by the process whereby two or more liquid droplets merge to form a single larger droplet. By contrast, droplets remain its own identity during flocculation process. The rate at which droplet flocculation occurs depends on the droplet-droplet collision frequency and collision efficiency. Droplet collisions due to Brownian motion in the dominant mechanism in systems containing relatively small droplets. In this case, collision frequency increases with increasing both dispersed phase content and homogenization rate.[25] Therefore, the increase of homogenization rate and/or dispersed phase content could produce flocculation during preparation. However, it should be noted that if the attractive interactions between the droplets in a floc are fairly weak then the floc may spontaneously dissociate due to Brownian motion or applied forces.[25] Hence, an excess on mechanical energy can break up flocs.

Figure 6.3 shows the mechanical spectra of 40 wt% emulsions processed at 6000,7000 and 8000 rpm. These emulsions exhibited storage modulus (G') higher than loss modulus (G'') in the frequency range studied. A minimum of G'' indicates that the mechanical spectra for these systems correspond to the plateau zone, which is a typical weak gel-like behaviour. However, there are no significant differences between 6000 and 7000

rpm whereas 8000 rpm emulsion showed lower values of G' and G''. A higher G' and G'' values was previously interpreted as a first indication of the existence of flocculation by Calero et al [26] Furthermore, this can be clearly detected by the changes in characteristic frequency (ω_c) and plateau modulus ($G_N^{\prime 0}$), which are shown in table 6.3. This fact may be attributed to a break down of flocs. It should be remarked that not significant differences were found in zero-shear viscosity for 40 wt% emulsions processed at 6000,7000 and 8000 rpm . Hence, Small Amplitude Oscillatory Stress (SAOS) technique was more sensitive to detect these slight structural changes as a consequence of oil droplet flocculation process. [26] Thus, systems which could not be differentiated by using flow tests showed different both viscoelastic functions (G', G'') and viscoelastic parameters (ω_c, $G_N^{\prime 0}$) resulting from SAOS tests. Therefore, SAOS tests are efficient tool to recognise slightly different grades of flocculation.

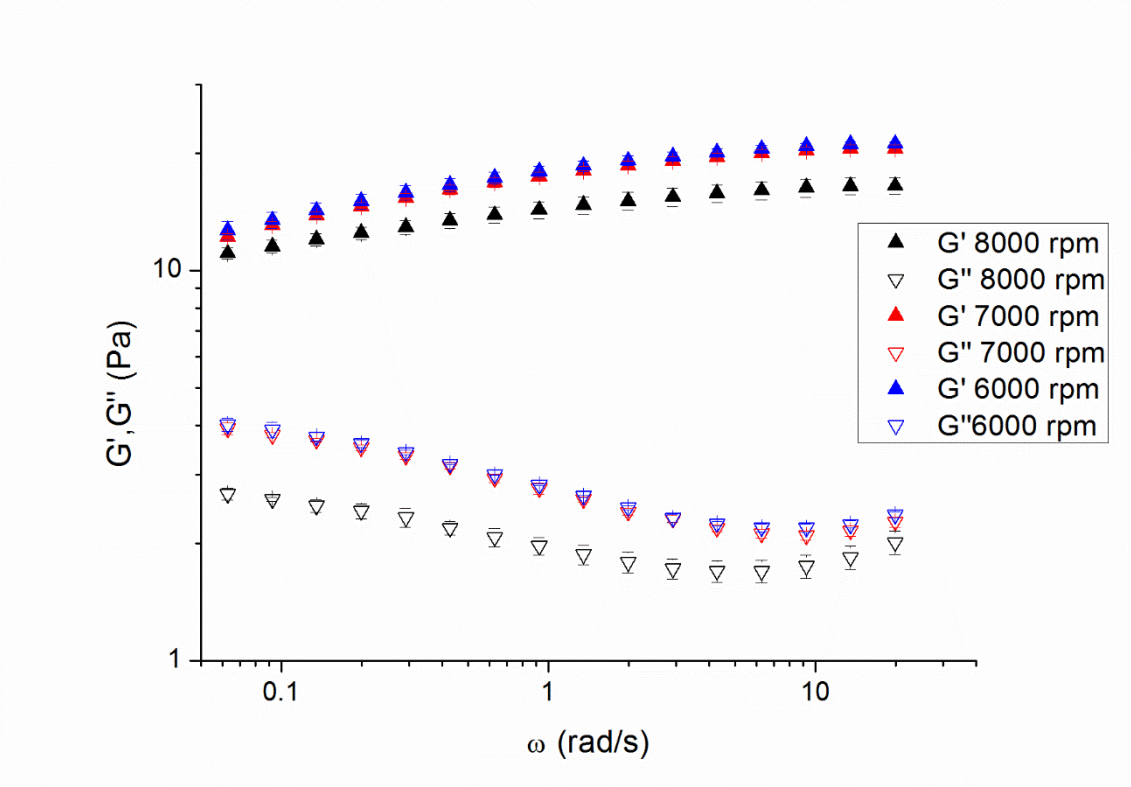

Figure 6.3. Mechanical spectra for 40 wt% emulsions as a function of homogenization rate.

Table 3. Characteristic frequency and Plateau modulus for emulsions which showed viscoelastic properties.

Homogenization rate (rpm)	ω_c (rad/s)	$G_N'^0$ (Pa)
6000	9.2	20.5
7000	9.2	20.3
8000	6.3	16.0

In order to quantify the coalescence in emulsions with aging time, the normalised difference of $D_{4.3}$ was used. We have defined this parameter as follows:

$$\Delta D_{4.3} = \frac{D_{4.3\,(day\,40)} - D_{4.3\,(day\,1)}}{D_{4.3\,(day\,1)}} \cdot 100 \quad \text{Eq (4)}$$

Figure 6.4 shows the influence of homogenization rate for 30 wt% and 40 wt% emulsions on $\Delta D_{4.3}$.

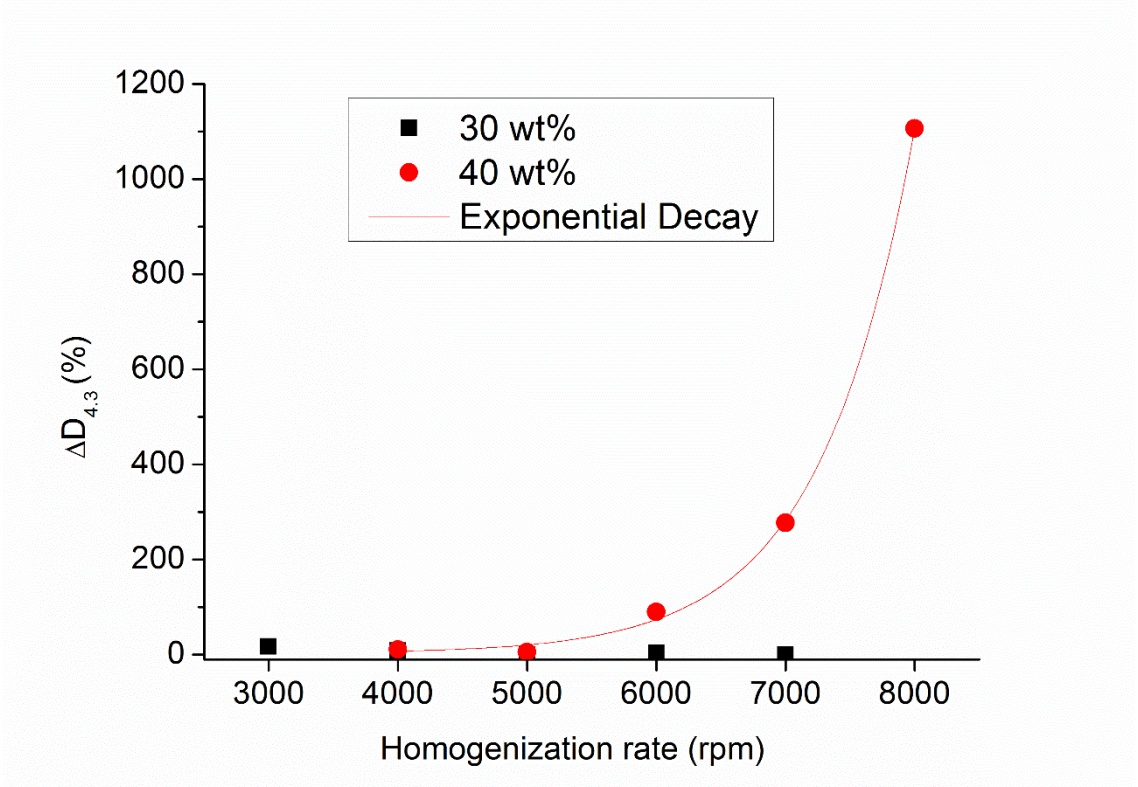

Figure 6.4. Influence of homogenization rate on $\Delta D_{4.3}$ as a function of dispersed phase content for the emulsions studied.

On the one hand, $\Delta D_{4.3}$ showed a value of nearly 0 for 30 wt% emulsions processed above 3000 rpm. This demonstrated that these emulsions did not undergo a significant coalescence process in 40 days. 30 wt% emulsions prepared at 3000 rpm showed a little value of $\Delta D_{4.3}$. Hence, a slight increase in volumetric diameter was observed with aging time.

On the other hand, 40 wt% emulsions up to 5000 rpm showed values of $\Delta D_{4.3}$ about 0 whereas above 5000 rpm showed high values of $\Delta D_{4.3}$. This fact point out a coalescence process, which is favoured by a previous flocculation mechanism since coalescence occurs when the droplets are in contact for a long time. In addition, there is no increase of $D_{4.3}$ for 40 wt% emulsions up to 5000 rpm which means that coalescence was not taking place. Therefore, only emulsions containing flocs underwent a significant coalescence process after 40 days.

Figure 6.5.A shows the influence of the aging time on zero shear viscosity for 30 wt% emulsions. An increase of zero shear viscosity was observed from day 1 to day 40 in all emulsions except for this processed at the minimum homogenization rate studied. This growth is related to higher content of the dispersed phase in the upper zone of the vial, which points out creaming and/or flocculation process. By contrast, emulsions processed at 3000 rpm showed a decrease of zero shear viscosity with aging time. This fact is due to an increase of the droplet size as a consequence of a coalescence phenomenon. Only the emulsion with the highest Sauter diameter at day 1 underwent

coalescence, which supports the direct relationship between coalescence rate and Sauter diameter [27].

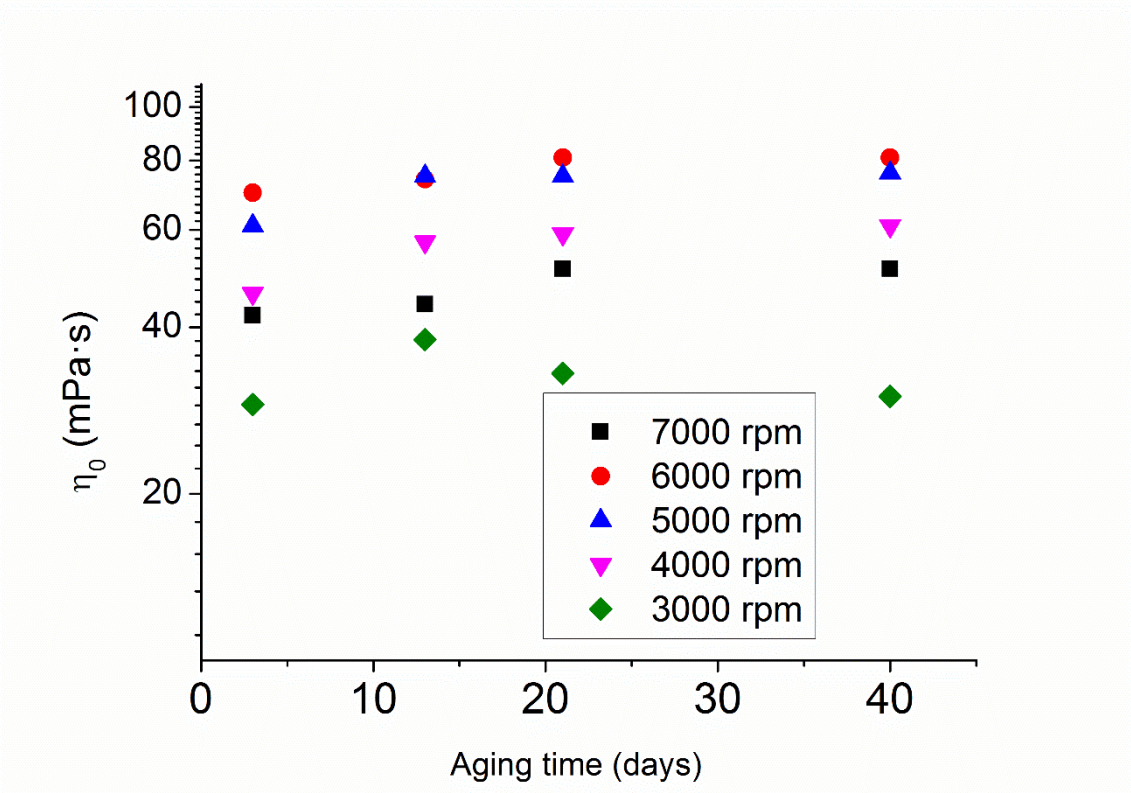

Figure 6.5.A. Zero shear-viscosity for 30 wt% emulsions with aging time as a function of homogenization rate.

Figure 6.5.B shows the influence of the aging time on zero shear viscosity for 40 wt% emulsions. Emulsions processed at higher homogenization rates (6000-8000 rpm), which possessed viscoelastic properties, showed a decrease of zero shear viscosity. This fact points out these emulsions underwent a destabilization process by coalescence. This is consistent with laser diffraction results. On the contrary, 40 wt% emulsions processed up to 5000 rpm showed an increase of zero shear viscosity with aging time, which can be attributed to the occurrence of oil droplet flocculation and/or creaming.

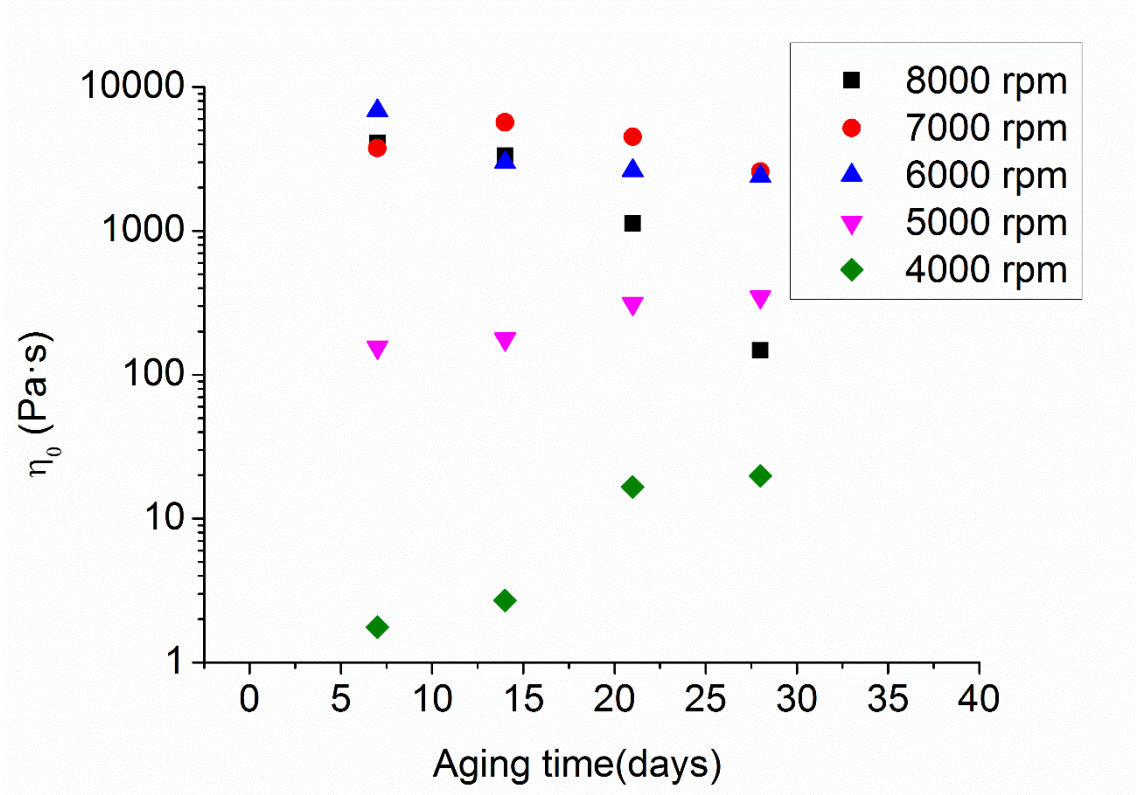

Figure 6.5.B. Zero shear-viscosity for 40 wt% emulsions with aging time as a function of homogenization rate.

The influence of aging time on $G_N'^0$ as a function of homogenization rate for 40 wt% emulsion was showed in figure 6.6. There is a clear falling down of $G_N'^0$ with aging time for these emulsions, which reveals coalescence phenomenon. It is interesting to remark that this parameter obtained from oscillatory tests are more sensitive than a parameter resulting from flow test, as previously mentioned. In this sense, emulsions processed at 7000 rpm did not show significant variation of zero shear viscosity with aging time. However, the plateau modulus underwent a clear decrease with aging time as a consequence of coalescence. Furthermore, emulsions processed at 6000 and 8000 rpm showed a decrease of plateau modulus as well as of zero shear viscosity. These rheological results support the interpretation of laser diffraction measurements.

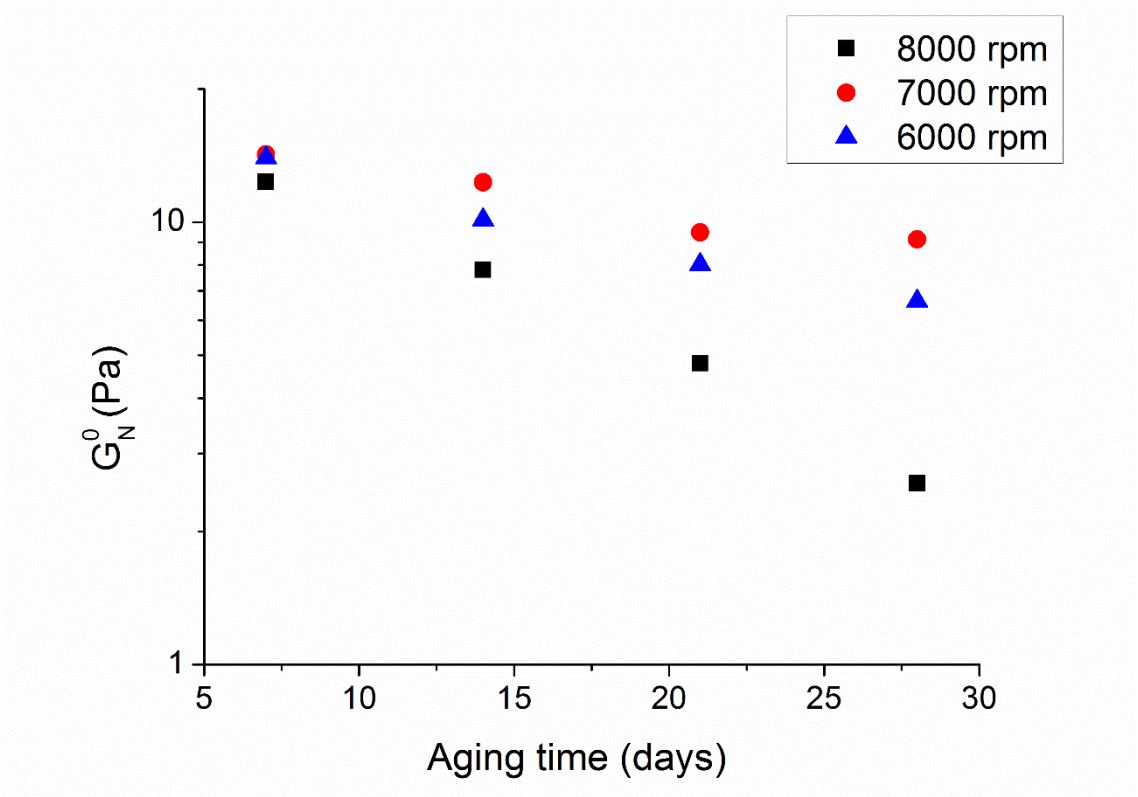

Figure 6.6. Plateau modulus with aging time as a function of homogenization rate for emulsions which showed viscoelastic properties.

In order to compare the physical stability of all emulsions studied, TSI global parameter for 30 days have been showed in figure 6.7. This parameter allows all the mechanisms involved in the destabilization of emulsions to be quantified. Consequently, it is a measure of not only creaming but also coalescence and/or flocculation; that is, TSI global parameter is the total contribution of each destabilization process. There is a decrease of TSI_{global} with homogenization rate followed by a trend to reach a constant value about 6000 rpm for 30 wt% emulsions. By contrast, an increase of TSI_{global} with homogenization rate was observed for 40 wt% emulsions. Thus, 30 wt% emulsions processed at 6000-7000 rpm and 40 wt% emulsions processed at 4000 rpm showed the best stability, respectively. It is important to remark that both optimum homogenization rate and destabilization mechanisms were different depending on dispersed phase

content. Hence, it is not adequate to extrapolate processing conditions even to a slightly different formulation.

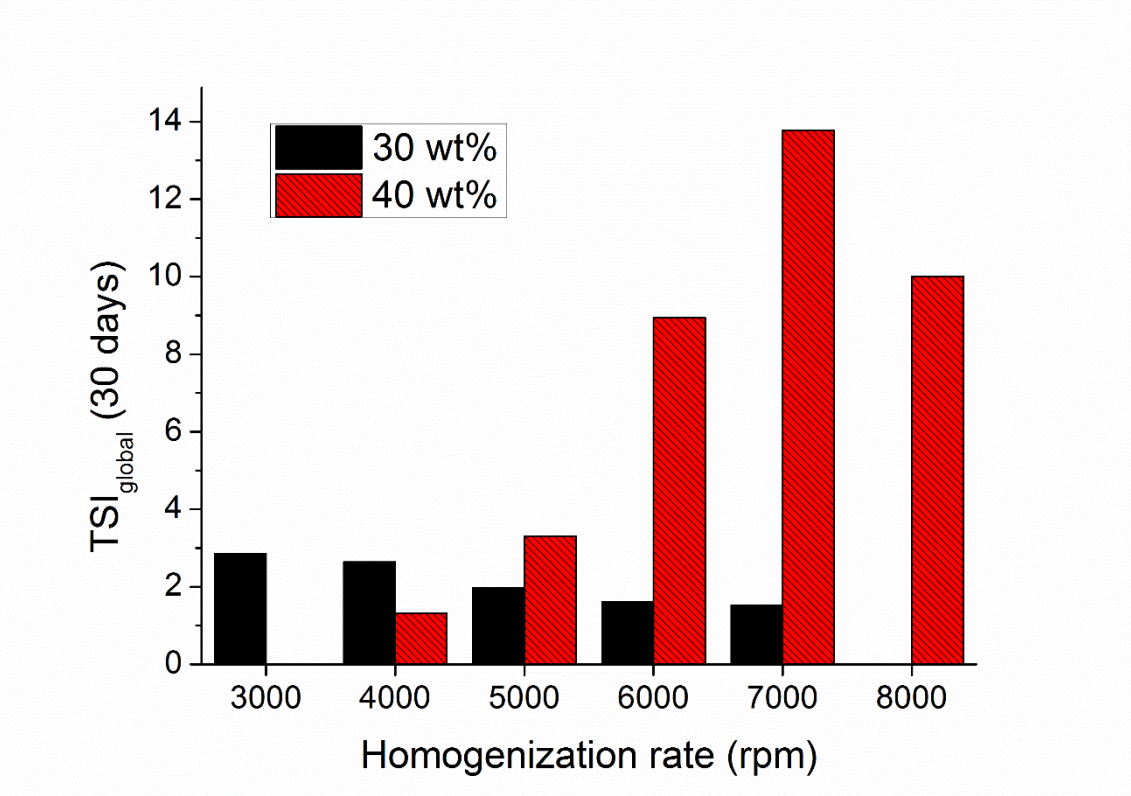

Figure 6.7. TSI global at 30 days of aging time as a function of homogenization rate for 30 and 40 wt% emulsions

Conclusions

DSD was strongly influenced by homogenization rate for 30 wt% emulsions but slightly influenced for 40 wt% emulsions due to a change of regime. By contrast, zero-shear viscosity changes more in 40 wt% than in 30 wt% emulsions with homogenization rate. This fact is related to a flocculation process induced by energy input (above 5000 rpm). These aforementioned emulsions showed viscoelastic properties. As a consequent, plateau modulus were calculated and was used to detect destabilization mechanisms by mean of its variation with aging time. In this sense, this rheological parameter was

demonstrated to be an useful tool in order to predict coalescence before visual observation and to distinguish between different grades of flocculation. Furthermore, flocculated 40 wt% emulsions showed coalescence with aging time while 30 wt% underwent creaming process due to the low zero shear viscosity shown. This supports the laser diffraction and rheology results. It is important to remark that the main destabilization mechanism is influenced by not only the dispersed phase content but also the homogenization rate. Hence, this study demonstrate the importance of flocculation induced by emulsification process in emulsions.

The most stable emulsion was 40 wt% processed at 4000 rpm in the rotor-stator device. Therefore, a more concentrated emulsion was achieved using less energy input, which fulfil the demands of a bio-based society.

References

1 D. J. McClements, *Food emulsions: principles, practices, and techniques*, CRC press, 2015.

2 H. A. Barnes, *Colloids Surfaces A Physicochem. Eng. Asp.*, 1994, **91**, 89–95.

3 S. Aben, C. Holtze, T. Tadros and P. Schurtenberger, *Langmuir*, 2012, **28**, 7967–7975.

4 E. Dickinson and M. Golding, *J. Colloid Interface Sci.*, 1997, **191**, 166–176.

5 E. L. Paul, V. A. Atiemo-Obeng and S. M. Kresta, *Handbook of industrial mixing: science and practice*, John Wiley & Sons, 2004.

6 E. L. Cussler and G. D. Moggridge, *Chemical product design*, Cambridge University Press, 2011.

7 P. T. Anastas and J. B. Zimmerman, *Environ. Sci. Technol.*, 2003, **37**, 94A–101A.

8 F. Liu and C.-H. Tang, *J. Agric. Food Chem.*, 2014, **62**, 2644–2654.

9 R. Pal, *AIChE J.*, 1996, **42**, 3181–3190.

10 J. Santos, L. A. Trujillo-Cayado, N. Calero, M. C. Alfaro and J. Muñoz, *J. Ind. Eng. Chem.*, 2016.

11 R. P. Borwankar, L. A. Frye, A. E. Blaurock and F. J. Sasevich, *J. Food Eng.*, 1992, **16**, 55–74.

12 P. T. Anastas and M. M. Kirchhoff, *Acc. Chem. Res.*, 2002, **35**, 686–694.

13 F. M. Kerton and R. Marriott, *Alternative solvents for green chemistry*, Royal Society of chemistry, 2013.

14 L. A. Trujillo-Cayado, P. Ramírez, M. C. Alfaro, M. Ruíz and J. Muñoz, *Colloids Surfaces B Biointerfaces*, 2014, **122**, 623–629.

15 L. A. Trujillo-Cayado, P. Ramírez, L. M. Pérez-Mosqueda, M. C. Alfaro and J. Muñoz, *Colloids Surfaces A Physicochem. Eng. Asp.*, 2014, **458**, 195–202.

16 T. F. Tadros, *Colloids in Agrochemicals, Volume 5: Colloids and Interface Science*, John Wiley & Sons, 2011.

17 J. Santos, L. A. Trujillo-Cayado, N. Calero and J. Muñoz, *AIChE J.*, 2014, **60**, 2644–2653.

18 L. Leclercq and V. Nardello-Rataj, *Eur. J. Pharm. Sci.*, 2016, **82**, 126–137.

19 J. Santos, N. Calero and J. Muñoz, *Chem. Eng. Res. Des.*, 2015, **100**, 261–267.

20 J. Santos, L. A. Trujillo, N. Calero, M. C. Alfaro and J. Munoz, *Chem. Eng. Technol.*, 2013, **36**, 1883–1890.

21 C. Lesaint, W. R. Glomm, L. E. Lundgaard and J. Sjoblom, *Colloids Surfaces A-Physicochemical Eng. Asp.*, 2009, **352**, 63–69.

22 L. M. Pérez-Mosqueda, L. A. Trujillo-Cayado, F. Carrillo, P. Ramírez and J. Muñoz, *Colloids Surfaces B Biointerfaces*, 2015, **128**, 127–131.

23 N. Vankova, S. Tcholakova, N. D. Denkov, I. B. Ivanov, V. D. Vulchev and T. Danner, *J. Colloid Interface Sci.*, 2007, **312**, 363–380.

24 R. Pal, *Chem. Eng. Sci.*, 1997, **52**, 1177–1187.

25 D. J. Mcclements, *Crit. Rev. Food Sci. Nutr.*, 2007, **47**, 611–649.

26 N. Calero, J. Muñoz, P. W. Cox, A. Heuer and A. Guerrero, *Food Hydrocoll.*, 2013, **30**, 152–162.

27 F. L.-C. Schmitt, S Arditty, in *Mishchuk, N. A., & Petsev, D. Emulsions: structure, stability and Interactions. Amsterdam–Tokyo: Elsevier.*, 2004, p. 351.

Chapter 7: Differences between Ostwald ripening and coalescence by analysing rheology, laser diffraction and MLS results.

Abstract

Two different mechanisms can provoke an irreversible droplet size increase: coalescence and Ostwald ripening. The latter is generally modelled with the well-know Lifshitz-Slyozov-Wagner (LSW) theory while coalescence follows the equation proposed by Weers and Kabalnov. This contribution deals with the study of the influence of surfactants ratio, a triblock copolymer (Pluronic PE9400) and a polyoxyethylene glycerol fatty acid ester (Levenol C201), in emulsions formulated with a mixture of two biosolvents. Emulsions containing Pluronic at any concentration underwent Ostwald ripening while coalescence took place in emulsions which contained only Levenol C201. This fact was analysed not only by mean of average diameters but also by rheological properties and a parameter derived from Multiple light scattering measurements with aging time. Pluronic PE9400 formed multilayers in the emulsions studied, which could promote both flocculation during processing and Ostwald ripening. By contrast, Levenol C201 showed a compact adsorbed layer with the molecules perpendicularly oriented to the interface. This difference of structure may be the reason of the different destabilization mechanisms that took place. This work studies the differences between Ostwald ripening and coalescence using different techniques such as Multiple Light Scattering, rheology and laser diffraction. Furthermore, the importance of the surfactant selection in the formulation of emulsions showing similar Droplet Size Distributions after preparation is demonstrated.

7.1. INTRODUCTION

Oil in water (O/W) emulsions are complex systems composed of an oil-dispersed phase and an aqueous continuous phase [1]. They are thermodynamically unstable but may

become kinetically stable depending on the formulation and processing [2][3][4]. Some of the most important characteristics are the solubility of the two phases, the amount and types of surfactants used as well as the volume ratio.[2] Different destabilization mechanisms can take place in emulsions involving droplet migration/aggregation or droplet size increase. Namely, irreversible droplet size increase may occur through two different mechanisms: Ostwald ripening and coalescence. Ostwald ripening involves a diffusive transfer of the dispersed phase from smaller to the larger droplets. Conversely, coalescence is the rupture of the thin film between droplets leading them to fuse into a single one.

The Ostwald ripening process is generally modelled by the well know Lifshitz-Slyozov-Wagner (LSW) theory, for O/W emulsions without excess of surfactant.

This theory is based on the assumption that the diffusion of oil through the water determines the overall Oswald ripening rate.[5] [6] This theory predicts that, at asymptotically long times, there is a constant Ostwald ripening rate ω_T which is determined by the growth in the cube of the number weighted mean droplet radius $\bar{r}$.

$$\omega_T = \frac{d\bar{r}^3}{dt} = \frac{8\gamma c_w^{eq} D_w V_m}{9kT} \quad (EQ.7.1)$$

Where, γ is the interfacial tension between oil and aqueous phases at the droplet surface, V_m is the molecular volume of the oil, c_w^{eq} is the aqueous oil solubility, D_w is the diffusivity of the oil molecule, k is Bottzmann´s constant and T is absolute temperature. This equation based on diffusion controlled ripening has been recognized in sub-micron diluted emulsions stabilized by ionic or non ionic surfactant. Diffusion could be

accelerated due to the micellar solubilization of oil in the aqueous phase. In addition, the micelles might act as a carrier that substantially increases the ripening rate [7].

Conversely, coalescence follows the following law [8]:

$$\frac{1}{{D_0}^2} - \frac{1}{D^2} = \frac{2\pi}{3}\omega t (EQ.7.2)$$

Where, D_0 is the initial diameter and D is the diameter at time t.

It has been reported that the combination of two mechanisms or the coarsening is sometimes determined first by Ostwald Ripening followed by coalescence. [9]

Green solvents fulfil the new necessities of the society and chemical industry and replace the non-ecological traditional solvents progressively. N,N-dimethyldecanamide (AMD-10) and D-Limonene are considered eco-friendly solvents that have been used in matrices for agrochemical products [10]. The latter, a natural hydrocarbon, is a natural biosolvent derived from the rinds of citrus fruits such as grapefruit, lemon, lime, and in particular, oranges. Also, ecological surfactants have been attracted much attention recently. Levenol C-201, a green emulsifier which possesses ecolabel, is a non-ionic surfactant derived from coconut oil.

Pluronics are non-ionic triblock copolymers also known as polaxamers. They are formed by two hydrophilic side chains of poly(ethylene oxide), PEO, and a central hydrophobic chain of poly(propylene oxide),PPO. They are usually denoted (PEOx-PPOy-PEOx), where x and y are the repeating PEO and PPO units, respectively. They have many applications in fields such as cosmetics, pharmaceutical industry, emulsification and foaming [11–13]

Laser diffraction, Multiple Light Scattering (MLS) and Rheology were used to study the physical stability of emulsions containing green solvents with different ratios of a polyoxyethylene glycerol ester (Levenol C-201) and a polymeric surfactant (Pluronic 9400). Furthermore, this work shows a rheological, MLS and droplet size analysis about the differences between coalescence and Ostwald ripening in emulsions.

7.2. Materials and methods

7.2.1. Materials

N,N Dimethyl Decanamide (Agnique AMD-10^{TM}, BASF) and D-Limonene (Sigma Chemical Company) were used as dispersed phase. Levenol C-201^{TM} (polyoxyethylene glycerol fatty acid ester, Glycereth-17 Cocoate), whose HLB is 13, was supplied by KAO. The triblock copolymer Pluronic PE9400 (PEO_{21}-PPO_{50}-PEO_{24}, Mw= 4600 g·mol^{-1} and HLB=12-18) was provided by BASF. HLB value of this Pluronic is defined as 20 $M_{W,PEO}/M_W$ where $M_{W,PEO}$ is the molecular weight of the hydrophilic PEO units and Mw is the total molecular weight. An antifoaming agent (RD antifoam emulsion, DOW CORNING) was used. All emulsions were prepared using deionized water.

7.2.2. Emulsion preparation

The aqueous phase contained deionized water, 0.1 wt% antifoam emulsion and 4 wt% of the mixture of surfactants. The ratios studied were Levenol C-201/PE 9400: 4/0,3/1,2/2,1/3,0/4. The oil phase (40 wt%) consisted of a mixture of two green solvents: AMD-10 and D-Limonene in a ratio of 75/25. This ratio of solvents was previously demonstrated to be optimum in 30 wt% emulsions by Santos et al., 2014.[10]

Emulsions were prepared using a rotor-stator homogenizer (Silverson L5M) with a mesh screen, at 8000 rpm during 60 seconds. This homogenization rate was the minimum homogenization rate needed to form all emulsions.

7.2.3 Droplet size distribution measurements.

Droplet size distributions and mean diameters of oil droplets were measured by laser diffraction technique (Mastersizer X, Malvern, Worcestershire, United Kingdom). All measurements were carried out in triplicate for each emulsion. The influence of aging time on droplet size distributions were carried out for 20 days.

The mean droplet diameters were expressed as Sauter diameter ($D_{3,2}$) and volume mean diameter ($D_{4,3}$):

$$D_{3,2} = \sum_{i=1}^{N} n_i d_i^{\,3} \Big/ \sum_{i=1}^{N} n_i d_i^{\,2} \qquad \text{(EQ.7.3)}$$

$$D_{4,3} = \sum_{i=1}^{N} n_i d_i^{\,4} \Big/ \sum_{i=1}^{N} n_i d_i^{\,3} \qquad \text{(EQ.7.4)}$$

where d_i is the droplet diameter, N is the total number of droplets and n_i is the number of droplets having a diameter d_i.

7.2.4. Rheological measurements.

Rheological tests were performed with a controlled-stress rheometer (Haake MARS, Thermo-Scientific, Germany). Emulsions studied were measured using a sandblasted double-cone geometry (angle: 0.017 rad; diameter: 60 mm). Flow curves were carried out from 0.05- 5 Pa. Small Amplitude Oscillatory Stress (SAOS) were conducted from 20 to 0.05 rad/s and at a shear stress lower than the critical stress.

7.2.5. Multiple light scattering

Multiple light scattering (Turbiscan Lab Expert) measurements were conducted with aging time at 20 ºC.

Turbiscan stability index (TSI) is a parameter that can be used for estimation of emulsion stability. This index is a statistical factor and its value is given by the following equation [14],[15]:

$$TSI = \sum_j \left| scan_{ref}(h_j) - scan_i(h_j) \right| \qquad \text{(EQ.7.5)}$$

Where $scan_{ref}$ and $scan_i$ are the initial backscattering value and the backscattering value at a given time, respectively, h_j is a given height in the measuring cell and TSI is the sum of all the scan differences in the measuring cell. When the TSI value increases the stability of the system decreases.

7.3. Results

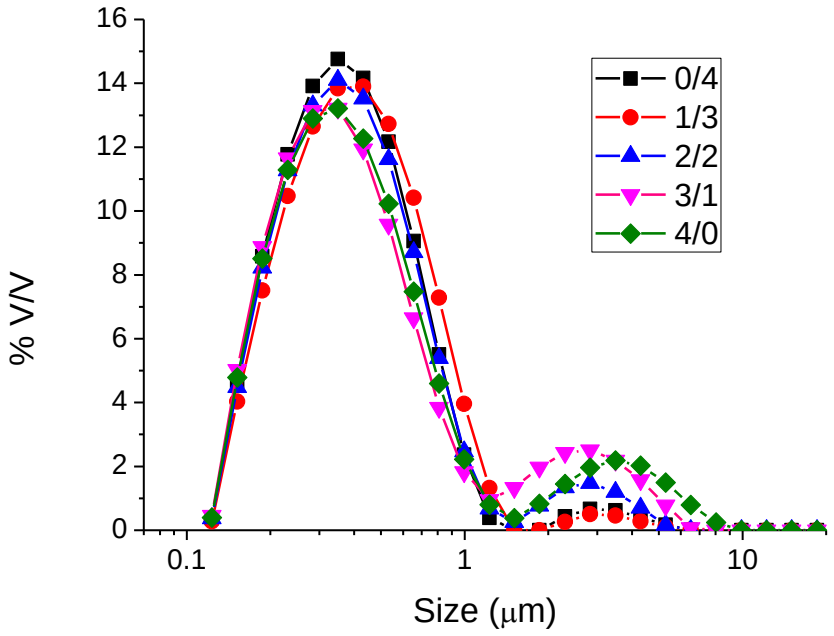

Figure 7.1A. Droplet size distribution for emulsions containing different ratio of surfactants at two hours of aging time.

Figure 7.1A shows Droplet Size Distribution (DSD) for emulsions with different ratios of Levenol C201/Pluronic PE9400 for 2 hours of aging time. All emulsions exhibited bimodal distributions: first population below 1 μm and second population above. This second peak is due a recoalescence phenomenon that took place during the processing. [10,16] Nevertheless, differences in the grade of recoalescence can be noted. In order to clarify this point, figure 7.1B shows Sauter and volumetric diameters as well as span for emulsions studied. There are no significant differences in Sauter diameters for emulsions studied. However, emulsions with higher content in PE9400 showed lower volumetric diameters and lower span. It is important to highlight the existence of a trend in volumetric diameter and span with the content of PE9400. This is a clear consequence of the reduction of recoalescence. Hence, emulsions with higher content in PE9400 showed less droplets in the second population, which is also seen in figure 7.1A. This fact indicates that PE9400 protects interface oil-water against recoalescence better than Levenol C-201.

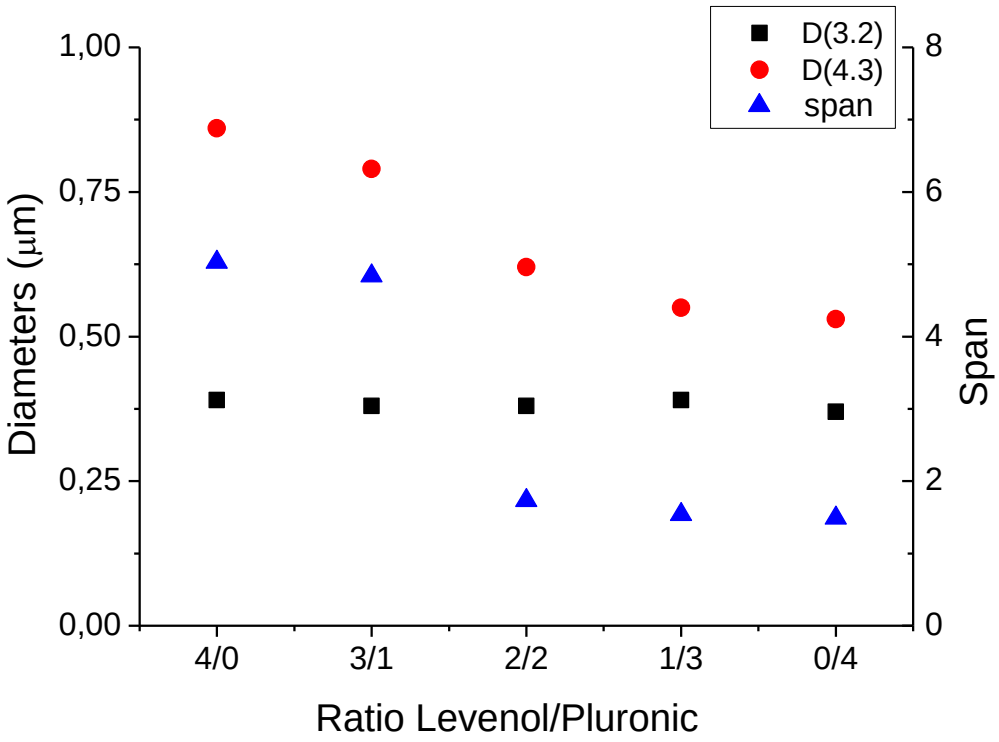

Figure 7.1B. Sauter, volumetric diameters and span for emulsions containing different continuous phases for 2 hours of aging time.

Figure 7.2 shows the influence of ratio Levenol/Pluronic that is contained in continuous phase on flow properties of emulsions studied. All emulsions exhibited shear-thinning behaviour and the data obtained were fitted fairly well by Cross model (R^2>0.99). Fitting parameters for this model are shown in table 7.1.

$$\eta = \frac{\eta_0}{1+\left(\frac{\dot{\gamma}}{\dot{\gamma}_c}\right)^{1-n}} \qquad \text{EQ. 7.6}$$

Where $\dot{\gamma}_c$ is related to the critical shear rate for the onset of shear-thinning response, η_0 stands for the zero-shear viscosity and (1-n) is a parameter related to the slope of the power-law region; n being the so-called “flow index”.

A decrease of zero shear viscosity with Pluronic concentration can be observed when the predominant surfactant is Levenol. This fact is consistent with the viscosity of continuous phases (Table 7.2) since emulsion with 4/0 ratio showed the highest viscosity followed by 3/1 ratio. On the contrary, when the predominant surfactant is Pluronic PE9400 and for the ratio 2/2, the increase of PE9400 provoked an increase of zero-shear viscosity. This is not consistent with Sauter diameter since all emulsions did not show significant differences. In addition, this trend cannot be explained by the viscosity of the continuous phases. Hence, this fact points out that there is an increase of viscosity due to flocculation. Interestingly, Pérez-Mosqueda et al. stated that there is a conformational change of Pluronic PE9400 molecules from a 2D conformation to a 3D brush/mushroom when Pluronic concentration increase [17]. Thus, pluronic would exhibit 3D conformation for the pluronic concentration used in these emulsions. This conformation is characterized by brush-brush forces and it could form multilayers in oil-water interfaces. [18,19] Therefore, this structure could promote the flocculation when pluronic is the predominant surfactant. By contrast, the study of the equilibrium surface pressure isotherms reported by Trujillo-Cayado et al. stated that Levenol C201 develops a compact adsorbed layer with the molecules perpendicularly oriented to the interface.[20] Hence, the structural difference could be the reason why Pluronic may lead to flocculated emulsions during preparation and Levenol does not. Furthermore, this could be also the explanation why Pluronic protected better the interface against recoalescence provoked by the processing. Apart from that, CMC of Levenol C-201-Limonene mixture is higher than their counterpart in Pluronic. [17,20]. This fact is related to a higher amount of micelles in Pluronic-based emulsion. These micelles could lead to a depletion flocculation process.

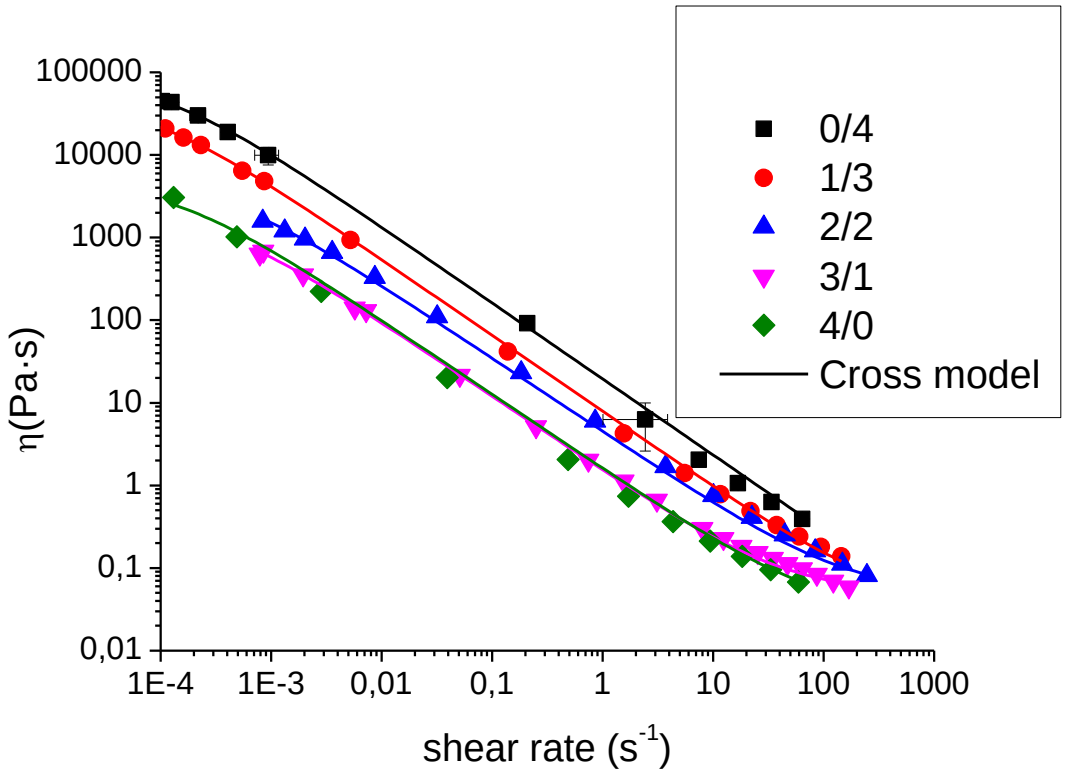

Figure 7.2. Flow curves for emulsions containing different continuous phases for 24 hours of aging time.

Table 7.1. Fitting parameters to Cross model for emulsions studied.

Ratio L/P	η_∞ (Pa·s)	η_0 (Pa·s)	k (s)	n
0/4	0.0001	86295	9215	0.08
1/3	0.04	49481	13447	0.08
2/2	0.05	5500	2962	0.11
3/1	0.05	2295	3368	0.10
4/0	0.03	5023	7724	0.10

Table 7.2. Continuous phase density and viscosity values at 20°C.

Ratio Levenol/Pluronic in continuous phase	δ (kg/m^3)	η (mPa·s)
4/0	1.0045 ± 0.0001	25.30 ± 0.7
3/1	1.0082 ± 0.0001	3.90 ± 0.02
2/2	1.0086 ± 0.0001	2.15 ± 0.04
1/3	1.0097 ± 0.0001	1.93 ± 0.02
0/4	1.0110 ± 0.0001	2.10 ± 0.02

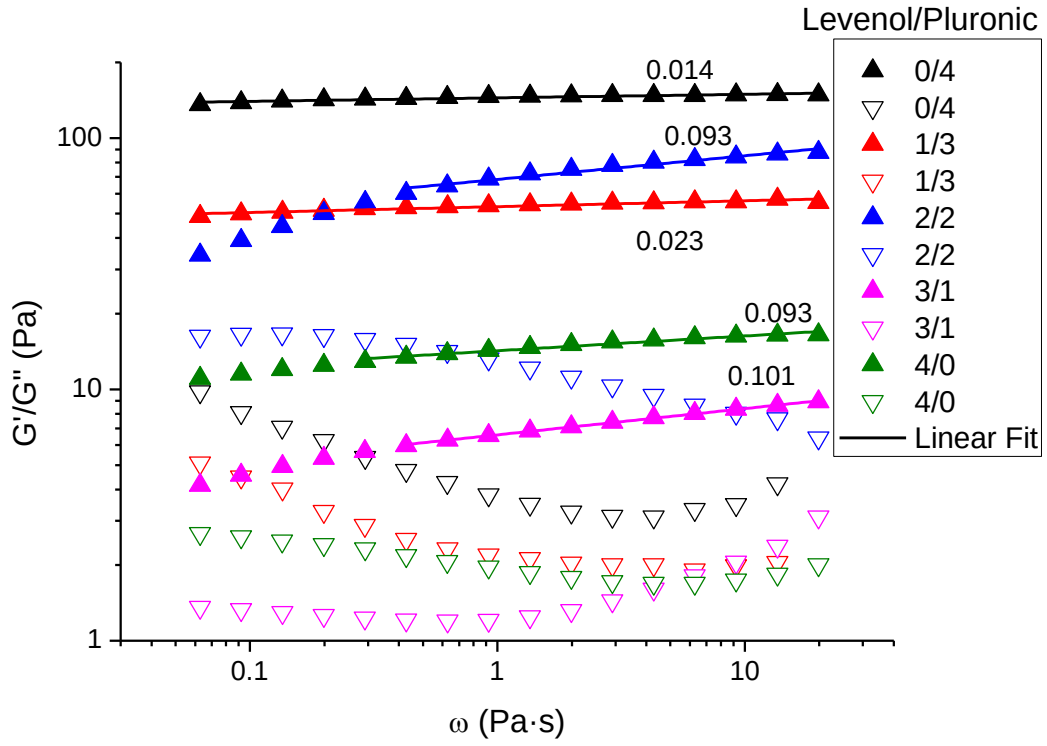

Figure 7.3. Mechanical spectra for 40 wt% emulsions as a function of ratio of Levenol C201/Pluronic PE9400 and the slope of G'.

Figure 7.3 shows mechanical spectra for all emulsions studied. G' is higher than G'' in the frequency range studied for all the samples. However, different slopes of G' were observed as a function of ratio of surfactants. When the main surfactant is Levenol (4/0, 3/1), a decrease of G' and G'' with Pluronic concentration can be detected. In addition, the slopes of G' and G'' for both emulsions are quite similar. This is pointed out that a weaker structure was formed when Levenol C201 was used alone. There are no enough concentration of PE9400 to form multilayers or brush interactions. Interestingly, the same slope was exhibited for 2/2 emulsion but with higher values of G' and G''. In this emulsion containing the same concentration of both surfactants, brush interaction

could be the reason why values of G' and G'' were higher. When PE9400 was the main surfactant, an increase of G' and G'' with PE9400 concentration was observed. This fact may be explained by the increment of multilayers formed with pluronic concentration. In addition, it is not only an increase of viscoelastic modulus but also a decrease of the slope of G'. Hence, the structure is becoming more solid-like.

Figure 7.4 shows the influence of aging time on DSD for the emulsion containing A) Levenol C-201 and B) Pluronic PE9400 as only surfactant in continuous phase. Both figures show an increase in droplet size. However, while in figure 7.4A, an increase of the second peak and a reduction of the population with smaller size with aging time is observed, in figure 7.4B, DSD follows a specific time-independent form that moves up the size axis. These facts indicate different destabilization mechanisms.[21,22] The multimodal final distribution shown in figure 7.4A is related to a coalescence phenomenon.[23] By contrast, Ostwald ripening can lead to a DSD sharpening [24], as shown in figure 7.4B. In order to gain a deeper insight into differences between DSD for figure 7.4A and 7.4B, figure 7.5 is shown.

Figure 7.5 shows the evolution of Sauter diameter, volumetric diameter and span with aging time for the emulsions studied. Sauter diameter increased with aging time for Pluronic emulsion. In addition, volumetric diameter increased similarly to Sauter diameter and interestingly, span decreased with aging time for the emulsion containing only Pluronic PE9400. Furthermore, growth rate of the diameters is continuously decreasing ($d^2D4.3/dt^2 \leq 0$). These observations reveal that Ostwald ripening is the predominant mechanism. [25] By contrast, emulsion with only Levenol C201 showed no differences in Sauter diameter, an increase in volumetric diameter from 150 hours, and

an increase of span with aging time. Therefore, this analysis allows two different trends in the increase of droplet size to be distinguished.

The Ostwald ripening process is generally modelled with the well-known Lifshitz-Slyozov-Wagner (LSW) theory, predicted by the following equation:

$$\omega_T = \frac{d\bar{r}^3}{dt} \ (EQ.7.7)$$

Being ω_T the constant ripening rate and $\bar{r}$ the number-weighted mean droplet radius. Therefore, the trend of Pluronic PE9400 is related to Ostwald ripening behaviour, as seen in figure 7.6A. Conversely, the trend of Levenol C-201 cannot be fitted to the Ostwald Ripening model proposed by LSW theory. Hence, the type of surfactant can be a determining factor not only in the stability of emulsions but also in the predominant destabilization process that takes place. Since the emulsions with Pluronic PE9400 could be flocculated, the direct contact of flocculated oil droplets might promote Ostwald ripening by reducing the diffusion path length [26]. Furthermore, the 3D brush/mushroom conformation of Pluronic and the formation of multilayers may promote Ostwald Ripening phenomenon. Interestingly, all emulsions of this study containing Pluronic PE9400 followed the same trend (data not shown). However, 1/3 and 2/2 emulsions presented oiling-off after one week of aging time. Hence, although the first destabilization mechanism would be Ostwald ripening, coalescence may take place later.

Nevertheless, the increase of droplet size for the emulsion that only contains Levenol C-201 is different. This trend follows the equation proposed by Kabalnov and Weers for coalescence rate (figure 7.6B).[8]

$$\frac{1}{D^2} = \frac{1}{D_0^2} - \frac{2\pi}{3}\omega t \text{ (EQ.7.8)}$$

where D_0 is the initial diameter, ω is the coalescence rate and t is the time.

This fact points out that the emulsion with only Levenol C201 showed an increase of droplet size due to coalescence. In addition, this emulsion presented the highest recoalescence during its preparation. Consequently, it is to be expected that the main destabilization process can be related to coalescence.

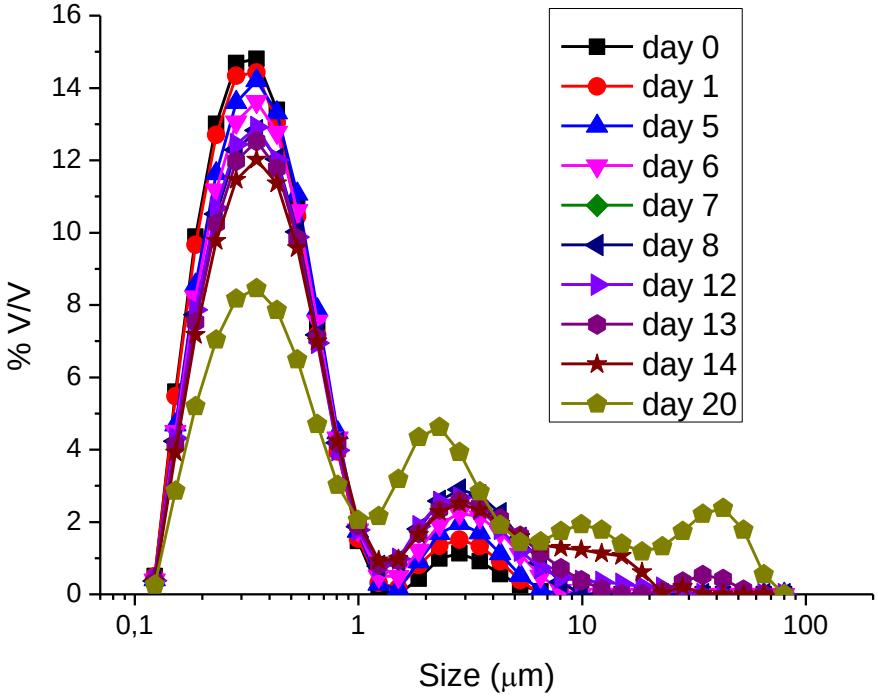

Figure 7.4A. Influence of aging time on DSD for emulsion that only contains Levenol C201 as surfactant.

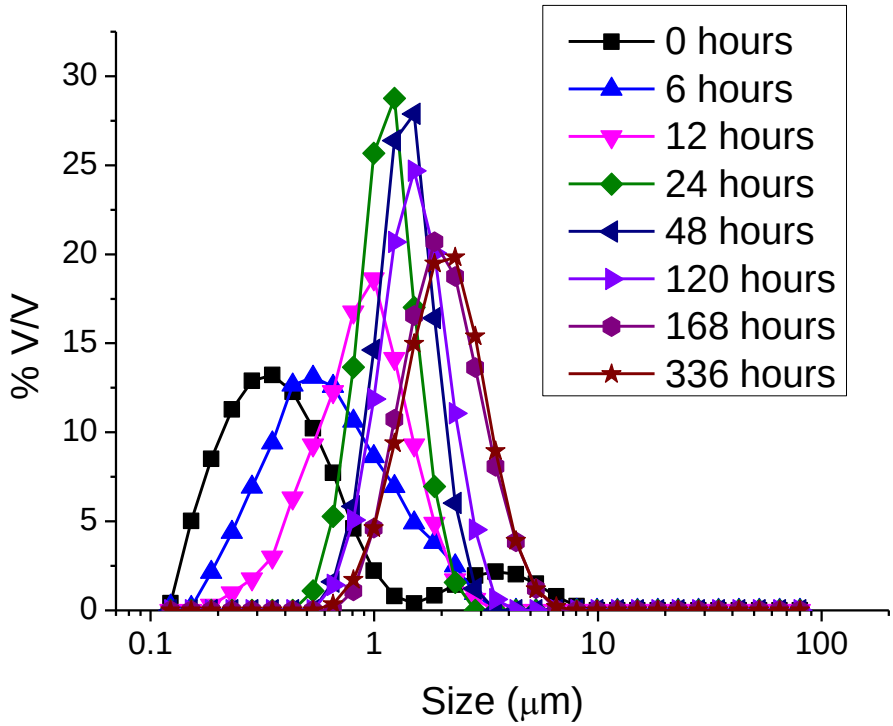

Figure 7.4B. Influence of aging time on DSD emulsion that only contains Pluronic PE9400 as surfactant.

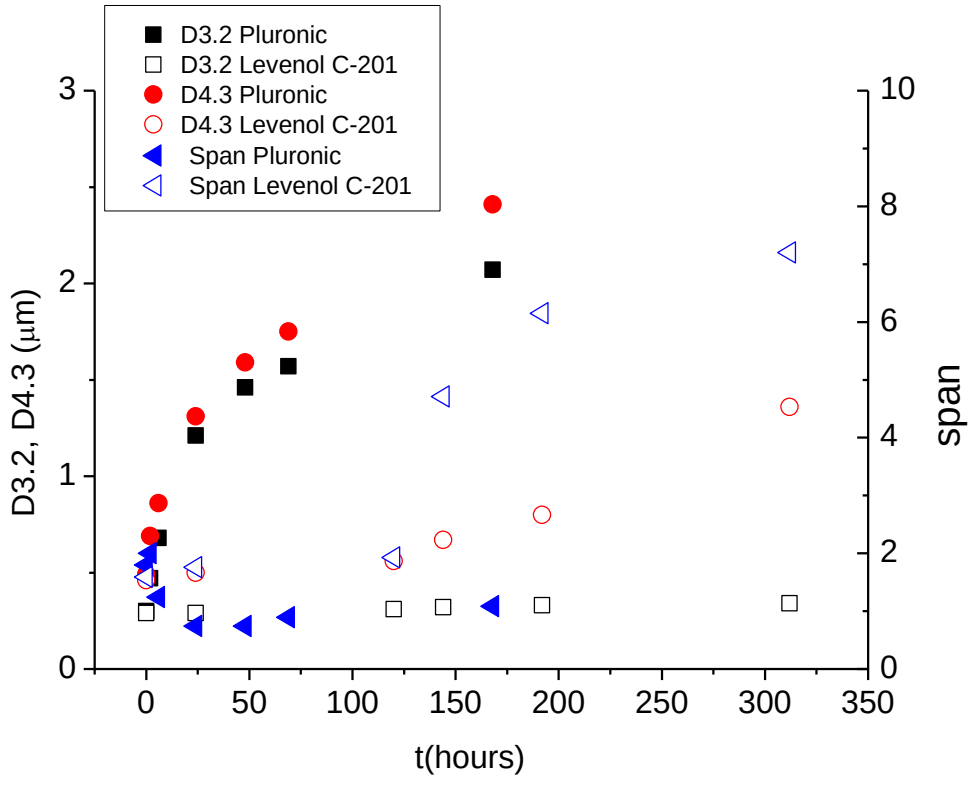

Figure 7.5. Influence of aging time on Sauter, Volumetric diameters and span for emulsions containing only one surfactant in continuous phase.

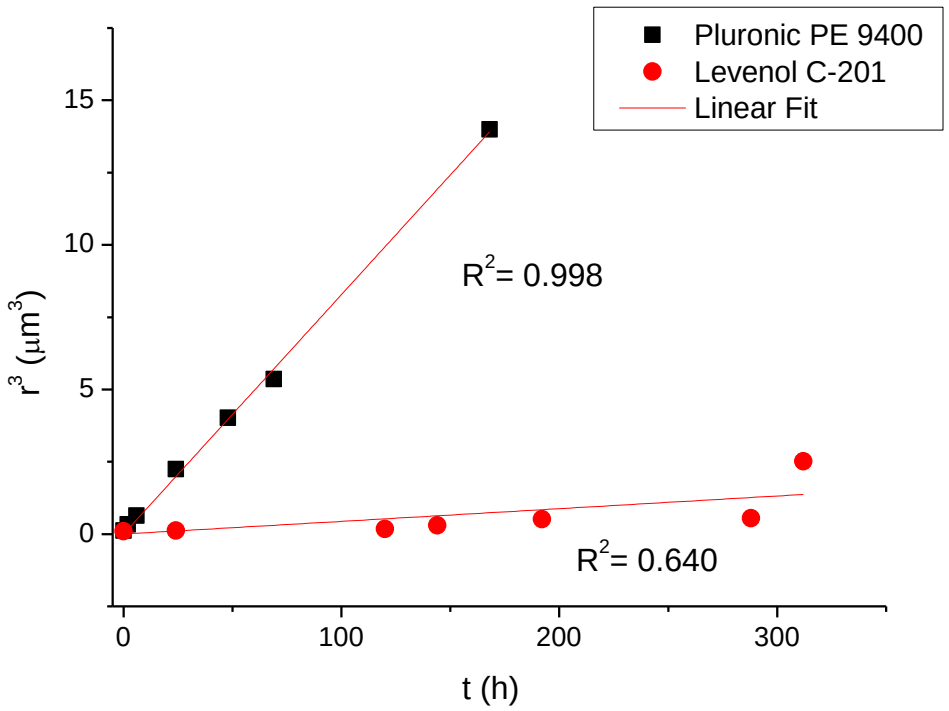

Figure 7.6A. Effect of continuous phase composition on time dependence of the cube of mean droplet radius (r^3) for eco-friendly emulsions during aging time at 20ºC.

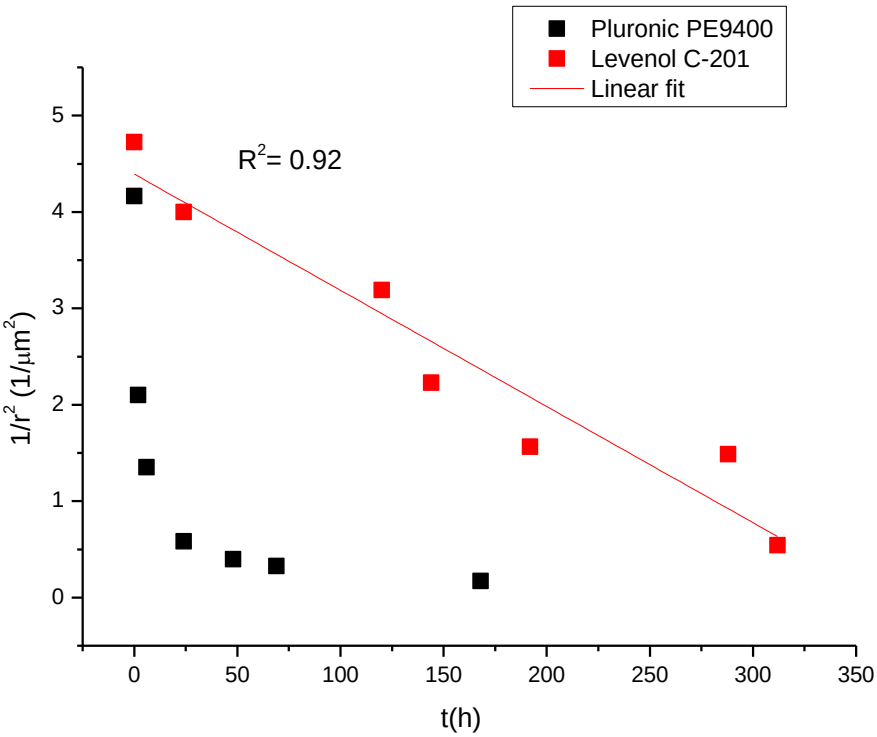

Figure 7.6B. Effect of continuous phase composition on time dependence of the inverse of the quadratic of mean droplet radius ($1/r^2$) for eco-friendly emulsions during aging time at 20ºC.

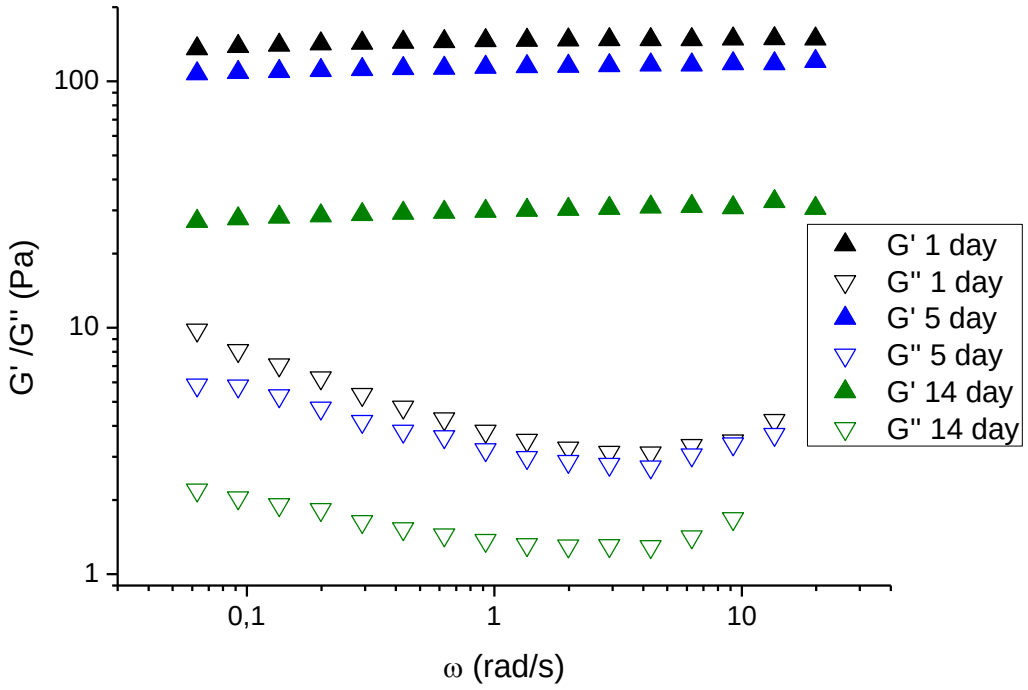

Figure 7.7A. Influence of aging time on mechanical spectra for emulsion containing only PE9400 as the only surfactant.

Figure 7.7 shows the influence of aging time on frequency sweeps for emulsions with A) Pluronic PE9400 and B) Levenol C201. In the figure 7.7A, G' was higher than G'' along the whole frequency range covered. Both moduli depend on frequency but following a different pattern. G' exhibited a weak frequency dependence, while G" showed a marked increase in its frequency-dependency above a certain frequency in the 0.07–1 rad/s range. This behaviour was observed for all aging times studied. In addition, both G' and G'' decreased with aging time being the decrease of G' more marked. This is related to an increase of droplet size, which supports the laser diffraction results. [27]

In figure 7.7B, G' was also higher than G'' in all the frequency range studied for all aging times. A pronounced decrease of G'' was observed from day 1 to day 5 while G' remained almost constant. This is related to an increase of the complex viscosity. This fact can be attributed to a process of flocculation or creaming. After that, a clear decrease of G' and a slight decrease of G'' from day 5 to day 14 can be observed. Hence, firstly Levenol emulsion underwent a flocculation and/or a creaming processes and secondly coalescence. It is very common that before a coalescence process, the flocculation takes place.

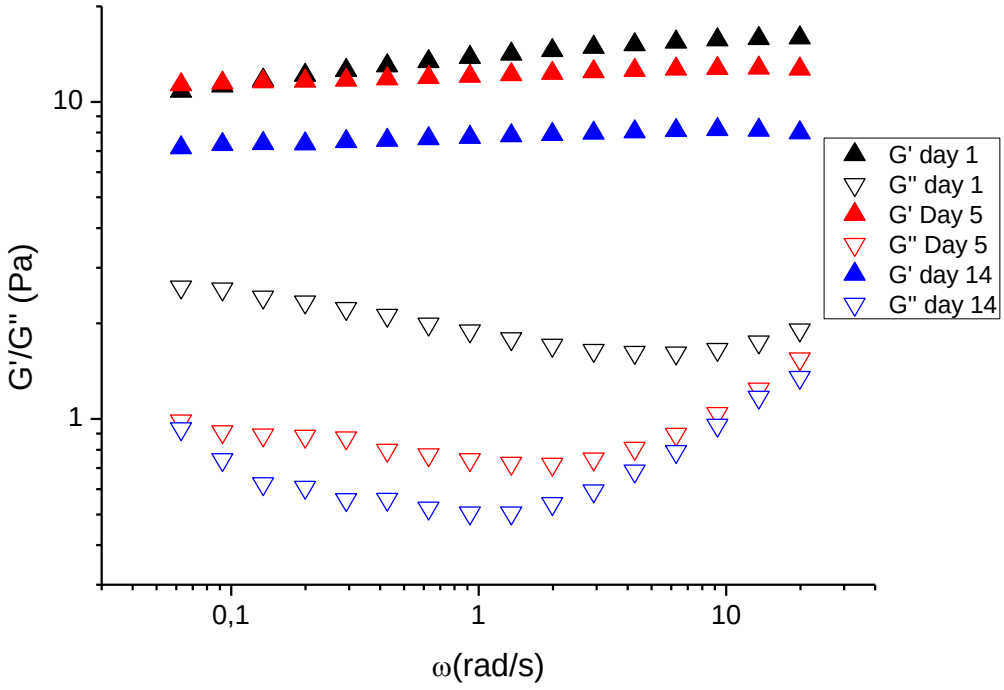

Figure 7.7B. Influence of aging time on mechanical spectra for emulsion containing only Levenol C201 as the only surfactant.

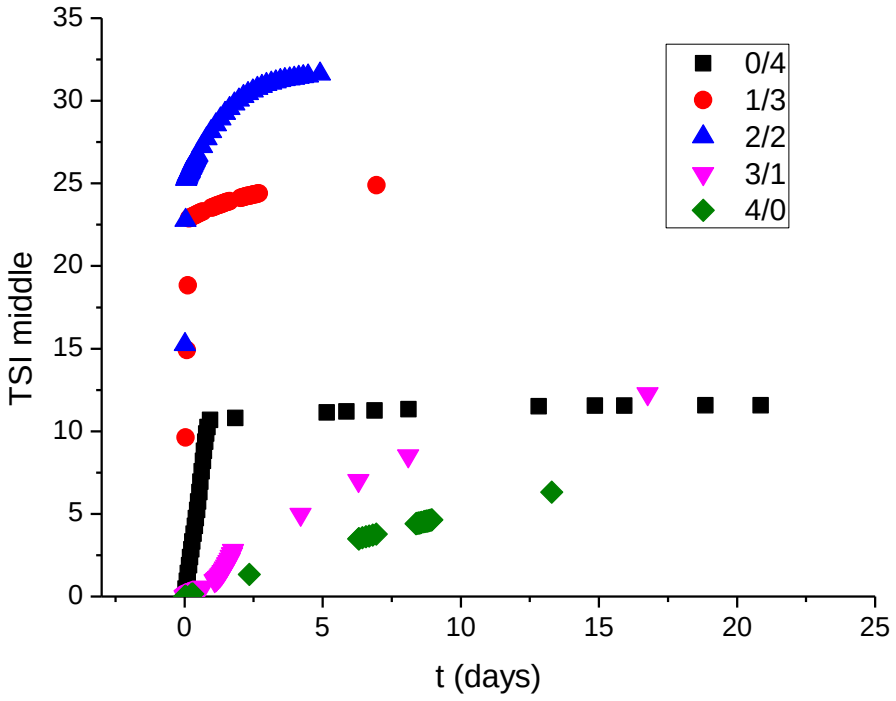

Figure 7.8. Turbiscan Stability Index (TSI) in the middle part of the samples for emulsions studied as a function of ratio of Levenol C201/Pluronic PE9400.

Figure 7.8 shows Turbiscan Stability Index (TSI) for the middle part of the measuring cell for all emulsions studied. TSI was chosen in the middle part because it is where the kinetics of increase of droplet size is analysed. All emulsions showed an increase of TSI with aging time. However, a marked increase of TSI with aging time was observed after one day of aging time for all emulsions containing pluronic. At higher aging time, this increase mellowed. This fact is related to Ostwald ripening mechanism. These emulsions exhibited two trends with aging time. By contrast, the emulsion with levenol showed a linear increase of TSI during the study time. Hence, there is a clear difference of trends of increase of droplet size analysing MLS results. This fact supports laser diffraction results. Taking into account these results, 4/0 emulsion presented the best stability considering the droplet size increase.

Conclusions

An increase of recoalescence during processing of emulsion with Levenol C-201 concentration was detected. Hence, Pluronic PE9400 protects better the interface against recoalescence. Rheological properties of these emulsions reveal an increase of rheological parameters (η_0, G', G'') with pluronic concentration when it is the predominant surfactant or for 2/2 ratio of surfactants. This fact is related to a flocculation process during the processing since Sauter diameters were very similar for all emulsions studied. This flocculation could be due to a depletion flocculation process or due to the 3D brush/mushroom conformation and the formation of multilayers of Pluronic. The latter may be the reason why the protection of the interface is better with Pluronic. An increase of droplet size with aging time were observed in all emulsions but

with different trends. There are some evidences that point out different destabilization mechanisms. Emulsions with only Levenol C201 as surfactant showed an increase of volumetric diameter, a decrease of span and an almost constant Sauter diameter with aging time. Conversely, a great increase of Sauter and volumetric diameter and a decrease of span were observed for the pluronic emulsion. These facts have been corroborated by analysing the droplet size increase fitting to the LWT theory about Ostwald ripening and to the coalescence equation proposed by Weers and Kabalnovov. The 3D brush/mushroom conformation and the formation of multilayers of Pluronic in the emulsions studied could be the reason why these systems underwent Ostwald ripening and not coalescence. This conformation would promote Ostwald ripening and reduce coalescence. By contrast, structure induced by Levenol did not protect perfectly the interface and coalescence was observed. Furthermore, some differences can also be seen in rheology and MLS results with aging time for the two extreme systems. Hence, this work demonstrates the importance of the type of surfactant in a formulation regardless these possess droplet size distributions very similar after preparation. On top of that, the surfactant type has demonstrated to be a key factor in which destabilization process emulsions will undergo.

References

[1] D.J. McClements, Food emulsions: principles, practices, and techniques, CRC press, 2015.

[2] J. Bibette, F.L. Calderon, P. Poulin, Emulsions: basic principles, Reports Prog. Phys. 62 (1999) 969.

[3] I. Capek, Degradation of kinetically-stable o/w emulsions, Adv. Colloid Interface Sci. 107 (2004) 125–155.

[4] U. El-Jaby, M. Cunningham, T.F.L. McKenna, Comparison of emulsification devices for the production of miniemulsions, Ind. Eng. Chem. Res. 48 (2009) 10147–10151.

[5] A.J. Ardell, The effect of volume fraction on particle coarsening: theoretical considerations, Acta Metall. 20 (1972) 61–71.

[6] C. Solans, P. Izquierdo, J. Nolla, N. Azemar, M.J. Garcia-Celma, Nano-emulsions, Curr. Opin. Colloid Interface Sci. 10 (2005) 102–110.

[7] S. Ariyaprakai, S.R. Dungan, Influence of surfactant structure on the contribution of micelles to Ostwald ripening in oil-in-water emulsions, J. Colloid Interface Sci. 343 (2010) 102–108.

[8] A. Kabalnov, J. Weers, Kinetics of mass transfer in micellar systems: surfactant adsorption, solubilization kinetics, and ripening, Langmuir. 12 (1996) 3442–3448.

[9] D.N. Petsev, Emulsions: structure, stability and interactions, Academic Press, 2004.

[10] J. Santos, L.A. Trujillo-Cayado, N. Calero, J. Muñoz, Physical characterization of eco-friendly O/W emulsions developed through a strategy based on product engineering principles, AIChE J. 60 (2014) 2644–2653.

[11] X.Y. Xiong, K.C. Tam, L.H. Gan, Polymeric nanostructures for drug delivery applications based on pluronic copolymer systems, J. Nanosci. Nanotechnol. 6 (2006) 2638–2650.

[12] M. Gonzales, K.M. Krishnan, Phase transfer of highly monodisperse iron oxide nanocrystals with Pluronic F127 for biomedical applications, J. Magn. Magn. Mater. 311 (2007) 59–62.

[13] J.J. Escobar-Chávez, M. López-Cervantes, A. Naik, Y. Kalia, D. Quintanar-Guerrero, A. Ganem-Quintanar, Applications of thermo-reversible pluronic F-127 gels in pharmaceutical formulations, J. Pharm. Pharm. Sci. 9 (2006) 339–358.

[14] C. Lesaint, W.R. Glomm, L.E. Lundgaard, J. Sjoblom, Dehydration efficiency of AC electrical fields on water-in-model-oil emulsions, COLLOIDS SURFACES A-PHYSICOCHEMICAL Eng. Asp. 352 (2009) 63–69. doi:10.1016/j.colsurfa.2009.09.051.

[15] L.M. Pérez-Mosqueda, L.A. Trujillo-Cayado, F. Carrillo, P. Ramírez, J. Muñoz, Formulation and optimization by experimental design of eco-friendly emulsions based on d-limonene, Colloids Surfaces B Biointerfaces. 128 (2015) 127–131.

[16] R. Pal, Effect of droplet size on the rheology of emulsions, AIChE J. 42 (1996) 3181–3190.

[17] L.M. Pérez-Mosqueda, J. Maldonado-Valderrama, P. Ramírez, M.A. Cabrerizo-Vílchez, J. Muñoz, Interfacial characterization of Pluronic PE9400 at biocompatible (air–water and limonene–water) interfaces, Colloids Surfaces B Biointerfaces. 111 (2013) 171–178.

[18] G. Gotchev, T. Kolarov, K. Khristov, D. Exerowa, Electrostatic and steric interactions in oil-in-water emulsion films from Pluronic surfactants, Adv. Colloid Interface Sci. 168 (2011) 79–84.

[19] P. Ramírez, J. Muñoz, V.B. Fainerman, E. V Aksenenko, N. Mucic, R. Miller, Dynamic interfacial tension of triblock copolymers solutions at the water–hexane interface, Colloids Surfaces A Physicochem. Eng. Asp. 391 (2011) 119–124.

[20] L.A. Trujillo-Cayado, P. Ramírez, L.M. Pérez-Mosqueda, M.C. Alfaro, J. Muñoz, Surface and foaming properties of polyoxyethylene glycerol ester surfactants, Colloids Surfaces A Physicochem. Eng. Asp. 458 (2014) 195–202.

[21] V. Schmitt, C. Cattelet, F. Leal-Calderon, Coarsening of alkane-in-water emulsions stabilized by nonionic poly (oxyethylene) surfactants: The role of molecular permeation and coalescence, Langmuir. 20 (2004) 46–52.

[22] G. Urbina-Villalba, A. Forgiarini, K. Rahn, A. Lozsán, Influence of flocculation and coalescence on the evolution of the average radius of an O/W emulsion. Is a linear slope of R^3 vs. t an unmistakable signature of Ostwald ripening?, Phys. Chem. Chem. Phys. 11 (2009) 11184–11195.

[23] T. Delmas, H. Piraux, A.-C. Couffin, I. Texier, F. Vinet, P. Poulin, M.E. Cates, J. Bibette, How to prepare and stabilize very small nanoemulsions, Langmuir. 27 (2011) 1683–1692.

[24] E. Nazarzadeh, T. Anthonypillai, S. Sajjadi, On the growth mechanisms of nanoemulsions, J. Colloid Interface Sci. 397 (2013) 154–162.

[25] F. Leal-Calderon, V. Schmitt, J. Bibette, Emulsion science: basic principles, Springer Science & Business Media, 2007.

[26] A.M. Djerdjev, J.K. Beattie, Enhancement of ostwald ripening by depletion flocculation, Langmuir. 24 (2008) 7711–7717.

[27] N. Calero, J. Muñoz, P.W. Cox, A. Heuer, A. Guerrero, Influence of chitosan concentration on the stability, microstructure and rheological properties of O/W emulsions formulated with high-oleic sunflower oil and potato protein, Food Hydrocoll. 30 (2013) 152–162.

Chapter 8: Influence of processing temperature on stability of eco-friendly emulsions.

Abstract

This work is based on tuning the preparation temperature of ecofriendly emulsions in order to reduce the flocculation induced by processing. Rheology, laser diffraction and Multiple Light Scattering have been used to characterize the properties and to detect and quantify the destabilization mechanisms of these emulsions. Emulsions prepared up to 15 ºC showed a cross-over point in the mechanical spectra while a gel-type behavior was shown for emulsions processed above this temperature. This fact pointed out two different grades of flocculation since there was no droplet-size effect. A combined analysis of complex viscosity values, volumetric diameter and variation of backscattering with aging time reached to the conclusion that the most stable emulsion was prepared at 5 ºC since there was a reduction of collision frequency and therefore, a reduction of flocculation. Therefore, this work demonstrated the direct relation between flocculation and processing temperature for these green emulsions.

8.1. Introduction

Emulsions are a kind of disperse systems consisting of two immiscible liquids. The liquid droplets (the disperse phase) are dispersed in a liquid medium (the continuous phase).[1] They have applications in several fields like coatings, food, agrochemicals as well as cosmetics. Long-term stability is a pre-requisite for these systems. Many destabilization processes can take place in emulsions such as creaming, flocculation, coalescence and Ostwald ripening. The flocculation of emulsions could be a double-edged sword since it can provoke an increase of viscosity, which could enhance stability against creaming, but coalescence could take place after a period of time for a flocculated emulsion.[2] [3]

Flocculation occurs when there is not sufficient repulsion to keep the droplets apart to distances where the van der Waals attraction is weak [1]. The repulsion forces can be ionic repulsion or steric repulsion. Steric repulsion is produced by using nonionic surfactants or polymers, for example, alcohol ethoxylates, or A-B-A block copolymers. Not only the surfactant nature and concentration but also the processing parameters (emulsification temperature, speed and time) are crucial in the formation of emulsions and in their physical stability.[4][5][6] However, there is no much information about the influence of processing temperature on the physical stability, flocculation and rheology of emulsions. Furthermore, changes in solubility of polyoxyethylene-type non-ionic surfactants with temperature can be produced. [7][8] The surfactant is hydrophilic at low temperatures but becomes lipophilic with increasing temperature due to dehydration of the polyoxyethylene chains. [9]

Organic solvents has played a vital role in the development of agrochemical products in the past. No attention has been paid to avoid the release of these harmful chemicals in the land and sea. However, during the last decade special emphasis has been made towards green solvents and surfactants. [10][11] [12] In this work, we have used a mixture of ecofriendly solvents (N,N-dimethyldecanamide and D-Limonene) [13][14] and an ecologic surfactant (polyoxyethylene glycerol fatty acid ester, Glycereth-17 Cocoate) that possesses the ecolabel (DID list: 2133) to prepare concentrated green emulsions.

These concentrated ecofriendly emulsions have been studied previously at room temperature [15] and they showed important flocculation problems. One method to reduce this destabilization process is to tune the emulsification temperature. Hence, a

systematic study of the influence of processing temperature has been carried out in order to enhance the stability of these ecological emulsions.

8.2. Materials and methods

8.2.1. Materials

N,N Dimethyl Decanamide (Agnique AMD-10^{TM}) and D-Limonene, was kindly supplied by BASF and Sigma Chemical Company respectively. A non-ionic surfactant derived from cocoa oil (polyoxyethylene glycerol fatty acid ester, Glycereth-17 Cocoate) was used as emulsifier. Its trade name is Levenol C-201^{TM} and it was received as a gift from KAO. An antifoaming agent (RD antifoam emulsion, DOW CORNING) was used. All emulsions were prepared using deionized water.

8.2.2. Emulsion preparation

The aqueous phase was a solution of deionized water, 0.1 wt% antifoam emulsion and 4 wt% of the green surfactant. The oil phase (40 wt%) consisted of a mixture of two ecofriendly solvents: AMD-10 and D-Limonene in a ratio of 75/25. This ratio of solvents was previously demonstrated to be optimum by Santos et al., 2014.[16]

Emulsions were prepared using a rotor-stator homogenizer (Silverson L5M), equipped with a mesh screen, at 8000 rpm during 60 seconds in a thermostatically-controlled water bath at 5, 15, 25, 35 or 45 ºC. Dispersed and continuous phase were previously tempered in the same bath.

8.2.3 Droplet size distribution measurements.

Droplet size distributions and mean diameters of oil droplets were measured by laser diffraction technique (Mastersizer X, Malvern, Worcestershire, United Kingdom). All

measurements were carried out in triplicate for each emulsion. The influence of aging time on droplet size distributions were carried out 1, 7, 13, 21 and 28 days after preparation.

The mean droplet diameters were expressed as Sauter diameter ($D_{3,2}$) and volume mean diameter ($D_{4,3}$):

$$D_{3,2} = \sum_{i=1}^{N} n_i d_i^{\,3} \Big/ \sum_{i=1}^{N} n_i d_i^{\,2} \qquad \text{Eq.8.1}$$

$$D_{4,3} = \sum_{i=1}^{N} n_i d_i^{\,4} \Big/ \sum_{i=1}^{N} n_i d_i^{\,3} \qquad \text{Eq. 8.2}$$

where d_i is the droplet diameter, N is the total number of droplets and n_i is the number of droplets having a diameter d_i.

8.2.4. Rheological measurements.

Rheological tests were performed with a controlled-stress rheometer (Haake MARS, Thermo-Scientific, Germany). Emulsions studied were measured using a sandblasted double-cone geometry (angle: 0.017 rad; diameter: 60 mm). Flow curves were carried out from 0.05- 5 Pa using a multi-step protocol.

8.2.5. Multiple light scattering

Multiple light scattering measurements were conducted with a Turbiscan Lab Expert until 30 days at 20 ºC in order to study and quantify the destabilization mechanisms in the emulsions prepared. Multiple light scattering is a sensitive and non-intrusive tool to allow physical stability of complex fluids to be analysed. [17], [18]

8.2.6. Microscopic observation

For cryo-scanning electronic microscopy (cryo-SEM), samples were placed on a sample holder and plunged into nitrogen slush. Frozen samples were etched and coated with gold and subsequently were kept at -120ºC for observation.

8.2.7. Statistical analysis.

Laser diffraction and rheological tests were carried out in triplicate, and the resulting data was analysed using one-way analysis of variance (ANOVA). This was carried out using Microsoft excel 2013. All statistical calculations were conducted at a significance level of p= 0.05.

8.3. Results and discussion

Figure 8.1 shows Droplet Size Distribution (DSD) for emulsions as a function of processing temperature at one day of aging time. All emulsions showed bimodal distributions, even trimodal distribution for emulsion processed at 15 ºC. This polidispersion is characteristic of this type of system containing these ecofriendly solvents. [16] [19] There are no significant changes in DSD in emulsions processed up to 35 ºC. However, there is a shift towards bigger droplet sizes from 35 ºC to 45 ºC. This fact could be related to a recoalescence process, which might be attributed to the increased molecular movement and the enhanced collision probability between droplets at higher emulsification temperatures. [5] In spite of this fact, all emulsions showed submicron mean diameters (Table 8.1).

Table 8.1. Sauter diameter for green emulsions as a function of processing temperature.

T (ºC)	D(3.2)
5	0.34
15	0.34
25	0.34
35	0.33
45	0.44

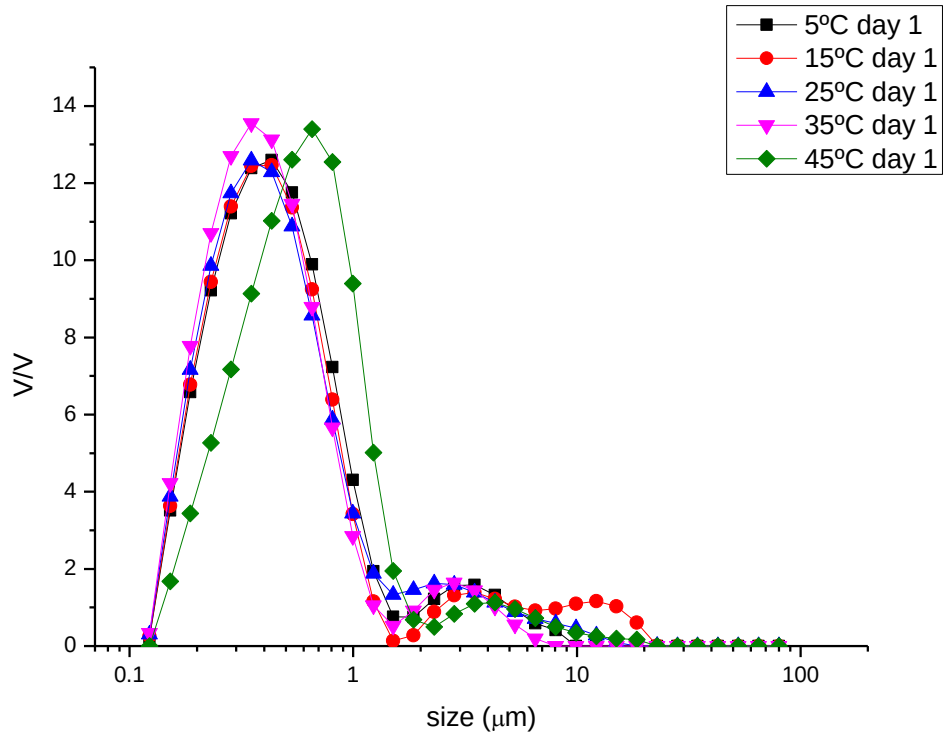

Figure 8.1. Influence of processing temperature on droplet size distributions for emulsions studied.

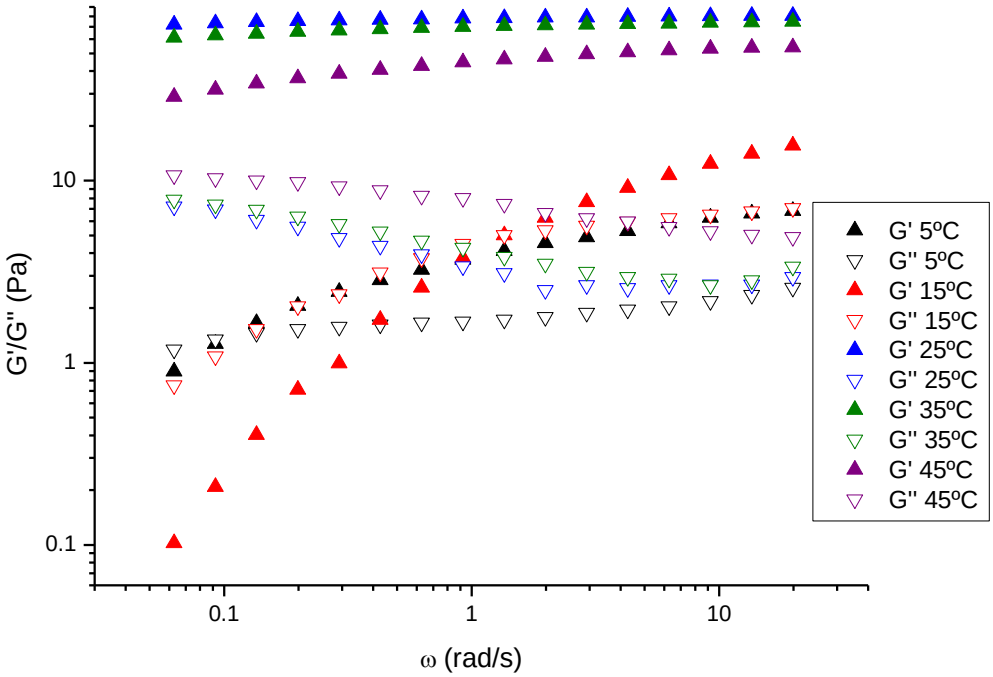

Figure 8.2A. Mechanical spectra for emulsions studied as a function of processing temperature at 20 ºC.

Fig 8.2A illustrates the mechanical spectra for emulsions processed at different temperatures measured at 20 ºC. There are two different behaviours: while emulsions processed above 15 ºC show G' higher than G'' in all the frequency range studied, emulsions processed at 5 ºC and 15 ºC show a crossover point. The latter is typical of weakly structured materials. In this sense, *G*' is lower than *G*" in the lower frequency regime up to the crossover point (ω*), and *G*' is higher than *G*" in the higher frequency regime above ω*. This crossover frequency determines the onset of the terminal relaxation zone. The terminal relaxation time (t_r) was calculated as the inverse of ω* and decreased from 5 to 15 ºC processing temperature. This fact indicates a reduction in the elastic nature of the system, which is related to a loss of structure. Shorter relaxation times lead to relatively fast rearrangements and correlate well with the instability of emulsions against creaming. Conversely, longer relaxation times point out that the droplet-droplet interactions are stronger. This is currently correlated with greater macroscopic stability against creaming in emulsions and suspoemulsions [20][18] Therefore, the emulsion processed at 5 ºC is more structured than those processed at 15 ºC. It is important to highlight that the emulsion processed at 15 ºC showed a third population in DSD. Hence, this fact could be the cause of the structure loss. However, the increase of processing temperature above 15 ºC provokes an increase of both viscoelastic parameters (G' and G'') that is not related to droplet-size effect. This fact could be due to an increase of the flocculation since the collision frequency is higher with temperature. Hence, there would be a significant increase of flocculation from 15 ºC to 25 ºC since it presented the jump in viscoelastic parameters but the same DSD. Nevertheless, emulsions processed at 45 ºC exhibited lower viscoelastic functions than those prepared at 35 and 25 ºC. This is due to the higher droplet size that this system showed. Furthermore, 25 and 35 ºC emulsions presented a minimum of G'' at the characteristic frequency (ω_c), which is a typical weak gel-like behaviour. The plateau modulus associated to ω_c are 79.25 and 74.03 rad/s, respectively. This parameter has been previously used to distinguish between grades of flocculation by Santos et al, 2016. [15] In this case, 25 ºC emulsion could be more flocculated than its counterpart processed at 35 ºC.

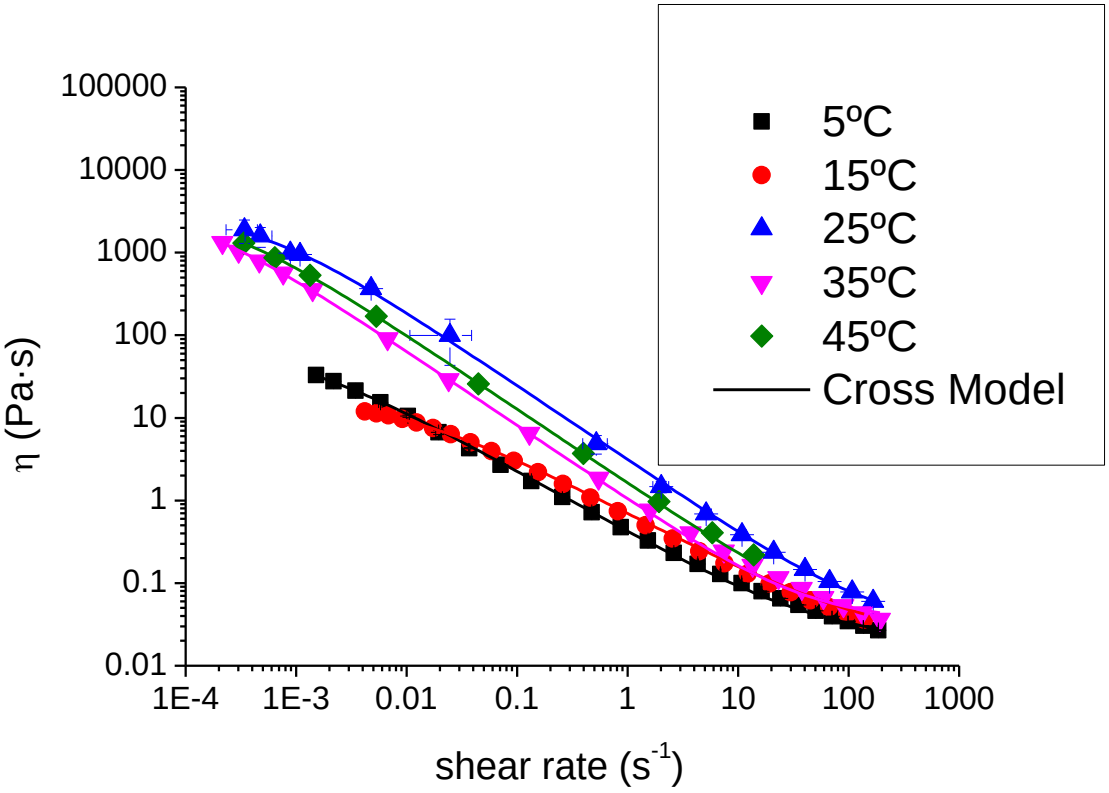

Figure 8.2B. Flow curves as a function of processing temperature for emulsions studied at 20 ºC. Lines represented the fitted to Cross model.

Table 8.2. Fitting parameters to Cross model as a function of processing temperature.

Processing temperature (ºC)	η∞ (Pa·s)	η_o (Pa·s)	k (s^{-1})	n
5	0.02	82.7	1193	0.25
15	0.02	19.4	115	0.30
25	0.03	3000	2073	0.10
35	0.03	2750	4440	0.10
45	0.03	2230	1300	0.10

Standard deviation of the mean (3 replicates) for η_0, η_∞ < 8%

Standard deviation of the mean (3 replicates) for $\dot{g}_c$ < 10%

Standard deviation of the mean (3 replicates) for n < 10%

Figure 8.2B shows flow curves for emulsions processed at different temperatures. All emulsions exhibited shear thinning behaviour with a trend to reach a Newtonian region at a very low shear rate. All curves were fitted fairly well to Cross model (R^2> 0.998) (Equation 8.3). The fitting parameters are shown in table 8.2.

$$\eta = \frac{\eta_0}{1+\left(\frac{\dot{\gamma}}{\dot{\gamma}_c}\right)^{1-n}} \qquad \text{EQ. 8.3}$$

Where $\dot{\gamma}_c$ is related to the critical shear rate for the onset of shear-thinning response, η_0 stands for the zero-shear viscosity and (1-n) is a parameter related to the slope of the power-law region; n being the so-called "flow index".

Results of the ANOVA test demonstrated that there are significant differences in the zero shear viscosity of emulsions studied. The same trend showed in mechanical spectra is presented in zero shear viscosity (η_o). Zero shear viscosity of emulsions processed at 5 and 15 ºC are in two lower decades than for the emulsions processed at higher temperatures. In addition, there is a slight decrease in zero shear viscosity from 35 ºC to 45 ºC emulsions due to the droplet-size effect. Furthermore, it is important to highlight the differences between flow index (n) for the emulsions studied. Flow index for emulsions processed above 15 ºC are much lower than those processed below this temperature. These low values have been shown previously in flocculated emulsions [15][21] Hence, it supports the SAOS results that pointed out these emulsions were more flocculated than those prepared at lower temperature.

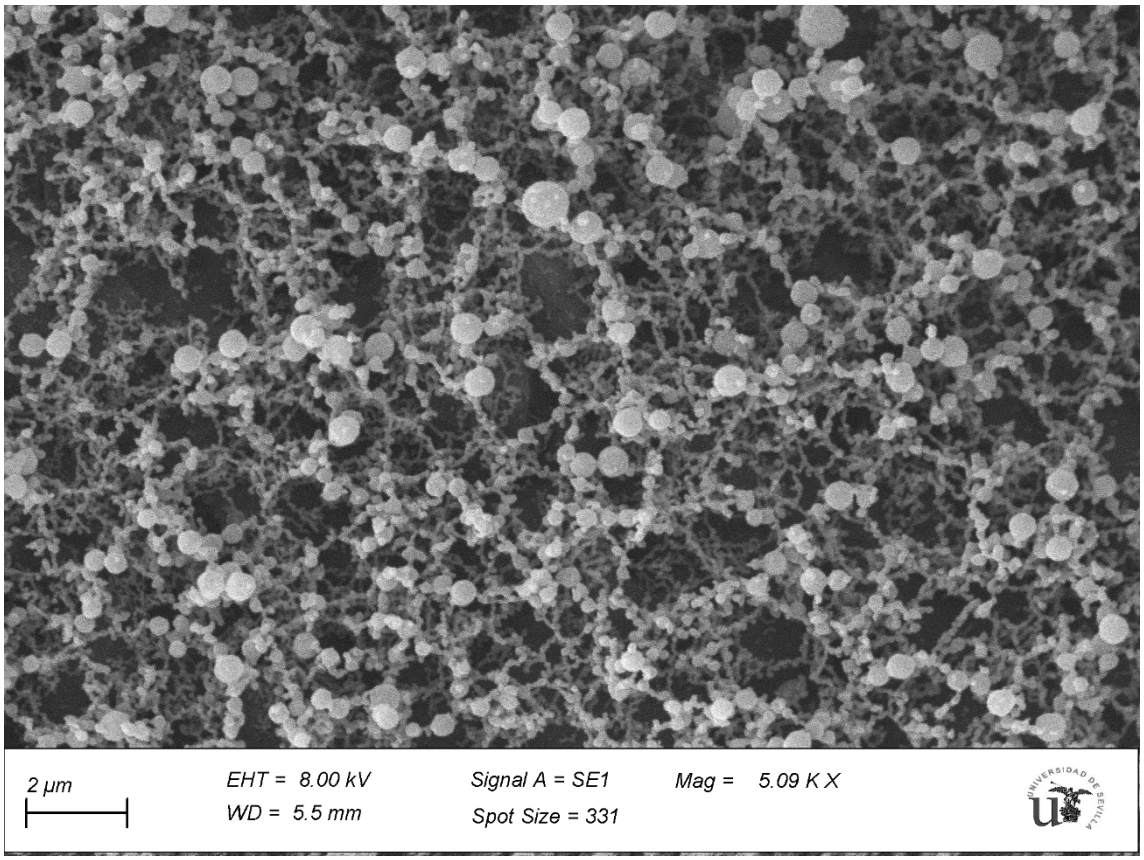

Figure 8.3A. Cryo-SEM micrograph of green emulsion processed at 5°C.

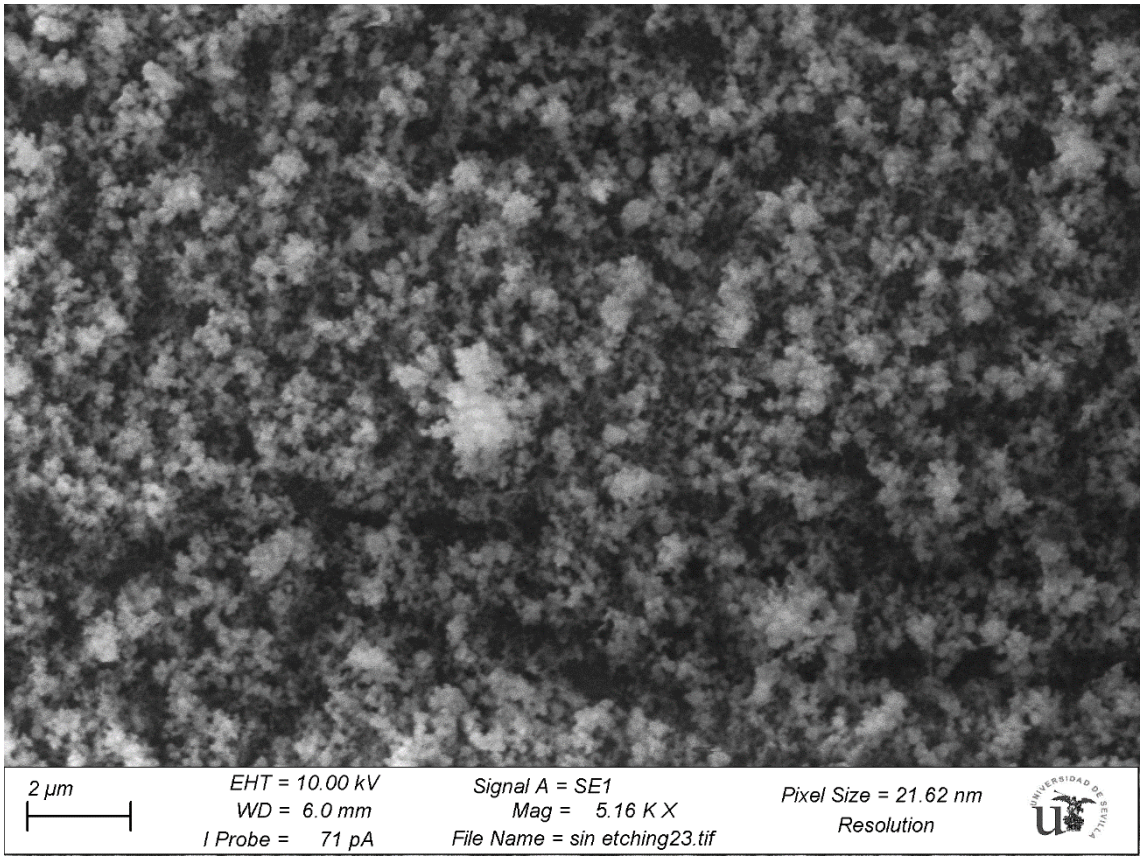

Figure 8.3B. Cryo-SEM micrograph of green emulsion processed at 35ºC.

Figure 8.3 show cryo-sem micrographs of emulsion processed at A) 5ºC and B) 35ºC. All the droplets form interconnected chains but single droplets can be differenciate in figure 8.3A. However, a diffuse mass of droplets is shown in figure 8.3B. This fact is directly related to the high flocculation grade of this emulsion. Hence, emulsion processed at 35ºC is much more flocculated than emulsion processed at 5ºC. Furthermore, these micrographs support laser diffraction results about droplet size.

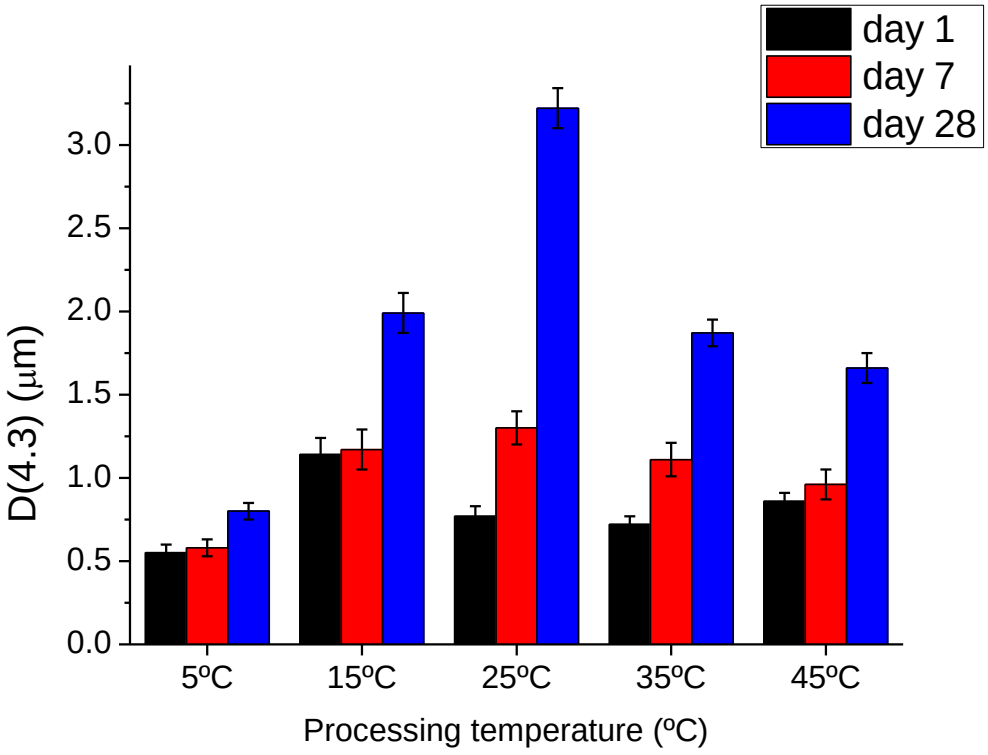

Figure 8.4. Influence of processing temperature on volumetric diameter with aging time.

Figure 8.4 shows the influence of aging time on volumetric diameter for emulsions processed at different temperatures. Results of the ANOVA test demonstrated that there are significant differences in volumetric diameter of day 1 with day 28 of

emulsions studied. There is an increase of volumetric diameter in all emulsions studied but in different grade and in different aging times. Whereas emulsions processed above 15 ºC showed an increase of volumetric diameter from day 7 of aging time, emulsions prepared at 15 ºC or below did not present this increase until day 28. In addition, the emulsion which showed the greatest coalescence was those prepared at 25 ºC. This emulsion seemed to be the most flocculated analysing rheology results. Hence, this points out that the droplets merged after a period of flocculation. On the top of that, the lowest increase is shown by the emulsion which was the least flocculated (5 ºC emulsion). Therefore, these results supports the hypothesis about the different grades of flocculation.

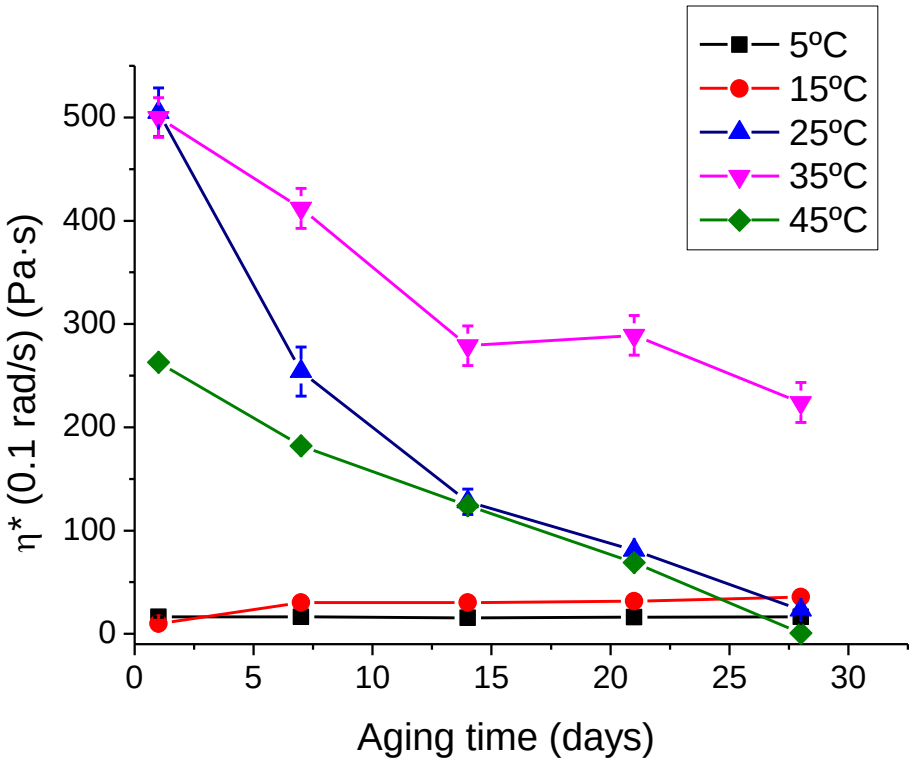

Figure 8.5. Influence of aging time on complex viscosity at 0.1 rad/s as a function of processing temperature.

Figure 8.5 shows the influence of aging time on complex viscosity as a function of processing temperature. 25, 35 and 45 ºC emulsions presented a decrease of complex viscosity with aging time, which is related to an increase of droplet size. However, 15 ºC showed a slight increment of this parameter. This fact indicates a flocculation and/or creaming process. Hence, 15 ºC not only underwent coalescence but also flocculation

and/or creaming. Furthermore, 5 ºC emulsions did not present significant changes in complex viscosity with aging time (ANOVA test). This may be a cause of opposites mechanisms that simultaneously takes place. In order to clarify this point, a Multiple Light Scattering study has been carried out.

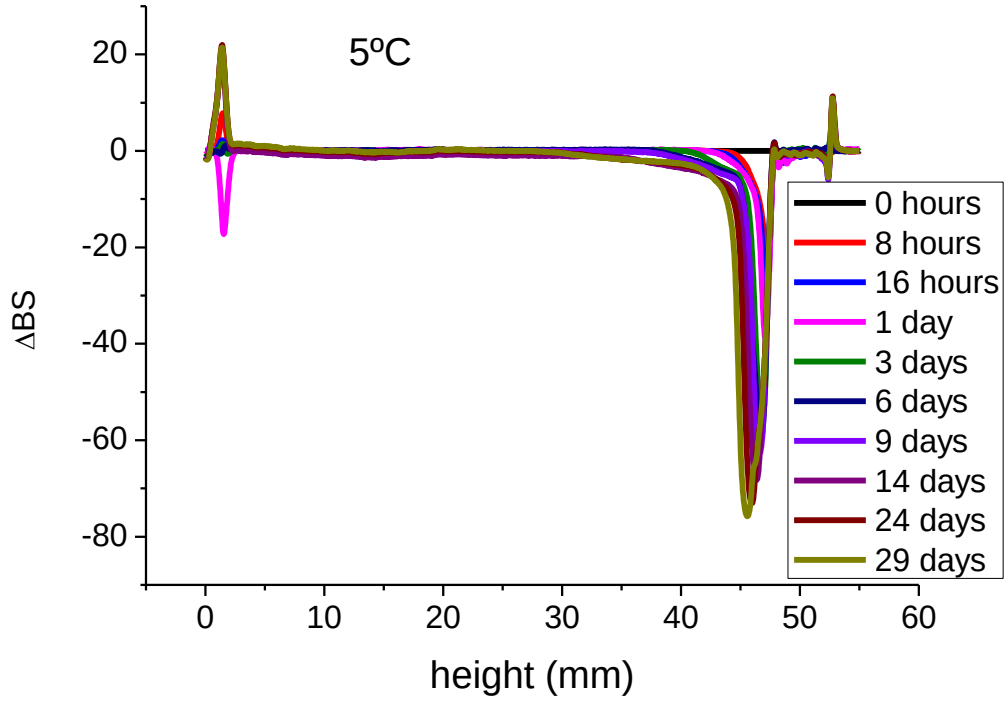

Figure 8.6A. Variation of backscattering versus measuring cell height as a function of time for the emulsion prepared at 5ºC.

Figure 8.6A and 8.6B show the variation of Backscattering (BS) as a function of measuring cell height with aging time for emulsions prepared at 5 ºC and 15 ºC, respectively. Figure 8.6B has been chosen as a way of example of samples prepared at 15 ºC and above since the BS curves for 25ºC, 35 ºC and 45 ºC emulsions presented the same trends with different values. Figure 8.6A presents a decrease of BS in the low zone of the measuring cell until one day of aging time, followed by an increase of BS in the same part above this aging time. The decrease of BS in the low zone is directly related to a clarification process. This fact points out a creaming mechanism at the beginning which leads to a flocculation mechanism in the bottom of the measuring cell. Furthermore, this creaming and flocculation provokes an oiling off process in the upper zone of the measuring cell. No variation in BS in the middle part was shown. Hence, the coalescence is not extensive

in all the measuring cell. Coalescence took part just in the top zone of this sample. Therefore, there was a creaming process firstly that lead to flocculation/coalescence and oiling off mechanism.

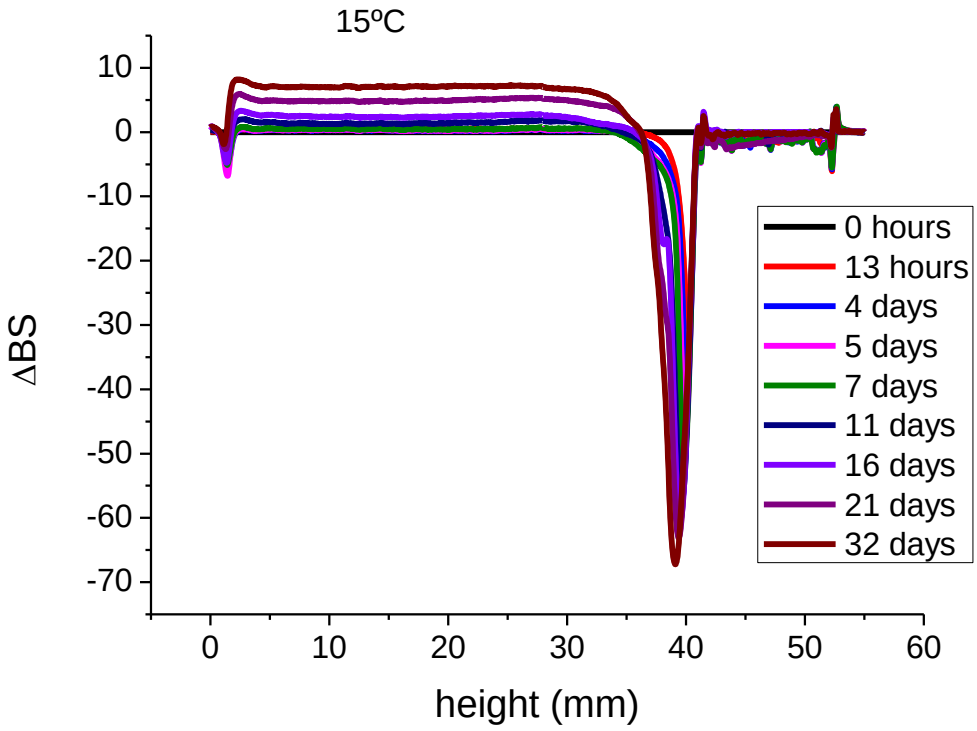

Figure 8.6B. Variation of backscattering versus measuring cell height as a function of time for the emulsion prepared at 15ºC.

Figure 8.6B presents a decrease of BS in the low zone of the vial until 16 days of aging time. After this time, there is an increase of BS in this part. However, this increase is due to the extensive coalescence and/or flocculation that takes place in all the measuring cell since an increase of BS is shown in the low and middle part of the vial. Thus, that creaming could be cover up by flocculation and/or coalescence after day 16. Furthermore, there is a decrease of BS in the upper part that is related to oiling off. A similar behaviour was shown for emulsions prepared at 25 ºC, 35 ºC and 45 ºC. It is important to highlight that just the destabilization of emulsions prepared above 25 ºC were detected by naked-eye in the study time.

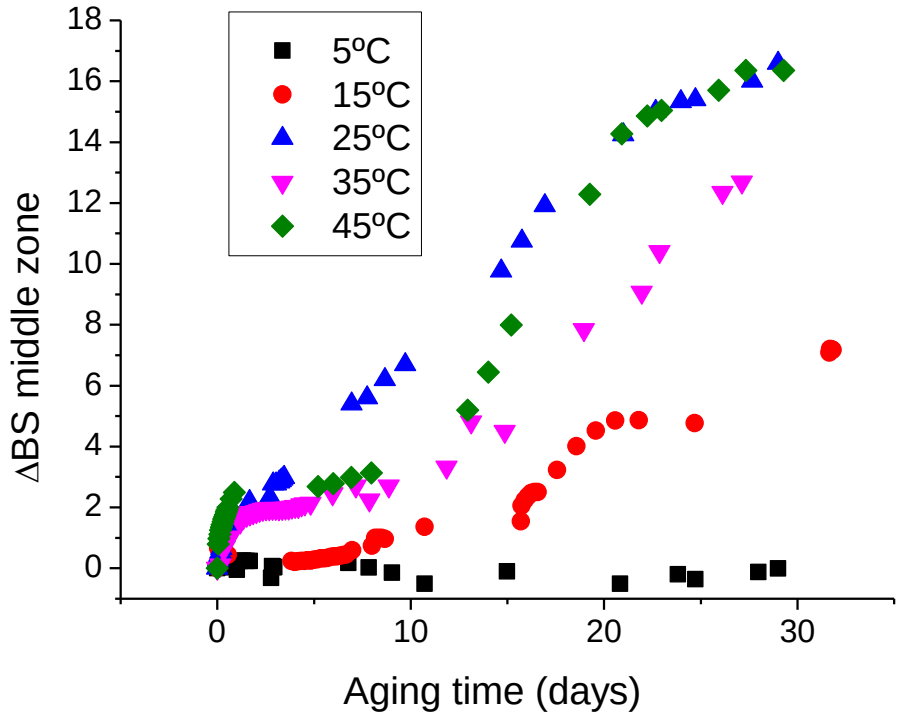

Figure 8.7. Variation of backscatering in the middle zone of the measuring cell (5-25 mm) as a function of processing temperature at room temperature.

Only the increase of BS in the middle part of the measuring cell has been analysed since the creaming process in the emulsions studied could be cover up by flocculation/coalescence. Figure 8.7 shows the BS variation in the middle zone of the measuring cell with aging time for emulsions prepared at different processing temperatures. The variation of BS in the middle zone is directly related to the increase of droplet size or floc size. This method can not distinguish between a floc or a droplet. No variation in BS was presented for emulsion prepared at 5 ºC, being the most stable emulsion studied. Conversely, there was a clear increase of BS for the other emulsions studied in different grades. Flocculated emulsions (those prepared above 15 ºC) exhibited higher increases than emulsion prepared at 15 ºC. MLS results supports laser diffraction and rheology results.

Conclusions

Processing temperature did not show a big influence on DSD below 35 ºC. But interestingly, emulsions prepared at 5 ºC and 15 ºC exhibited viscoelastic properties

typical of weakly structured materials while emulsions prepared at 25 ºC, 35 ºC and 45 ºC showed a weak-gel behaviour. 25 ºC and 35 ºC emulsions presented very similar behaviour but with different values of Plateau modulus. Those differences in this parameter pointed out different grades of flocculation of these emulsions since there was no droplet-size effect. Flow curves showed shear-thinning behaviour for all emulsions studied. Emulsions prepared above 15 ºC exhibited very low values of flow index, which is consistent with flocculated emulsions. All emulsions presented coalescence but in different grades being 5 ºC the emulsion which showed the least increase in droplet size with aging time. Laser diffraction results and rheology with aging time supported the hypothesis about different grades of flocculation induced by processing temperature. Hence, a tight control of the preparation temperature is necessary in order to tune flocculation grade and slow down the destabilization process. Furthermore, rheology has demonstrated to be a powerful tool to show the slight structural differences between emulsions with similar DSD but with different stability. Multiple Light Scattering has been an important method to clarify the destabilization mechanisms which were taking place simultaneously in these emulsions. It was another way to quantify coalescence reaching to the same conclusion that laser diffraction and rheology results: emulsion prepared at 5 ºC showed the best stability due to the low flocculation grade.

References

[1] T. F. Tadros, *Applied surfactants: principles and applications*. John Wiley & Sons, 2006.

[2] H. A. Barnes, “Rheology of emulsions—a review,” *Colloids Surfaces A Physicochem. Eng. Asp.*, vol. 91, pp. 89–95, 1994.

[3] D. J. McClements, *Food emulsions: principles, practices, and techniques*. CRC press, 2015.

[4] R. G. Dos Santos, A. C. Bannwart, M. I. Briceno, and W. Loh, “Physico-chemical properties of heavy crude oil-in-water emulsions stabilized by mixtures of ionic and non-ionic ethoxylated nonylphenol surfactants and medium chain alcohols,”

Chem. Eng. Res. Des., vol. 89, no. 7, pp. 957–967, 2011.

[5] L. Fengyan, Z. Wenli, Z. Tianbo, D. Danghui, and Y. Fang, "Factors influencing droplet size of silicone oil emulsion with high solid content," *China Petro. Process Petrochem. Tech*, vol. 13, pp. 21–26, 2011.

[6] D. J. Mcclements, "Critical review of techniques and methodologies for characterization of emulsion stability," *Crit. Rev. Food Sci. Nutr.*, vol. 47, no. 7, pp. 611–649, 2007.

[7] M. Naous, J. A. Molina-Bolívar, and C. C. Ruiz, "Micelle size modulation and phase behavior in MEGA-10/Triton X-100 mixtures," *Thermochim. Acta*, vol. 598, pp. 68–76, 2014.

[8] G. Vitiello, G. Mangiapia, E. Romano, M. Lavorgna, S. Guido, V. Guida, L. Paduano, and G. D'Errico, "Phase behavior of the ternary aqueous mixtures of two polydisperse ethoxylated nonionic surfactants," *Colloids Surfaces A Physicochem. Eng. Asp.*, vol. 442, pp. 16–24, 2014.

[9] S. L. Ee, X. Duan, J. Liew, and Q. D. Nguyen, "Droplet size and stability of nano-emulsions produced by the temperature phase inversion method," *Chem. Eng. J.*, vol. 140, no. 1, pp. 626–631, 2008.

[10] D. Y. Xing, W. Y. Dong, and T.-S. Chung, "Effects of different ionic liquids as green solvents on the formation and ultrafiltration performance of CA hollow fiber membranes," *Ind. Eng. Chem. Res.*, vol. 55, no. 27, pp. 7505–7513, 2016.

[11] A. M. Yehia and H. M. Mohamed, "Green approach using monolithic column for simultaneous determination of coformulated drugs," *J. Sep. Sci.*, vol. 39, no. 11, pp. 2114–2122, 2016.

[12] X. Li, Y. Qin, C. Liu, S. Jiang, L. Xiong, and Q. Sun, "Size-controlled starch nanoparticles prepared by self-assembly with different green surfactant: The effect of electrostatic repulsion or steric hindrance," *Food Chem.*, vol. 199, pp. 356–363, 2016.

[13] F. M. Kerton and R. Marriott, *Alternative solvents for green chemistry*, no. 20.

Royal Society of chemistry, 2013.

[14] Z. Li, K. H. Smith, and G. W. Stevens, “The use of environmentally sustainable bio-derived solvents in solvent extraction applications—a review,” *Chinese J. Chem. Eng.*, vol. 24, no. 2, pp. 215–220, 2016.

[15] J. Santos, N. Calero, and J. Munoz, “Optimization Of A Green Emulsion Stability By Tuning Homogenization Rate.,” *RSC Adv.*, 2016.

[16] J. Santos, L. A. Trujillo-Cayado, N. Calero, and J. Muñoz, “Physical characterization of eco-friendly O/W emulsions developed through a strategy based on product engineering principles,” *AIChE J.*, vol. 60, no. 7, pp. 2644–2653, 2014.

[17] P. Szumała and N. Luty, “Effect of different crystalline structures on W/O and O/W/O wax emulsion stability,” *Colloids Surfaces A Physicochem. Eng. Asp.*, vol. 499, pp. 131–140, 2016.

[18] J. Santos, L. A. Trujillo, N. Calero, M. C. Alfaro, and J. Munoz, “Physical Characterization of a Commercial Suspoemulsion as a Reference for the Development of Suspoemulsions,” *Chem. Eng. Technol.*, vol. 36, no. 11, pp. 1883–1890, 2013.

[19] J. Santos, G. T. Vladisavljević, R. G. Holdich, M. M. Dragosavac, and J. Muñoz, “Controlled production of eco-friendly emulsions using direct and premix membrane emulsification,” *Chem. Eng. Res. Des.*, vol. 98, pp. 59–69, 2015.

[20] S. Aben, C. Holtze, T. Tadros, and P. Schurtenberger, “Rheological investigations on the creaming of depletion-flocculated emulsions,” *Langmuir*, vol. 28, no. 21, pp. 7967–7975, 2012.

[21] R. Pal, “Dynamics of flocculated emulsions,” *Chem. Eng. Sci.*, vol. 52, no. 7, pp. 1177–1187, 1997.

Conclusions

1. A dependence of homogenization rate and the ratio of solvents with emulsion stability and DSDs was demonstrated. The use of mixtures of green solvents led to obtain emulsions with submicron droplet mean diameter above 5000 rpm in Silverson L5M. In addition, an increment of droplet size with aging time was observed for emulsions with the higher content in D-limonene. However, emulsions containing high AMD-10/D-limonene ratio remained stable against coalescence. Coalescence information obtained by laser diffraction and multiple light scattering supported each other. In addition, the results provided by multiple light scattering revealed that 65/35 & 70/30 emulsions underwent not only coalescence but also creaming. Emulsion with 75/25 solvent ratio exhibited intermediate delay time for the onset of incipient creaming but it did not undergo coalescence. Rheology cleared up the destabilization mechanism for high-limonene content emulsions. First, creaming was dominant (increasing η_0) and later coalescence became predominant (decreasing η_0). From a methodological point of view, monitoring the cooperative information provided by rheology, laser diffraction, multiple light scattering and CSLM for a short aging time is a powerful tool to get a comprehensive panoramic view of the destabilization mechanism and kinetics of emulsions, especially when several mechanisms are simultaneously taking place.

2. The influence of the surfactant concentration in the range of 1.5-4 wt% was studied. The influence in DSD, rheological properties and physical stability in the range of 2-3 wt% was not really significant. However, 1.5wt% of surfactant is not enough to cover the surface of the interface and it led to higher Sauter and volumetric mean diameters. Consequently, this emulsion has the lowest zero-shear viscosity and the highest flow index. Emulsion containing above 3.5wt% of surfactant showed an accused depletion flocculation process since its preparation. The combination of measurements of laser diffraction, flow curves and multiple light scattering at different aging times showed the destabilization phenomenon in the emulsions in short period of time. These techniques have complemented each other leading to the conclusions:
   - ❖ 1.5 wt% emulsion showed creaming as a predominant mechanism.

- ❖ 2-3 wt% emulsions exhibited low creaming rates being 3wt% emulsion which showed the greatest stability.
- ❖ 3.5-4 wt% emulsion showed flocculation, creaming and coalescence. 4wt% emulsion showed the major increase in the droplet size due to the depletion flocculation showed since its preparation.

The emulsions in the range 2-3wt% were highly stable and this excellent result can be explained by considering that the emulsion prepared at intermediate surfactant concentrations showed enough viscosity to prevent creaming and cover the interface. Also, it is not excessive surfactant concentration that may lead to a depletion flocculation process.

3. The production of eco-friendly emulsions with a median droplet diameter ranging from 21 to 69 μm has been demonstrated using direct and premix membrane emulsification (ME) in a simple paddle-bladed stirred cell. An increase of the content of AMD-10 solvent in the dispersed phase caused a decrease in the mean droplet size and an increase of polidispersity of the emulsion droplets size, probably due to lower interfacial tension and higher polarity of the solvent blend compared to pure d-limonene. In direct ME, the mean droplet size decreased with increasing the stirring speed and decreasing the transmembrane flux. The droplet-to-pore size ratio was 2.2-4.6 and 1.5-3.5 for the membrane with a pore size of 10 and 20 μm, respectively. The minimum droplet-to-pore size ratio of 1.5 was smaller than 3 reported in direct ME with SPG membrane, probably due to very low interfacial tension of 1 mN/m when 25/75 solvent mixture was used. The most uniform droplets were obtained at the flux of 600 L m^{-2} h^{-1} and the stirrer speed of 620 rpm, which corresponded to the peak shear stress on the membrane surface of 7 Pa. For a constant surfactant/oil ratio (R) of 0.10, the mean droplet size decreased with increasing the dispersed phase content in the emulsion.

   In premix ME, the mean droplet size exponentially decreased with increasing transmembrane flux from an initial value greater than 50 μm in a pre-emulsion to a final value lower than the pore size in the emulsions processed at the flux above 2000 L m^{-2} h^{-1}. The mean droplet size was additionally reduced using two

or three passes through the membrane, but the particle size distribution was relatively broad.. The effect of pore size on the mean droplet size was more pronounced in premix than in direct ME. The mean droplet size lower than 6 µm was achieved using both 10 and 20 µm membrane. O/W emulsions with a dispersed phase content of 40 wt% showed shear thinning behaviour and viscoelastic properties, due to structuration in the emulsion. Premix ME with repeated only two passes through nickel micro-engineered membrane enables to obtain O/W emulsions with very small mean droplet sizes compared to the pore size. The mean droplet size lower than 6 µm was achieved using both 10 and 20 µm membrane, but more uniform droplets were obtained with a 20 µm membrane.

O/W emulsions with a dispersed phase content of 40 wt% showed viscoelastic properties, due to structuration in the emulsion. On the other hand, O/W emulsions with a dispersed phase content of 30 wt% exhibited Newtonian behaviour with the viscosity values in a good correlation with the mean droplet sizes.

4. Microfluidization was capable of producing nano-emulsions for 30 wt% eco-friendly emulsions, regardless of the homogenization pressure used. These emulsions showed re-coalescence due to an over-processing undergone during their preparation. In spite of the fact that all microfluidized emulsions did not show significant changes in the DSD, these emulsions exhibited different values of zero shear viscosity. Emulsions processed at lower homogenization pressures showed higher values of zero shear viscosity; this is related to flocculated emulsions. This flocculation led to a coalescence process. Furthermore, slightly flocculated emulsions did not show an increase of the droplet size, but rather the creaming process took place. Consequently, moderate pressure of 15000 psi responded better than higher or lower pressures due to the lack of creaming and a lower coalescence. Hence, rheology was a relevant and decisive tool to allow us to understand why different destabilization mechanisms occur depending on homogenization pressure in emulsions with very similar DSD.

5. DSD was strongly influenced by homogenization rate for 30 wt% emulsions but slightly influenced for 40 wt% emulsions due to a change of regime in rotor-stator device. By contrast, zero-shear viscosity changes more in 40 wt% than in 30 wt% emulsions with homogenization rate. This fact is related to a flocculation process induced by energy input (above 5000 rpm). These aforementioned emulsions showed viscoelastic properties. As a consequent, plateau modulus were calculated and was used to detect destabilization mechanisms by mean of its variation with aging time. In this sense, this rheological parameter was demonstrated to be an useful tool in order to predict coalescence before visual observation and to distinguish between different grades of flocculation. Furthermore, flocculated 40 wt% emulsions showed coalescence with aging time while 30 wt% underwent creaming process due to the low zero shear viscosity shown. This supports the laser diffraction and rheology results. It is important to remark that the main destabilization mechanism is influenced by not only the dispersed phase content but also the homogenization rate. Hence, this study demonstrate the importance of flocculation induced by emulsification process in emulsions.

   The most stable emulsion was 40 wt% processed at 4000 rpm in the rotor-stator device. Therefore, a more concentrated emulsion was achieved using less energy input, which fulfil the demands of a bio-based society.

6. An increase of recoalescence during processing of emulsion with Levenol C-201 concentration for 40 wt% emulsions containing Levenol C-201 and Pluronic PE9400 was detected. Hence, Pluronic PE9400 protects better the interface against recoalescence. Rheological properties of these emulsions reveals an increase of rheological parameters (η_0, G', G'') with pluronic concentration when it is the predominant surfactant or for 2/2 ratio of surfactants. This fact is related to a flocculation process during the processing since Sauter diameters were similar for these emulsions. This flocculation could be due to a depletion flocculation process or due to the 3D brush/mushroom conformation and the formation of multilayers of Pluronic. The latter may be the reason why the protection of the interface is better with Pluronic. An increase of droplet size

with aging time were observed in 40 wt% emulsions but with different trends. There are some evidences that point out different destabilization mechanisms. Emulsions with only Levenol C201 as surfactant showed an increase of volumetric diameter, a decrease of span and an almost constant Sauter diameter with aging time. Conversely, a great increase of Sauter and volumetric diameter and a decrease of span were observed for the pluronic emulsion. These facts have been corroborated by analysing the droplet size increase fitting to the LWT theory about Ostwald ripening and to the coalescence equation proposed by Weers and Kabalnovov. The 3D brush/mushroom conformation and the formation of multilayers of Pluronic in the emulsions studied could be the reason why these systems underwent Ostwald ripening and not coalescence. This conformation would promote Ostwald ripening and reduce coalescence. By contrast, structure induced by Levenol did not protect perfectly the interface and coalescence was observed. Furthermore, some differences can also be seen in rheology and MLS results with aging time for the two extreme systems. Hence, the study of the different surfactants for these eco-friendly emulsions demonstrates the importance of the type of surfactant in a formulation regardless these possess droplet size distributions very similar after preparation.

7. Processing temperature did not show a big influence on DSD below 35 ºC. But interestingly, emulsions prepared at 5 ºC and 15 ºC exhibited viscoelastic properties typical of weakly structured materials while emulsions prepared at 25 ºC, 35 ºC and 45 ºC showed a weak-gel behaviour. 25 ºC and 35 ºC emulsions presented very similar behaviour but with different values of Plateau modulus. Those differences in this parameter pointed out different grades of flocculation of these emulsions since there was no droplet-size effect. Flow curves showed shear-thinning behaviour for all emulsions studied. Emulsions prepared above 15 ºC exhibited very low values of flow index, which is consistent with flocculated emulsions. All emulsions presented coalescence but in different grades being 5 ºC the emulsion which showed the least increase in droplet size with aging time. Laser diffraction results and rheology with aging time supported the hypothesis about different grades of flocculation induced by processing temperature. Hence, a tight control of the preparation temperature is necessary in order to

tune flocculation grade and slow down the destabilization process. Furthermore, rheology has demonstrated to be a powerful tool to show the slight structural differences between emulsions with similar DSD but with different stability. Multiple Light Scattering has been an important method to clarify the destabilization mechanisms which were taking place simultaneously in these emulsions. It was another way to quantify coalescence reaching to the same conclusion that laser diffraction and rheology results: emulsion prepared at 5 ºC showed the best stability due to the low flocculation grade.